NTNU – Trondheim
Norwegian University of
Science and Technology

Optimizing CO2-injection by Compositional Simulation

Tor Arild Melby

Petroleum Geoscience and Engineering (2 year)
Submission date: June 2014
Supervisor: Odd Steve Hustad, IPT

Norwegian University of Science and Technology
Department of Petroleum Engineering and Applied Geophysics

NTNU

Det skapende universitet

Norwegian University of Science and Technology

Master's Thesis

TPG 4915

Optimizing CO_2-Injection by Compositional Simulation

Author:
Tor Arild Melby

Supervisor:
Prof. Odd Steve Hustad

June 6, 2014

Department of Petroleum Engineering and Applied Geophysics

Acknowledgements

I would like to express my gratitude to my supervisor, Odd Steve Hustad, who has during this semester helped and guided me in making my thesis complete. I would also like to give my thanks to Olav R. Hansen, Bamshad Nazarian and Statoil for helping and supplying me with the necessary equipment and data. I would also like to give my thanks to Lastly, I would like to give my thanks to family and friends for supporting me through my studies, especially Joakim Leboulvais Børkja and Gunnar Sie Dahle who took their time reading and correcting my thesis.

Tor Arild Melby, *June* 6, 2014

Abstract

Reservoir simulation is used to predict flow of fluids through porous media. The purpose is to get an insight into how the reservoir performs by for example employing certain injection methods and/or modelling options in order to optimize investment decisions. In this thesis reservoir simulation is used as a tool to aid in the process of simulating hysteresis in one of Statoil's field models. Hysteresis affects the pattern of fluid flow in the reservoir. In order to optimize oil prediction this phenomena is studied. Hysteresis is seldom employed in field models due to its complexity and requirement of computational resources. However, it is an important phenomena which causes change in saturation direction and trapping of fluid phases. Water-alternating-gas injection (WAG) is a method causing rapid changes in saturation direction, but in this thesis CO_2-injection has been the main focus.

In order to employ hysteresis to the field model, new relative permeability- and capillary pressure curves were made based on experimental data. Corey correlation was used to make gas-oil and water-oil relative permeability curves for the 5 different rock types in the model. Only k_r hysteresis was studied due to the fact that enabling capillary pressure caused too many problems for the simulator. Eclipse300 was the selected simulation tool used to simulate the different two-phase hysteresis models available; Carlson's-, Killough's- and Jargon's methods. Carlson's method gave the most optimistic oil predictions while Killough's method gave the least. Jargon's method proved to be the least computational heavy method. However, what all the methods had in common was that a bigger saturation of gas was left in the reservoir compared with the case of no hysteresis selected. A comparison between the different injection methods are also given, where simultaneous water and gas injection proved to be the most cost efficient in terms of oil volumes produced versus the amount of CO_2 injected. Injecting at different BHPs was tested to simulate immiscible- and miscible CO_2 behavior. An increase in numerical instabilities was observed when BHP was set to miscible conditions, causing severe inconsistencies in calculated relative permeability curves, ultimately resulting in non-physical behavior of the fluid flow.

Lastly, a sensitivity analysis of the three-phase models was done, including ODD3P. The ODD3P model predicts less ultimate oil recovery compared to the traditional models, even though it extends the three-phase saturation range. However, an increase in oil prediction was observed pre-injection. This is due to a different table input and a different way of handling saturation changes, compared to the traditional models. Based on earlier published results done on WAG simulations comparing experimental data with numerical (hysteresis- and non-hysteresis) models[23], the IKU3P model, which ODD3P is an extension of, gave the closest match to the experimental data. Based on this the ODD3P model possibly estimates a more realistic oil prediction compared to the traditional models.

Sammendrag

Reservoarsimulering blir brukt til å prediktere strømning av fluider gjennom porøse media. Hovedformlet er å få en innsikt i hvordan reservoaret oppfører seg ved eksempelvis forskjellige injeksjonsmetoder, slik at en kan optimalisere investeringsbeslutninger. Hovedfokuset for denne avhandlingen har vært å implementere hysterese på en av Statoils feltmodeller, og studere hvordan dette har påvirket strømningsmønsteret i reservoaret. Hysterese er sjeldent anvendt i feltmodeller på grunn av dets kompleksitet og krav når det kommer til dataressurser. Likevel er det et viktig fenomen som forekommer i prosesser som fører til endring i metningsretningen. Alternerende vann-og gassinjeksjon forårsaker store endringer i metningsretning, men i denne avhandlingen har CO_2-injeksjon vært hovedfokuset.

For å kunne bruke hysterese i feltmodellen ble nye relative permeabilitet - og kapillærtrykkskurver generert basert på eksperimentelle data . Corey korrelasjon ble brukt til å lage gass-olje- og vann-olje relative permeabilitetskurver for de 5 forskjellige steintypene i modellen. Eclipse300 var det valgte simuleringsverktøyet som ble brukt til å simulere de ulike to-fase hysteresemodellene; Carlsons- , Killoughs- og Jargons metoder . Carlsons metode gav de mest optimistiske oljeprediksjonene mens Killoughs metode gav de laveste. Jargons metode viste seg å være den minst beregningstunge metoden. En sammenligning mellom de forskjellige injeksjonsmetodene er også gitt, simultaneous gas-and water injeksjon viste seg å være den mest kostnadseffektive i forhold til oljevolum produsert mlt mot mengder CO_2 injisert . Injisering på ulike bunnhullstrykk ble testet for å simulere ikke-blandbar og blandbar CO_2 forhold. En økning av numeriske ustabiliteter ble observert når BHP ble satt til blandbare forhold, som førte til at relativ permeabilitietskurver og skannekurver kalkulert ikke stemmer overens med virkeligheten.

Til slutt ble det utført en sensitivitetsanalyse av tre-fase modeller, inkludert ODD3P. ODD3P modellen predikterer mindre oljeutvinning i forhold til de tradisjonelle modellene, selv om den har et større tre-fase metningsområde. Men en økning i olje utvunnet ble observert før injeksjon. Dette er på grunn av en annen tabellinnputt, sammenlignet med de tradisjonelle modellene. Basert på tidligere publiserte resultater gjort på WAG- simuleringer med IKU3P modellen[23], som ODD3P er basert på, vil ODD3P mest sannsynlig gi en mer realistisk olje prediksjon i forhold til de tradisjonelle modellene.

Contents

List of Figures

List of Equations

1 Introduction

1.1 Background

There are many factors to take into account before CO_2-injection can be executed in a field. Simulating different scenarios by compositional simulation is one of the factors that needs to be taken into consideration. In order to minimize errors related to reservoir simulation, and approximate the model as much as possible to the reality, it is important that the input data in the model is correct and that the fundamental reservoir mechanics are included. Hysteresis, or phase trapping, is a well known phenomena occurring in the reservoir. However, many reservoir engineers neglect this effect when simulating full-scale field models, due to its complexity (e.g. swelling into oil and water which causes changes in IFT and P_c) and requirement of computational resources. In order to simulate hysteresis, drainage and imbibition relative permeability curves, and capillary pressure curves need to be made. SCAL data are used for this purpose. Corey type relative permeability correlation is a way of correlating laboratory data. Corey correlation is a simple power-law function with only one empirical parameter, the power itself. The correlation generates smooth relative permeability curves. There has also been suggested improvements to the correlation by Chierici[6] and Sigmund and McCaffery[27] due to shortcomings in the original Corey correlation. However, in this thesis the general Corey correlation will be used in order to make the two-phase relative permeability curves based on experimental data in order to simulate hysteresis.

1.2 Study Objectives

The main objective of this study is to analyse the effect of implementing hysteresis into a full-scale reservoir model through CO_2-injection. Different hysteresis methods will be considered in order to optimize reservoir simulation. In order to employ hysteresis, correct relative permeabilities of the different rock types need to be made. PVT and phase behavior analysis need to be done in PVTsim to study the behavior of CO_2 in contact with the reservoir crude, in order to describe what happens when the reservoir crude comes in contact with the CO_2 at different pressures.

1.3 Description of Employed Softwares

1.3.1 Eclipse300

Eclipse is a simulation software owned by Schlumberger. It is used in relation to black oil, compositional, thermal, and streamline reservoir problems. It offers a robust set of numerical solutions for fast and accurate prediction of dynamic behavior for all types of reservoirs and development schemes. The ECLIPSE simulator suite consists of two simulators: ECLIPSE100 and ECLIPSE300, where E100 is the black oil simulation software, while E300 is the compositional simulation software. Eclipse 300 allows to model multicomponent hydrocarbon flow. In order to get a detailed description of phase behavior- and compositional changes, E300 uses cubic equation of state, pressure dependent K-values and black oil fluid treatments. E300 was used in this thesis to investigate the effect of implementing hysteresis in one of Statoil's fields in the North Sea.

1.3.2 PVTsim

PVTsim is a simulation program developed for reservoir engineers, flow assurance specialists, PVT lab engineers and process engineers. It is utilized as a tool to combine fluid characterization procedures with efficient regression algorithms to match fluid properties and experimental data with a given EOS. In the database, 25 years of data material is collected to give accurate approximations. PVTsim can simulate slim-tube-displacement process to calculate MMP, including finding MMP by a given EOS. PVTsim is used in this thesis to get detailed description of the phase behavior of the reservoir crude and the CO_2.

2 CO_2-Injection: In Retrospect

CO_2-injection is a fairly young method for extracting remaining oil in place of mature reservoirs. During the 1950's the earliest results of CO_2 combined with flue gas were seen as a potential of enhanced oil recovery (EOR)[25]. The research continued through the 60's and included early field pilots as well as laboratory experiments. Results were of varying outcome, some showed great potential, others did not. In the 1970's there was a major development of CO_2 pipelines in the Permian basin, due to positive results from the earlier years.

CO_2-injection has been a method used to recover oil for over 40 years. There are classic texts related to EOR potential of CO_2, where Fred Stalkup (1983) describes "Miscible Displacement" in SPE Monograph 8. The studies conducted, describes various processes behind EOR due to CO_2, and the influence of various parameters such as composition, temperature, pressure, salinity and capillary number. The studies also describe immiscible/miscible displacement in relation with minimum miscible pressure (MMP). In addition, CO_2 behavior is also mentioned, where CO_2 rich phase sometimes gets heavier than the oil, which in turn forces the oil to switch place with the CO_2 rich phase.

It is of utter importance to understand the reservoir characterization of the field where CO_2 injection is going to be implemented. This includes an understanding of how the fluids flow in the reservoir, and an understanding of the reservoirs' internal structure. It was due to lack of this knowledge that many EOR projects encountered problems related to EOR floods in the past.

When injecting carbon dioxide into sandstone- or carbonate reservoirs, the pressure in the formation will increase. At the same time, when the oil gets in contact with the CO_2, it swells and the viscosity is being reduced. For light oil reservoirs, multiple-contact miscibility can be developed. Parts that are being swept above the MMP results in a remaining oil in place of $0 \rightarrow 5$ %, depending on sweep efficiency. With large amounts of natural gas available, growing networks of CO_2 pipelines, low residual oil after CO_2 flooding, and effective separation of CO_2 for recycling,

IOR-technology by CO_2 flooding has been proven to be more profitable during recent years. [9]

CO_2 has a great potential enhancing and increasing oil recovery. However, it does not recover all the oil, regardless of whether the reservoir has been previously flooded with water. Typically, primary recoveries constitutes 5 % - 15 % of OOIP. Secondary recovery gives additional 20 - 40 %. As described earlier, CO_2 is capable of displacing nearly all oil in the reservoir, but a typical recovery addition with CO_2 displacement is around 10 - 20 %, if it is under miscible conditions by injecting an equivalent of 80 % HCPV with CO_2. Immiscible displacements give much less recovered oil, only 5 - 10 % at most. The fundamentals causing these low oil recoveries can be traced back to the mechanisms behind CO_2 flooding. If the injection process is stable in vertical direction, the displacement will be very effective. If the process is miscible, heterogeneities will have a less effect. However, barriers will have a negative impact for these processes.

3 Fundamentals and Concepts

In order to understand what is happening in the reservoir, it is important to have a perceptive view of the fundamental reservoir mechanics. The interplay of forces existing and occurring during an injection process, and the related basic concepts, are important to understand. As this study mainly focuses on CO_2-injection, it is a necessity to include the phase behavior of CO_2 as well.

3.1 Forces in Porous Media

3.1.1 Interfacial tension

An interface is known as a boundary between two bulk phases. The equilibrium bulk phases can be: liquid-vapor, liquid-solid, liquid-liquid or vapor-solid. Gases are generally miscible, however, N_2, CO_2 and HC-gases may be immiscible depending on pressure, temperature and composition. When oil is poured into a cylindrical tube containing water, the pressure will increase to negate the effect of interfacial tension between the two fluids. This will make a curved shape in the contact surface. The physical phenomenon occurring is also related to the energy required to establish the surface area. The molecules near the interface have less kinetic energy than the bulk phase, and will therefore move less freely. Additionally, the composition at the interface is different from the bulk composition. Since the total energy is dependent on temperature, the potential energy of the molecules is greater in the interface section than in the rest of the volume. The potential energy is proportional to the surface area of the system, and since equilibrium is attained at lowest potential energy state, the surface area of the system is always minimized. Keeping temperature, pressure and the amount of material present in the system constant, the interfacial tension, σ, may be expressed as a function of Gibbs free energy[19]:

$$\sigma = \frac{\delta G}{\delta A} \tag{1}$$

Where G is Gibbs free energy, and A is the contact area. The unit of surface tension is therefore energy per area, J/m^2, or more commonly used mN/m.

σ is also related to pressure, temperature and composition. The pressure difference that the interfacial tension creates is called capillary pressure, and is given by the Laplace equation (1806):

$$P_c = P_{nonwetting} - P_{wetting}$$

For a waterwet system the expression becomes:

$$P_c = P_o - P_w = \sigma(\frac{1}{R1} + \frac{1}{R2})$$

where σ = oil-water interfacial tension, P_c = capillary pressure, P_o= pressure in the oil phase, P_w= pressure in the water phase, R1, R2 = radii of curvature of the oil-water interface measured perpendicular to one another.

By convention, capillary pressure is defined by the pressure in the reference phase minus the non-reference phase. This means that there are two possible solutions depending on which one is the reference phase. Thus, if a negative pressure is a solution, the pressure will point in the opposite direction of the pressure chosen as a reference. For two immiscible displacement fluids, the surface tension will be positive, due to the reduction of surface area. In the case of two miscible fluids, the surface tension will be zero. This means that the fluids will be mixed together, and/or even react with each other. For an ideal homogeneous water-wet cylindrical tube R1 and R2 can be expressed as R which then again can be written as: R = radius of the tube/ cosine of the contact angle. This results in the equation above being simplified to[19]:

$$P_c = \frac{2\sigma cos\theta}{r} \tag{2}$$

3.1.2 Wettability

From thermodynamics the definition of wettability is:" *The tendency of one fluid to spread or adhere on a solid surface in the presence of other immiscible fluids.*[3] The wettability of a reservoir can be evaluated through measurements of interfacial tensions, tensions between fluid-fluid and rock-fluid interfaces, and the contact angle. The theoretical foundation of the contact angle was first described by Young[36] in 1805. The mathematical equation was, however, formally derived by Laplace[17], and can be regarded as a mechanical force balance illustrated in Fig.1.

$$\sigma_{os} = \sigma_{ws} + \sigma_{ow} cos\theta \tag{3}$$

Where os = oil-solid, ws = water-solid, ow = oil-water

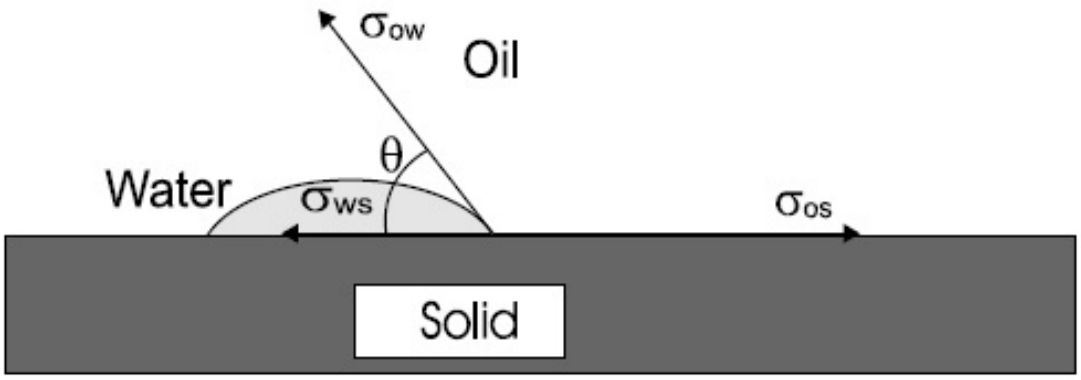

Figure 1: Illustration of mechanical forces influencing a droplet of water on a solid surface[30].

When measuring which phase is the wetting phase, θ is being evaluated. Water is most commonly used as the reference phase. This means that if θ is between 0-90 degrees, the solid is water wet. It prefers water in contrast to the other phase. If θ is 90 degrees, the solid has neutral wetting properties. For θ bigger than 90 degrees, the solid is oil wet. This is illustrated in Fig.2. It is important to note that when the contact angle increases or decreases, the preferability of the solid does as well. This means that if the wetting preferability for water decreases the contact angle

increases, for this particular system. Wettability is an important parameter when it comes to enhancing oil recovery, because it affects the distribution, location and flow of oil and water in the reservoir. Due to varying wetting conditions throughout the reservoir the flow of injection fluid may pass pores, and oil will be left as residual saturation. [3]

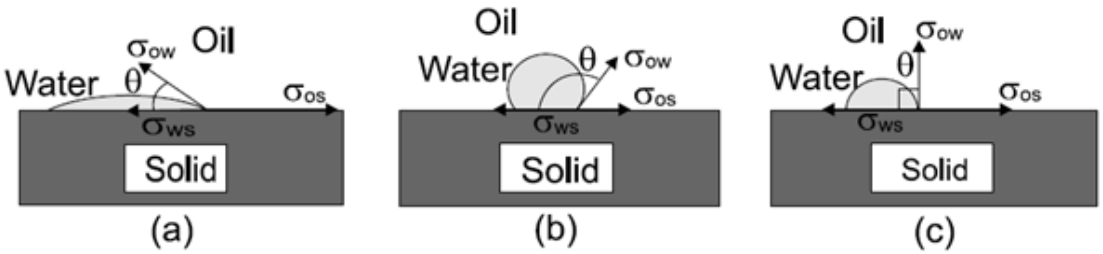

Figure 2: **a**. water-wet, **b**. oil-wet, **c**. neutral-wet.[30]

When CO_2 is injected, it reduces the pH of the formation brine. There exist experimental evidence that wettability changes to less water-wet conditions as pH decreases.[5] Different methods of injection have been recommended depending on wetting conditions. If the reservoir is water-wet, continuous gas injection is optimal, while oil-wet conditions suggest that WAG is the optimal choice of injection.[25]

3.1.3 Effect of Gravity

When two immiscible fluids are in contact with each other, there will be a pressure difference between them. If the fluid with the lowest density is underneath the other one, it will experience an upward pointing pressure, due to the buoyancy effect. This can be observed by pouring water into a burette with oil. The oil will flow upwards, due to pressure/density differences. This is all due to Archimedes principle. In the reservoir, density difference, height of the liquid column, permeability and capillary pressure are some of the most important factors influencing gravity forces during fluid movements.[32]

However, Ypma (1985) states that under certain conditions, capillary forces are of minor importance. Ypma has defined a dimensionless capillarity/gravity number which incorporates gas/oil interfacial tension to describe this statement:

$$N_{cg} = \frac{\sigma\sqrt{(\phi\tilde{J}/k)}}{\Delta\rho g H} \tag{4}$$

ϕ = porosity, k = absolute permeability, $\tilde{J}$ = average Leverett J-function, H = is layer thickness in stratified reservoirs or total reservoir thickness. N_{cg} is related to the dimensionless recovery expression:

$$\frac{(E - E_{min})}{(E_{max}) - E_{min})}$$

For N_{cg} less than 0.1, capillary forces start to affect the recovery process. For high

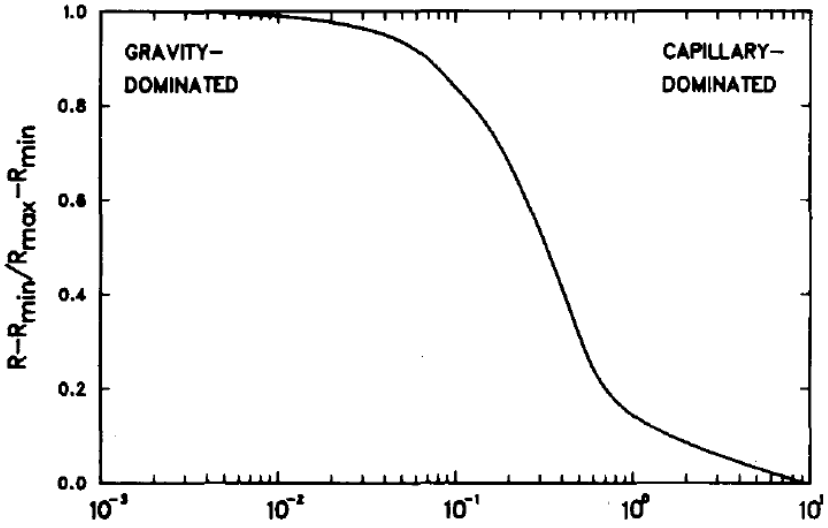

Figure 3: Effect of Gas/Oil capillary pressure on gravity drainage in dipping layer. X axis is CG-number[37].

permeable reservoirs with low interfacial tension, capillary forces will not have a major impact on oil recovery. However, it is not certain how low the interfacial tension can be to make this statement valid.[37]

3.1.4 Viscous Forces in Porous Medium

It is not unusual to express viscous forces in relation to capillary forces. The term used to do this is called capillary number, N_{ca}. In fluid dynamics, the capillary number represents the relative effect of viscous forces versus surface tension acting across an interface between two immiscible fluids.

$$N_{ca} = \frac{v\mu}{\sigma} \tag{5}$$

μ is the viscosity of the displacing phase, while σ is the IFT between the displaced and the displacing phases, and v is the interstitial velocity. What the capillary number does is correlating data, which it does pretty well. However, there is a significant scatter in the data. When the capillary number is relatively low, 10^{-6} and less, the residual oil is no longer a function of N_{ca}. Although values on the order of 10^{-7} are most common. This indicates that waterflood recoveries should be independent of injection rate over the range of values that can be accomplished in practice. It has also been shown by Moore and Slobod that waterflood recoveries from laboratory cores were just as good as when water was injected at typical rates used in the field [21]. The capillary number also shows that for values above 10^{-5} the residual oil saturation decreases. For values at 10^{-2} the residual oil saturation becomes virtually zero.[10]

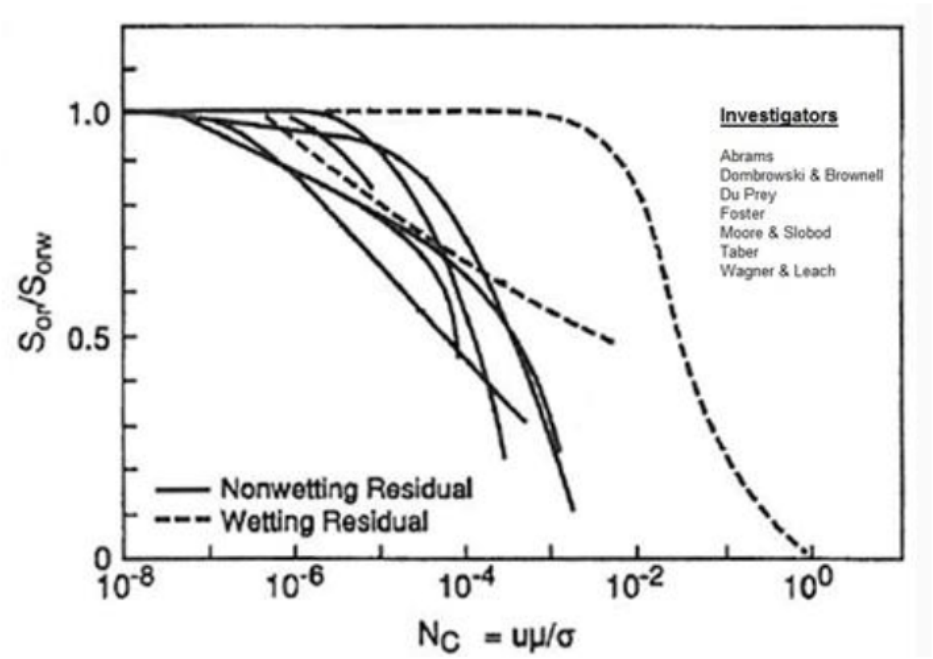

Figure 4: Capillary number[10][16].

3.2 Fluid Flow in Porous Media

When forces are either supplied or taken from the reservoir, in terms of injection and production, it causes a net force imbalance. The result is that the fluid within the pore space of the rock will begin to move. The simplest way of describing fluid movement in porous media is through Darcy's law.

3.2.1 Darcy's Law

Darcy's law relates fluid velocity and viscosity to fluid potential through a porous medium by:

$$u = \frac{k\rho}{\mu}\frac{d\Phi}{dl} \tag{6}$$

where u is fluid velocity, dl is length of the porous media, μ is fluid viscosity, ρ is fluid density and k represents absolute permeability, and dϕ is fluid potential

between the ends of the media

$$d\Phi = \frac{dp}{\rho} + gdz$$

where the second term represents the hydrostatic head.

Under normal conditions the absolute permeability is independent of the nature of the fluid, however, when encountering real gas flow, at very low pressures there is a slippage between the gas molecules and the walls of the porous media, resulting in an apparent increased permeability. This phenomenon is called the Klinkenberg effect.[7] Hence, it is important to make corrections when doing laboratory experiments calculating permeabilities through air flow rates in core plugs.

3.2.2 Relative Permeability

Permeability is the medium's ability to conduct fluid flow. In systems where two or more fluids are flowing simultaneously, each fluid will have its own effective permeability. These permeabilities are dependent on the saturations of each fluid. The sum of the effective permeabilities are always less than the absolute permeability. Consider two points on the effective permeability curve for water. Initially the water saturation is 1. At this point the rock is entirely saturated with water, and K_w = k, the absolute permeability. When S_w has been decreased to S_{wc} (drainage) there will be no flow of water, since the residual water is immovable. At this point K_w = 0. Between the end-points, the effective permeabilities are assumed the shapes as shown in Fig.5. The main factors influencing the shapes of the curves are pore size, pore size distribution, wettability, saturation and saturation history (drainage or imbibition).[29] Important to point out is that relative permeability is special for flow through porous media. For a two-phase system $K_{rj} + K_{ri} \leq 1$, which is also a specific attribute of flow behavior due to relative permeability. This is a result of the phases competing to flow through pore throats. From Fig.5, the effective permeability curves and relative permeability curves have exactly the same shapes. The only difference is that the relative permeabilities scales from 0 to 1. Relative permeabilities are used due to mathematical convenience since in many displacement

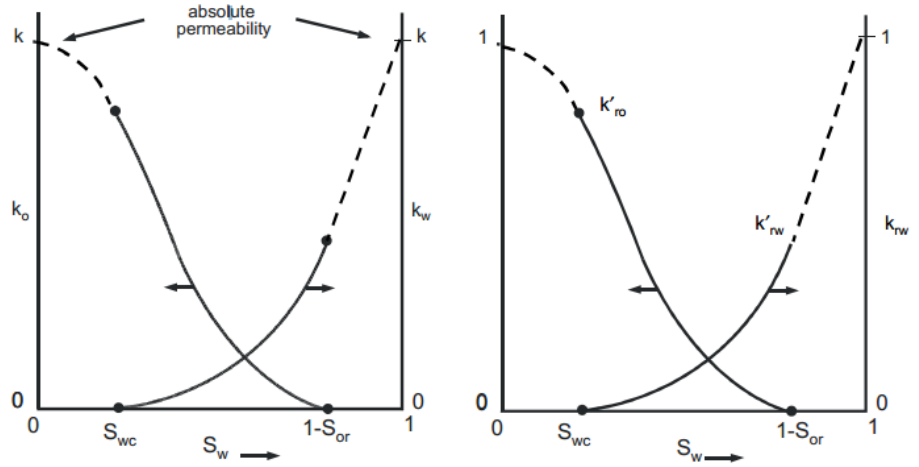

Figure 5: **a**.Effective and **b**. Corresponding relative permeabilities.[7]

calculations, the ratio of effective permeabilities can be simplified to:

$$\frac{K_o(Sw)}{K_w(Sw)} = \frac{K \times K_{ro}(S_w)}{K \times K_{rw}(S_w)} = \frac{K_{ro}(S_w)}{K_{rw}(S_w)} \tag{7}$$

For two-phase flow, one usually presents relative permeability in plots, where non-wetting phase and wetting phase are plotted versus increasing non-wetting saturation. Considering an oil-water drainage and imbibition in a completely water-wet system, the drainage curves are represented by Fig.6. Initial water saturation is 1, decreasing to S_{wir}.

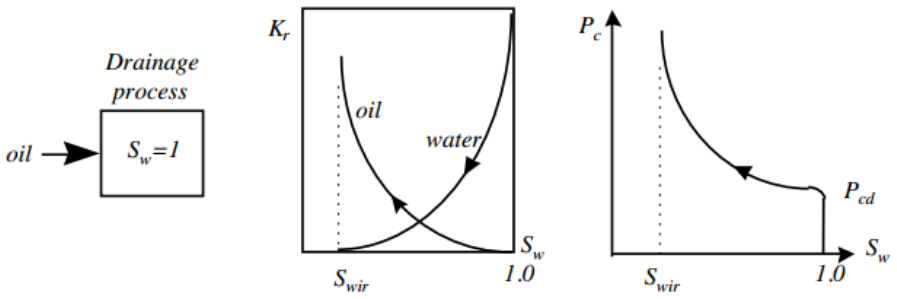

Figure 6: Oil-Water Drainage process.[15]

During imbibition the porous media is filled with both oil and water at initial

conditions, where $S_w = S_{wir}$. In this case the wetting phase is increasing in saturation.

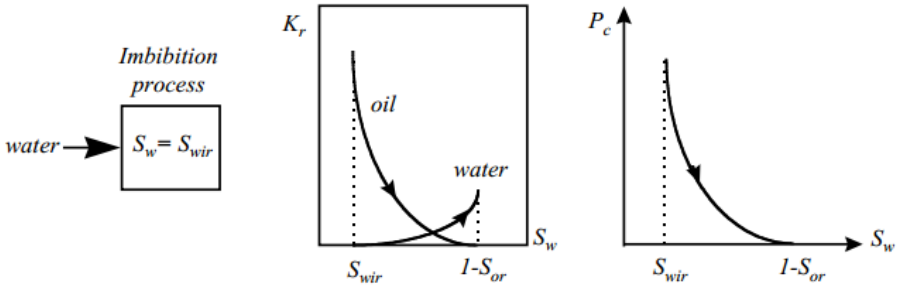

Figure 7: Oil-Water Imbibition process.[15]

For systems which are less water-wet the capillary pressure curves will have a negative part at high water saturations. Drainage and imbibition are common processes occurring in the reservoir where injection takes place. During initial stages of pressure depletion, imbibition is the main process direction. This is however dependent of how active the water aquifer is. In the case of water injection the saturation process will revers, causing drainage to occur. When wetting fluid is increasing and decreasing in saturation, this causes hysteresis, and ultimately results in pore-trapping of fluid.

3.3 Relative Permeability Models

Relative permeability can be modelled depending on how many phases there are in the system. There are certain models related to two-phase systems and others related to three-phase systems. In this section, a short outline will be given for the most used models for both two-phase- and three-phase systems.

3.3.1 Two-Phase Systems

A couple of correlations for modelling two-phase relative permeability curves have been proposed in earlier studies, such as Wyllie and Gardner's correlation[35], Torcaso and Wyllie correlation[33], Pirson's correlation and Corey's power-law correlation. Since the latter one is employed, only this model will be studied in depth.

3.3.1.1 Corey Correlation

A commonly used approach to generate the relative permeability and capillary pressure curves, is the Corey-correlation. It has its base in normalized saturation. For water/oil system:

$$S_{on} = \frac{1 - S_w - S_{or}}{1 - S_{wir} - S_{or}} = 1 - S_{wn} \tag{8}$$

$$S_{wn} = \frac{S_w - S_{or}}{1 - S_{wir} - S_{or}} \tag{9}$$

$$K_{ro} = S_{on}^{N_{o,p}} \tag{10}$$

$$K_{rw} = S_{wn}^{N_{o,p}} \tag{11}$$

Important to note is that the Corey exponents are different for each process, p, representing either imbibition or drainage.

Since laboratory experiments are carried out with an irreducible water saturation, The oil/gas equations becomes:

$$S_{on} = \frac{1 - S_g - S_{or}}{1 - S_{wir} - S_{or}} \tag{12}$$

$$S_{gn} = \frac{S_g - S_{gc}}{1 - S_{wir} - S_{org} - S_{gc}} \tag{13}$$

$$K_{ro} = S_{on}^{N_{o,p}} \tag{14}$$

$$K_{rg} = S_{gn}^{N_{g,p}} \tag{15}$$

Variations of these equations have been used when generating the relative permeability curves used in this study. The equations have been modified according to the end-point values, and are somewhat simplified in some cases. This will be explained in further detail in the "Simulation Study" chapter.

3.3.2 Three-Phase Systems

Phases considered in a three-phase system are: water, oil and gas. Definitions of the relative permeabilities and capillary pressures of oil, water and gas are functions of saturations considered in a completely water wet system with no contact between gas and water phases. The parameters are thus functions of the following: $\mathrm{K}_{rw}(\mathrm{S}_w)$, $\mathrm{K}_{rg}(\mathrm{S}_g)$, $\mathrm{K}_{ro}(\mathrm{S}_w, \mathrm{S}_g)$, $\mathrm{P}_{cow}(\mathrm{S}_w)$, $\mathrm{P}_{cog}(\mathrm{S}_g)$.
To estimate three-phase relative permeability, two sets of two-phase data are needed water-oil and gas-oil data. From water-oil data K_{rw} and K_{row} are obtained as functions of water saturation. Similarly, K_{rg} and K_{rog} are obtained from oil-gas data as functions of gas-saturation. Hysteresis effects are also taken into consideration. Consider a water-wet system in which oil saturation is decreasing, imbibition data should

be used for water-oil data, and drainage data for oil-gas data. For decreasing water saturations, drainage data should be used for water-oil system. Generally it is not feasible to treat complicated hysteresis effects caused by oscillating saturations.[31]

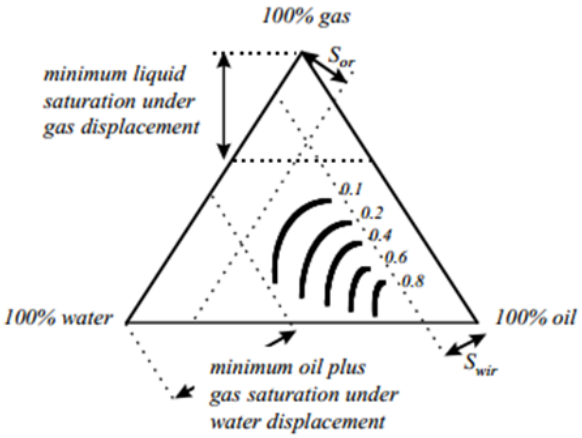

Figure 8: 3-Phase relative permeability graph.[31]

In a three-phase flow situation, the oil relative permeability would be a function of both water and gas saturation. Plotting the data in a triangular diagram, so that each saturation is represented by one of the sides, oil isoperms can be defined by the systems maxima and minima saturations. By following one of the isoperms, saturation changes occurring within a pore can maintain a certain relative oil permeability. The simplest method to generate three-phase permeability curves is simply to multiply oil-water and gas-oil relative permeabilities:

$$K_{ro} = K_{row} \cdot K_{rog}$$

This model, however, is very flawed due to different factors affecting the limiting saturations in three phase flow compared to two-phase flow. For example, S_{or} is process dependent in three-phase flow and very difficult to estimate.

3.3.2.1 ECLIPSE Default Model

The default model implemented in eclipse is rather simple, but effective. It assumes complete segregation of gas and water within each cell. However, water in the gas zone is equal to S_{wco}. The oil saturation is assumed to be constant and equal to the block average value, S_o, throughout the cell. In total $S_o + S_g + S_w = 1$, and assuming the block average saturations are S_o, S_g and S_w. The saturation equations for the gas zone cells and water zone cells are as follows: Gas zone cell (in a fraction of the cell)

$$\frac{S_g}{(S_g + S_w - S_{wco})} \tag{16}$$

Where S_o is the oil saturation, S_{wco} is water saturation (since $S_w = S_{wco}$ here). S_g+S_w-S_{wco} is the gas saturation.

In the water zone, the fraction of the cell becomes:

$$\frac{S_w - S_{wco}}{S_g + S_w - S_{wco}} \tag{17}$$

Where S_o is the oil saturation. The gas saturation is 0, and the water saturation is given by $S_g + S_w$.

The oil relative permeability is then given by:

$$K_{ro} = \frac{S_g K_{rog} + (S_w - S_{wco}) K_{row}}{S_g + S_w - S_{wco}} \tag{18}$$

Where K_{rog} is the oil relative permeability for a system with oil, gas and connate water. K_{row} is the oil relative permeability for a two-phase system with oil and water.

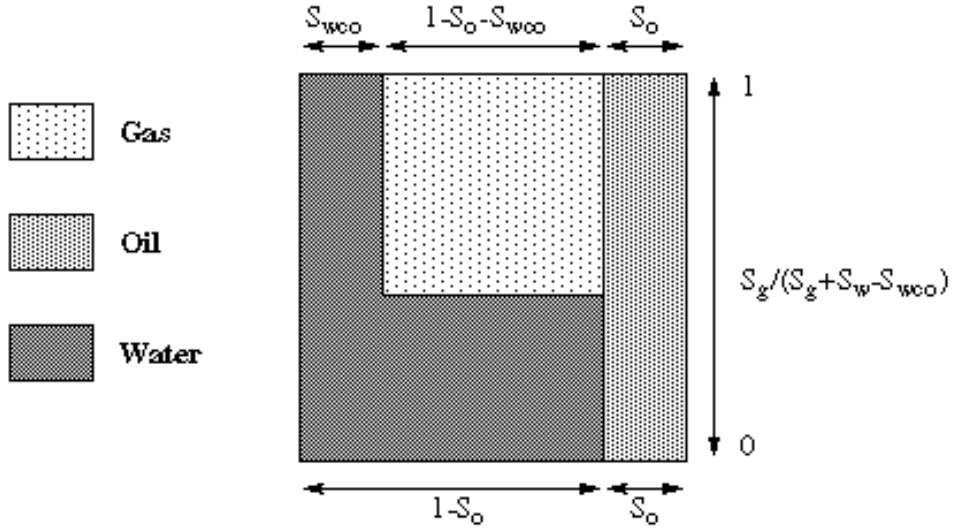

Figure 9: The ECLIPSE default three-phase oil relative permeability model.[26]

3.3.2.2 Stone's First Model

The most commonly used correlations are the so-called Stone-models. They are fairly simple and are defined as follows:

$$S_{oD} = \frac{S_o - S_{or}}{1 - S_{wir} - S_{or}} \tag{19}$$

This is valid for $S_o \geq S_{or}$

$$S_{wD} = \frac{S_w - S_{wir}}{1 - S_{wir} - S_{or}} \tag{20}$$

Which is valid for $S_w \geq S_{wir}$

$$S_{gD} = \frac{S_g - S_{gr}}{1 - S_{wir} - S_{or}} \tag{21}$$

Where $S_{gr} \neq 0$.

These equations represent normalized fluid saturations, and treats connate water and irreducible residual oil as immobile fluids. The sum of the normalized saturations are equal to 1. When the saturation of normalized oil is 100 %, K_{ro} is also 100 %. A decrease in S_{oD} causes a decrease in relative oil permeability, and as a result gas and/or water saturation will increase. The reduction in K_{ro} is not proportional with the reduction in the normalized saturation, and therefore needs to be multiplied by a factor, β_w and β_g, to correct this disproportion.

$$\beta_w = \frac{K_{row}}{1 - S_{wD}} \tag{22}$$

$$\beta_g = \frac{K_{rog}}{1 - S_{gD}} \tag{23}$$

The relative permeability of oil can be written as:

$$K_{ro} = \frac{S_{oD}\beta_g\beta_w}{K_{rocw}} \tag{24}$$

The water/gas saturation dependent factors above are calculated from two-phase data. By putting β_g or β_w equal to zero, it is possible to calculate the corresponding factor. Due to shortcomings in Stone's first model, modifications were made by Hustad and Holt[12] in their improved "Stone Exponent" model.

3.3.2.3 Stone Exponent Model

The Stone Exponent model is a modified Stone's First Model, where an exponent term, n, is introduced to the normalized saturations.

$$K_{ro} = \frac{K_{row}K_{rog}}{(K_{ro})_{Swc}}\beta^n \tag{25}$$

Where

$$\beta = \frac{S_o^*}{(1 - S_w^*)(1 - S_g^*)}$$

$$S_o^* = \frac{S_o - S_{om}}{1 - S_{wc} - S_{om} - S_{gc}}$$

$$S_g^* = \frac{S_g - S_{gc}}{1 - S_{wc} - S_{om} - S_{gc}}$$

$$S_w^* = \frac{S_w - S_{wc}}{1 - S_{wc} - S_{om} - S_{gc}}$$

The β term may be interpreted as a variable that varies between one and zero for high-oil and low-oil saturations, respectively. If the exponent equals to one, the correlation reduces to Stone's first model. Increasing the exponent beyond unity, causes the oil isoperms at low oil saturations to spread from another. Decreasing the exponent below unity, causes the opposite effect. High β values produces a Stone 2 type oil isoperms.

3.3.2.4 Stone's Second Model

Stone's second model tries to estimate S_{or} implicitly by the following expression:

$$K_{ro} = (K_{rog} + K_{rg})(K_{row} + K_{rw}) - (K_{rw} + K_{rg}) \tag{26}$$

When K_{ro} approaches negative values, the residual oil saturation is found. These two methods give different relative permeabilities, so one should be careful when selecting which model to use in each situation. For numerical simulation of WAG injection, Stone's second model severely underestimates the relative oil permeability in the regions with low oil saturations.[28] Experimental results have also shown that for water-oil-gas system where S_w and S_o are decreasing and S_g is increasing, Stone's method 2 predicted three-phase permeabilities better than method 1 at low gas saturations, but both failed to predict correctly at high gas saturations. In the case of increasing S_w and S_o and decreasing S_g, method 2 predictions were not correct, while method 1 approximated to experimental data.[24]

3.3.2.5 ODD3P

The ODD3P method provides a coupled hysteretic model for three-phase relative permeability and capillary pressures. Three-Phase properties are obtained through a weighting scheme of two-phase data.[11] The hysteresis formulation is based upon two limiting scanning curves for increasing and decreasing saturations. When a saturation process changes direction, capillary pressure is made continuous at the turning-point saturation by renormalizing the saturation range relative to end-point and turning-point saturations. The same method is applied for making the relative permeabilities continuous.

A typical ternary diagram of the ODD3P model is shown below with its respective two-phase end point values.

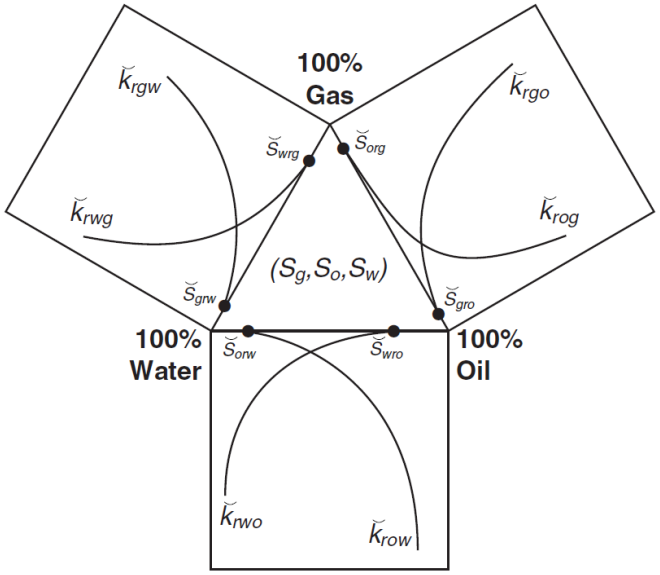

Figure 10: Ternary representation of saturation values with two-phase data.[11]

As input data the model employs gas-oil, gas-water and oil-water two-phase capillary pressure and relative permeability data as functions of one of the phase pair's saturations. The capillary pressure must possess a non-zero gradient. The gas-oil data differ from the traditional data in that the gas-oil data are at zero water saturation. If conventional data are used as a basis of input, a transformation of

these is needed. There are a couple of ways of transforming the conventional data. The first method is to transform the data along the constant gas lines. The second method is to transform the data along the constant oil lines. Arguably the latter is more correct, this will however be discussed in section 6. Gas-water data are represented by the oil-water data. The data are then assigned on regional or block to block basis, represented by the keywords PSTNUM, ISTNUM and DSTNUM. These keywords contain primary saturation data, increasing saturation data and decreasing saturation data. It is possible to set ISTNUM = DSTNUM, however, no hysteretic effects will be accounted for after the increasing saturation process. This will impact WAG injection, as this method alternates between both increasing and decreasing saturation processes. During the calculation procedure, the input saturations are normalized with respect to their end-point saturations by:

$$S_i = \frac{S_i - S_{irj}}{1 - S_{irj} - S_{jri}}, \ i, j = g, o, w \tag{27}$$

The three-phase saturations are formulated based on the three gridblock saturations and the six gridblock end-point saturations, the minimum and maximum saturations are calculated as follows:

$$\bar{S}_{imn} = \frac{\bar{S}_j \bar{S}_{irj} + \bar{S}_k \bar{S}_{irk} + \bar{S}_{irj} \bar{S}_{irk} (\bar{S}_i - 1)}{\bar{S}_j (1 - \bar{S}_{irk}) + \bar{S}_k (1 - \bar{S}_{irj})} \tag{28}$$

and

$$\bar{S}_{imx} = \frac{\bar{S}_j \bar{S}_{kri} + \bar{S}_k \bar{S}_{jri} + \bar{S}_{jri} \bar{S}_{kri} (\bar{S}_i - 1)}{\bar{S}_j (1 - \bar{S}_{kri}) + \bar{S}_k (1 - \bar{S}_{jri})} \tag{29}$$

where, i,j and k represents either the gas,oil or water phase, and i $\neq$ j $\neq$ k. The gridblock saturations are then normalized by:

$$S_i = \frac{\bar{S}_i - \bar{S}_{imn}}{\bar{S}_{imx} - \bar{S}_{imn}} \tag{30}$$

Generally, the equation above does not sum to 1 when three phases are present. However, at the two-phase boundaries the two normalized saturations sum to 1.

The gridblock saturations may then be used to obtain representative two-phase relative permeabilities from the normalized two-phase relative permeabilities. In total there are two relative permeabilities for each phase, one from each of the two-phase system. These are used in calculating three-phase relative permeabilities by a weighting scheme:

$$k_{ri} = \frac{\bar{S}_j}{\bar{S}_j + \bar{S}_k}\hat{k}_{rij} + \frac{\bar{S}_k}{\bar{S}_j + \bar{S}_k}\hat{k}_{rik} \tag{31}$$

As shown in the equation above, the relative permeability for a particular phase is a function of its own saturation only without the presence of a third phase. This is different compared to the traditional models where gas and water are functions of their respective saturations, while oil is a function of both water and gas saturations.

When it comes to capillary pressure in ODD3P, six choices of saturation dependencies are possible. This is illustrated in Fig.11

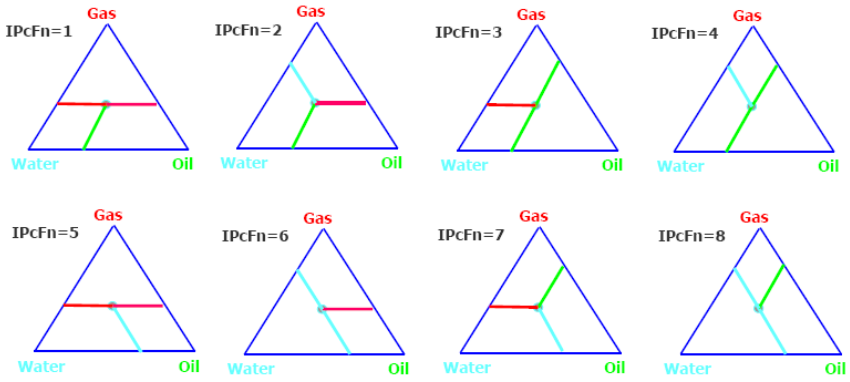

Figure 11: Demonstration of hysteresis.[11]

By specifying IPCFN = 0, 0 is put in the pressure equation in ECLIPSE.

3.4 Hysteresis

In order to get the relative permeability models correct, hysteresis needs to be employed in the models. Hysteresis refers to the changes in saturation. Hysteresis is distinguished between relative permeability hysteresis and capillary pressure hysteresis.

3.4.1 Relative Permeability Hysteresis

Relative permeability values for many porous medias are not a unique function of saturation. It is common to use different relative permeability values for different increasing/decreasing saturations. Consider a 100 % water-wet system being oil-flooded reducing water saturation from a point A to B. From point B, a water-flood is being initialized, going from path B to C. Subsequently a new oil-flood is being done, going from C to B. Due to capillary trapping, the water-flooding will not drain out all of the oil, preventing getting 100 % water in the system. This is referred to as hysteresis phenomena.

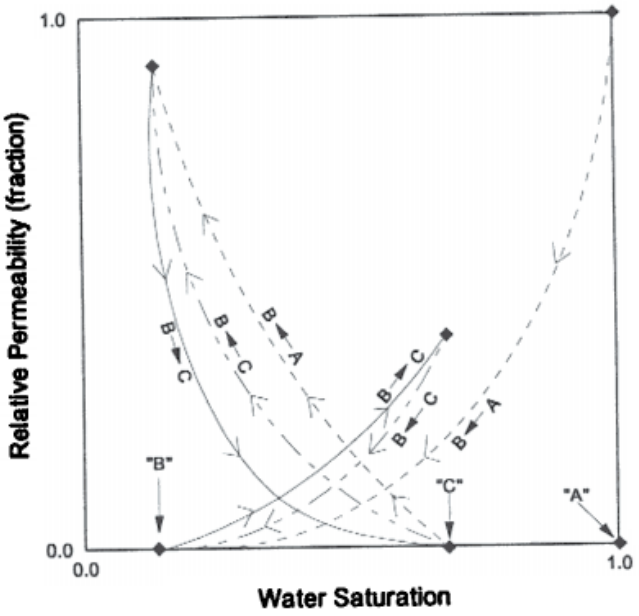

Figure 12: Demonstration of hysteresis.[4]

In reservoir engineering relative permeability hysteresis can be modelled in a couple of ways. It is possible to either employ hysteresis to the non-wetting phase, or the wetting phase.

3.4.1.1 Hysteresis in the non-wetting phase

Typical non-wetting relative permeability curves are given in Fig.13. Curve 1-2 and 2-3 are user supplied drainage and imbibition curves, respectively. If the drainage or the imbibition process are reversed at some point, it will not simply reverse following the same curve, but rather along a scanning curve. Consider a full drainage process starting at point 1, (critical non-wetting residual saturation for drainage, S_{ncrd}), the end-point will be at 2 (S_{nmax}), from this point the imbibition will start and end at point 3, (critical non-wetting residual saturation for imbibition). If the imbibition process started somewhere in between 1 and 2, it would need to follow a scanning curve, 4-5. The saturation remaining at point 5 is the trapped critical saturation, which is a function of maximum non-wetting saturation (S_{hy}).

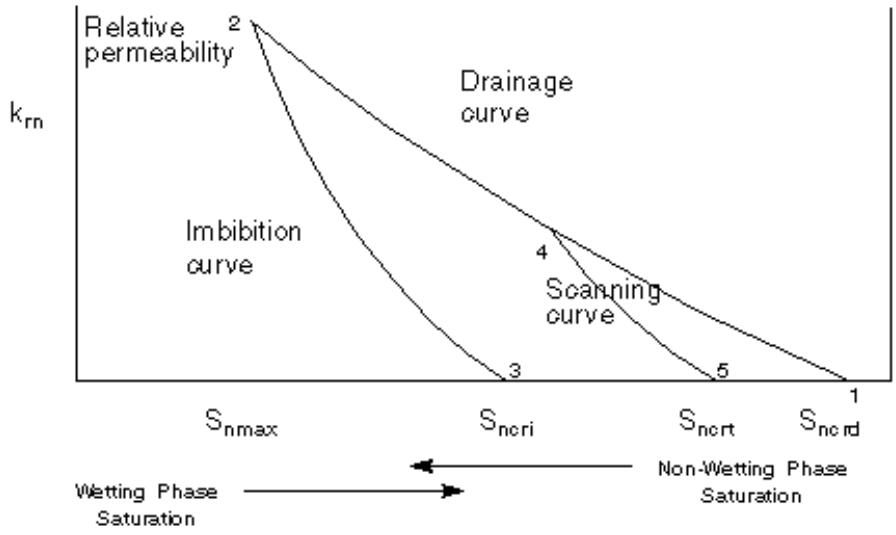

Figure 13: non-wetting phase hysteresis.

3.4.1.2 Hysteresis in the wetting phase

For hysteresis in the wetting phase, curve 1-2 and curve 2-3 are the user specified drainage- and imbibition curves, respectively. To ensure consistency, the two curves must meet at the connate saturation. A primary process would follow the path from 1 to 2 during a full drainage. At point 2 the imbibition will start and end up at point 3 at 1-S_{ncri} (maximum wetting phase saturation that can be reached starting from S_{wco}). Assume that an imbibition process is initiated at an arbitrary point on the primary drainage curve, 4. The process will follow a scanning curve from 4 to 5, where the saturation equals 1-S_{hy}, and S_{hy} is the maximum saturation that can be reached on the scanning curve. If a secondary drainage process is initiated, it will retrace the same scanning curve from 5 to 4.

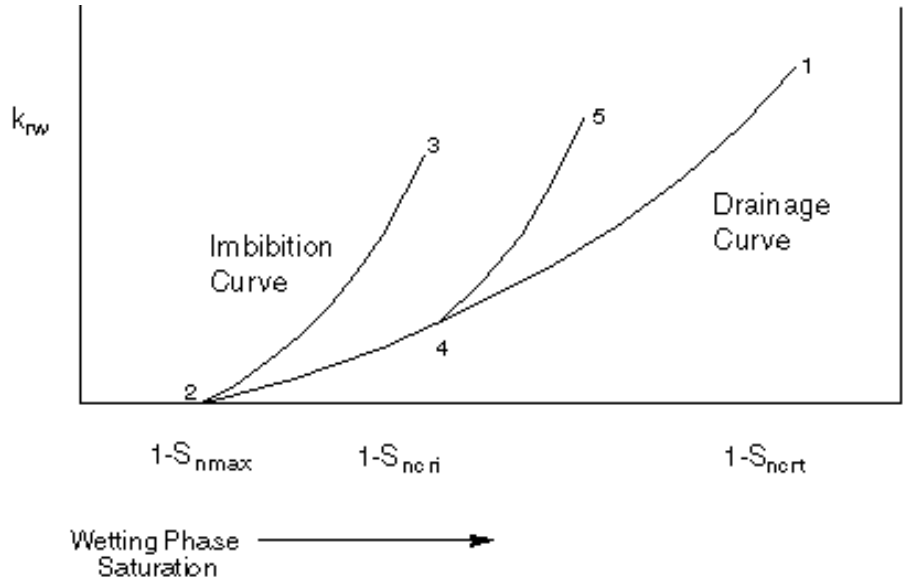

Figure 14: wetting phase hysteresis.[26]

3.4.1.3 Methods

There are three choices of modelling hysteresis in ECLIPSE. Those three are: Carlson's method, Killough's method and Jargon's method.

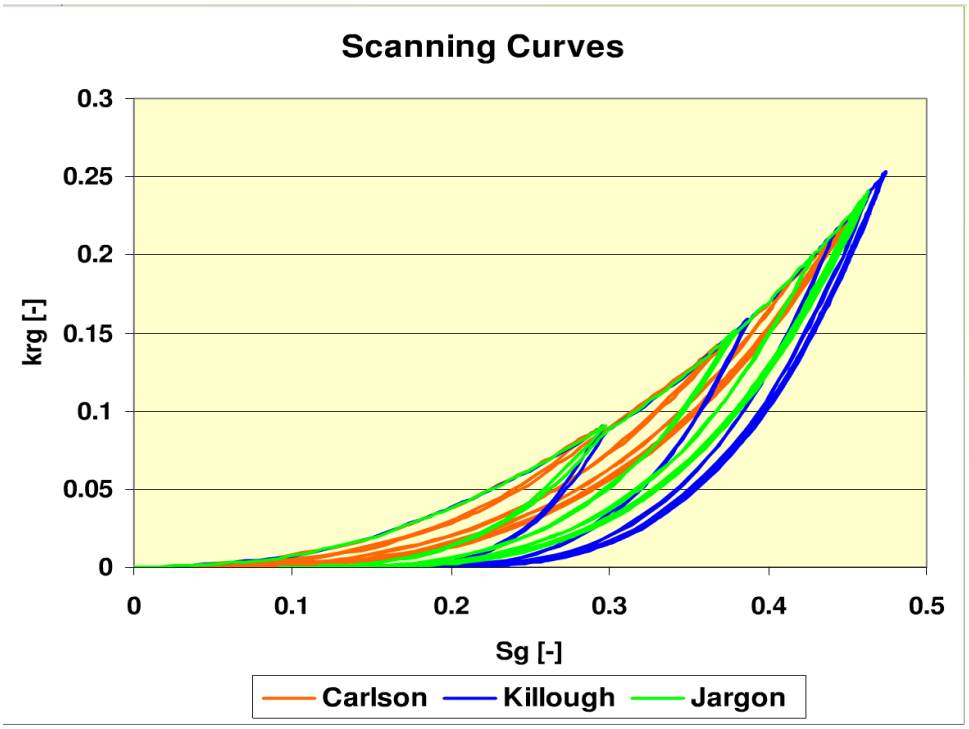

Figure 15: non-wetting phase hysteresis by different methods.[8].

Carlson's Method

Carlson's method creates a scanning curve parallel to the imbibition curve. It can easiest be visualized by a horizontal shift of the imbibition curve from Fig.14 where curve 2-3 is shifted to 4-5. A criteria for this method is that the imbibition curve needs to be steeper than the drainage curve. If this is not the case, it may produce negative values of S_{ncrt}.

Killough's Method

Killough's hysteresis method can be employed both on the wetting phase and the non-wetting phase. By using an interpolation formula between input bounding curves, Killough developed a method to calculate scanning curves from intermediate values.[14] For a given value of S_{hy}, the trapped critical saturation can be

calculated as:

$$S_{ncrt} = S_{ncrd} + \frac{S_{hy} - S_{ncrd}}{1 + C(S_{hy} - S_{ncrd})} \tag{32}$$

Where the constant C is a formulation of Land's trapping formula:

$$C = \frac{1}{S_{ncri} - S_{ncrd}} - \frac{1}{S_{n,max} - S_{ncrd}} \tag{33}$$

The relative permeability for a particular saturation phase can be calculated as follows:

$$K_{rn}(S_n) = \frac{K_{rni}(S_{norm})K_{rnd}(S_{hy})}{K_{rnd}(S_{n,max})} \tag{34}$$

In this equation K_{rnd} and K_{rni} represent relative permeability on the bounding drainage and imbibition curve, respectively, and

$$S_{norm} = S_{ncri} + \frac{(S_n - S_{ncrt})(S_{n,max} - S_{ncri})}{S_{hy} - S_{ncrt}}$$

The trapped critical saturation calculated with Killough's method will always lie between S_{ncrd} and S_{ncri}, unless drainage and imbibition curves are made to coincide. The scanning curve will then not necessarily follow this combined curve, except at its end point values.

Jargon's Method

In Jargon's hysteresis method the trapped saturation, S_{ncrt}, is constructed by moving the drainage critical saturation towards the imbibition critical saturation by the same fraction that the hysteresis saturation has moved towards the maximum non-wetting saturation:

$$S_{ncrt} = S_{ncrd} + \frac{(S_{ncri} - S_{ncrd})(S_{hy} - S_{ncrd})}{S_{n,max} - S_{ncrd}} \tag{35}$$

A function, R(X), is now constructed, representing the ratio of imbibition and

drainage curves as a function of the saturation value scaled between the drainage curve end point and the maximum saturation:

$$R(X) = \frac{K_{ri}(S_n)}{K_{rd}(S_n)} \tag{36}$$

X in the equation is defined from the non-wetting saturation S_n by:

$$X = \frac{S_n - S_{ncrd}}{S_{n,max} - S_{ncrd}} \tag{37}$$

Obviously, the interval in which X lies in must be between 0 and 1, where R goes from 0 at X = 0 to 1 at X = 1, where the two curves meet. A consequence of the drainage curve being above the imbibition curve, is that R must be between 0 and 1. R is now evaluated at a value of X and then multiplied by the drainage curve value in order to create scanning relative permeability values. X reflects the fractional distance of the current saturation between drainage and imbibition curve end point and the hysteresis saturation.

$$K_{rn} = R(X_s)K_{rnd}(S_n) \tag{38}$$

Where

$$X_s = \frac{S_n - S_{ncrd}}{S_{hy} - S_{ncrd}}$$

The function R(X) was defined above and can be substituted into the equation for the scanning curve, resulting in:

$$K_{rn} = \frac{K_{ri}(\bar{S})}{K_{rd}(\bar{S})}K_{rnd}(S_n)$$

where

$$\bar{S} = S_{ncrd} + (S_n - S_{ncrd})\frac{(S_{n,max} - S_{ncrd})}{S_{hy} - S_{ncrd}}$$

3.4.2 Capillary Pressure Hysteresis

In this section capillary pressure hysteresis will be considered, where primary drainage and imbibition curves are available. Capillary pressure hysteresis occurs in three-phase- and gas-water cases, and is therefore important to note.

3.4.2.1 Water Capillary Pressure Modelling

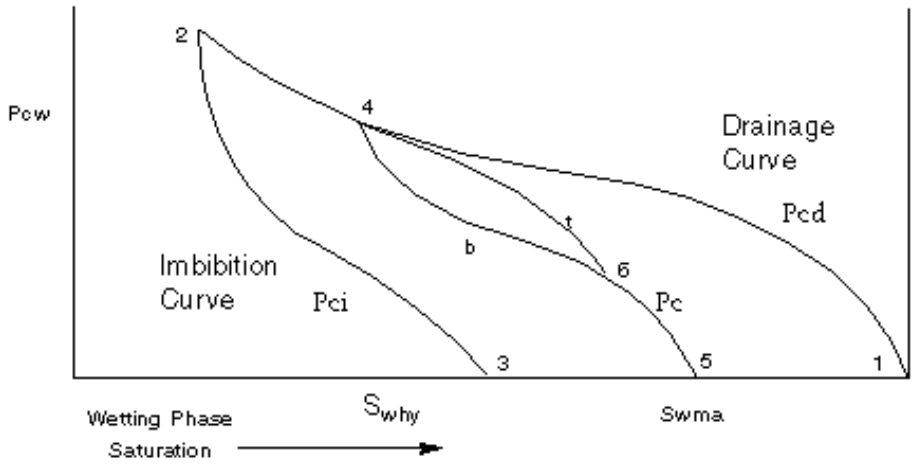

Figure 16: Water Capillary Pressure.[26]

From Fig.16 consider that the drainage process, starting at point 1, is reversed at an arbitrary value between 1 and 2 (point 4 in this case). The capillary pressure will then move along a scanning curve from point 4 to the trapped critical non-wetting phase saturation at point 5. This curve is formed as a weighted average of the drainage and imbibition curves, starting with 100 % of the drainage curve at point 4. Killough has suggested the form:

$$P_c = P_{cd} + F(P_{ci} - P_{cd}) \tag{39}$$

Where F represents:

$$F = (\frac{1}{S_w - S_{why} + E} - \frac{1}{E})/(\frac{1}{S_{wma} - S_{why} + E} - \frac{1}{E}) \tag{40}$$

E is a curvature parameter of the order of 0.1

S_{why} is the water saturation at the hysteresis reversal point 4. (minimum historical water saturation in the cell)

S_{wma} is the maximum water saturation attainable for the trapped non-wetting phase saturation. In ECLIPSE the curvature parameter, E, is specified in item 1 in the EHYSTR keyword.

Assume that instead of following the scanning curve all the way to point 5, the imbibition process is reversed at point 6, and a secondary drainage process is initiated. The values will not follow the already generated scanning curve, but may follow a new drainage-imbibition-drainage curve that returns to point 4 through "t" from Fig.16. The "t" curve is represented by

$$P_c = P_{cd} + G(P_{ci} - P_{cd}) \tag{41}$$

Where G represents:

$$G = (\frac{1}{S_{dep} - S_w + E} - \frac{1}{E})/(\frac{1}{S_{dep} - S_{why} + E} - \frac{1}{E}) \tag{42}$$

Where S_{why} is the water saturation at the hysteresis reversal point 4, and S_{dep} is the departure saturation, where G = 0.

3.4.2.2 Gas Capillary Pressure Modelling

The principle of gas capillary pressure hysteresis is similar to water capillary pressure hysteresis.

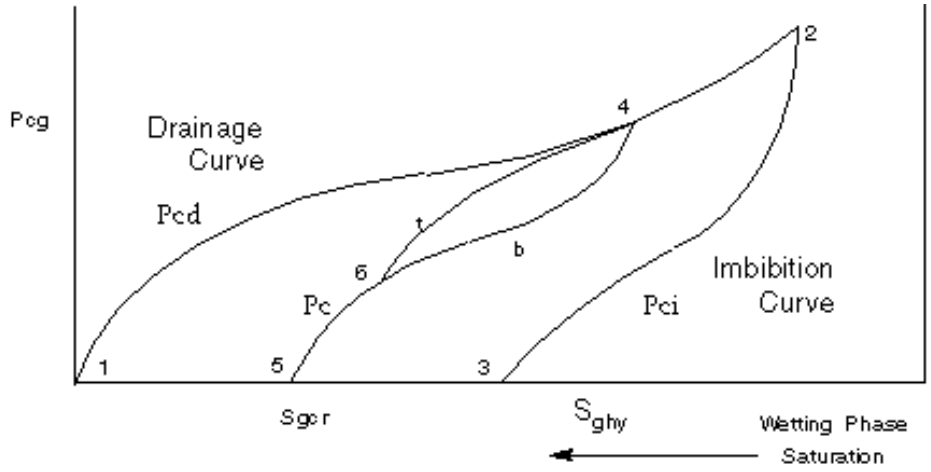

Figure 17: Water Capillary Pressure.[26]

Consider the same analogue for P_{cg} as it was for P_{cw}:

$$P_c = P_{cd} + F(P_{ci} - P_{cd}) \tag{43}$$

$$F = (\frac{1}{S_{ghy} - S_g + E} - \frac{1}{E})/(\frac{1}{S_{ghy} - S_{gcr} + E} - \frac{1}{E}) \tag{44}$$

Where the only difference is that S_{ghy} represents the gas saturation hysteresis reversal at point 4. S_{gcr} represents the maximum water saturation attainable for the trapped non-wetting phase saturation.

3.5 PVT Properties and Phase-Behavior

CO_2 is a stable, non-toxic compound found in gaseous state at standard conditions. For petroleum related applications, CO_2 exist as a liquid-like supercritical fluid or as a gas. When mixed with water it forms carbonic acid, which is a problem regarding injectivity in carbonate reservoir. The acid will react with the carbonate, eroding the formation. Corrosion of steel is also significant, so WAG projects require utter supervision when doing such operations with CO_2.

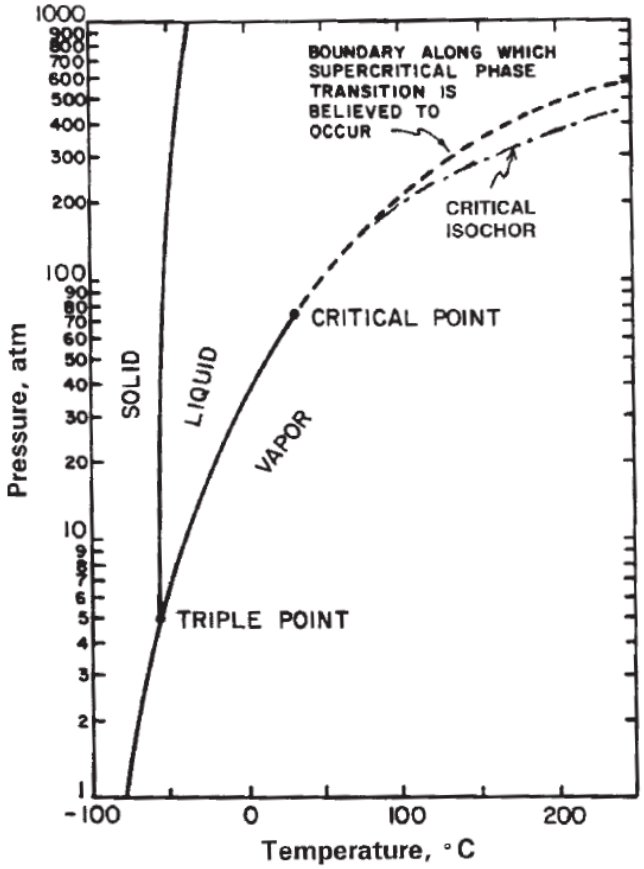

Figure 18: CO_2 Phase Diagram[34].

3.5.1 P-T Dependency

Fig.18 represents the phase diagram of CO_2, where phase transitions are shown for CO_2 at different pressures and temperatures. The line separating solid phase and liquid represents melting. The line separating solid and gas phase represents sublimation. The line separating liquid and vapor is also a boiling/condensing boundary. Phase transitions in this graph represents CO_2 in thermodynamic equilibrium. This means that it is possible for CO_2 to exist at a P-T coordinate corresponding to another phase. However, this is only temporarily. At stable conditions, CO_2 will eventually revert to the appropriate phase represented by the given pressure and temperature. At the critical point each phase boundary may or may not be eliminated, however, gas and liquid properties at this point are identical. The region above is commonly referred to as supercritical due to the fact that the fluid is neither a gas nor a liquid. Related to EOR, critical phenomena play an important part. Assume a laboratory pressure cell that contains a pure component on its vapor pressure curve. In these conditions it exists both as a gas and a liquid, and the cell will contain two fluid regions with different properties. One phase will separate to the top and another to the bottom of the cell. From the original point to the critical point, little change occur in the cell. However, when the conditions close in to the critical conditions, the sharp interface between the two phases (that occurred through segregation) becomes more and more blurred. Extending the conditions beyond the critical curve will turn the fluid more into a single phase fluid with gradual change in properties. A way to distinguish the phase transitions at the critical point is through a pressure-molar-volume diagram.

3.5.2 Pressure-molar-volume Dependency

A pressure-temperature diagram contains no information about the molar volume, just phase boundaries. A pressure-molar-volume plot gives information about liquid/vapor fractions in the fluid for a given isotherm. By keeping the temperature constant, and altering the pressure, the molar-volume will change and so will the fraction of vapor/liquid. The left side of the critical point represents 100 % liquid, while the right side represents 100 % vapor. This information is critical to understand when calculating the roots of the cubic EOS'.

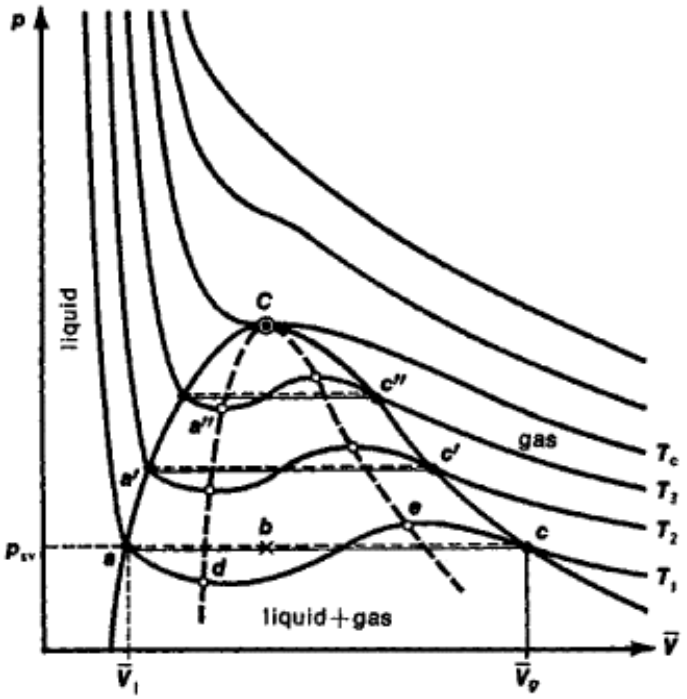

Figure 19: Schematic P-$\tilde{v}$ diagram..

Important to point out is the difference between molar volume and volume of a fluid. molar volume is defined as:

$$\tilde{v} = \frac{M}{\rho} \tag{45}$$

For a single component fluid. It is basically the volume occupied by one mole of a substance at a given temperature and pressure.

3.5.3 Mixtures

The main purposes of CO_2-injection is either to recover remaining oil in place, or to store it in the formation. In order to do this, a method to describe the behavior of the fluids when they come in contact with CO_2 is needed. Phase behavior of pure components is used as an aid to understand complex mixtures. A common way to describe such mixtures is to use pressure-composition and ternary diagrams as a result by comparing phase behavior of pure components to the mixture.

A compositional ternary plot contains little information about temperature. However, in return, compositional data is obtainable. The diagram can only show the composition of one fluid at a time. The information this gives is therefore insufficient compared to what is needed, due to a multitude of components that can form during an EOR displacement process. Ternary diagrams are usually used to describe the behavior of mixtures at a constant pressure and temperature. At each corner of the diagram 100 % of a component is presented, usually a pseudo-component containing several pure components.

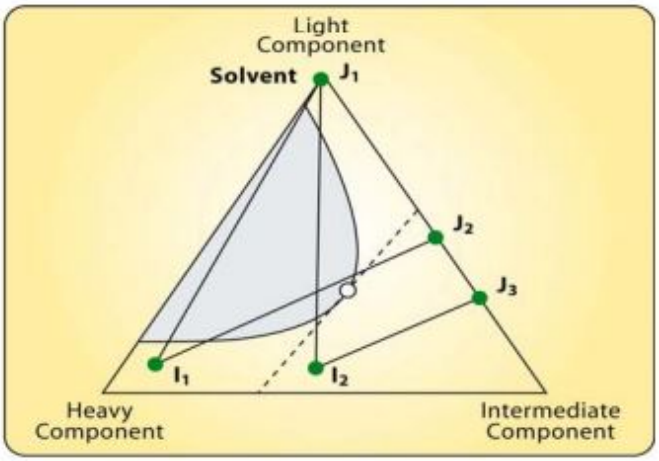

Figure 20: Conditions for different types of oil displacements by solvents[18].

Since composition of the crude changes with depth, the diagram is also representing a specific height in the reservoir. For naturally fractured reservoirs this is not the case due to the fact that these reservoirs generally have constant composition relations with regards to depth. By looking at the ternary diagram there is a couple of lines describing contact paths with increasing heavy, intermediate and light components. If the flooding process is represented by the pathway I_1 - J_1, the whole process is happening through the two phase envelope, which means that immiscible displacement is occurring.

I_2 - J_3: First contact miscible, due to the fact that the two-phase area is not involved in the pathway. When the initial and injected compositions are on the opposite side of the critical tie line, vaporizing drive or condensing drive occurs.
I_2 - J_1: Vaporizing gas drive
I_1 - J_2: Condensing gas drive
I_1 - J_1: Immiscible gas drive

3.5.4 Vaporizing Gas Drive

This is a process based on vaporization of intermediate components, ranging from C_5 to C_{12}, from the oil. These components will then "trade place" by, e.g. CO_2 gas. It is a viable method for light oil reservoirs. Vaporizing Gas miscible process can displace almost all the oil being contacted by the displacing gas. However, due to reservoir heterogeneities and relative permeabilities, the fraction of the reservoir oil being in contact with the gas may be low. Injection rates are typically higher for other gases than CO_2, because CO_2 has the ability to extract heavier components compared to hydrocarbon gas. At high pressure, lean gas can develop an in-situ gas that is sufficiently rich in C_2 through C_4 to develop miscibility with the reservoir oil. Another condition for developing miscibility by this process is that the reservoir should not have an initial free gas saturation. Which means that in order for the vaporizing-miscible drive mechanism to take place, the gas saturation in front of the displacement bank must always be zero.[34]

From Fig.21. Consider a pure light component solvent, and a light oil. Since the dilution path goes through the two-phase region it will not be first contact miscible. Since the gas-phase from the first cell is higher than the fluid, it will move on to the second cell, liquid 1 will continue to mix with fresh solvent. At a certain point the gas mixing with the reservoir crude will no longer develop two-phases and will instead be first contact miscible.

3.5.5 Condensing Gas Drive

When a gas is injected, and the gas and the oil are initially immiscible, this will result in multiple contacts condensing drive. If a hydrocarbon rich gas is injected, a miscible bank will form through condensation of intermediate components from gas

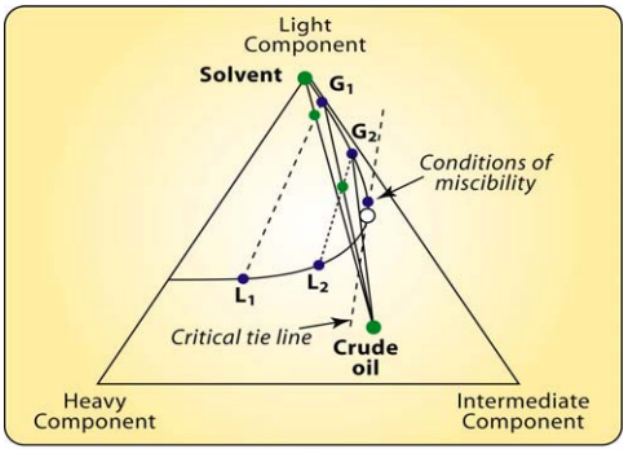

Figure 21: Multi-contact Vaporizing Drive[16].

into oil. Further out from the pressure source, the oil will become heavier, due to a pressure drop, which makes less and less gas condense into the oil.

The process is shown in the ternary diagram below. First mixing cell splits into G_1 and L_1, representing gas and liquid, respectively. L_1 will mix with pure solvent going to L_2 containing less liquid, and continue until it results in a single-phase fluid.

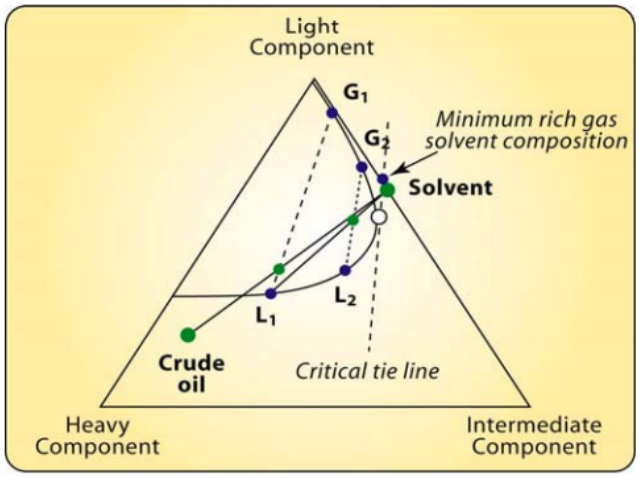

Figure 22: Multi-contact Condensing Drive[16].

3.5.6 Condensing/Vaporizing Mechanism

Zick[1] proposes a mechanism considering both condensing and vaporizing drive. The easiest way to understand it is to use an oil/gas system composed of four groups of components as an example. The first group consists of light components, such as methane, nitrogen and CO_2. The second group consists of light intermediate components; ethane, propane, butane. The third group contains middle intermediates which can be found in the oil, but not significantly in the gas, usually ranging from butane to decane. The fourth group consists of everything else. When the enriched gas comes in contact with the oil, a supply of light intermediate components condenses from gas into the reservoir oil, making the oil lighter. Since the gas injected is more mobile than the oil, a continuous stream of fresh gas constitutes with more intermediate components to the oil. If this continued, a the oil will at a certain point become miscible with the gas injected. This drive makes the condensing gas drive. For a real reservoir oil this is not the only drive occurring. As this drive takes place, middle intermediates vaporizes from the oil to the gas. After a few contacts the oil will be saturated with light intermediates but stripped from middle intermediate components. Since light intermediates cannot substitute loss of middle intermediates a net effect results in the oil becoming heavier than it initially was. Five zones can be interpreted from Fig.23:

1. Original oil zone.
2. Condensing zone.
3. Transition from condensing to vaporizing.
4. Vaporizing zone.
5. Tail end where oil residue and injected gas are in equilibrium. [34]

In conventional reservoirs composition is a function of depth. Light components tend to be on top of the reservoir formation, while heavier fractions are gradually increasing as the depth increases. If a rich solvent is injected, vaporizing drive can occur on top, and gradually transition to condensing drive in the bottom of the oil zone. Minimum miscible pressure (MMP) will therefore vary with depth.[22]

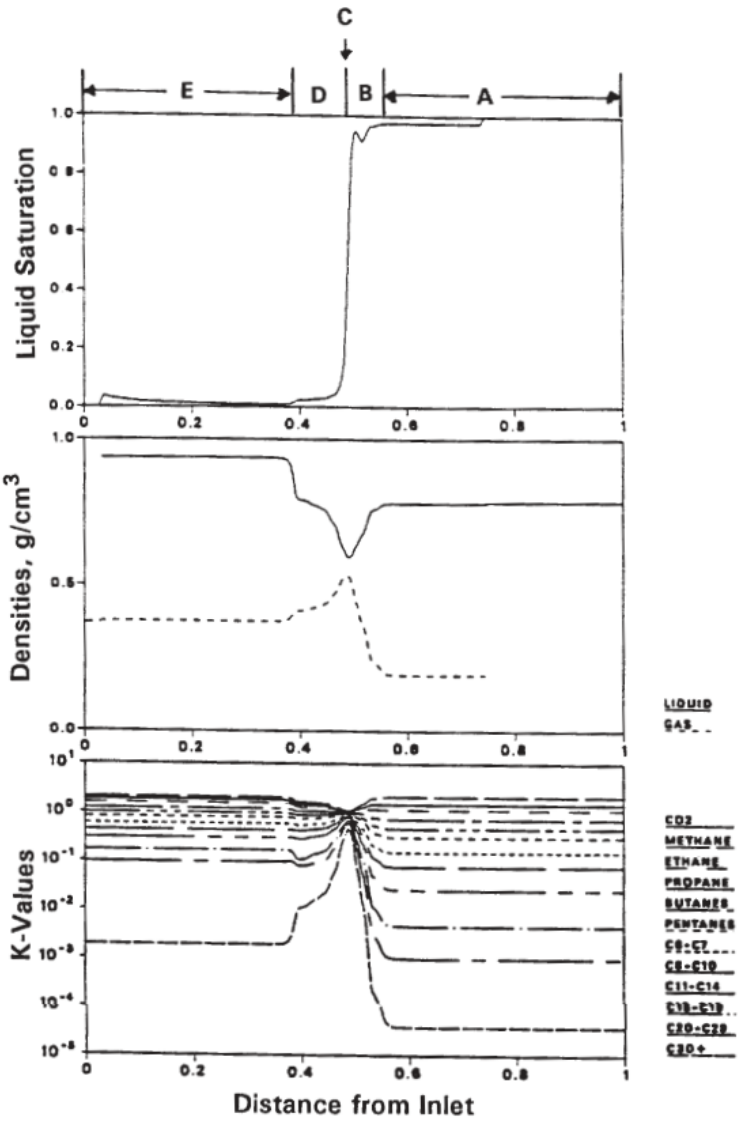

Figure 23: EOS-calculated slimtube-profiles for condensing/vaporizing gas drive.[34].

4 Simulation Study

4.1 Objectives

The main goal of this thesis is to implement hysteresis in the existing Statoil1 field model. In order to do that new relative permeability- and capillary pressure curves need to be made. Corey-correlation will be used to make drainage and imbibition curves based on given experimental data. In order to get a structural overview, the chapter is divided into three parts; Reservoir Description, Saturation Functions, and Workflow and Assumptions. In the Reservoir Description part, general information about the model is given, such as fluid description, permeability and porosity of the model, SATNUM regions, and so on. The second part consists of the newly generated saturation functions. The third part consists of assumptions made for the simulation study, and an overview of the working process.

4.2 Reservoir Description

The grid model dimensions are 89x104x207, totalling in 1915992 grid blocks. The model consists of 9 components, and Soave-Redlich-Kwong EOS is used. Oil, gas and water are present. Datum depth is at 2597 meters, at the OWC. The gas existing in the reservoir has been liberated from the oil. The pressure initially at the datum depth was 290 bar, however, at present it is around 80 bar. The allocation of the different permeabilities and porosities are randomly distributed throughout the model, which makes the model very heterogeneous. The reservoir model used in this study, Statoil1, is a replication of a field located in the North Sea.

4.2.1 Permeability and Porosity

The Statoil1 field model consists of 5 different rock types, assigned with 5 different relative permeability- and capillary pressure tables. Typically, the tables are assigned to different porosity- and permeability ranges, on either regions or facies level, or both. In ECLIPSE this is specified in the SATNUM/IMBNUM keyword, in the REGION section. SATNUM represents drainage tables while IMBNUM represents imbibition tables.

Table 1: Region Data

IMBNUM	**SATNUM**	**Rock Type**	**Permeability [mD]**	**Porosity [%]**
1	6	1	0,0-2000	0,177-0,272
2	7	1B	5,09-1962,8	0,138-0,372
3	8	2	5,0-50	0,12-0,34
4	9	3	2,0-5,0	0,125-0,316
5	10	4	0,01-2,0	0,0116-0,32

In the table above the different SATNUMs are given for the corresponding rock types. It is important to note that the permeability ranges in rock type 2, 3 and 4 are quite low, especially for 3 and 4. When implementing new relative permeability- and capillary pressure curves for these rocks, little change is expected for grid blocks given these SATNUMs, due to the flow's ability to be conducted through high

permeable layers. The implementation of hysteresis will most likely have most effect in the top layers (1-50) where most of the blocks consists of rock type 1 and 1B. From Fig.24,25,26,27 and 28 the distribution of the different rock types with regards to depth is shown. Layer 1-12 is mainly consisting of rock 1. Layer 18 to 50 consist of rock type 1B through 4, where the concentration of the latter ones, 2, 3 and 4, are increasing more and more with depth.

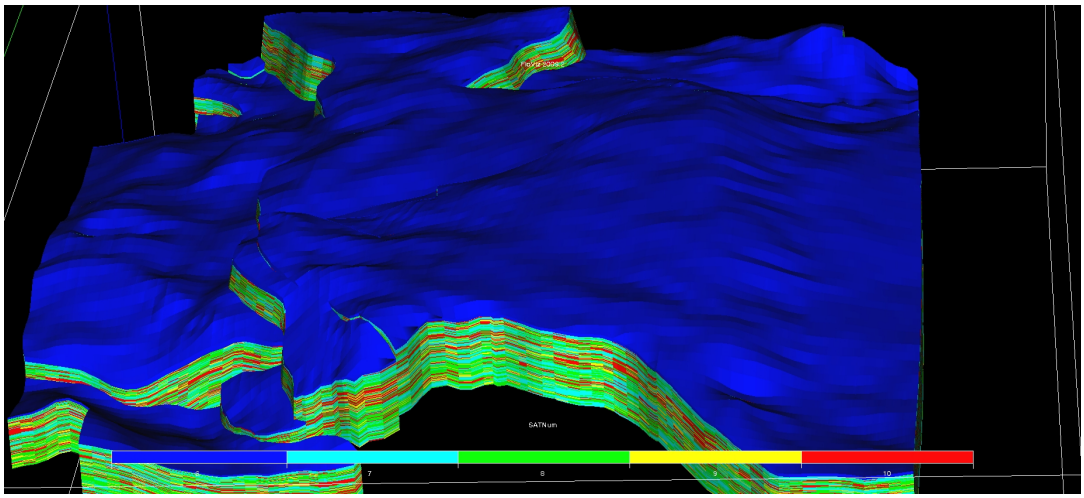

Figure 24: SATNUM allocations,top layer is layer 1. Color ranging from left to right represents SATNUM 6, 7, 8, 9 and 10, respectively.

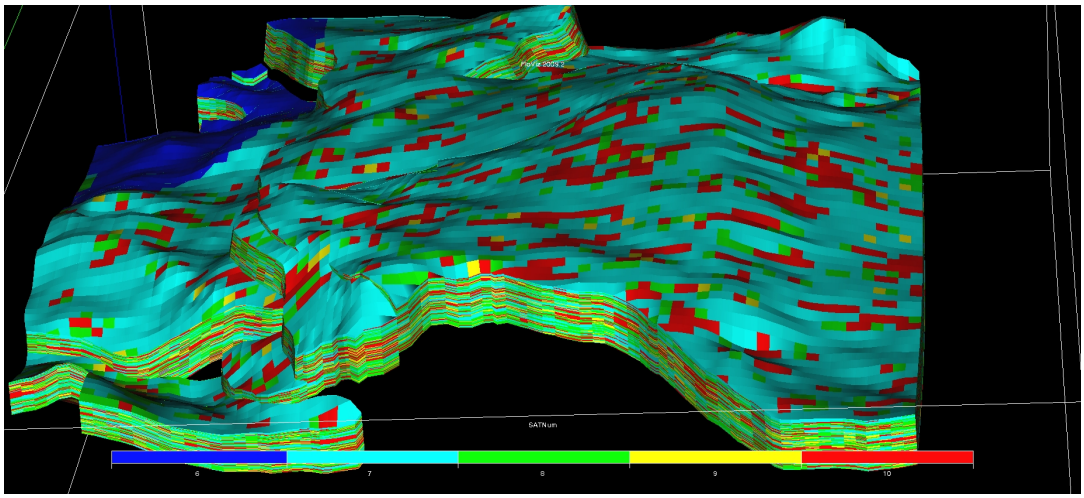

Figure 25: SATNUM allocations, top layer is layer 18. Color ranging from left to right represents SATNUM 6, 7, 8, 9 and 10, respectively

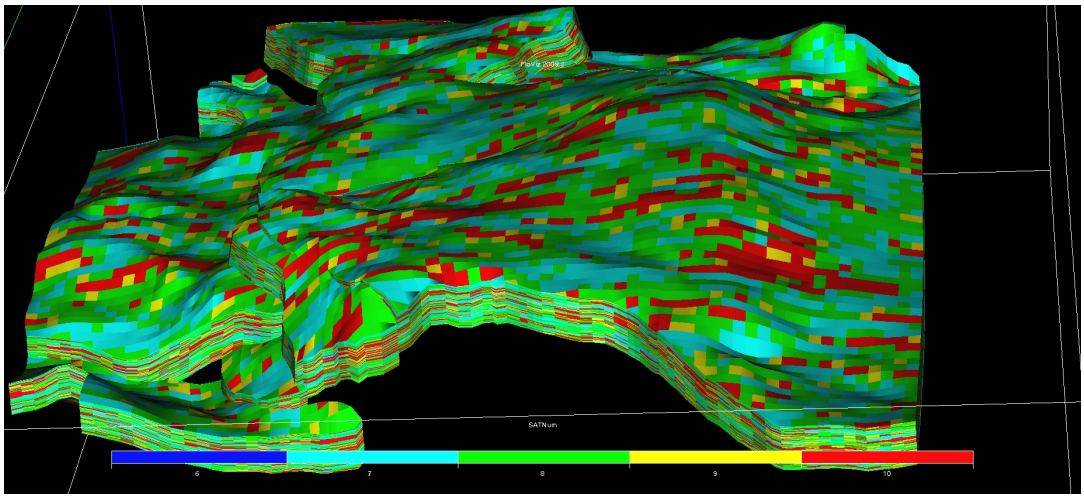

Figure 26: SATNUM allocations, top layer is layer 30. Color ranging from left to right represents SATNUM 6, 7, 8, 9 and 10, respectively

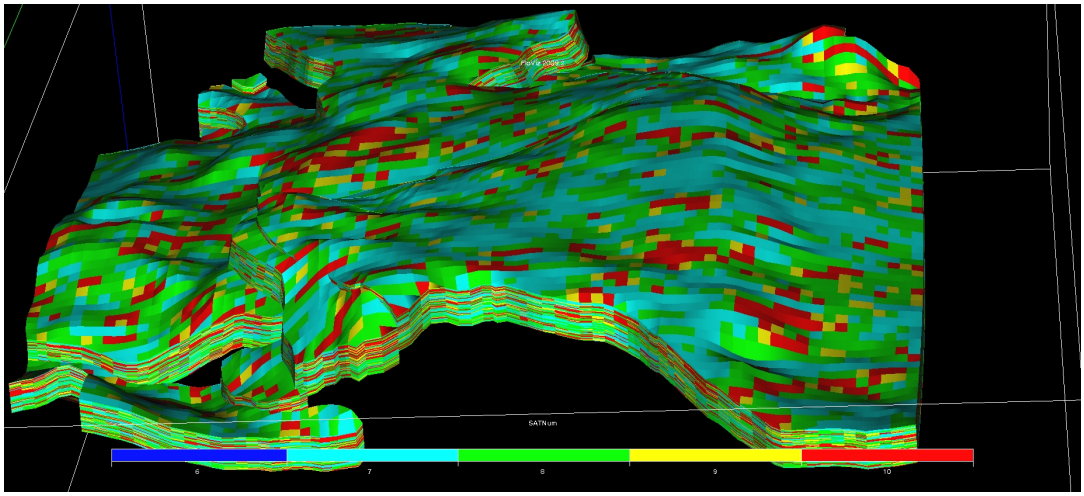

Figure 27: SATNUM allocations, top layer is layer 42. Color ranging from left to right represents SATNUM 6, 7, 8, 9 and 10, respectively

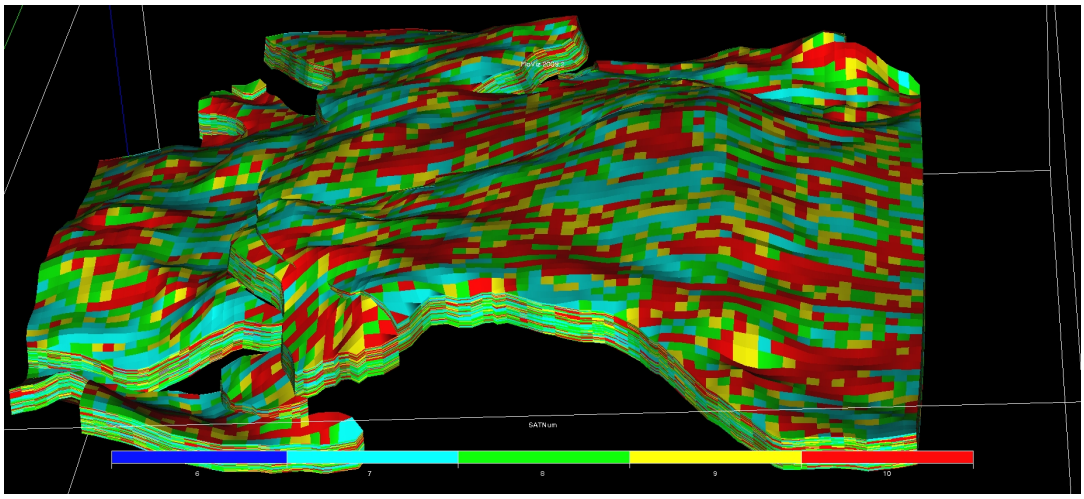

Figure 28: SATNUM allocations, top layer is layer 50. Color ranging from left to right represents SATNUM 6, 7, 8, 9 and 10, respectively

4.2.2 Fluid Description

In order to describe how and why the fluids flow and act as they do in the reservoir, they need to be characterized. The following chapter gives an outline of the fluids that are dealt with in the simulation study, and the selected equation of state for handling the different state variables.

4.2.2.1 Crude Properties

Initial surface volumes of the crude with respect to separator conditions (1 atm, 15 ^{o}C) are given below:

	Surface volume	
Oil	16.810631	M SM3
Gas	3094.230456	M SM3

Figure 29: Surface Volumes initially in-place

In reservoir conditions, initially, the oil volume is 27.56 M Rm^3. This correlates to a shrinkage factor of 1.63. The surface volume will be further used in calculating recovery factors. In reservoir simulation, having too many components would

mean requiring more computer resources without having a noticeable effect on the outcome. How many components should be used depends on the process being simulated. Normally, between 5-8 components should suffice in any reservoir process.[34] Excess components are therefore lumped together into so-called pseudo components. This simulation study is using 9 components, and are given in the table below.

Table 2: Composition of the Reservoir Crude

Component	$\mathbf{Z}_i$ **[Mole-frac.]**
CO_2	0.002398
N_2	0.015589
C_1	0.352157
C_2	0.151296
C_3	0.181475
C_4C_5	0.142502
C_6	0.061383
C_7C_{12}	0.06533
$C_{13}+$	0.02787
Total	1.00

4.2.2.2 CO_2 Properties

Isothermal CO_2 data based on Span-Wagner EOS for different reservoir pressures are given in table 3[13]. The CO_2 is supercritical at all table conditions. The table is used for illustrational purposes giving an idea of how CO_2 will behave in the reservoir. At 200-250 bar injection pressure, the CO_2 will be *denser* than the oil in place, while at pressures below 200 bar, the CO_2 will be *lighter* than the crude, at the time of injection with a reservoir pressure of 80 bar and a crude density of 500 kg/m^3.

Table 3: CO_2 Properties

Temperature (^{o}C)	**Pressure (Bar)**	**Density (kg/m^3)**	**Viscosity (cP)**
100	150	332.35	0.027785
100	200	480.53	0.03719
100	250	588.45	0.046365
100	300	661.87	0.054

4.2.2.3 CO_2-Oil Properties

From the input data of the reservoir crude at initial conditions, MMP was found from PVTsim to be 184.56 bara @ 100^{o}C reservoir temperature. Other reservoir parameters calculated are shown in the table below:

Table 4: CO_2-Oil Properties

Parameter	**Units**	
Initial reservoir pressure	bara	292
Saturation pressure	bara	177.14 (Pb)
Reservoir temperature	°C	100
First Contact MMP	bara	304.93
Critical pressure	bara	246.43
Multi Contact MMP	bara	184.56
Vaporizing Drive	%	95.36
Condensing Drive	%	4.64

4.2.2.4 Water Properties

The formation water has the following properties:

$\rho_w = 1000\ \frac{Kg}{m^3}$, $B_w = 1.0$, C_w = 4.0E-5 and $\mu_w = 0.4$ cP.

4.2.2.5 Equation of State

An equation of state, is an equation that relates pressure, volume, temperature and the amount of moles of fluids. EOS are differentiated into two main groups; phase specific EOS and cubic EOS. Phase specific EOS are equations related to single phase only, for example ideal gas law, which is a gas specific equation. Cubic EOS, however, applies to gases, liquids, fluids(combination of gas and liquid) and super-critical fluids. The main cubic EOSs used in the industry today are:

- Soave-Redlich Kwong, SRK.

- Peng-Robinson, PR.

Other alternatives that can be selected in ECLIPSE are Redlich-Kwong and Zudkevitch-Joffe. The best suited model is chosen based on experimental data for the actual reservoir. In E300 when one model is selected, this is used to obtain Z-factors and phase fugacities, to be used to find fluid densities and inter-phase equilibrium, instead of the traditional ideal gas law, PV = NRT. In this study the Soave-Redlich-Kwong, or SRK for short, is used. It is a modification of the RK EOS, and represents an attempt to take molecular geometry and polarity into account. Soave expanded the traditional RK EOS, which was only temperature dependent, to include the acentric factor as well in the functional dependency of "a". Acentric factor is a correction term to the constant "a" in the cubic equation of SRK. The term "cubic" is used due to the fact that the equation is a polynomial function of the 3rd order in the compressibility factor. (see equation 42)

In 1973 Abbott gave form to the general cubic EOS. By putting constants for θ, η, δ and ϵ, one can derive the Redlich-Kwong, Peng-Robinson, Van der Waals, Berthelot, Clausius, Wilson and Lee-Erbar-Edmister equations.[16]

$$P = \frac{RT}{\widetilde{v} - b} - \frac{\theta(\widetilde{v} - \eta)}{(\widetilde{v} - b)(\widetilde{v}^2 + \delta\widetilde{v} + \epsilon)} \tag{46}$$

To derive RK:

$$\theta = \frac{a}{T^{\frac{1}{2}}},$$

$$\eta = b$$

,

$$\delta = b,$$

$$\epsilon = o,$$

Which then results in the Redlich-Kwong equation:

$$P = \frac{RT}{\widetilde{v} - b} - \frac{a}{\sqrt{T}\widetilde{v}(\widetilde{v} + b)}$$

Soave modified this expression by replacing the temperature term with a more complex temperature-dependent expression, resulting in:

$$(P + \frac{\alpha a}{\widetilde{v}(\widetilde{v} + b)})(\widetilde{v} - b) = RT \tag{47}$$

$$\text{where } a = a(T, \omega) = \alpha - \gamma T^{-1.5}$$

and

$$\alpha = (1 + (0.48508 + 1.55171\omega - 0.15613\omega^2)(1 - \sqrt{T_r})^2$$

The constants a and b are,

$$a = 0.427480\frac{R^2(T_c)^2}{P_c}$$

$$b = 0.086640\frac{R^2(T_c)^2}{P_c}$$

The cubic form of the equation is introduced in the compressibility factor by defining A and B:

$$A = \frac{\alpha a P}{R^2 T^2}$$

$$B = \frac{bP}{RT}$$

$$Z = \frac{P\widetilde{v}}{RT}$$

Which results in the cubic equation[2]:

$$Z^3 - Z^2 + (A - B - B^2)Z - AB = 0 \tag{48}$$

Soave added a small modification for mixtures by introducing the "binary interaction parameters", k_{ij}.

$$(\alpha a)_m = \sum\sum y_i y_j (\alpha a)_{ij}; (\alpha a)ij = \sqrt{(\alpha a)_i (\alpha a)_j}(1 - k_{ij}), \tag{49}$$

$$b_m = \sum_i y_i b_i$$

The binary interaction parameter (BIP) is an additional term that takes into account the interaction between molecules, and is used to accurately obtain the partitions of the compositions in the different phases. The BIP parameters are different for different EOS. SRK and PR EOS calculates the vapor densities with very good accuracy, however, the liquid density calculated from these two deviates. In order to correct this deviation, Peneloux introduced volume translation, which shifts the whole curve slightly towards the liquid pressure. Consider a case where experimental data, at given pressure and temperature, gives a molecular volume equal to 0.8 at the liquid pressure and 50 at the vapor pressure. However, the EOS calculates the liquid and vapor pressure, and results in $\widetilde{v}$ to be 1 and 50, for their respective phase pressures. By subtracting 0.2, this would pretty much equal the experimental data. This is the so-called volume translation, and is represented as a constant, C_i. The volume-shift has very little influence on the vapor pressure, due to the fact that at the vapor pressure the $\widetilde{v}$ is much higher than it is for liquid pressure. Subtracting 0.2 from e.g. 50 (in this case) is only a 0.4 % deviation from the actual value, and can be neglected. However, a subtraction of 0.2 from 1 is quite significant. The result of the volume translation and BIPs is that for a given set of data it is possible to get an equally good approximation with either SRK or the PR equation of state.[34]

$\mathrm{SRK}((\mathrm{C}_i)^{SRK}),(\mathrm{k}_{ij})^{SRK}) \simeq \mathrm{PR}((\mathrm{C}_i)^{PR}),(\mathrm{k}_{ij})^{PR})$

4.3 Traditional Saturation Functions

The old model consisted of only gas-oil drainage curves and water-oil imbibition curves. The curves are only accurate if the simulation study is based on depletion only, where the saturation generally changes through one direction. Gas-oil drainage will occur at the top of the reservoir and water-oil imbibition at the OWC as the pressure drops. However, in addition to this there seems to be faults in the curves resulting from scaling. (Fig.30). In order to simulate different injection processes with a realistic outcome, new relative permeability- and capillary pressure curves need to be employed. Corey correlation was used to develop new two-phase relative permeability curves. The following section contains how the different relative permeability curves were derived, and a graphical overview of one of 5 rock types. The rest are given in appendix A.

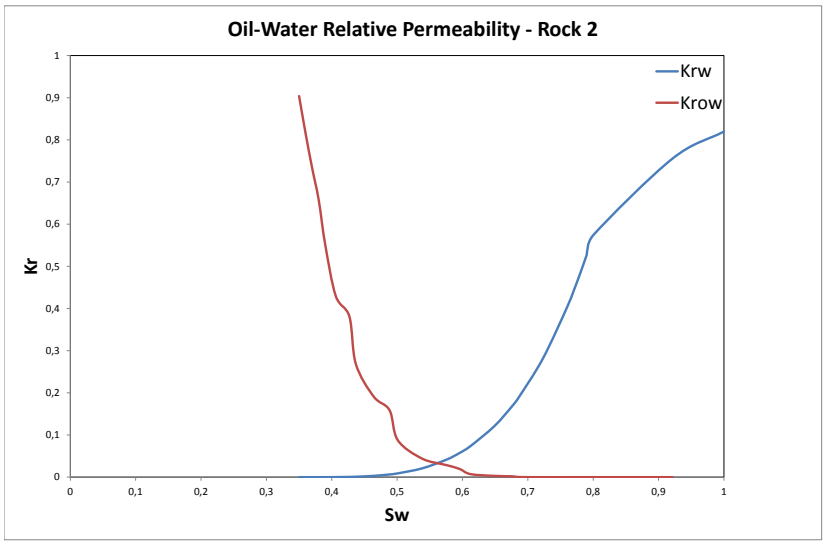

Figure 30: Old Oil-Water Imbibition Curve, Rock type 2.

4.3.1 Gas-Oil Relative permeability Curves

From this point on the saturation processes related to the gas-oil functions will be referred to as increasing gas saturation, indicated by subscript i, and decreasing gas saturation, indicated by subscript d. Given data to generate G-O relative permeability curves are tabulated below.

Table 5: Gas-Oil Relative permeability data

Rock Type	$\mathbf{S}_{wir}$	$\mathbf{S}_{gt}$	$\mathbf{S}_{gc}$	$\mathbf{S}_{org}$	$\mathbf{K}_{rog}(\mathbf{S}_{gt})$	$\mathbf{No}_d$	$\mathbf{No}_i$	$\mathbf{Ng}_d$	$\mathbf{Ng}_i$
1	0,2	0,3	0,035	0,2	0,069	3,8	3,2	1,7	1,6
1B	0,285	0,3	0,035	0,18	0,069	3,2	3,5	1,3	1,4
2	0,35	0,3	0,035	0,15	0,069	2,8	3,5	1,3	1,3
3	0,5	0,28	0,035	0,06	0,069	2,6	3,5	1,1	1,3
4	0,654	0,22	0,035	0,05	0,069	1,9	3	1,3	1,5

For the gas-oil curves, 4 equations were used. Since the experiments were conducted with an irreducible water saturation present, this needs to be accounted for in the calculations.

$$S_{on} = \frac{1 - S_g - S_{or}}{1 - S_{wir} - S_{or}}$$

$$S_{gn} = \frac{S_g - S_{gc}}{1 - S_{wir} - S_{org} - S_{gc}}$$

$$K_{ro} = S_{on}^{N_{o,p}} = (1 - S_{gn})^{N_{o,p}}$$

$$K_{rg} = S_{gn}^{N_{g,p}}$$

Where the subscript p represents the process direction, increasing or decreasing saturation of gas. In ECLIPSE the relative permeability inputs are not supposed to be in normalized saturations, so the equations need to be modified with regards to gas saturation and the end-points for the given process. The gas drainage curves have end-points at critical gas saturation, S_{gc} when $K_{rg} = 0$, which is used for increasing gas saturation. For decreasing saturation the process goes from irreducible water saturation to trapped gas saturation, S_{gt}. The equations for the respective processes

are:

$$S_{g,i} = S_{gn}(1 - S_{wir} - S_{gc}) + S_{gc} \tag{50}$$

where the normalized saturation ranges from 0 to 1. For the decreasing process, the gas curve end-points will be $K_{rg} = 0$ at $S_g = S_{gt}$, trapped gas saturation, and $K_{rg} = 1$ at $S_g = 1$ - S_{wir}.

$$S_{gn} = \frac{S_g - S_{gt}}{1 - S_{wir} - S_{gt}}$$

$$S_{g,d} = S_{gn}(1 - S_{wir} - S_{gt}) + S_{gt} \tag{51}$$

The gas saturations are then plotted against their corresponding K_{rg} values calculated from equation 50 and 51.

For the oil curves, the saturations are the same regardless of the process, and do not need to be transformed here. The relative permeability values changes due to different exponents.

$$S_{on} = \frac{1 - S_g - S_{or} - S_{wir}}{1 - S_{wir} - S_{org}} = 1 - S_{gn}$$

$$-S_{g,i/d} = (1 - S_{gn})(1 - S_{wir} - S_{org}) + S_{org} - 1 + S_{wir}$$

Which reduces to

$$S_{g,i/d} = S_{gn}(1 - S_{org} - S_{wir}) \tag{52}$$

The values are then plotted against the corresponding K_{ro} values. It is important to note that when the curves are implemented into ECLIPSE, the curves need to be enclosed into smooth loops in order to avoid errors when generating scanning curves. Even though the K_{ro} imbibition curves break off and becomes constant at trapped gas saturation, when inputting in ECLIPSE they will need to follow a smooth trend all the way to $S_g = 0$.

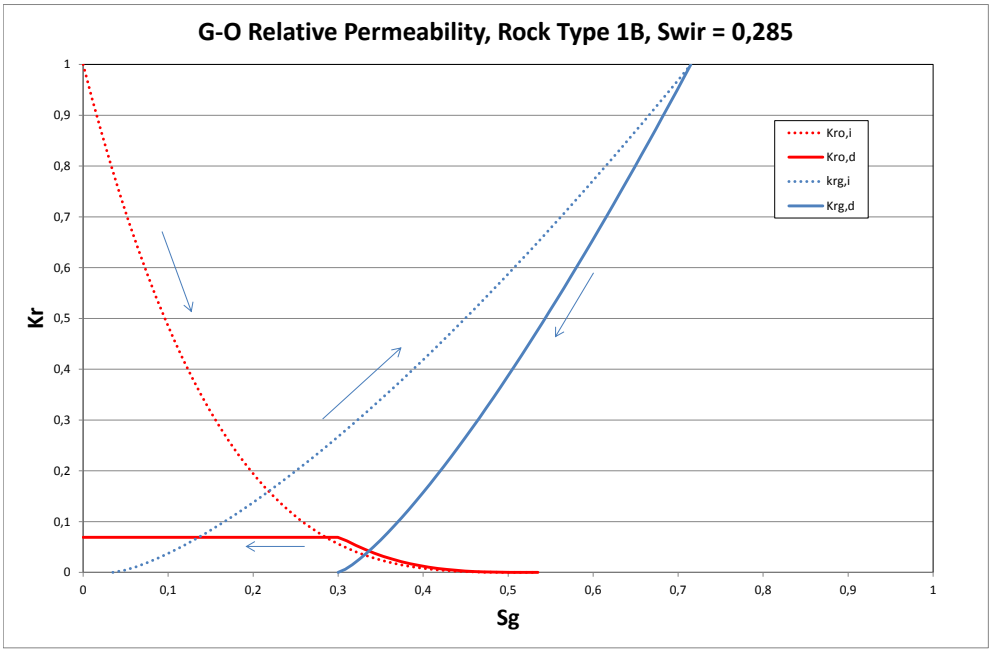

Figure 31: Gas-oil relative permeability, Rocktype 1B

4.3.2 Water-Oil Relative permeability Curves

The experimental data are given below.

Table 6: Water-Oil Relative permeability data

Rock Type	$\mathbf{S}_{wir}$	$\mathbf{S}_{orw}$	$\mathbf{K}_{rw}(\mathbf{S}_{orw})$	$\mathbf{No}_{imb}$	$\mathbf{No}_{dr}$	$\mathbf{Nw}_{imb}$	$\mathbf{Nw}_{dr}$
1	0,2	0,2	0,7	4,5	1,85	3,8	4
1B	0,285	0,2	0,7	4,5	1,5	3,8	3,5
2	0,35	0,2	0,7	4,5	1,5	3,8	3,5
3	0,5	0,2	0,7	4,5	1,5	3,8	3,5
4	0,654	0,2	0,7	4,5	1,5	3,8	3,5

The same principle used for the gas-oil curves is applied for the water-oil relative permeability curves. However, other equations have been used. With the basis in normalized saturation, and considering that normalized saturations cannot be used as input data in ECLIPSE, the equations are therefore modified. The process is either drainage with subscript dr, or imbibition with subscript imb, for decreasing and increasing water saturation, respectively.

End-point data for drainage are: $K_{rw} = 1$ at $S_w = 1$, and $K_{rw} = 0$ at $S_w =$ at S_{wir} Saturations are calculated as follows:

$$S_{wn} = \frac{S_{w,dr} - S_{wir}}{1 - S_{wir}}$$

$$S_{w,dr} = S_{wn}(1 - S_{wir}) + S_{wir} \tag{53}$$

where the normalized saturation ranges from 0 to 1. The imbibition end-points are: $K_{rw} = K_{rw}(S_{orw})$ at $S_w = 1\text{-}S_{orw}$, and $K_{rw} = 0$ at $S_w = S_{wir}$, the equation becomes:

$$S_{wn} = \frac{S_{w,imb} - S_{wir}}{1 - S_{wir} - S_{orw}}$$

Modified with regards to $S_{w,imb}$ it becomes:

$$S_{w,imb} = S_{wn}(1 - S_{wir} - S_{orw}) + S_{wir} \tag{54}$$

The corresponding relative permeabilities are calculated through:

$$K_{ro,p} = S_{on}^{N_{o,p}} = (1 - S_{wn})^{N_{o,p}} \tag{55}$$

$$K_{rw,p} = S_{wn}^{N_{w,p}} \tag{56}$$

The end-point data need to be connected to a closed loop to avoid errors in ECLIPSE here as well. For instance, the imbibition end-point needs to be connected to the drainage start-point at $S_w = 1$.

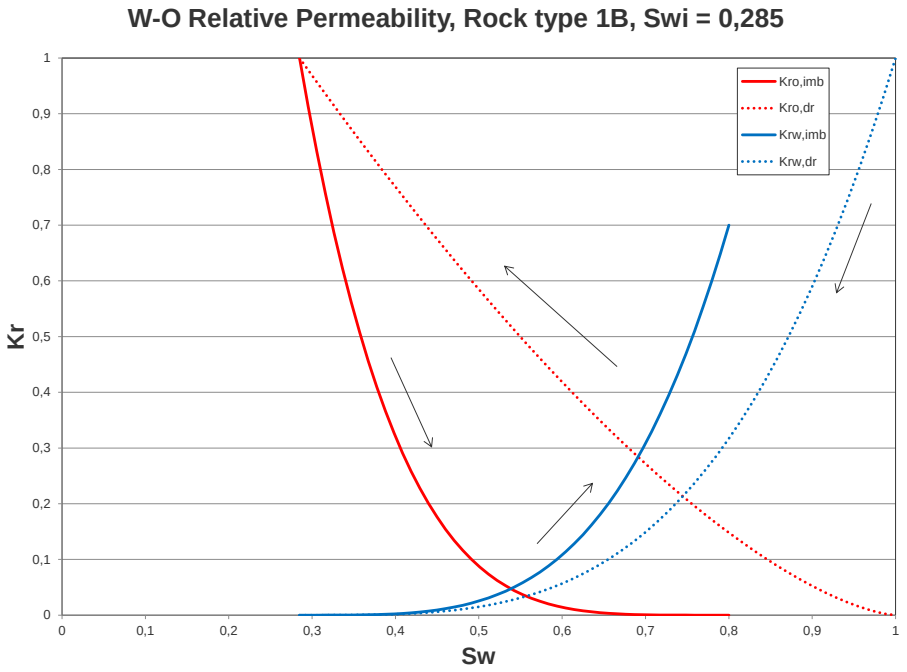

Figure 32: Oil-water relative permeability, Rocktype 1B

4.3.3 Capillary Pressure Curves

The capillary pressure curves for the gas-oil data can be calculated based on:

$$P_{cog} = \frac{\sigma_{og}}{\sigma_{ow}} P_{cow} \tag{57}$$

However, since the interfacial tension of oil-gas is just a small fraction compared to oil-water, P_{cog} is approximated to 0. The oil-water capillary pressure curves are given in Fig.33 where pp and sp are drainage and imbibition process, respectively.

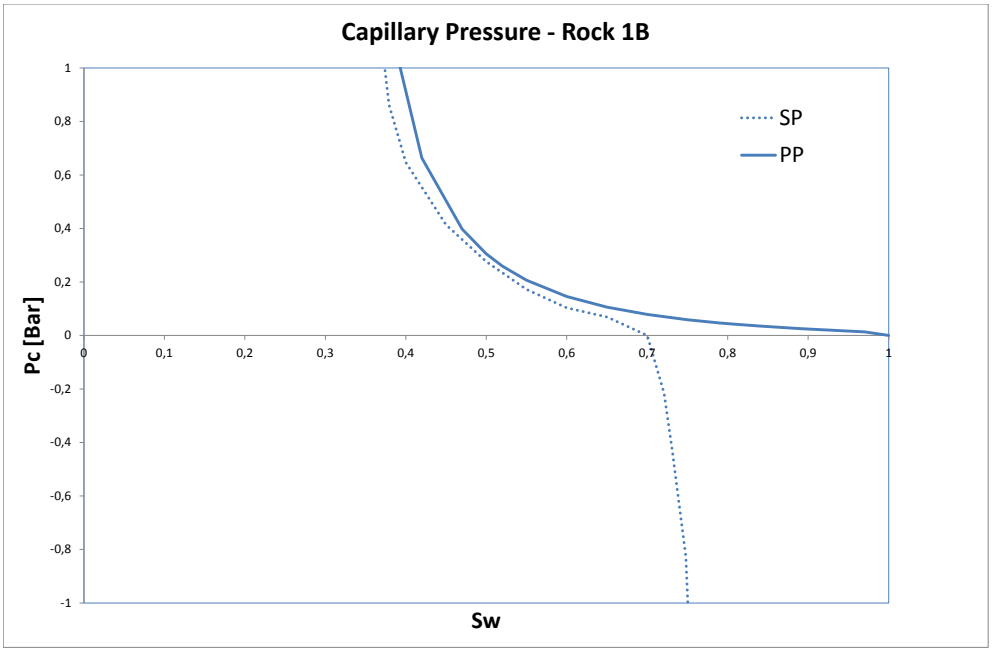

Figure 33: Oil-water capillary pressure, Rocktype 1B. Solid line represents primary drainage, while dashed line represents imbibition.

4.4 ODD3P Saturation Functions

The ODD3P model option in ECLIPSE requires a different type of saturation function input compared to the traditional models. This is due to the fact that each phase is a function of its own saturation without a third phase present. Only a slight modification is needed to transform the traditional data into ODD3P data. Water-oil data is the same, however, gas-oil data need to be converted from an initial S_{wir} = Constant, to 0. In order to do that one can either convert the data with regards to the constant gas lines or the constant oil lines.

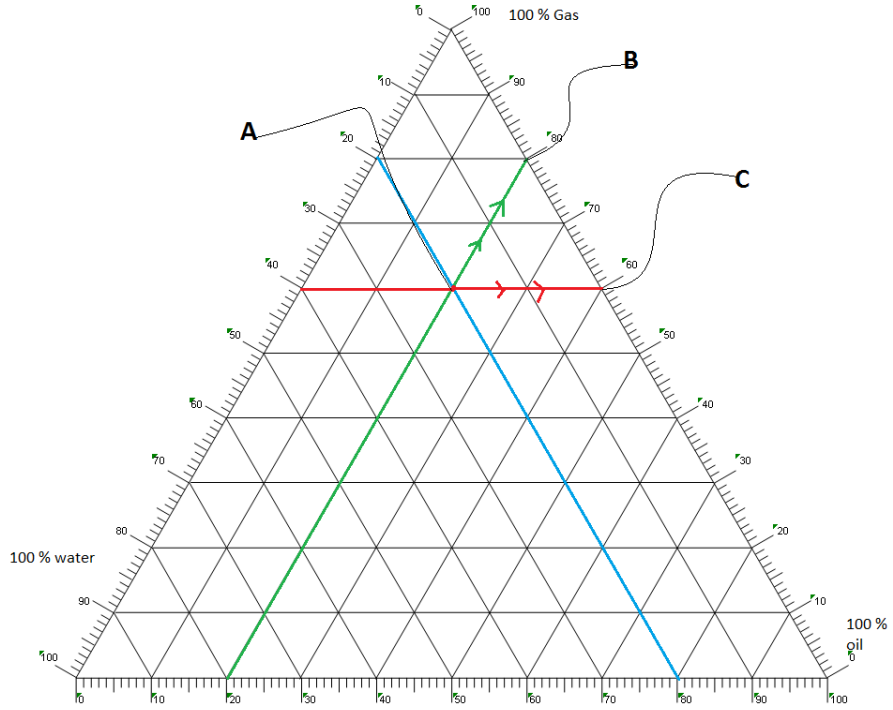

Figure 34: Ternary representation of traditional data conversion. S_{wir} = 0.2 and S_{org} = 0.2.

From Fig.34 this particular example considers S_{wir} = 0.2 and S_{org} = 0.2, representing rock type 1. The blue line represents conditions where on every point along the axis the water saturation is constant. That is, representing Stone's models and default model data input. The green line represents constant oil saturation values, while the red represents gas. The intersection of all the lines is the S_{org} of the sys-

tem at irreducible water saturation. There are a couple of ways of transforming the traditional data. As illustrated above, one can either follow the green line (A to B) or the red line (A to C), this is done to ensure end-point consistency. By converting the data along the constant gas-lines this results in a new system with a relatively high residual oil saturation. In this case the transformation of S_{org} becomes 0.4. As the irreducible water saturation increases the transformation of the residual oil saturation in the gas-oil system becomes more and more pessimistic. Experimental data has shown that $S_{g,max}$ is much higher than 1-S_{wir}-S_{org}[12]. A transformation along the constant oil-lines will therefore represent a more realistic behavior than a transformation along the constant gas-lines. In this study both transformations will be done to illustrate the difference between the two.

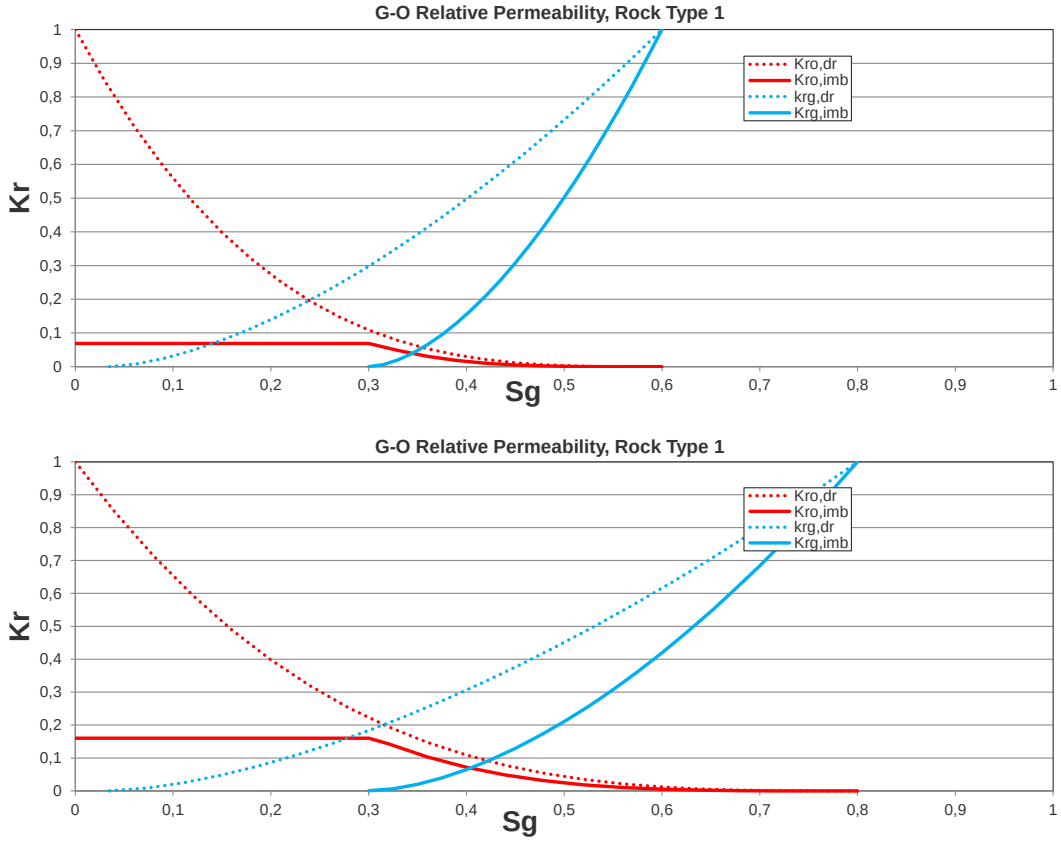

Figure 35: Transformed data, along gas-lines (top), along oil-lines (bottom).

From Fig.35 the differences between the two methods of transforming the data can be observed. Note that at S_{gt} the relative oil permeability has been modified as well. This is due to the fact that the saturation of mobile oil is much larger at the trapped gas saturation compared to the other method. From Fig.36 the two ways of transforming traditional data have been plotted in a single diagram. It is important to note the hysteresis end-points from the two transformations. The differences will have a significant impact on two-phase relative permeability calculations at high gas saturations.

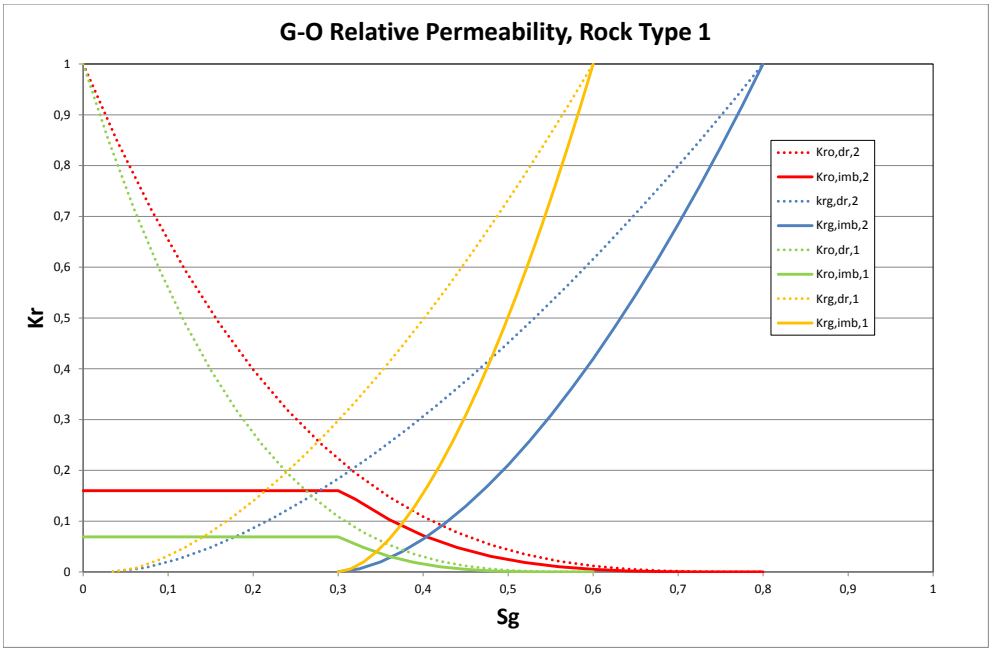

Figure 36: Transformed data, along gas-lines (green and yellow), along oil-lines (red and blue).

Gas-oil capillary pressure curves were calculated through:

$$P_{cog} = \frac{\sigma_{og}}{\sigma_{ow}} P_{cow} \tag{58}$$

Fig.37 represents one of five data sets of relative permeability and capillary pressure curves used in the field model (transformed along the oil-lines). For the simulation setup of ODD3P IPCFN was set to 0 with no K_r scaling in order to get a valid comparison between the other three-phase models. Note that from Fig.37 the tertiary data is equal to the secondary data. Since gas injection mainly influences one direction, ISTNUM = DSTNUM (no hysteresis after primary displacement process) is a reasonable approximation.

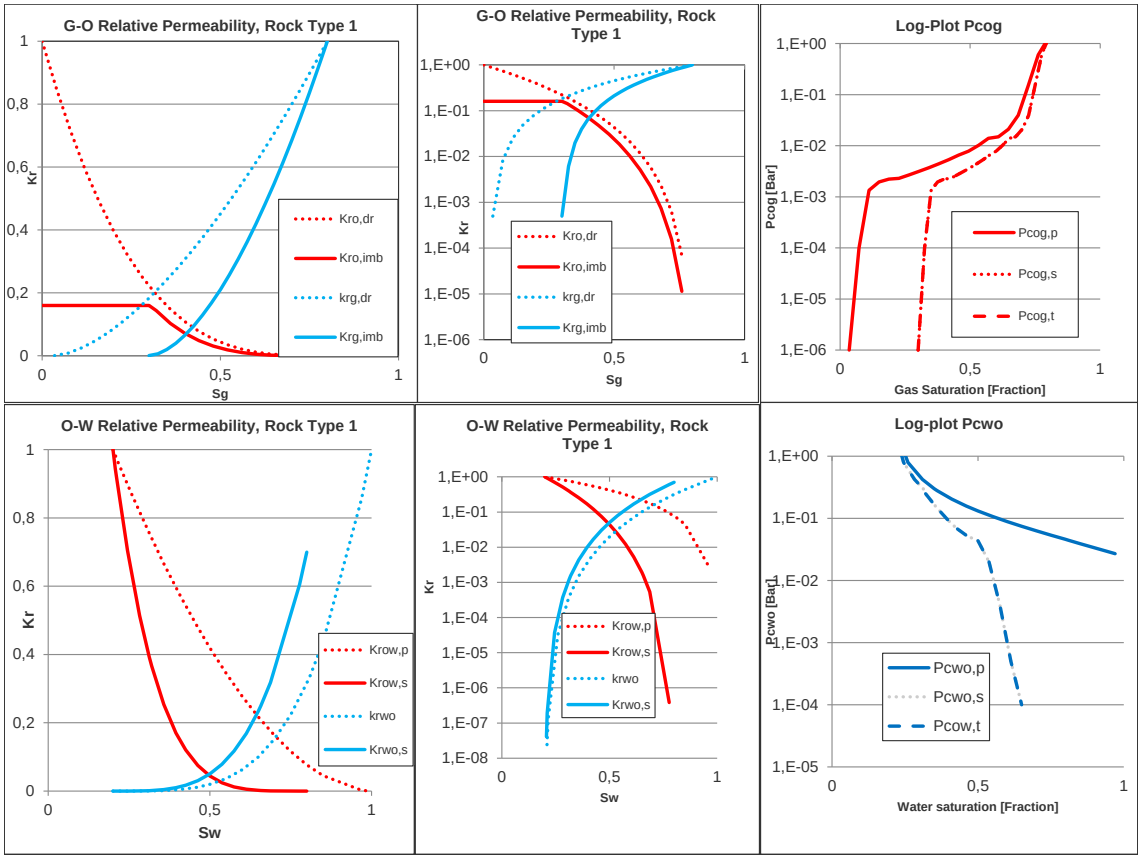

Figure 37: Rock type 1 data set for ODD3P.

4.5 Workflow and Assumptions

The new curves have been implemented into the field model, and are ready to be run in ECLIPSE. A list is shown below of the different variables which can be changed in in the simulation study.

1. Relative permeabilities
2. Injection Processes
3. Hysteresis methods
4. Pressure steps
5. Results

Within each option exist several possibilities. In the relative permeability case there are old relative permeabilities (no hysteresis select) and new relative permeabilities (hysteresis select). Injection processes are divided into gas-injection, WAG, simultaneous-water-and-gas (SWAG) and water-injection. Hysteresis methods are divided into: Carlson's method, Killough's method and Jargon's method for non-wetting phase, and drainage, imbibition and Killough for wetting phase. For each option the simulation scenarios multiply by the amount of options available. It is therefore important to make a reference case. Since this study revolves around CO_2-injection, this will be the chosen reference process. Choice of reference hysteresis model is based on following assumptions:

• The relative permeability curves represent a typical water-wet system which is being translated into this system.

• During injection of gas, saturation of non-wetting phase will increase. Therefore drainage curves will be used for modelling hysteresis in the wetting phase.

• Choice of hysteresis method for the non-wetting phase is Killough's method, due to the fact that this model is based on approaching real, physical data[14]. Carlson's method is based on moving the imbibition curve, and Jargon's method is based on a scaling method. It is important to note that the latter method is unpublished so one should be careful when employing such a method in the model. The reason is that there are little scientific proof of the model's validity.

• The pressure interval chosen for the gas-injection cases are such that immiscible injection and miscible injection are taken into account. Based on data from PVTsim the BHP control node for the injection well will be set to 150 bar, 190 bar and 310 for immiscible, multi-contact and first contact drive, respectively.

• The injection well location is fixed and assumed to be the most optimal choice. It is a horizontal dog-leg well located right above the OWC. The limitations put on the producer are: 15 bar tubing head pressure and 300 Sm^3/D water production rate.

5 Results and Observations

Results and observations done through the simulation study are given in this section. It is important to note that all simulation runs are done with P_c turned off. The effect of the simulation study considers K_r hysteresis only, due to the fact that by enabling capillary pressure required an excessive amount of computational resources.

5.1 No Hysteresis Select

For the "No Hysteresis Select" a new basecase was made. Fig.38 is a comparison of the implemented curves (black) and already employed curves (red line). Since these cases are depletion only, gas-oil drainage curves and water-oil imbibition curves were used. The differences are due to different relative permeability curves, causing mobility changes of the fluids in the reservoir.

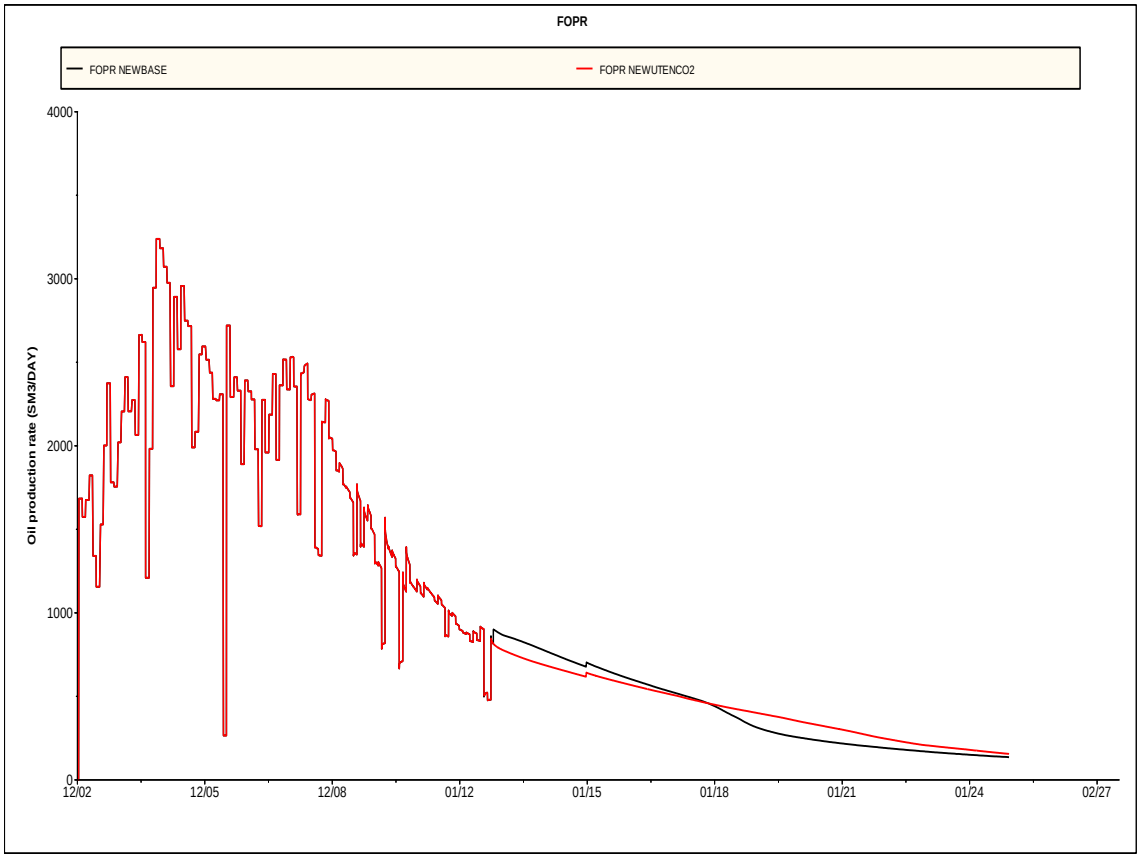

Figure 38: New (black line) and old (red line) depletion case, FOPR vs time

5.1.1 CO_2-Injection

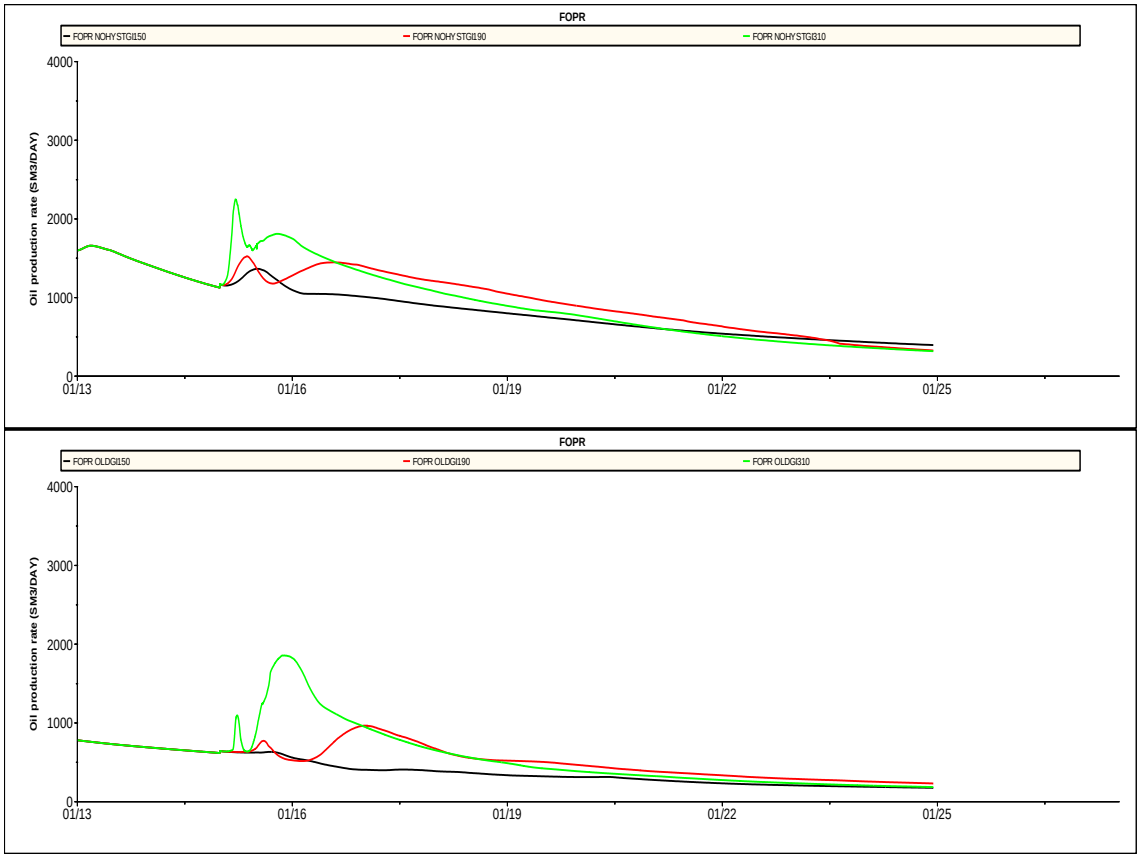

Figure 39: New curves (top) and old curves (bottom). FOPR vs time for 150,190 and 310 bar.

From Fig.39 it can be seen that by implementing the new curves give an upward shift in FOPR. The difference between the two cases is that drainage gas-oil and water-oil curves are used for the curves shown in the top graph. For the lower graph, the old gas-oil drainage and water-oil imbibition curves are used. The effect of this is further discussed in section 6.1.1

5.2 Hysteresis Select

5.2.1 Hysteresis vs No hysteresis

In order to get a valid comparison of no hysteresis versus hysteresis, the saturation point of origin in the relative permeability curves should be approximately the same. The old relative permeabilities will therefore be compared with the hysteresis select cases, where the point of origin is at the imbibition curve and not the drainage curve. Fig.40,41 and 42 show the difference between CO_2-injection at 150,190 and 310 bar, respectively. The trend appearing from all the figures is that water production is at a constant lower level in the case of hysteresis, which in turn results in higher oil production.

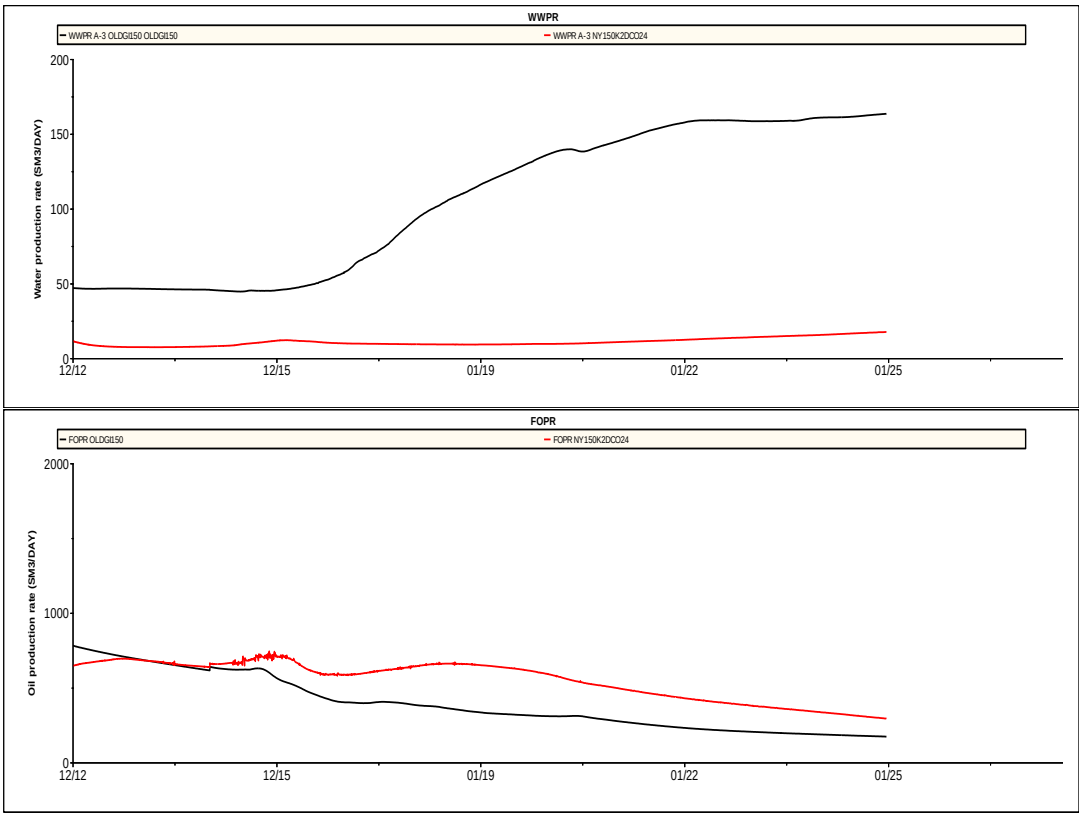

Figure 40: Upper graph (WWPR) and lower graph (FOPR) showing GI hysteresis (red line) and GI without hysteresis (black line) at 150 bar.

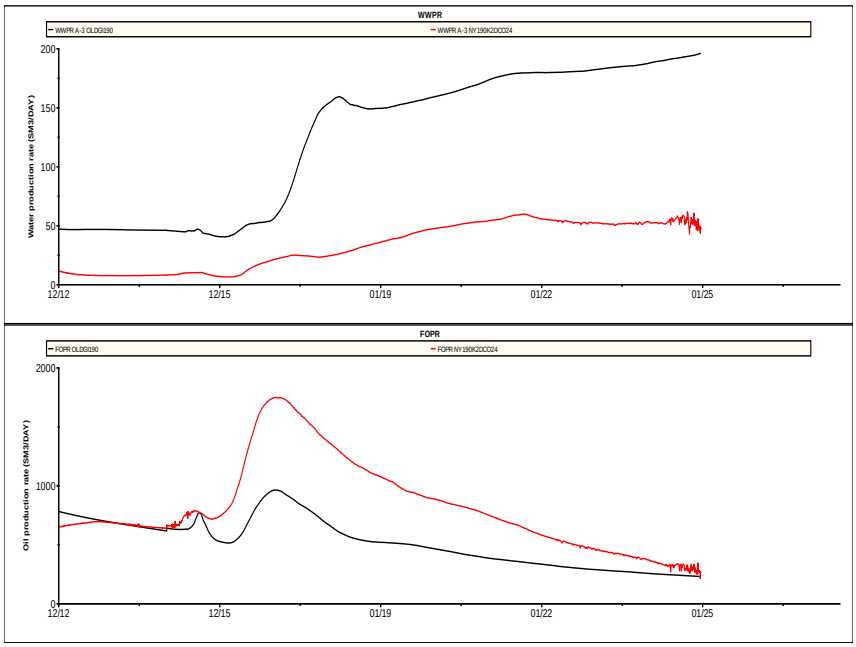

Figure 41: Upper graph (WWPR) and lower graph (FOPR) showing GI hysteresis (red line) and GI without hysteresis (black line) at 190 bar.

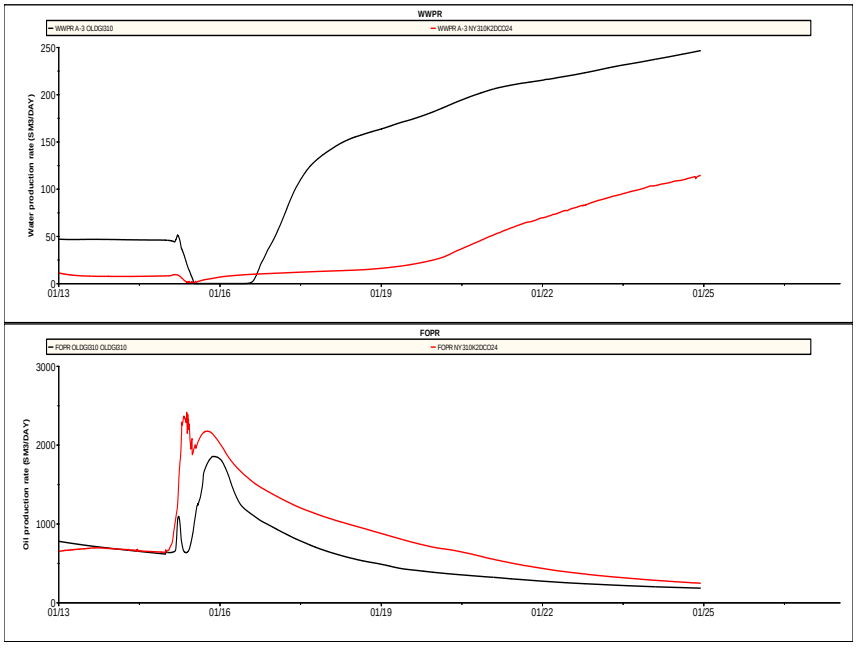

Figure 42: Upper graph (WWPR) and lower graph (FOPR) showing GI hysteresis (red line) and GI without hysteresis (black line) at 310 bar.

5.2.2 Immiscible vs Miscible CO_2-Injection

Fig.43 and 44 show the FOPR and FOPT, respectively, by different BHP control modes. The black line is the basecase without hysteresis, but with implemented corey curves. Red, green and blue lines represent a BHP injection control of 150, 190 and 310 bars. It is important to note the multi-contact miscible case (green line) where oscillations can be observed within the predicted data. This is due to convergence problems, and will be commented in the discussion section.

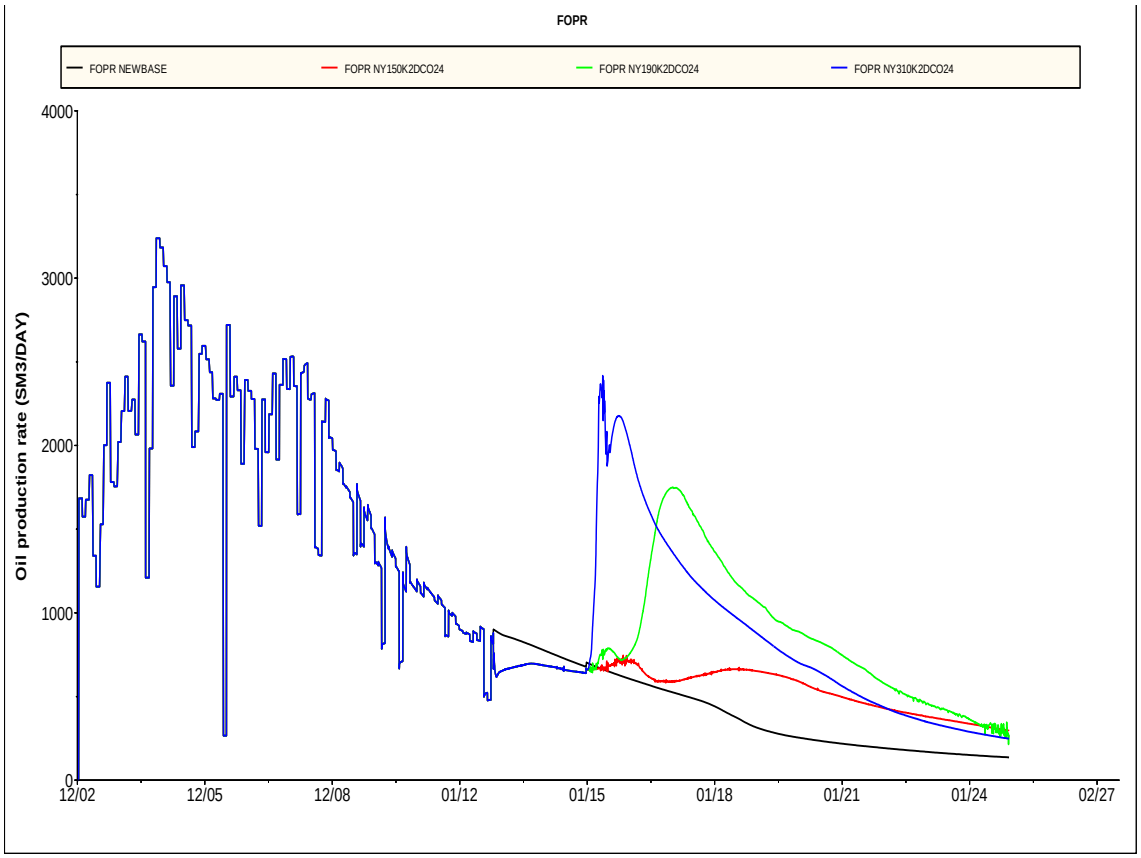

Figure 43: FOPR vs time

The main observation from the different graphs in Fig.43 is that maximum FOPT is obtained at 190 bar. By increasing the CO_2 injected, an increase in FOPR at an earlier stage is achieved, however, ultimate FOPT stays approximately the same at the end of the predicted period. The CO_2 amount required (Fig.45) to maintain the injection BHP target is 2.250.000 Sm^3 for 190 bar vs 10.000.000 Sm^3 for 310 bar, initially. After a certain period of time the required amount of CO_2 needed to maintain BHP drops due to development of a gas channel between the injector and producer. When this happens, less volume of CO_2 is needed to maintain the BHP.

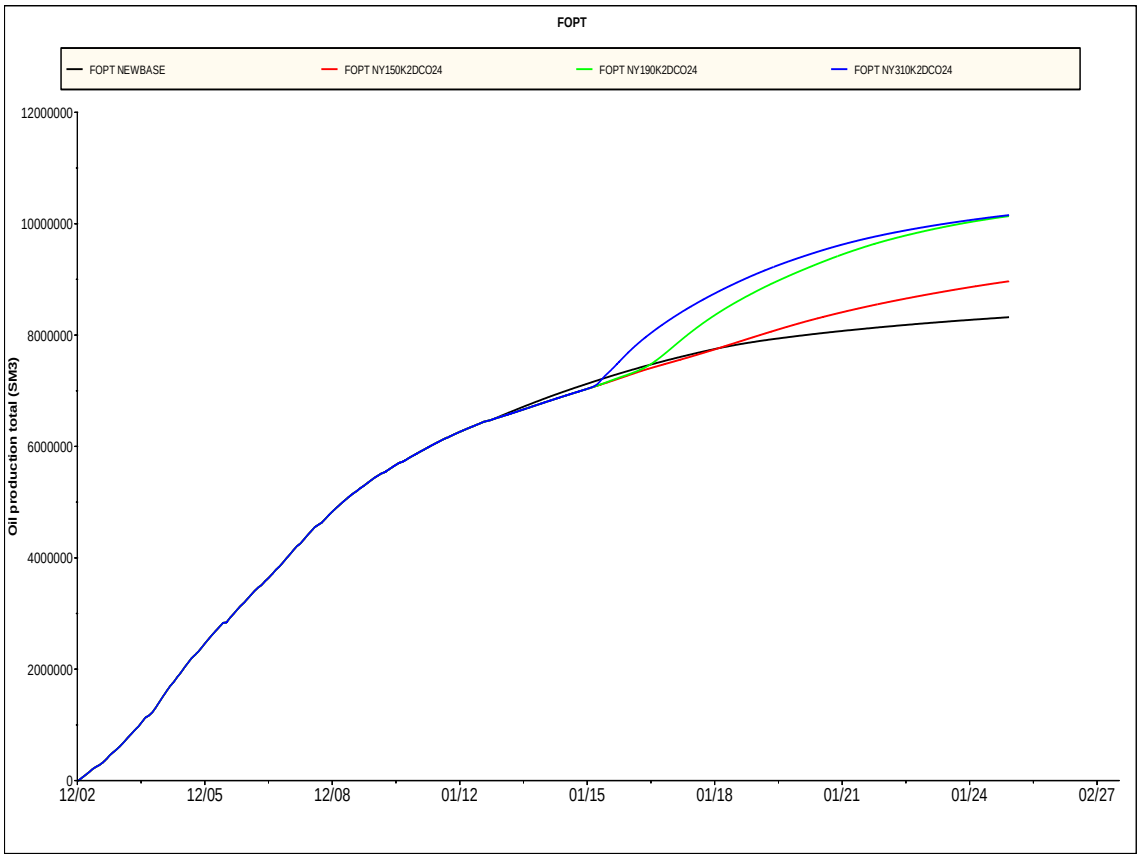

Figure 44: FOPT vs time

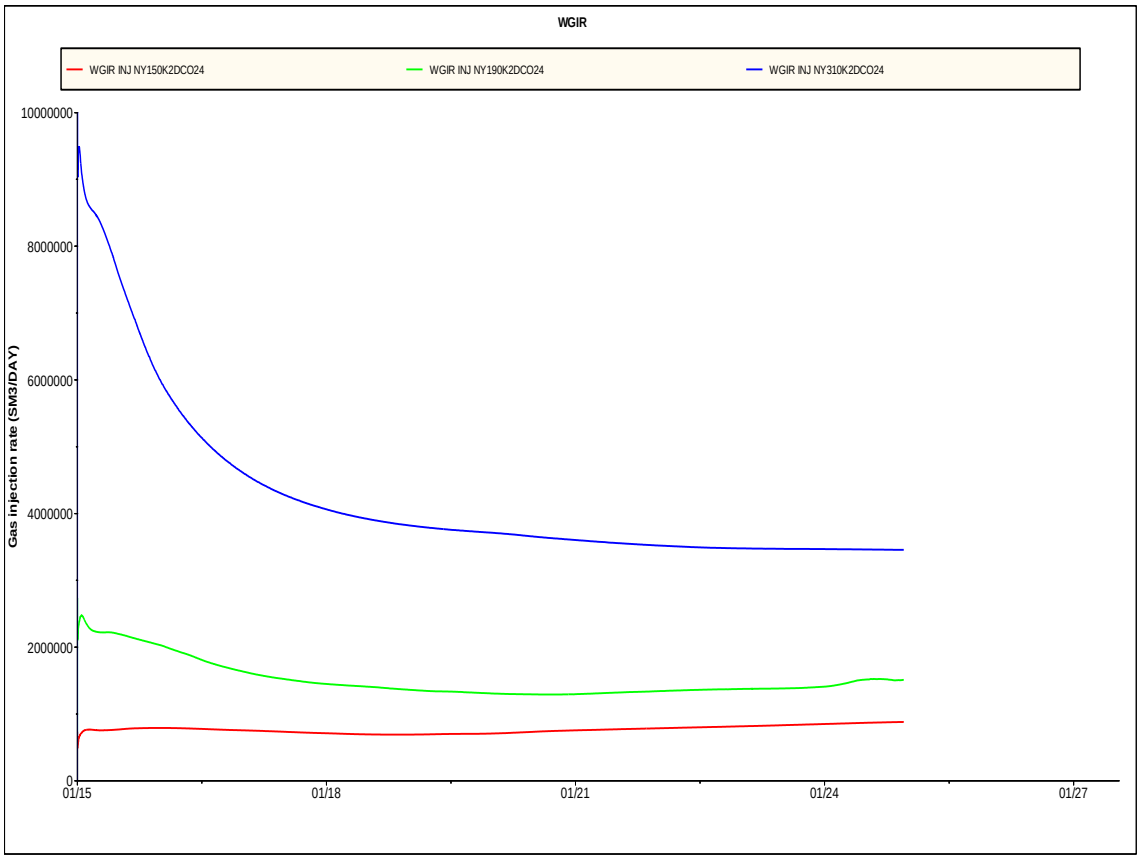

Figure 45: CO_2 Injected vs time

5.2.3 Non-wetting Hysteresis Methods

Injecting at 190 and 310 bar caused alot of instability and convergence problems for the simulator. These cases are omitted for comparison due to the fact that severe instability issues causes inconsistent relative permeabilities, and will therefore not give a representative picture of how it is in reality. (Further discussed in section 6.1.3) Immiscible cases were on this basis chosen for further comparison.

Killough, Jargon and Carlson's methods for handling hysteresis are different, and have been studied earlier in what ways they differ. In the field related simulation study it can be seen from the FOPR the differences in the hysteresis methods. From Fig.46 Carlson's method is the most optimistic model in handling hysteresis, while Killough's method is the least optimistic.

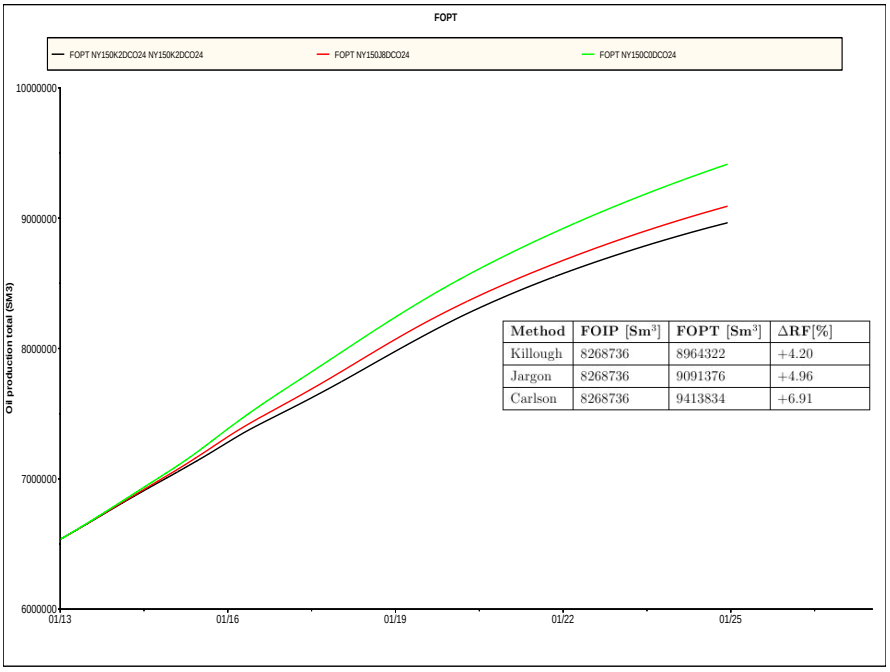

Method	FOIP [Sm^3]	FOPT [Sm^3]	ΔRF[%]
Killough	8268736	8964322	+4.20
Jargon	8268736	9091376	+4.96
Carlson	8268736	9413834	+6.91

Figure 46: Killough's (black), Carlson's (green) and Jargon's (red) method for handling hysteresis giving an additional RF of 4.20, 4.96 and 6.91 %, respectively.

From Fig.46, it can be seen that the outcome of the different hysteresis methods is noticeably big with regards to FOPT. FOIP represents field produced total initially without hysteresis.(GI basecase)

5.3 Flow Pattern

5.3.1 Immiscible CO_2-Injection

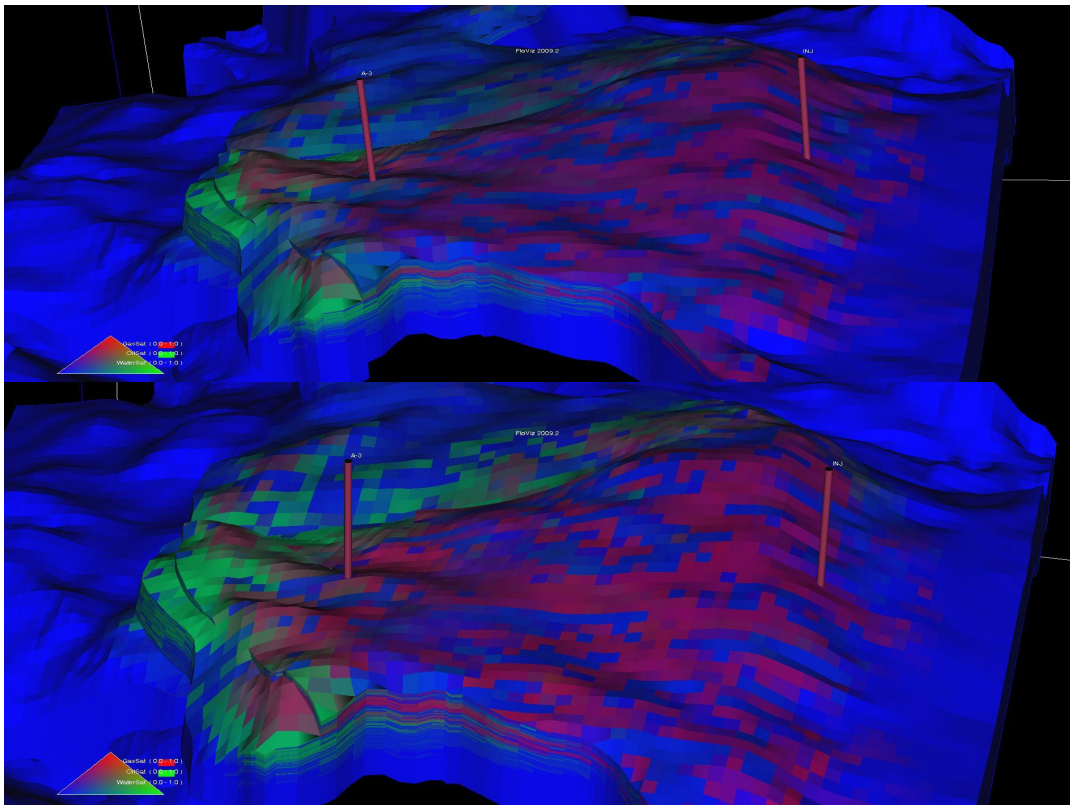

Figure 47: Layer 10.

Fig.47 is used for illustrational purposes to point out differences in the flow pattern of the injection fluid without hysteresis(upper) and with hysteresis selected(lower). The figure represents layer 10 in the reservoir model containing a SATNUM of mainly 6 and 7 at the end of predicted period. With the same well conditions it can be seen from Fig.47 that fluid saturations are different throughout the reservoir, where red is gas saturation, green is oil saturation and blue is water saturation. The sweep efficiency is somewhat different, however, the same high permeable blocks are mainly contributing to transporting the injection fluid. It is important to note that with hysteresis enabled the saturation of gas in the reservoir becomes higher compared to the model without hysteresis enabled. Ultimately increasing oil prediction.

5.3.2 Miscible CO_2-Injection

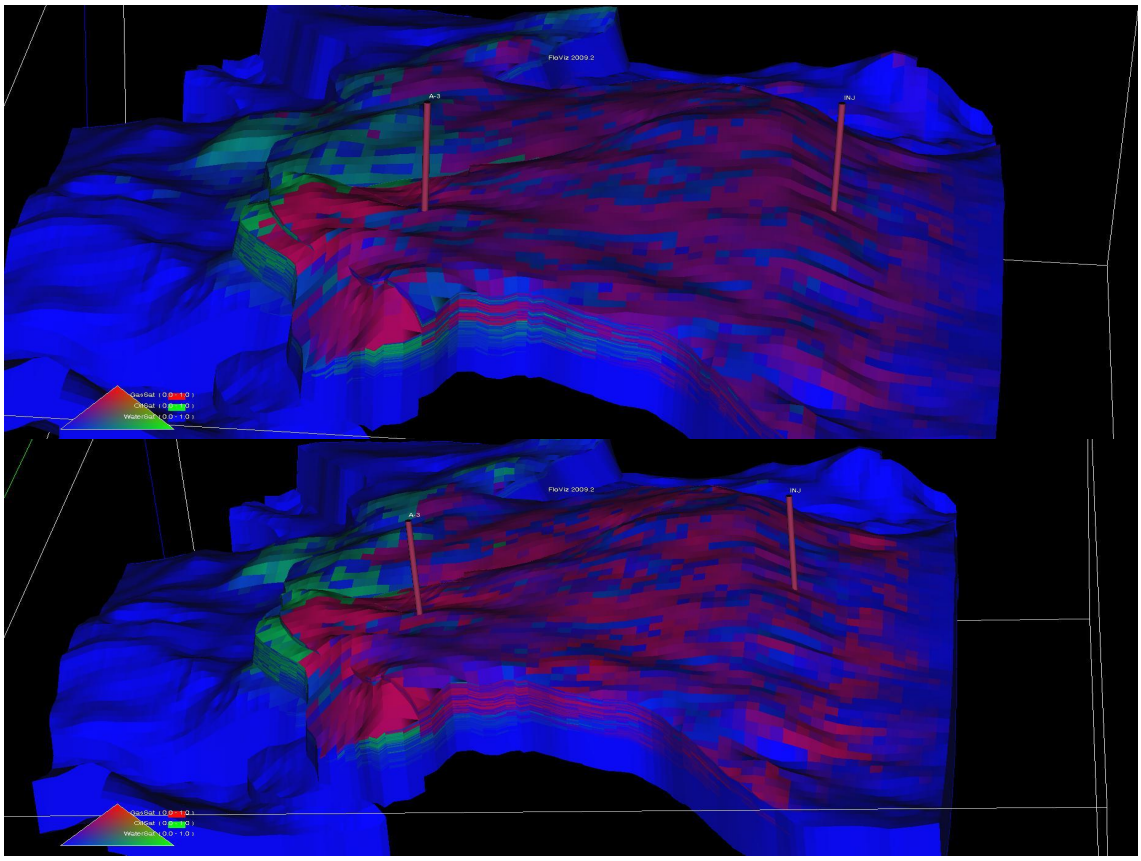

Figure 48: Layer 10.

For the miscible injection cases Fig.48 has been chosen to illustrate saturation- and flow pattern changes. As can be seen from the figure, the saturation changes become less and less prominent as the injection pressure increases. (Further details are discussed in section 6.1.3)

5.4 Other Methods of Injection

Hysteresis influence the pressure gradient, saturation history and trapped saturation. An interesting aspect to study is what effect hysteresis has on water injection, WAG and SWAG. Since hysteretic effects are more prominent at low injection pressure, and to avoid stability issues, a BHP control mode of 150 bar at the injector will be used for all cases.

Water Injection

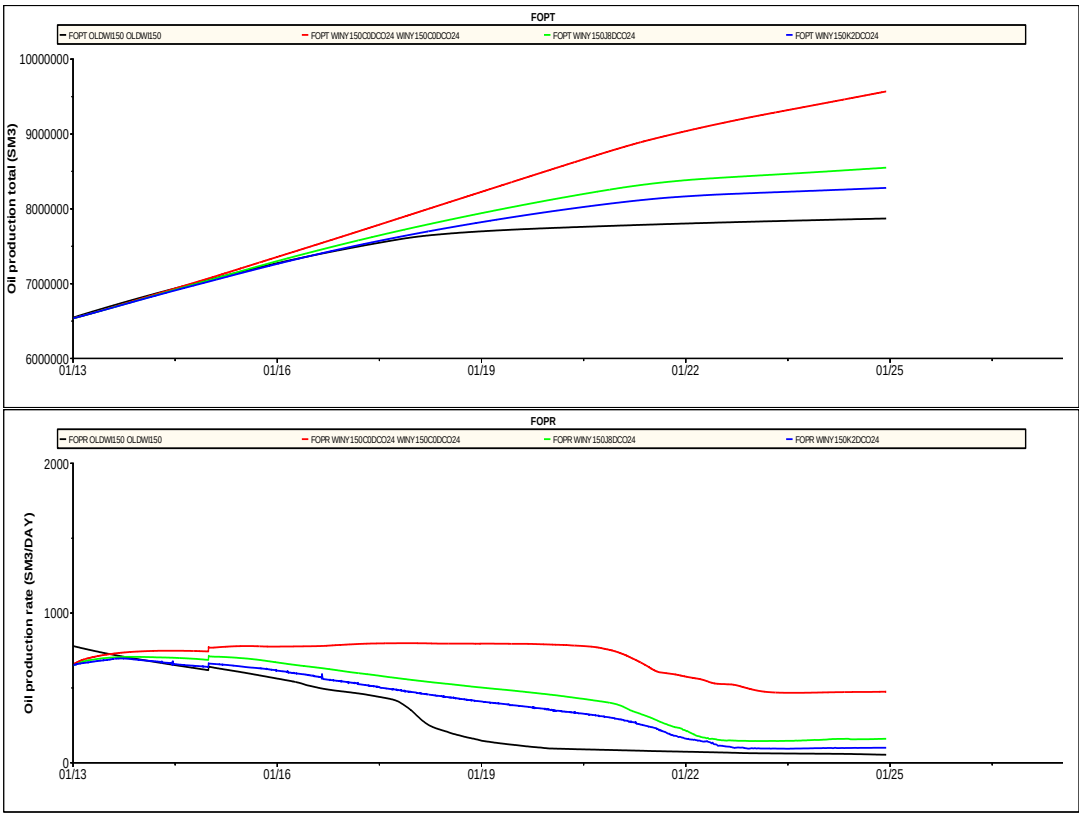

Figure 49: Effect of hysteresis on water injection. No hysteresis (black), Carlson's method (red), Killough's method (blue) and Jargon's method (green).

By implementing hysteresis, an increase in oil production is observed from Fig.49 Again, Carlson's method giving the most optimistic results, and Killough the least. A net change in FOPT was observed to be $\sim$ 5.0E5 Sm^3 for the most pessimistic case. This gives an addition to the recovery factor of 2.9 %.

WAG Injection

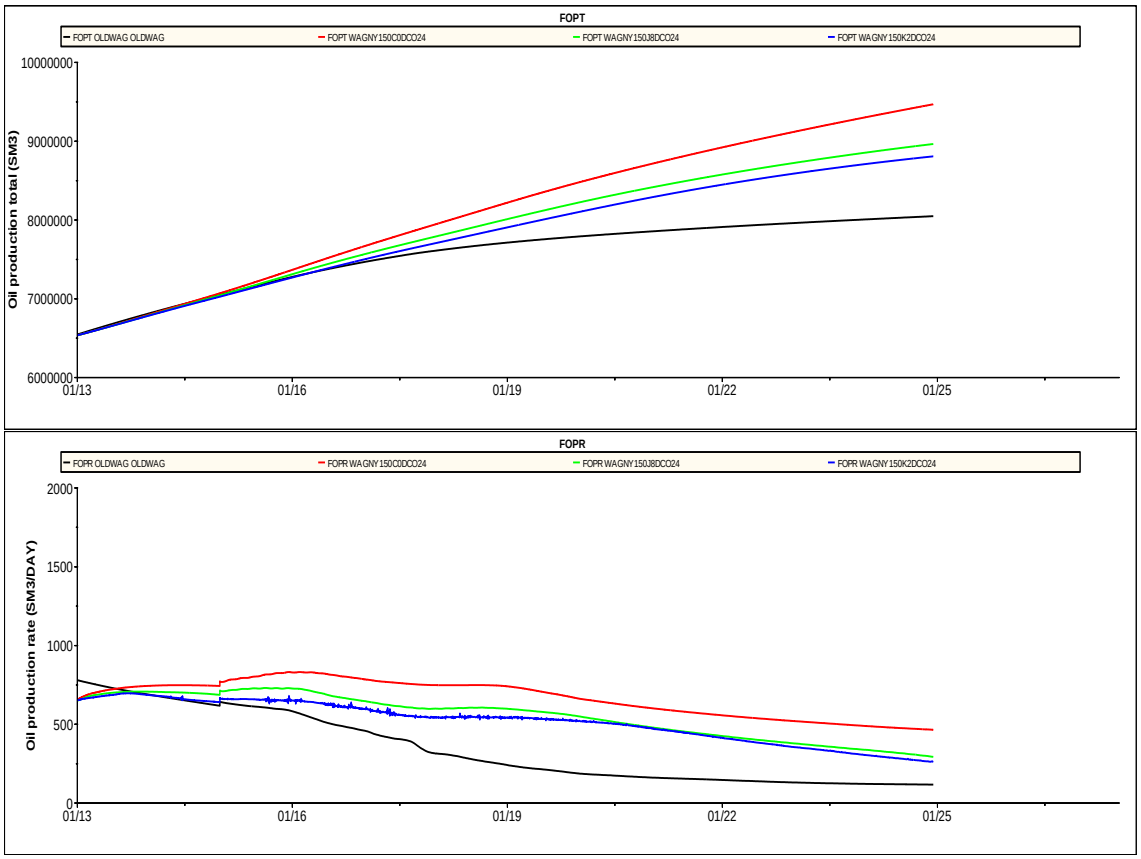

Figure 50: Effect of hysteresis on WAG-injection. No hysteresis (black), Carlson's method (red), Killough's method (blue) and Jargon's method (green).

An increase in oil production was also observed in the WAG simulations. (Fig.50) Net change in FOPT was observed to be ∼7.5E5 Sm^3 for the most pessimistic case. The cycling options were set to 3 months by each fluid, CO_2 and water.

SWAG Injection

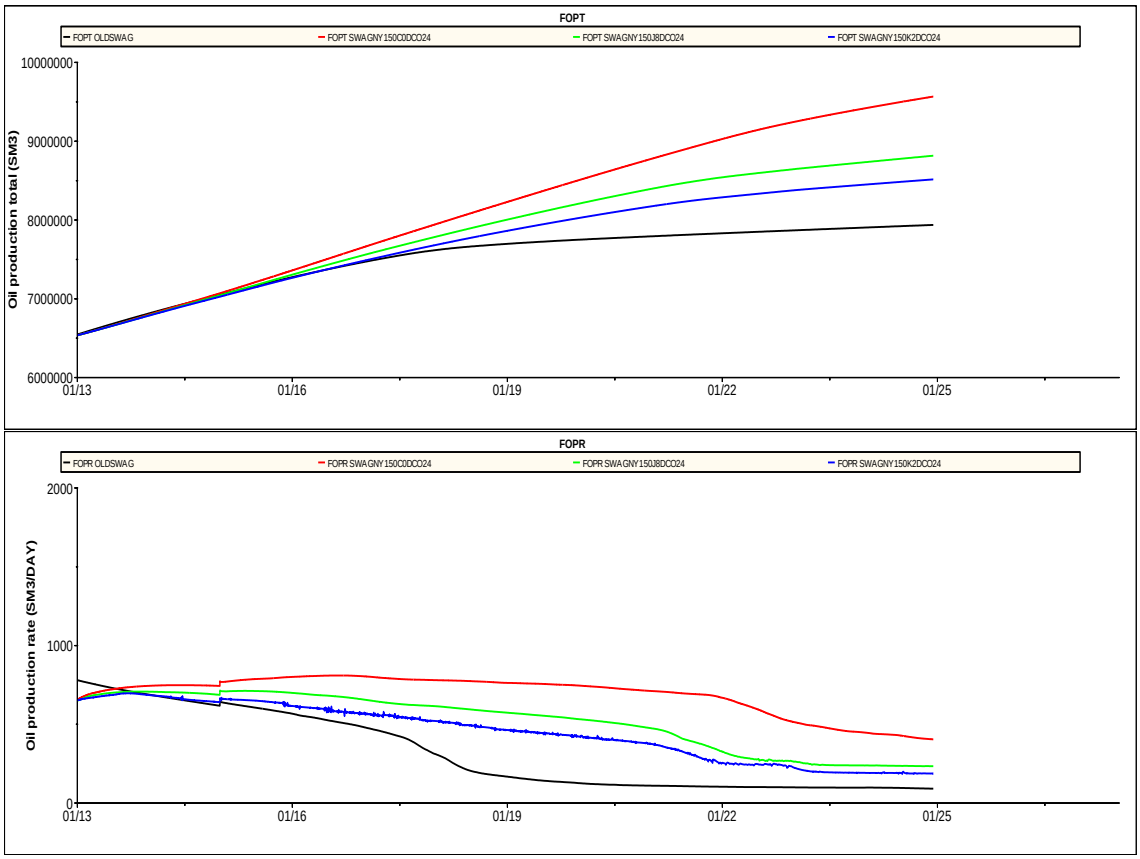

Figure 51: Effect of hysteresis on SWAG-injection. No hysteresis (black), Carlson's method (red), Killough's method (blue) and Jargon's method (green).

An increase in oil production was also observed in the SWAG simulations. (Fig.51)

Comparison

In the comparison section Jargon's method was chosen on the basis that Killough's method experienced too many stability issues. A reasonable approximation to this was then to use Jargon's method, since this was the closest match on the simulation results. Relevant information to obtain in the comparison between the methods of injection is; 1. How many pore volumes does the injected fluid displace and 2. how much more oil is it possible to produce for a given unit of CO_2 injected. Fig.52 is a representation of this.

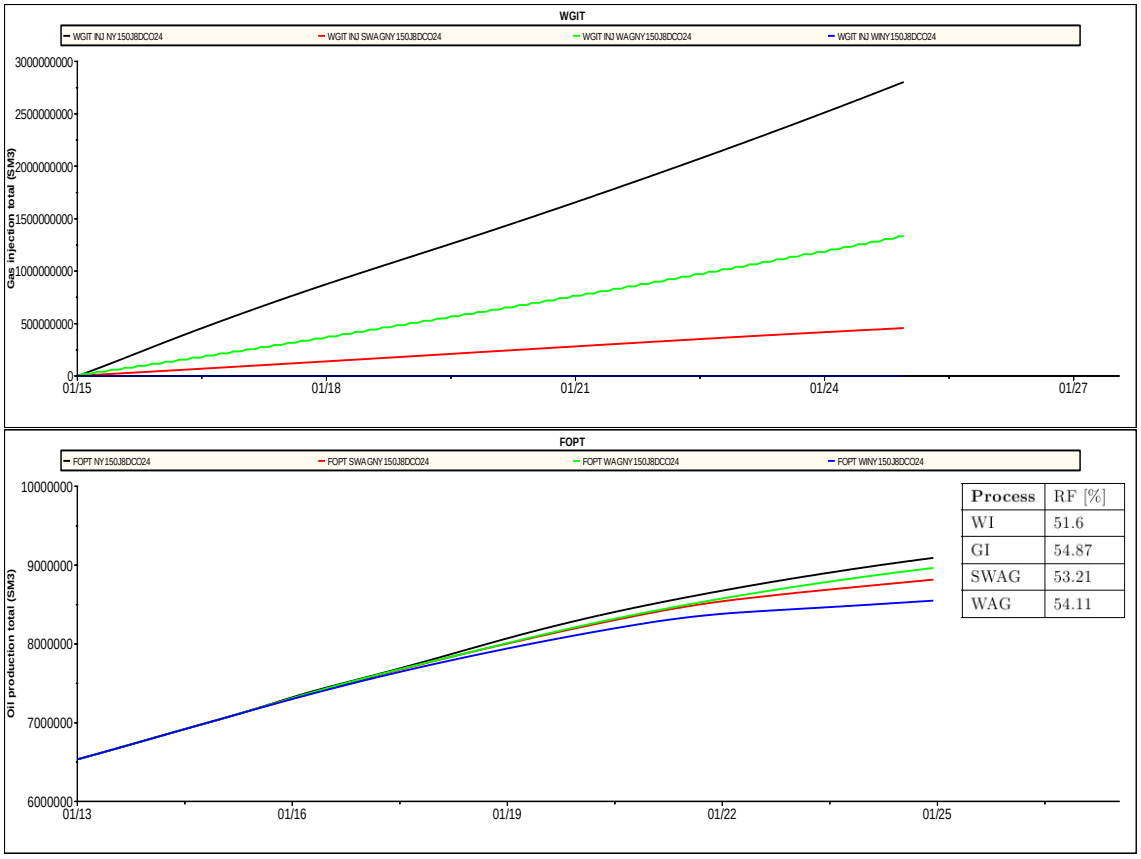

Figure 52: CO_2 injected relative to FOPT for GI (black), SWAG (red), WAG (green) and WI (blue).

In terms of reservoir volumes at injection conditions of 150 bar and 100 ^{o}C the CO_2 has a density of 332 kg/m^3 (from table 3). Assuming that CO_2 has a density at standard conditions of 1,87 kg/m^3, the volume shrinkage of CO_2 at the given reservoir conditions becomes:

$$X_{shrinkage,CO2} = \frac{\rho_{CO2}}{\rho_{CO2,sc}} = 177 Sm^3/m^3 \tag{59}$$

Considering the case of GI; In 2025 the estimated gas injected total is 3E9 Sm^3, which at reservoir conditions is 1.695E7 m^3. Total pore volume (PV) is equal to 375.78E6 m^3 and HCPV = 20.39E6 m^3 at the start of injection. Total PV displaced is therefore:

$$PV_{diplaced} = \frac{V_{CO2}}{V_{pore}} = 0.045 \tag{60}$$

Assuming that all the volumes of CO_2 injected travels through high permeable layers, containing mostly hydrocarbons, the estimated hydrocarbon pore volume displaced becomes:

$$HCPV_{displaced} = \frac{PV_{diplaced}}{HCPV/V_{pore}} = 0.827 \tag{61}$$

Since the HCPV displaced is much bigger than the recovery factor, the following statements can be assumed;

• The CO_2 cycles through the same high-permeable zones (SATNUM 6 and 7), which leaves low-permeable areas with oil unswept (mainly with SATNUM of 8,9 and 10).

• The injected CO_2 is not displacing HCPV only, resulting in an increase in HCPV displaced, while RF remains constant.

In the case of how much more oil it is possible to produce one needs a conversion factor to convert data to appropriate units. From Fig.52 after 3650 days of injection the multiplication factor converting Sm^3 to ton/d becomes:

$$X = \frac{kg/Sm^3}{kg/ton} \cdot \frac{1}{D} = \frac{1.87}{1000} \cdot \frac{1}{3650} = 5.123 \cdot 10^{-7} \frac{ton/d}{Sm^3} \tag{62}$$

The last column represents how much the additional oil requires in terms of volumes of CO_2. For instance the GI case; In order to produce the additional 542468 Sm^3 of oil, the required amount of CO_2 would be 1430 tons per day. The amount of oil produced per volume of CO_2 injected would be 378.15 $\frac{Sm^3}{ton/d}$. The most amount of oil produced per unit gas injected would be from the SWAG process. In a case where supply of CO_2 is unlimited, regular gas injection of CO_2 would be the optimal choice due to the higher RF. However, since CO_2 comes with a price, SWAG is more economically viable.

Table 7: Injection Method Comparison Data

Process	**FGIT [Sm^3]**	**FGIR [ton/d]**	**FOPT [Sm^3]**	**ΔFOPT [Sm^3]**	$\frac{\Delta FOPT}{CO_2}$ $[\frac{Sm^3}{ton/d}]$
WI	0	0	8548908	0	0
GI	2.8E9	1430	9091376	542468	378.15
SWAG	4.56E8	234	8815398	266490	1140.69
WAG	1.33E9	681	8963956	415048	609.11

5.5 Three-phase Models Comparison

Up until this point the simulation study has only considered the default model when handling three-phase situations. A sensitivity needs to be done with regards to the other models available. CO_2-injection has been chosen as base method in this comparison, with Jargon's method as hysteresis model for the default- and Stone's models. To minimize convergence problems the BHP was set to be 150 bar on the injection well. Fig.53 represents FOPT for the selected three-phase models. Time of injection is 800 days after the file restart (01.01.2015), marked with a dotted line.

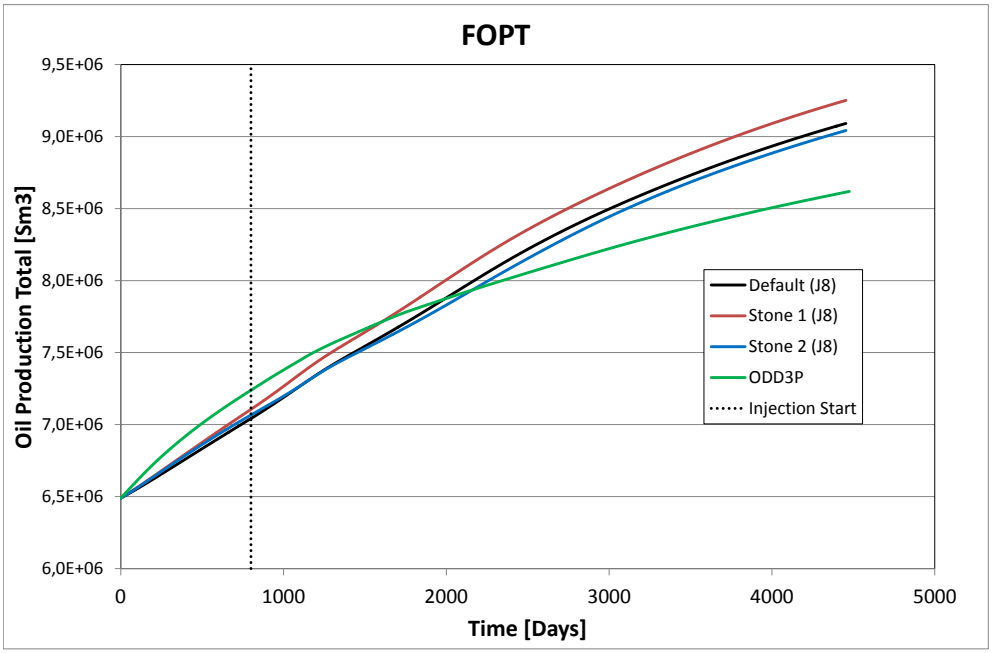

Figure 53: ECLIPSE default model (black) compared with Stone's 1st model (red) and Stone's 2nd model (blue) and ODD3P option (green).

From Fig.53 there is a minor difference between the three-phase models where Jargon's hysteresis method has been applied. Difference in recoveries are due to different oil isoperms. Comparing with the ODD3P model, there is a major difference in handling hysteresis. Even though ODD3P contains an extension of the three phase saturation range compared to the stone's models and the default model, a less recovery factor was observed. However, the effect of the saturation extension can be observed the first 1500 days elapsed, where the oil is much more mobile initially. A recent study done on WAG simulations in water-wet and mixed-wet systems[23] has shown that coupling relative permeability hysteresis models generally overestimate oil recovery prediction, with the exception of the IKU model. The IKU model gives better performance in correlating experimental data in the initial stages of injection (first gas injection, then cycling with water injection). ODD3P is an extension of the IKU model, and therefore gives a reason to believe that the ODD3P model simulates oil prediction more accurately than the other hysteresis models.

Table 8: Three-phase Model RFs

Model	**FOPT** [$\mathbf{Sm^3}$]	**RF**[%]
No-hyst.	8268736	49.20
ODD3P	8619224	51.27
Stone 2	9042447	53.79
Default	9091376	54.08
Stone 1	9251713	55.03

From Fig.54 the differences in field oil production total can be observed for the different ODD3P transformation methods. Method 2 gives an increase in FOPT due to the fact that the gas-oil relative permeabilities are mobile beyond the irreducible saturation range of method 1.

The difference in change in flow pattern can also be observed from Fig.55, which shows saturation distribution of the top layer of the reservoir. Layer 10,20,30,40 and 50 are given in the appendix. The main difference between ODD3P and the default model is that for the ODD3P model, the gas saturation is much higher in the top

layers of the reservoir, which mainly consists of rock type 1 and 1B.

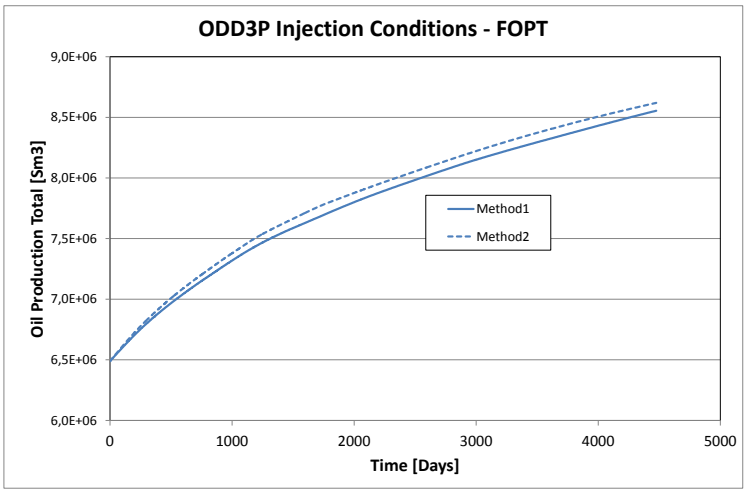

Figure 54: ODD3P model transformations, method 1 (along gas-lines) and method 2 (along oil-lines).

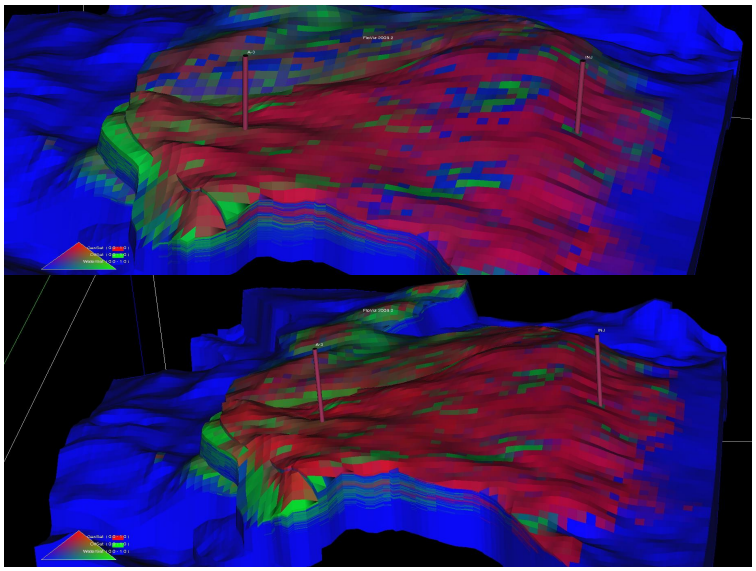

Figure 55: Top layer of the reservoir. Upper picture represents default model, while the lower one represents ODD3P. Note that ODD3P gives better sweep in high permeable layers. Upper picture shows more blue spots, which is water saturation. Additional pictures are given in Appendix.

6 Discussion

This chapter is divided into two parts; discussion of the simulation results and model validity.

6.1 Simulation Results

6.1.1 No Hysteresis Select

During gas injection, the non-wetting saturation in the grid blocks will increase. Therefore drainage curves should be used for both gas-oil and oil-water for proper modelling. However, by employing these curves a spike in oil prediction is observed as well as a sharp decrease in water production. (Fig.56)

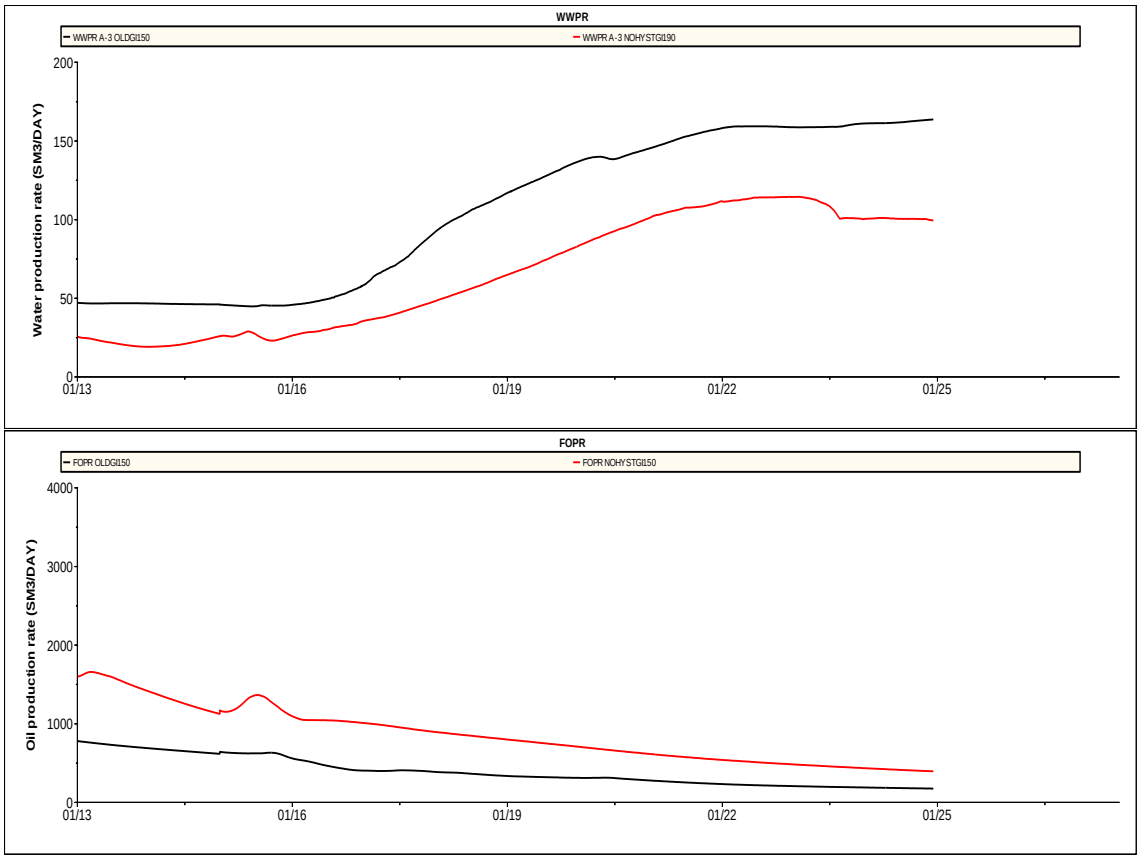

Figure 56: Implementing new relative permeability curves (red line)

The only difference between the two graphs in Fig.56 is the implementation of water-oil drainage curves instead of using water-oil imbibition curves. Fig.57 is used to illustrate what is happening.

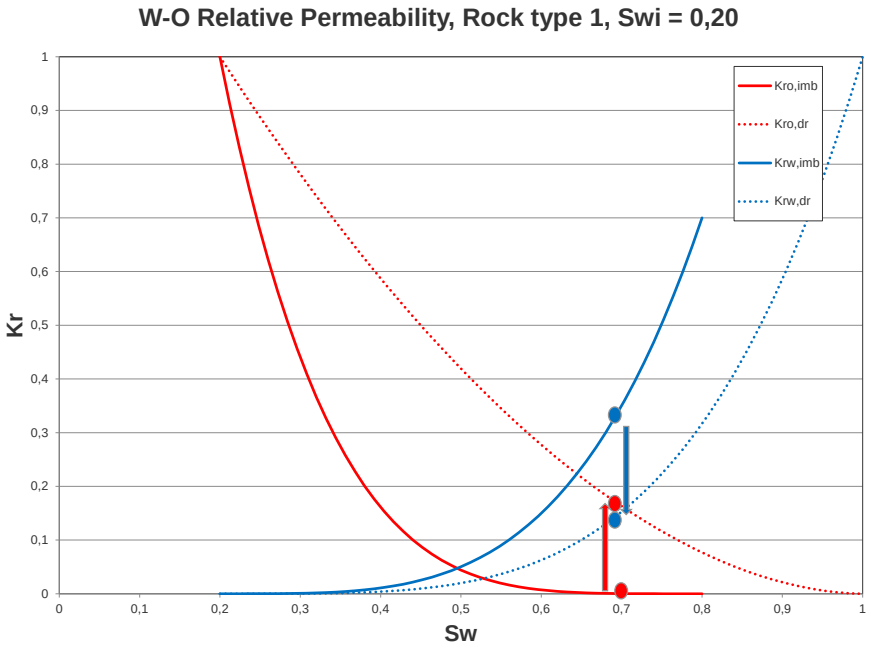

Figure 57: Illustrational example

The effect of using drainage curves instead of imbibition curves is that for a given saturation of wetting phase (assuming $S_w = 0.7$ in Fig.57), the relative permeability of water will be less compared to what it originally was. K_{ro} will drastically increase, making the oil phase more mobile. Ultimately, this gives an increase in oil production and a lower water production, as seen from Fig.56. These cases have been neglected for comparison due to not representing physical behavior.

This problem does not occur when hysteresis is selected since water-oil imbibition curves are included, and all changes related to saturations and relative permeabilities are done through scanning curves.

6.1.2 Hysteresis Method Evaluation

6.1.2.1 Immiscible CO_2-Injection

Two blocks were chosen in order to evaluate the different hysteresis methods during immiscible gas injection. The criteria of what blocks to pick was based upon high or low gas saturation, and that reservoir fluids are mobile within the block, generally blocks from the top layer of the reservoir with SATNUM 6 and 7.

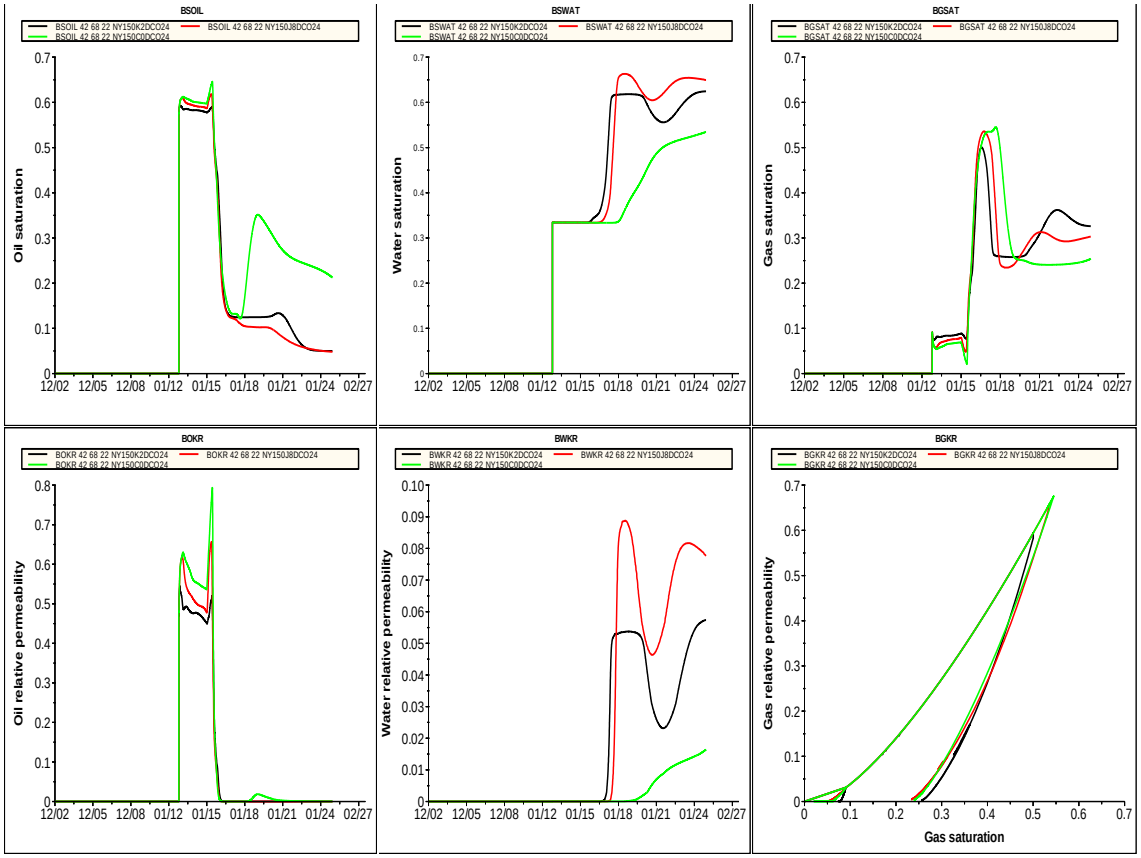

Figure 58: Block 42 68 22 Data, High gas saturation.

Fig.58 shows different parameters. From top left to bottom right, the S_o, S_w, S_g, K_{ro}, K_{rw} with respect to time lapsed and K_{rg} versus S_g are given. The black line represents Killough's model, green represents Carlson's model and red represents Jargon's model.

From the bottom left graph it can be seen that Carlson's model calculates the highest oil permeabilities, which causes the highest oil production curves.

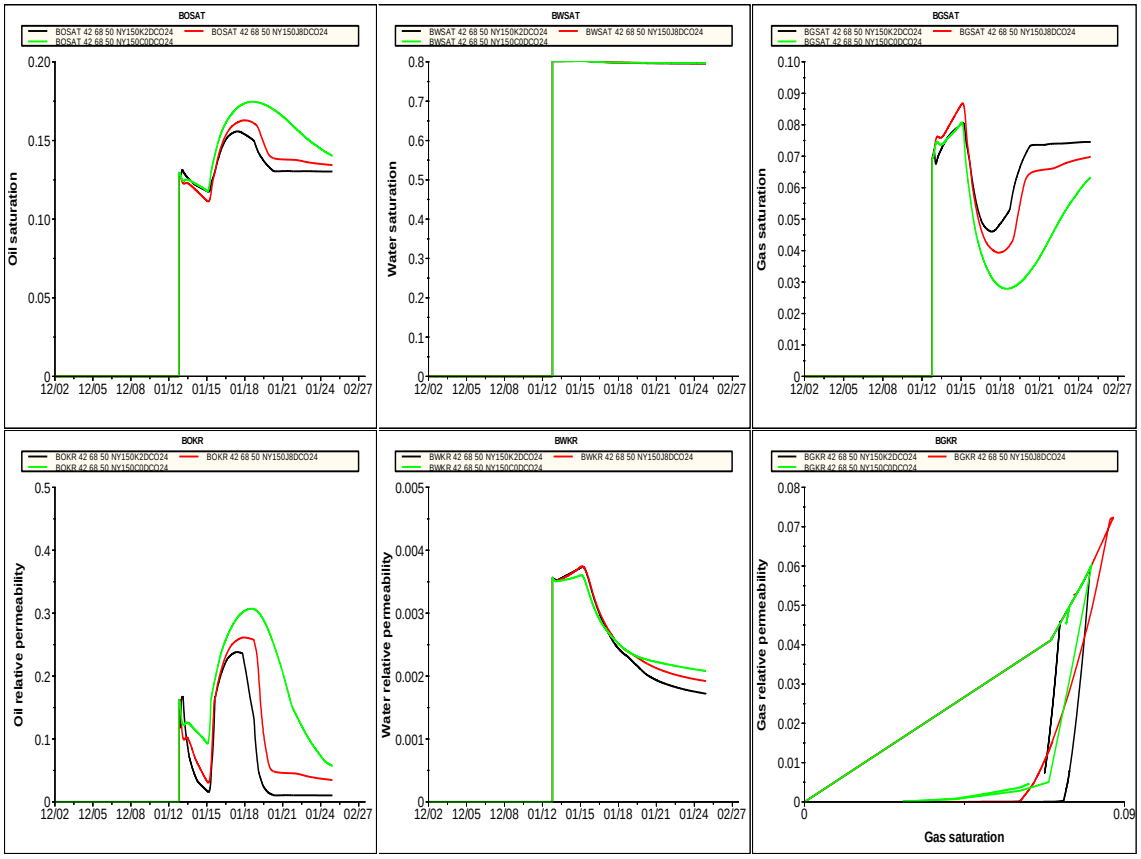

Figure 59: Block Data, Low gas saturation, layer 50 of the reservoir

In the high gas saturated block, the relative permeabilities are smooth lines. The black line represents Killough's hysteresis method, while the red and green line represent Jargon's method and Carlson's method, respectively. However, in the block with low gas saturation, small changes in the saturation occur, and inconsistencies are observed in Jargon's- and Carlson's method. Important to note is that all the selected hysteresis methods models reversible processes through intermediate values through a single generated scanning curve. This is arguably not the case in reality.

6.1.2.2 Miscible CO_2-Injection

In order to analyze what happens within a block exceeding minimum miscible pressure, an arbitrary block from one of the top layers was chosen. From top left corner of the graph outlay to the bottom right is the density, saturation, pressure and K_{rg} vs S_g shown.

Fig.60 represents block data relating change in gas and oil densities/saturations and relative permeabilities as pressure increases from immiscible conditions to miscible conditions. Killough's hysteresis method is selected in this case.

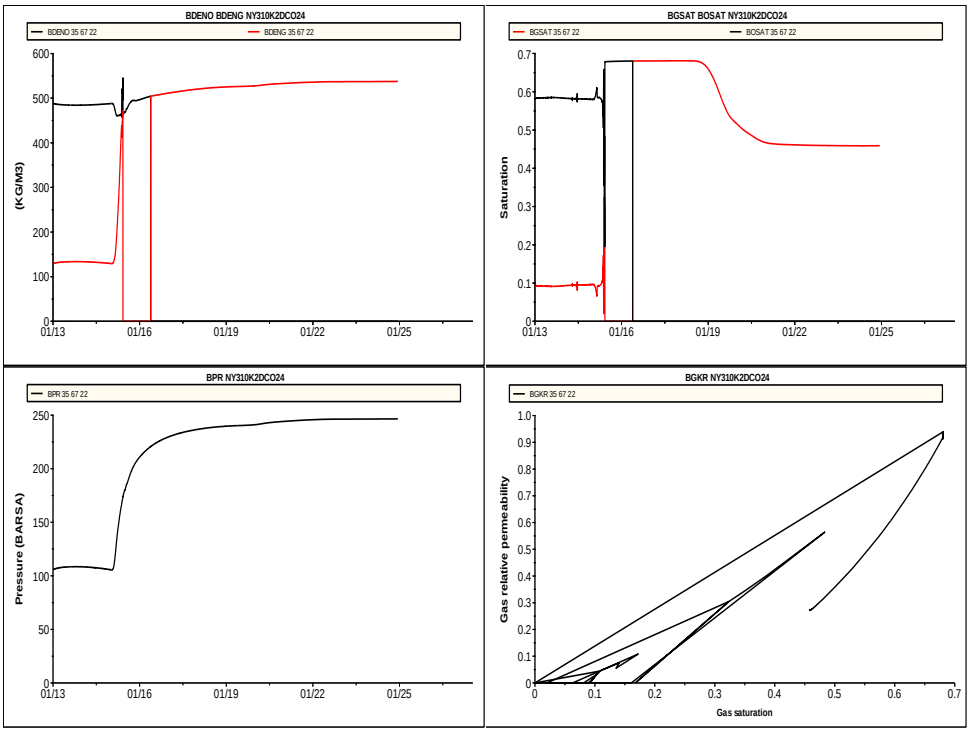

Figure 60: Block 35 67 22 data, red line representing gas and black represents oil.

As the reservoir conditions becomes higher than the MMP, the density of gas approaches the density of oil. This causes problems in ECLIPSE. From Fig.60 phase labelling changes which in turn gives inconsistent relative permeability curves. The same inconsistencies in the relative permeabilities can be seen in Carlson's and Jargon's method as well. This results in improper scanning curves, which ultimately affects the flow pattern of the fluids.

Additionally, it causes numerical problems for the simulator. Important to note is that the fluid injected has a higher density than the oil in place. Flow pattern will change due to density differences as well.

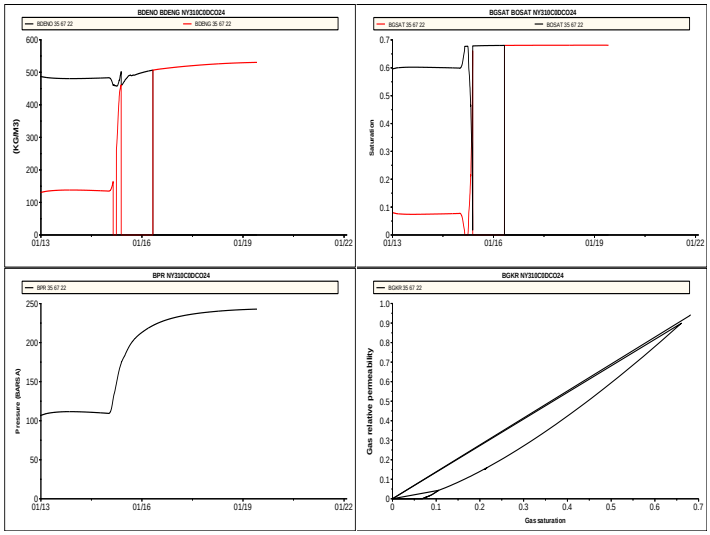

Figure 61: Block 35 67 22 data, Carlson's Method, red line representing gas and black represents oil.

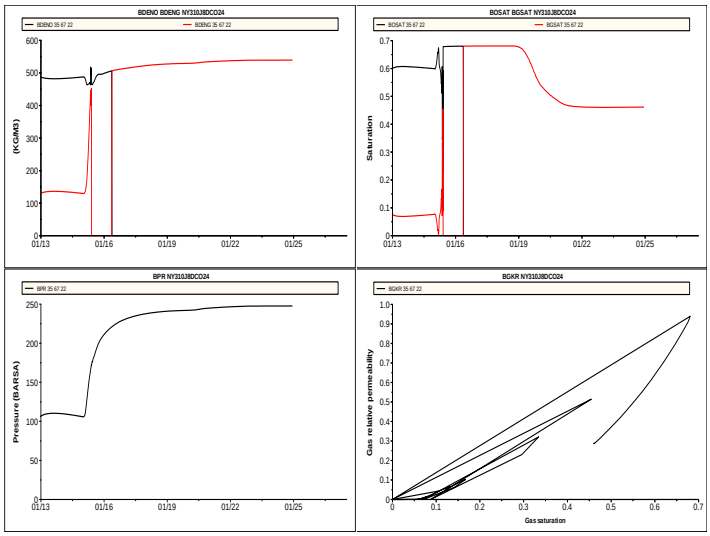

Figure 62: Block 35 67 22 data, Jargon's Method, red line representing gas and black represents oil.

6.1.2.3 ODD3P

The way ODD3P treats hysteresis and miscibility problems is different compared to the other hysteretic models. Consider the immiscible cases done for high gas satuation from Fig.58. The differences caused are due to different ways of handling three-phase situations including K_r hysteresis. It can be seen from the ODD3P model, Fig.63, that by observing the gas saturation as a function of time, and the developed gas relative permeability curves, the model promotes no hysteresis in this case. This is due to the fact that ODD3P does not engage hysteresis unless the gas saturation is bigger than S_{gt}. However, at gas saturations higher than S_{gt} it developes new curves through intermediate values by scaling and compressing shown in Fig.64.

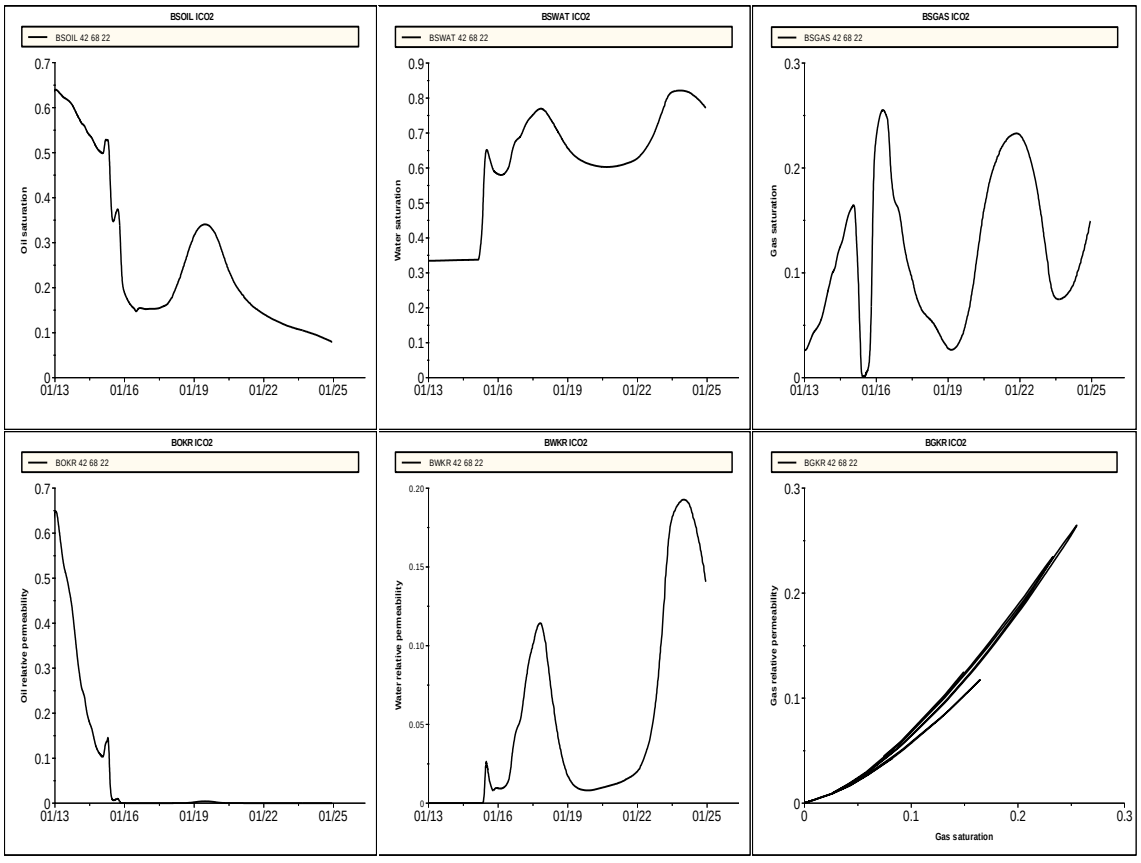

Figure 63: Block 42 68 22 data, immiscible conditions, ODD3P model, no hysteresis engaged.

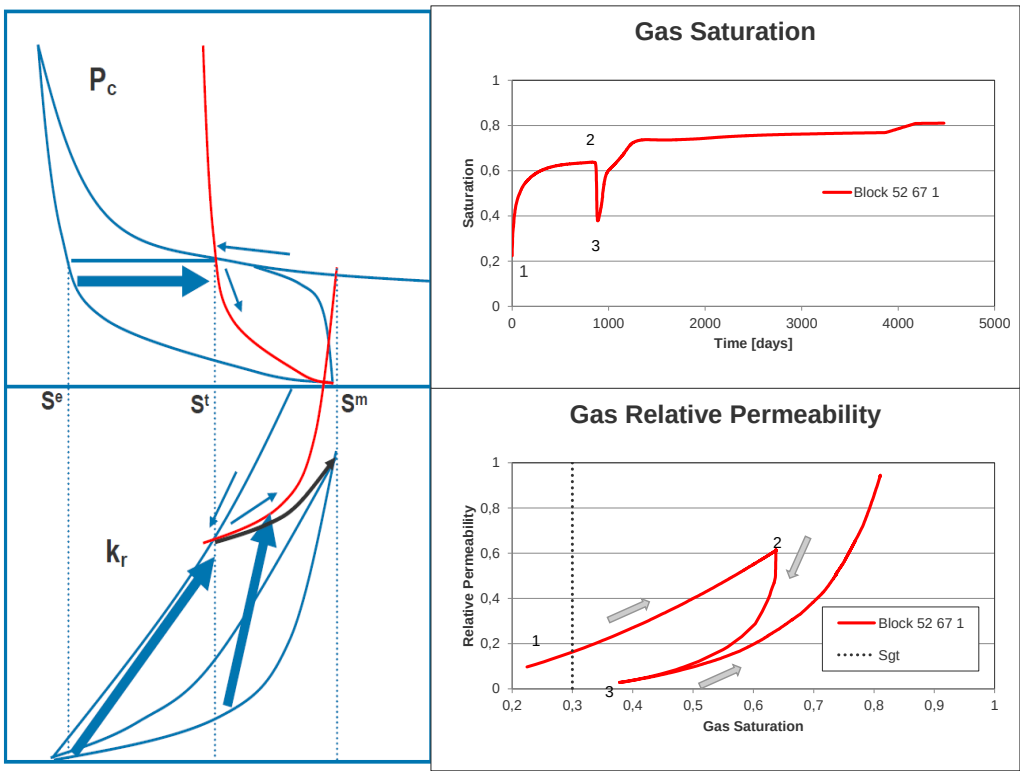

Figure 64: to the left; Capillary pressure and relative permeability mode switching in ODD3P[11], to the right; Block 52 67 1 showing how ODD3P handles hysteresis for immiscible CO_2 conditions. (increasing to decreasing to increasing saturation)

From Fig.64 to the top left and and bottom left; the two thin arrows indicate the switch from decreasing to increasing saturation mode. The thick arrows in the lower left diagram show the transformation of increasing K_r curve to (S^t,S^m), and how it is added to the turning point saturation, S^t. Important to note is that when saturation is in increasing mode the K_r might trace out a "flat" value due to the saturation scale transformation, resulting from the use of the increasing saturation mode curve for the scanning curve(From Fig.65). Also note that from Fig.64, that the gas relative permeability does not trace back to the same curve. In the case of Jargon's, Killough's and Carlson's methods, where saturation changes through intermediate values, the relative permeabilities follow the same scanning or bounding curve.

In the case of miscible conditions ECLIPSE experienced numerical instabilities illustrated with the arrows represented in Fig.65. The "flattening" part is also shown at $S_g = 0.25$, $K_{rg} = 0.3$.

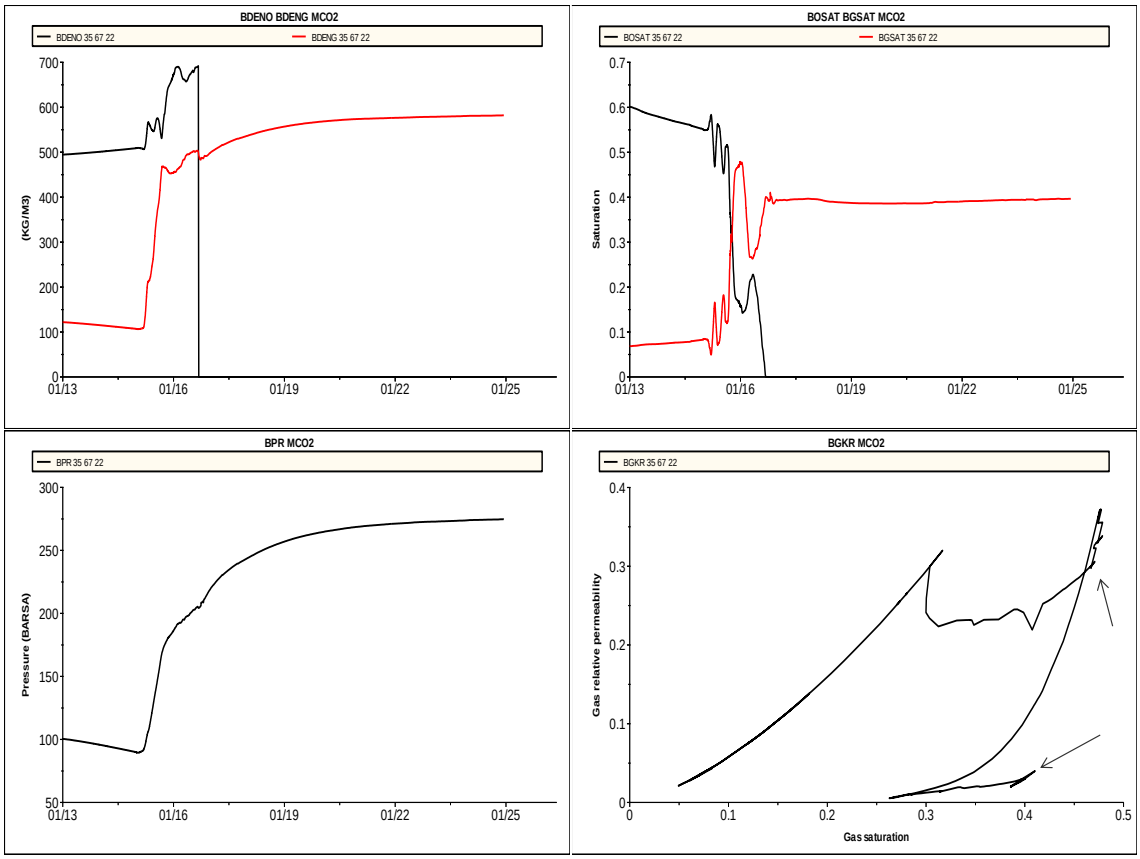

Figure 65: Block 35 67 22 data, miscible conditions, ODD3P model.

6.1.3 Flow Pattern

To demonstrate the change in flow pattern due to hysteresis, one can simply analyze the relative permeabilities and saturations on block level for the different models. Fig.66,67 and 68 represent immiscible conditions for block 49 68 22 with no hysteresis, hysteresis enabled (default), and ODD3P, respectively.

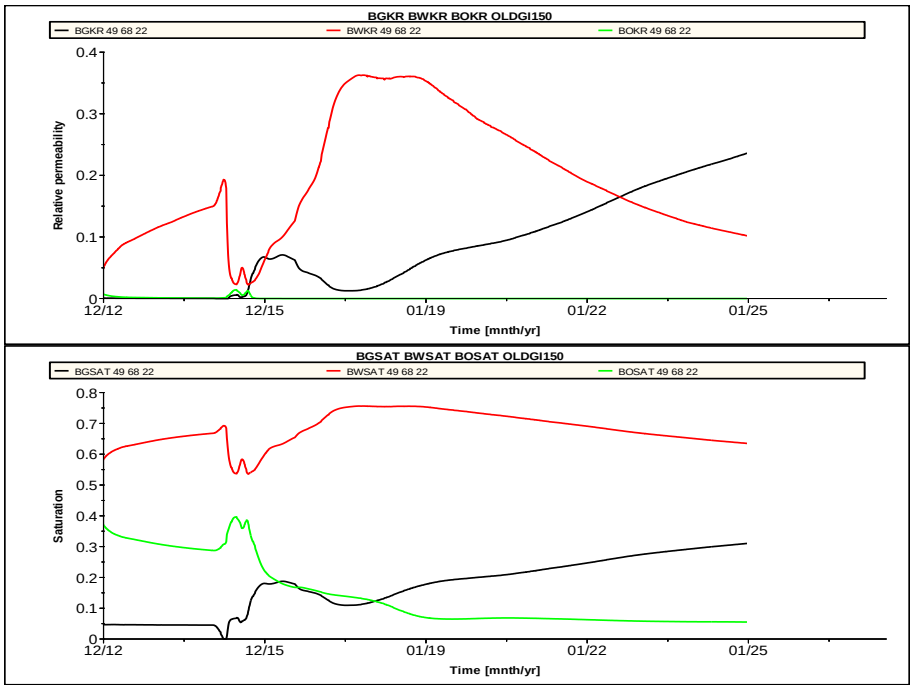

Figure 66: Block 49 68 22 data, no hysteresis, black line represents gas data, red represents water data and green represents oil data. Upper picture shows change in relative permeabilities, while the lower shows change in saturations.

The observations made based on Fig.66,67 and 68 are that the saturations and relative permeabilities are all completely different. The flow pattern is therefore different for the different models.

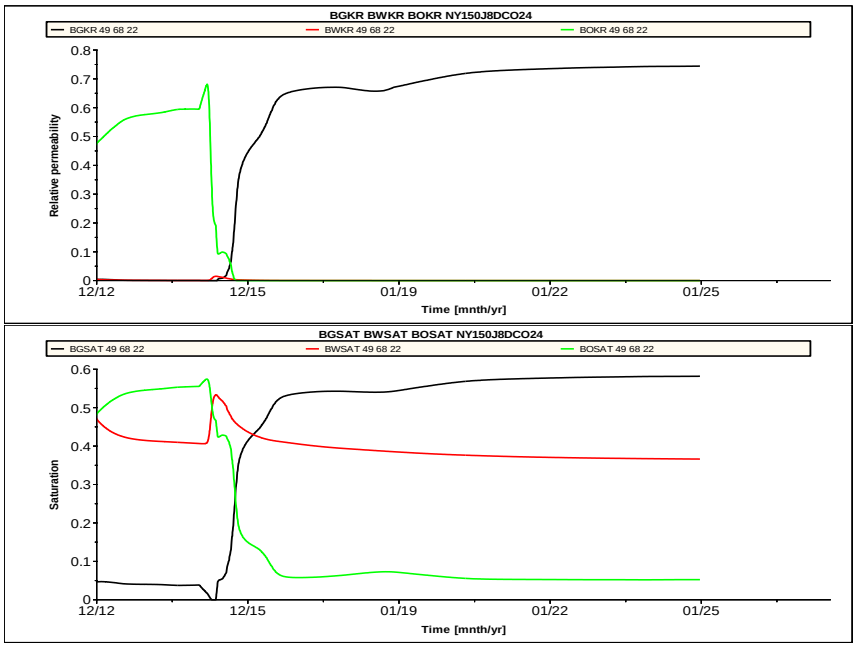

Figure 67: Block 49 68 22 data, hysteresis enabled, black line represents gas data, red represents water data and green represents oil data.

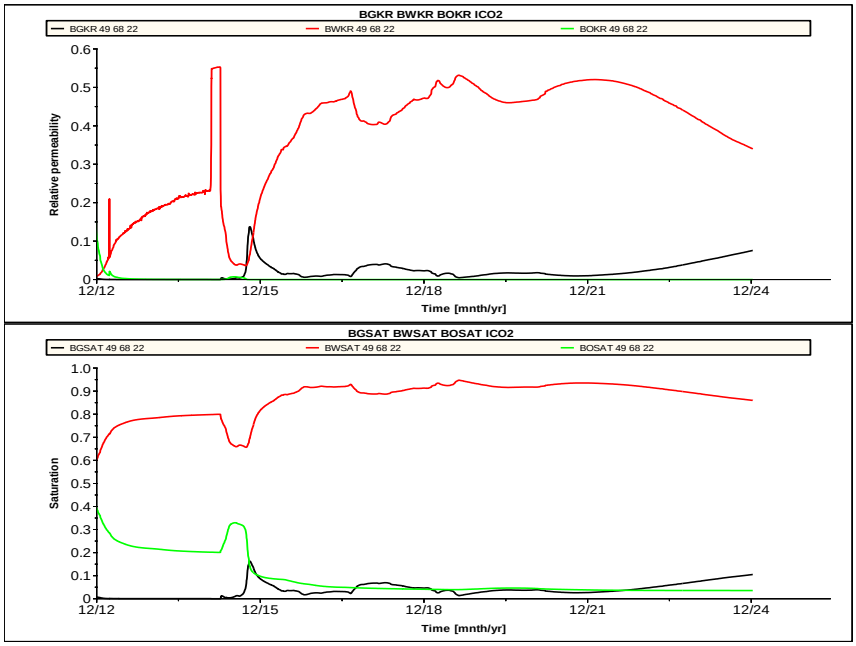

Figure 68: Block 49 68 22 data, ODD3P model, black line represents gas data, red represents water data and green represents oil data.

6.1.4 Importance of Hysteretic Effects

In this section a comparison of the curves used in the model before implementing hysteresis and the new curves will be done. For illustrational purposes a very simple example will be given. Consider a 100 % water wet system with a given permeability and porosity. At initial conditions the rock is 100 % saturated with water. Injection of non-wetting phase (oil) will be performed. Two cases are evaluated;

1. No hysteresis selected, with similar curves used in the field model.

2. Hysteresis selected.

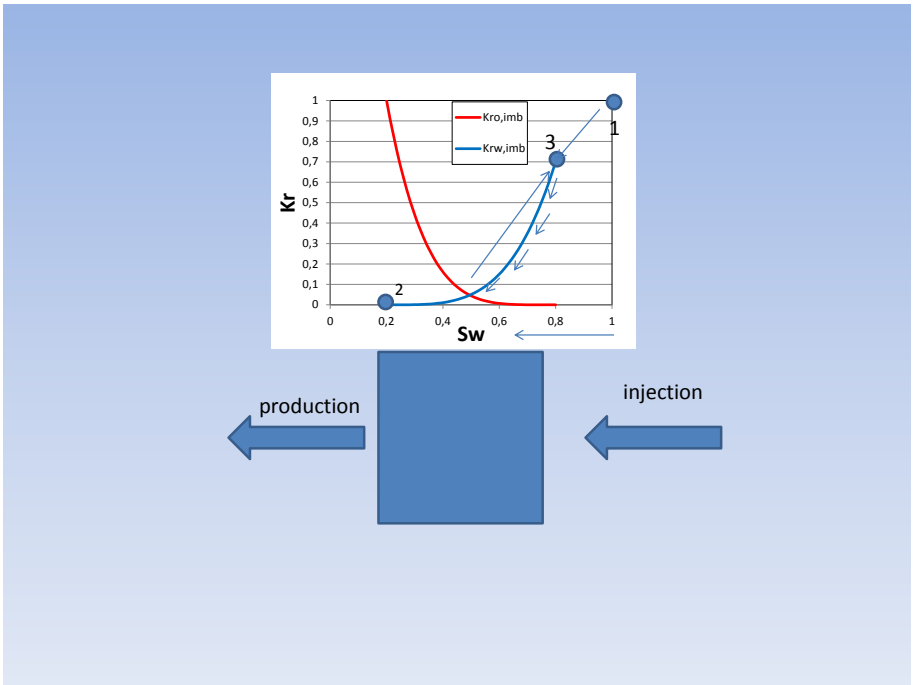

Figure 69: Case 1, system without hysteresis

W-O Case 1 As oil is injected into the system, the water and oil relative permeabilities will follow their respective imbibition curves. This is wrong due to the fact that imbibition curves are used related to the secondary process. A full drainage run is then done, and reversed at Swir, initiating a water injection. The secondary process ends at 1-Sor. For all values between 1-Sor and Swir The relative

permeabilities have the exact same values independent of the saturation process. A consequence of this is that during the primary process, water is much more mobile than it is supposed to be, which in turn makes the oil less mobile.

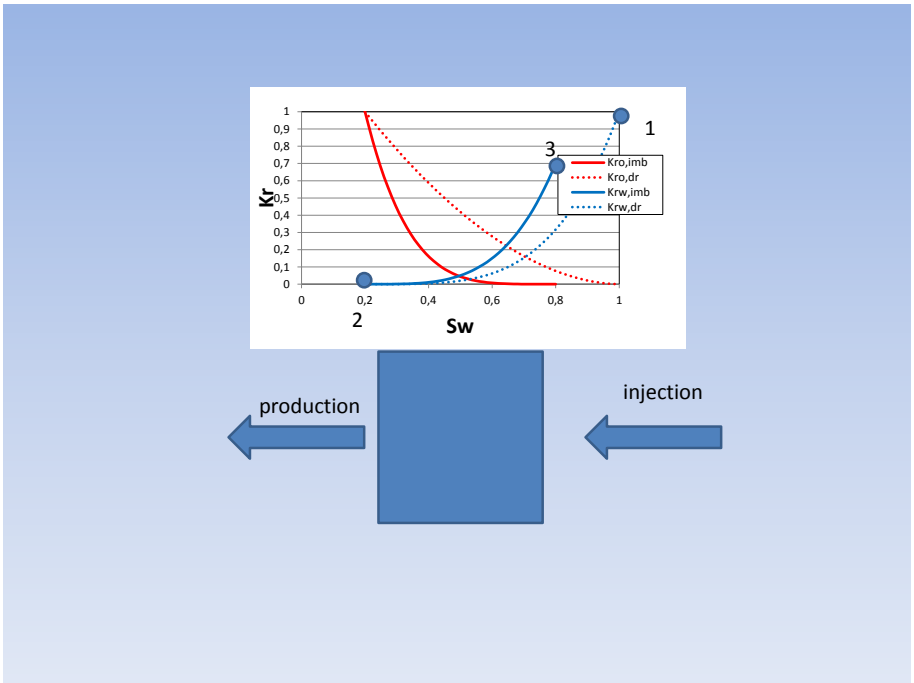

Figure 70: Case 2, system with hysteresis

W-O Case 2

Consider the same example as was given for case 1, the only difference being the use of w-o drainage and imbibition curves. For a given saturation between 1 and Swir during primary process, the water relative permeability will be less compared to case 1 and the oil relative permeability will be higher. As a result more oil will be displaced. The crude is more mobile compared to the water phase, ultimately changing the fluid's flow pattern in the reservoir.

This is just for illustrational purposes, however, it is due to this that oil production will be larger by employing hysteresis in this model.

In the case of CO_2-injection it is important to note the input of gas-oil data as well. In ECLIPSE when employing hysteresis, it is important that all the curves are enclosed loops to ensure consistency with the respective hysteresis models. The red solid line from Fig.71 should in reality be constant, instead the input data is such that it is steadily increasing until zero gas saturation. This means that the oil relative permeability calculated during decreasing saturation process is being overestimated for values less than S_{gt}. However, this is not the case for the ODD3P model, where this is accounted for.

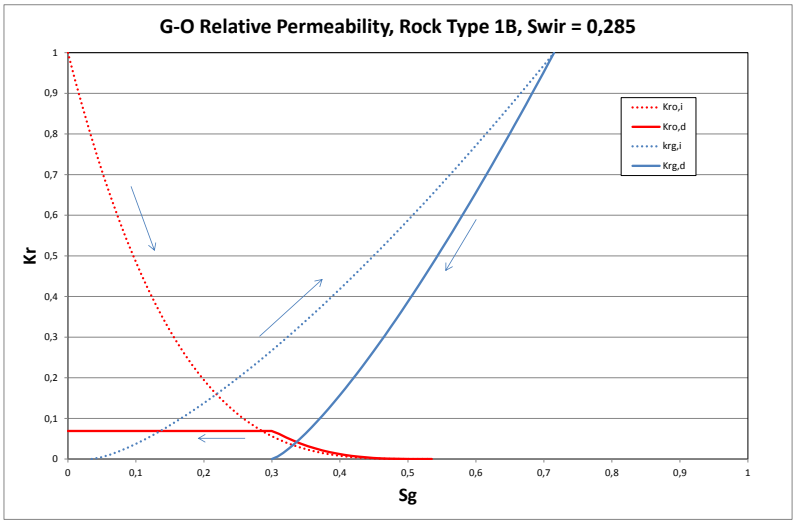

Figure 71: Gas-oil relative permeability, Rocktype 1B

6.1.4.1 ODD3P versus the Traditional Models

As shown in the result section, there is a major difference between transforming traditional data into ODD3P format. This is all due to the effect of the hysteresis end-points. Alteration of the end-points causes change in single, two-phase and three-phase saturation areas. This is represented in Fig.72 and Fig.73.

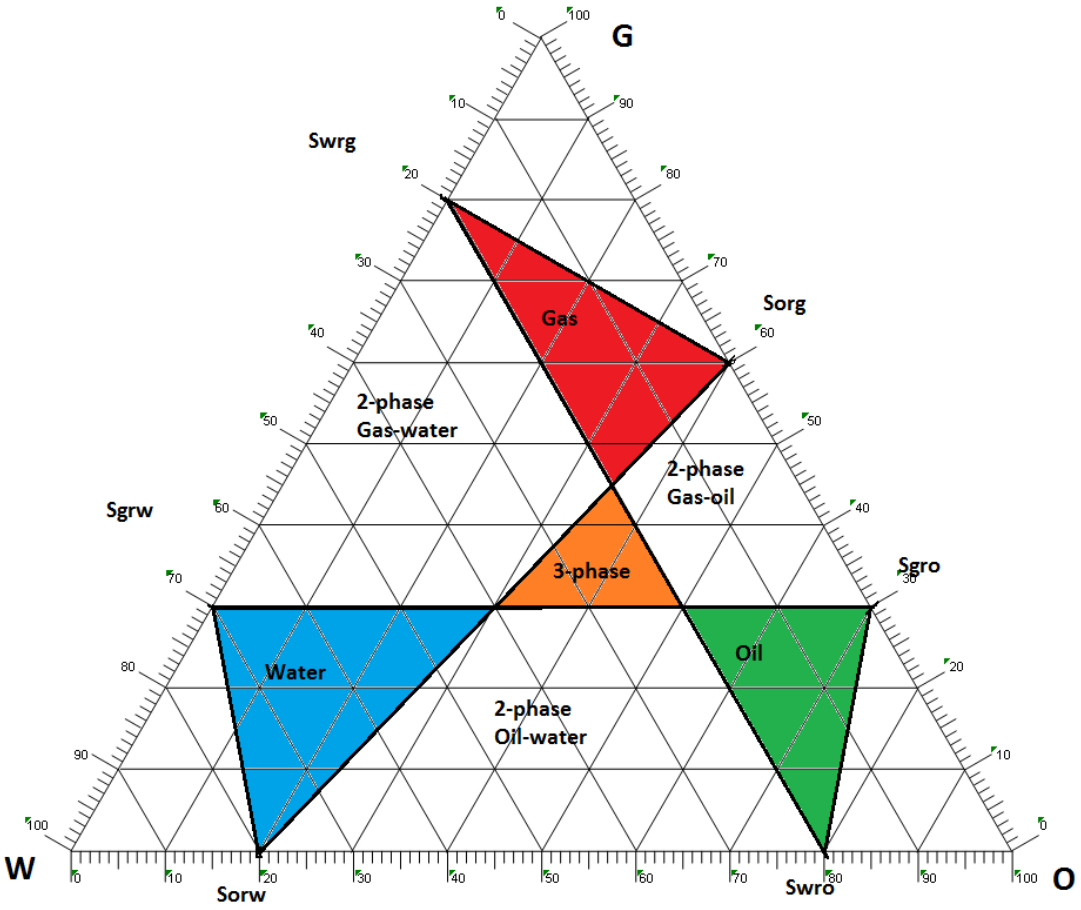

Figure 72: Flow areas of transformation through method 1, Rock type 1.

The small triangle in the middle of the figure represents the saturation area where all three phases are mobile. The other triangles colored with red,blue and green represent saturation areas where gas, water and oil are the only mobile phases, respectively. The white areas in between represent only two phases being mobile, while the solid lines connecting the residual end-points represent single-phase sat-

uration maximas for oil, water and gas. This is due to the fact that the saturations cannot exceed the line limited by the combined residual end-point saturations. Fig.72 represents transformed data along the constant gas lines. By transforming along the constant oil lines, represented by Fig.73, an extension of the three-phase area is observed, and the two-phase area of gas-oil has increased. This results in more mobile oil at higher gas saturations, thus, giving an increase in oil prediction. The dashed line represents the limiting S_{orw} - S_{org} from method 1.

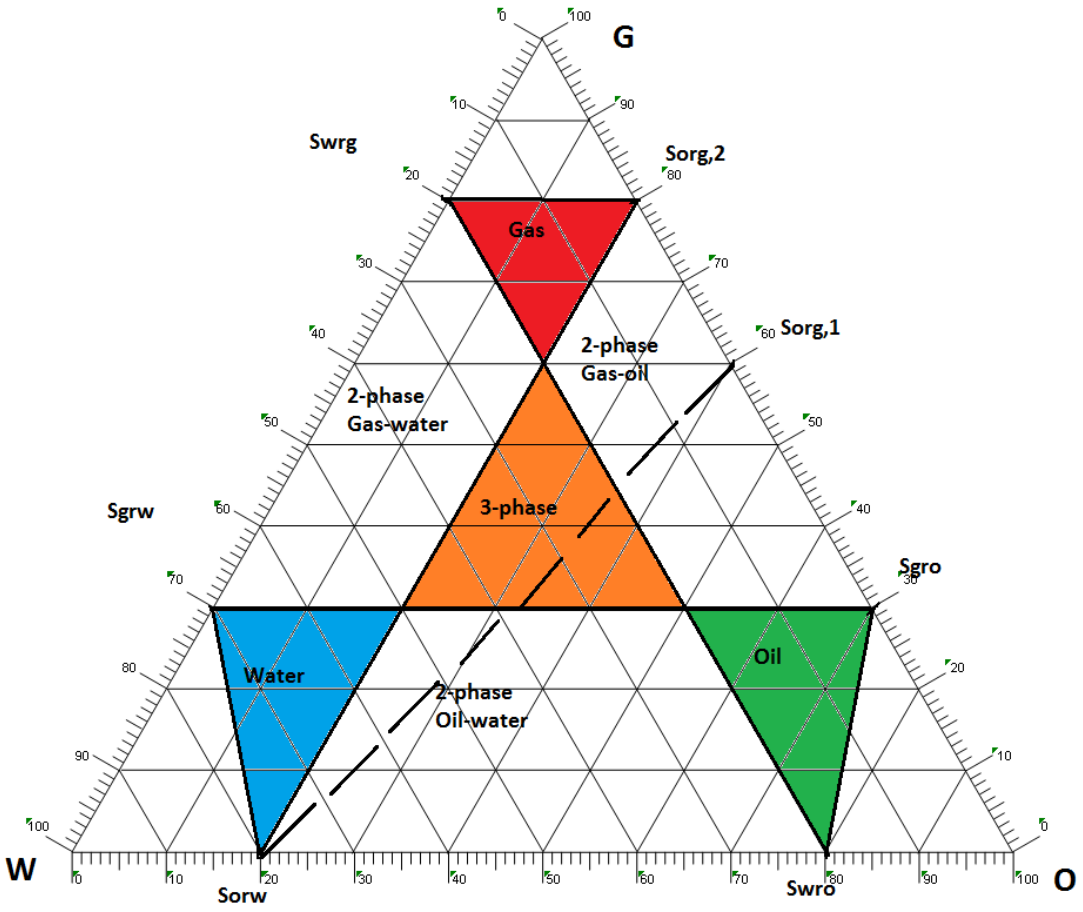

Figure 73: Flow areas of transformation through method 2, Rock type 1.

By observing Fig.74, the different ways of calculating oil isoperms by Stone's first- and second model are shown (ECLIPSE default model is between these two lines). The red dots on the figure show the same relative permeability value calculated from the two models. It can be seen that the first model estimates typically a mobile oil at low oil saturations, where Stone's second model calculates the same value at higher oil saturations.

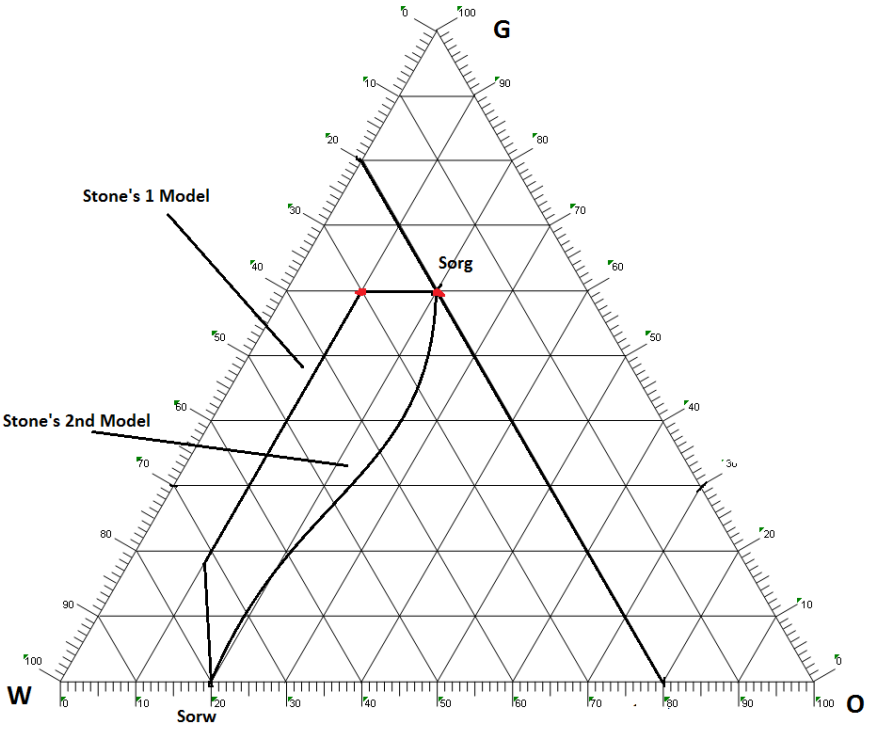

Figure 74: Illustration of typical Stone-type isoperms, Rock type 1.[12]

For simplicity reasons ODD3P model transformed along the gas lines is used in Fig.75. The line separating S_{orw} and S_{org} represents the boundary in which the oil is not mobile (upper part) and mobile (lower part). The oil predictions made from the different three-phase models are based on how the oil isoperms are calculated, where the Stone's models calculate mobile oil in saturation areas where ODD3P calculates immobile oil.

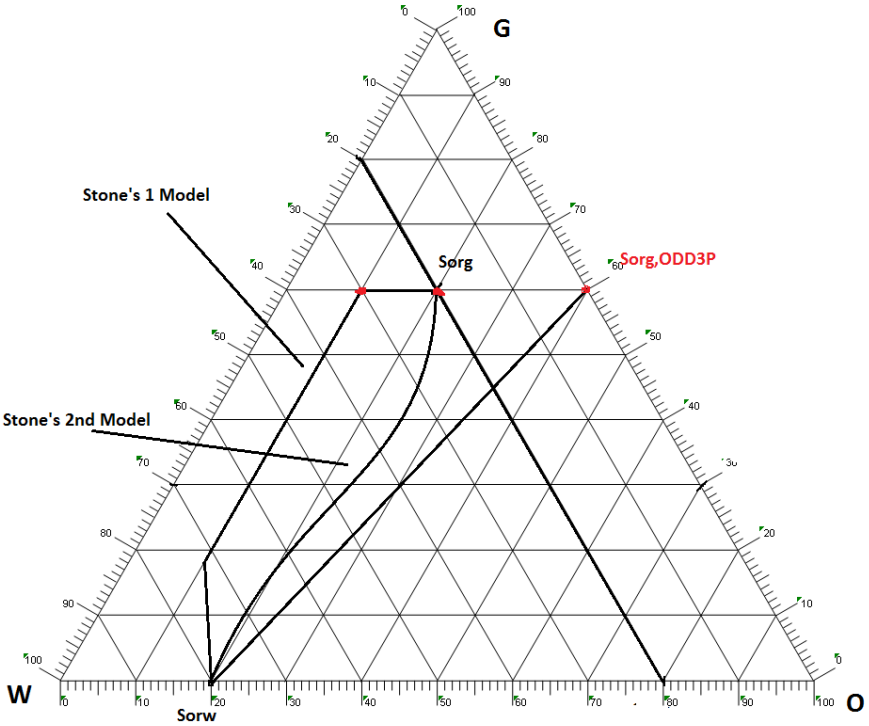

Figure 75: Illustration of typical Stone-type isoperms, Rock type 1, including ODD3P transformation method 1.

6.2 Model Validity

An increase in simulation time and increasing convergence problems have been a big issue. In order to fix these problems some limitations have been set to the reservoir model. Necessary model simplifications will be further explained in the following chapter.

6.2.1 No Hysteresis Select

The problems occurred already at the initial stages when hysteresis was turned off (changing the already implemented g-o drainage curves and w-o imbibition curves with the new ones). A typical message output would look like this:

MnNC; 4600.2 2.00E-02 388.30 .01669 652.92 11.079 2.5E05 132.04 0.0 0.0 7.2E05 20 0.01

@–Message at 4600.18997 Days 26 Jul 2015

@ Accepting time step at iteration 20 as unable to reduce.

Basically, ECLIPSE accepts the actual time-step calculated based on the limiting amounts of iterations given by the simulation-mode or the TUNING keyword. Too many "Minimum Not Converged" timesteps are a bad sign. Usually it is not so easy to tell where the MnNC error lies. However, since the simulations went well before implementing the capillary pressure- and relative permeability curves, an error might have occurred in these data. The problem lies within the capillary pressure data, since no errors were observed within the relative permeability data. The transition from the old Pc curves to the new curves causes serious instabilities for ECLIPSE. In the "no-hysteresis" an increase in CPU-usage and time-requirement per simulation-run were observed. An estimated time of 604.800 seconds to finish a run without hysteresis is too large relative to the size of the field model, especially when a depletion run with the old curves required only $\frac{1}{20}$ of the time needed. There are two options available in order to fix this; either increase the amount of iterations by decreasing the stability criterias, or freeze the capillary pressure (no change in

capillary pressure). The latter one will be the more optimal one, due to the fact that by increasing the iteration limit, ECLIPSE will only use more computer resources to try to solve the problem, thus increasing the time required. FREEZEPC can be used in ECLIPSE to prevent stability problems in runs which involves large capillary pressures (which is the case here). The results of applying this keyword is given in Fig.76 below:

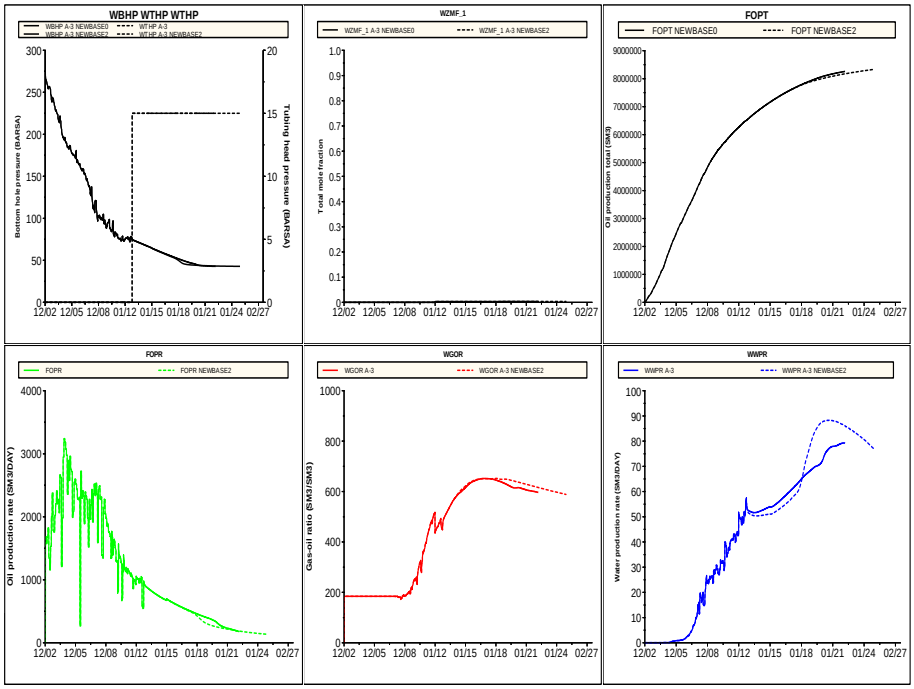

Figure 76: Overview of NEWBASE0 and NEWBASE2 which are Pc enabled and Pc frozen, respectively. x-axis represents time lapsed in years.

From Fig.76 top left to bottom right represents BHP, WZMF (which is 0.3 %), FOPT, FOPR, GOR and WPR. By observing these graphs there are certain differences in oil production rate, gas production and water production. However, since these changes are minor compared to the estimated time it takes to make a full run (with Pc enabled), FREEZEPC will be enabled in the "Hysteresis select" cases. There is of course a fundamental difference between enabling capillary pressure and freezing it, and the impact depends on how active the water is in the reservoir.

6.2.2 Hysteresis Select

Three main cases were studied in the hysteresis select; immiscible CO_2-injection, multi-contact miscible CO_2-injection, and first contact miscible CO_2-injection. The BHP at the injector are 150 bar, 190 bar and 310 bar, respectively. See Fig.77 below:

```
RESTART written Step  137 time   8047.000  1 Jan 2025
        369  Reading GADVANCE
        370  Reading ENDINC..
        371  Reading END.....

Actual well dimensions required in run
Number of wells in the model           2 (WELLDIMS item 1 was     3)
Max number of connections per well    69 (WELLDIMS item 2 was   207)
Number of groups in the model          2 (WELLDIMS item 3 was     5)
Max number of wells  per group         1 (WELLDIMS item 4 was     5)
Max number of groups per group         1 (WELLDIMS item 4 was     5)

 1) # ACTIVE CELLS =197750
 2) # ACTIVE CELLS =173546
 3) # ACTIVE CELLS =173236
 4) # ACTIVE CELLS =140674
@--Message at 8047.00000  Days  1 Jan 2025
@ For this parallel job with 4 processes.....................................
@ The required number of off processor completions.........................
@ needed in the 10th argument of WELLDIMS is 23............................
         994 Mbytes of storage required.....................................
  5.1470     KB/active cell.................................................
         792 Mbytes (image size)............................................


Unconverged stability checks          765       0
Unconverged flash calculations          0       0
Unconverged Psat  calculations          0
Cubic solns with no positive root       0
Unconverged well  model calls           0       0

Error summary.
Comments               0
Warnings              44
Problems               0
Errors                 0
Bugs                   0
Final cpu  246484.72 elapsed  283498.62
Process CPU time       Total storage  Image size
 1          246484.7      994.0 Mb       792.4 Mb
 2          248224.0      783.7 Mb       767.5 Mb
 3          247587.2      944.9 Mb       791.0 Mb
 4          242635.3      862.1 Mb       733.8 Mb
Total number of time steps forced to be accepted          2
```

Figure 77: An extract from the printfile of immiscible CO_2-injection.

It can be seen from the summary of the printfile that there are 765 unconverged stability checks. This means that there are 765 blocks that do not satisfy the converging criterias set by the simulation mode. The problem might lie in the VLE calculations. In order to check this, the injection fluid can be diluted and/or CVCRIT can be implemented in order to give ECLIPSE a less intensive run. (changing converging criterias)

6.2.2.1 Diluted CO_2

When simulating CO_2-injection with 100 % pure CO_2, problems near-critical conditions will occur, unless the injection fluid is diluted to a certain degree. If pure CO_2 is injected no phase envelope will be formed, instead it will be a straight line. However, if there is a very small fraction of C1 and N2, the mixture will form a phase-envelope and ECLIPSE will have a bigger margin of calculating phase properties. The phase properties should be approximately equal to that of pure CO_2 if the fractions of the impurities are very small. The injection gas composition is shown in the table below.

Table 9: Composition of the injected gas

Component	$\mathbf{Z}_i$ **[Mole-frac]**
CO_2	0.998
N_2	0.001
C_1	0.001
Total	1.00

It is important to note that in reality the CO_2 injected will always contain some impurities. Additionally, by injecting pure CO_2 it may cause the grid blocks to only contain CO_2. This causes problems for ECLIPSE, since two or more components are needed to perform a flash calculation.

6.2.2.2 Convergence near critical conditions

During CO_2-injection it is important to not have convergence problems near the critical state. In order to determine proper phase behavior and ease the simulator's computational processing, certain keywords were included.

CVCRIT

This keyword modifies the convergence criteria used to control the simulator in the SCHEDULE subsection. In this case this keyword is used to give the simulator a more relaxed run.

Table 10: CVCRIT cases

Case	**DPM**	**-**	**CompDV**	**USC**	**Time**[s]
DCO2	-	-	-	760	282211.33
DCO23	1.5	5*	0.1	137	31307.07
DCO24	2	5*	0.2	115	26070.33
DCO25	1.5	5*	0.5	91	32589.65

The table above represents the CVCRIT sensitivity cases. DPM represents the first position of the keyword and CompDV represents the seventh position. DPM is the maximum pressure change over an iteration. CompDV is maximum component specific volume change over an iteration. This is effectively the contribution to the saturation change due to any component. If the value is less than this the solution is accepted. USC represents unconverged stability checks, and "Time" is time lapsed for the respective simulation run. The impact of the CVCRIT cases is shown in Fig.78:

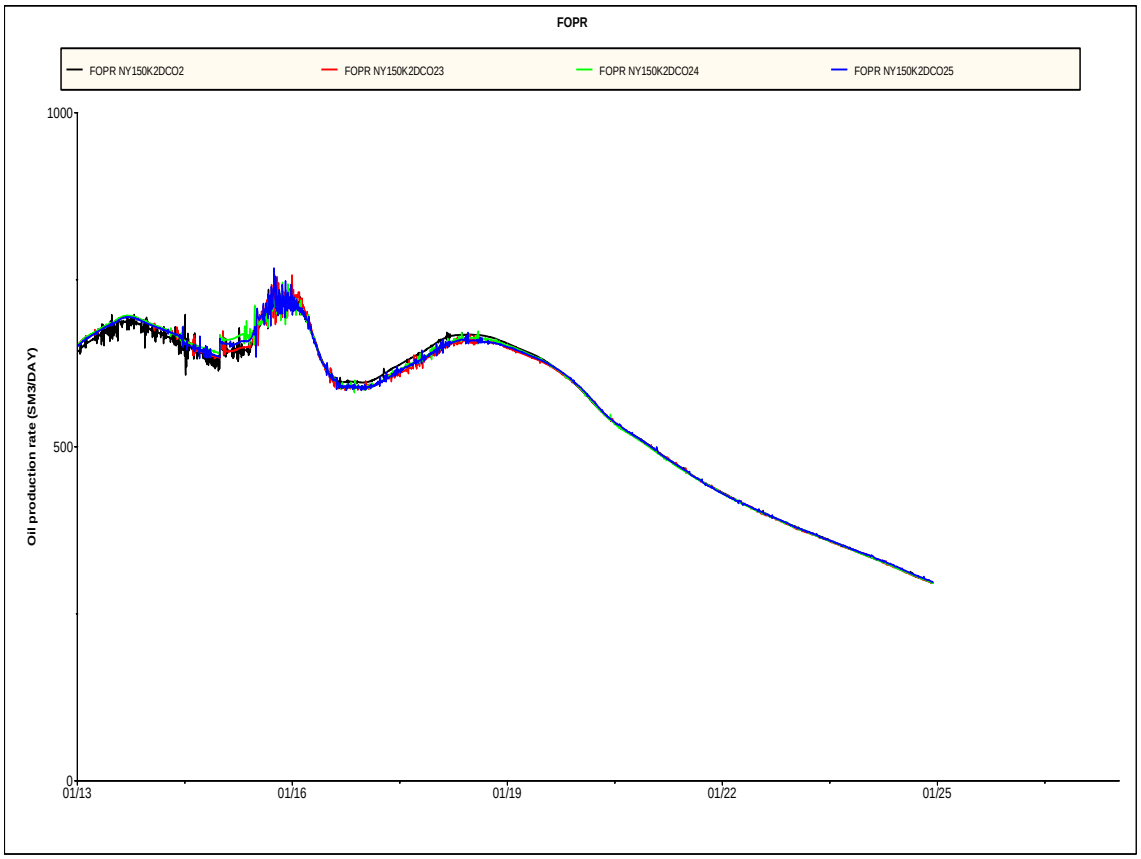

Figure 78: Effect of CVCRIT on FOPR vs time

From Fig.78 typical oscillations can be observed due to convergence problems. The graphs almost coincide with each other, which means that the effect of easing the convergence criteria has little effect on the overall simulation results, but have a major impact on the time required to make a full run.

NOHCSCAL

If the HCSCAL option is enabled in ECLIPSE, an extra scaling of hydrocarbon relative permeabilities is performed. In compositional simulation oil can change to gas without passing through the two-phase state. At very low K_{rg} and K_{ro} discontinuity can occur as the system goes to or from two-phase. In order to avoid discontinuity near two-phase conditions, NOHCSCAL is enabled.

6.2.2.3 History-matched data Comparison

Consider Fig.79 and 80, where there is a timeline divided into two parts; the past history data, and the future predicted data. If the boundary, dividing history and prediction, is shifted to the left, the predicted data will be correlated against history observed data. The result of this is shown in Fig.82

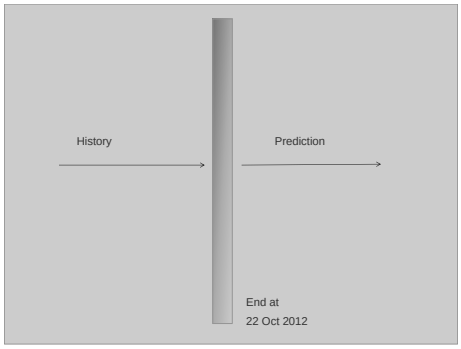

Figure 79: Restartstep initially

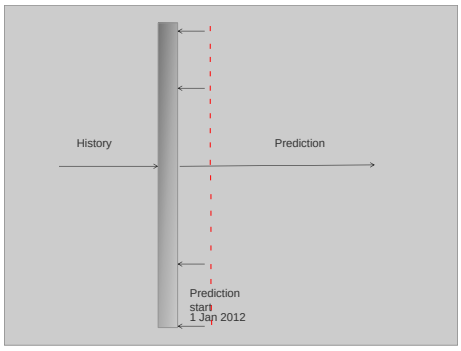

Figure 80: Restartstep post shift.

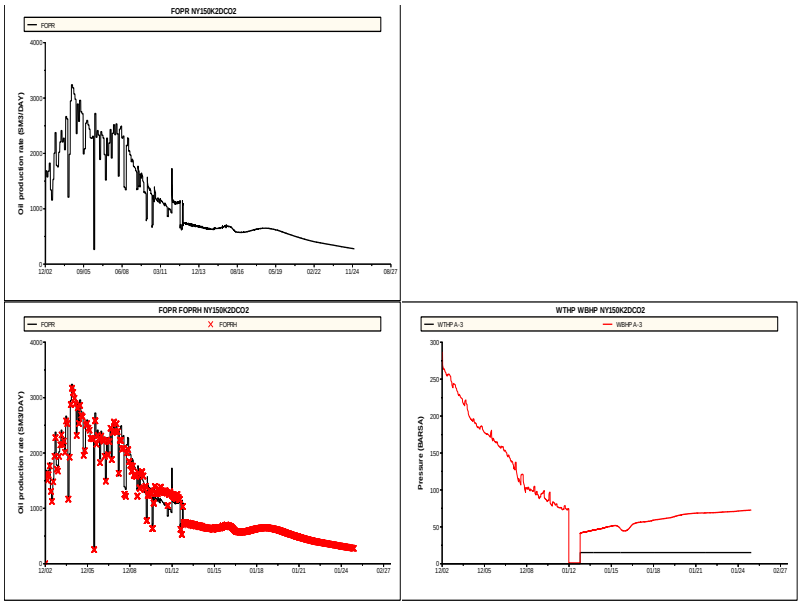

Figure 81: Historymatching hysteresis

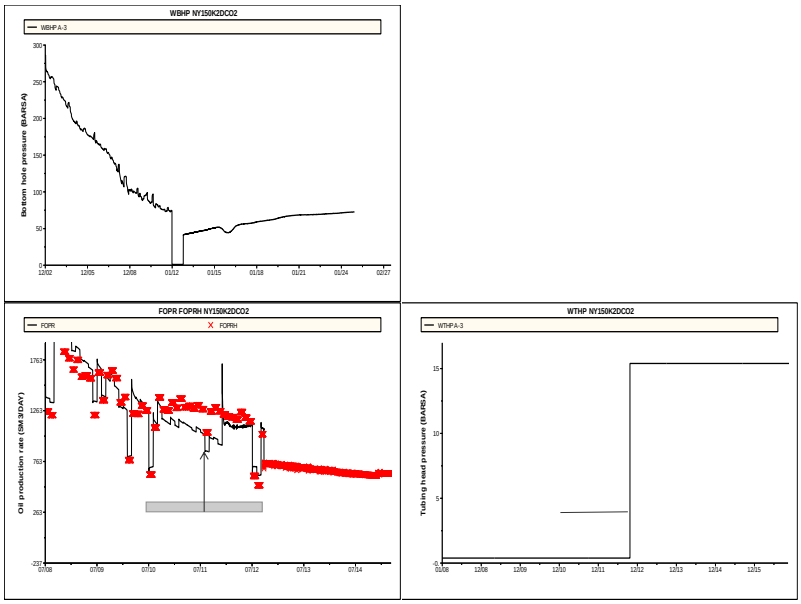

Figure 82: Historymatching hysteresis, zoomed view on BHPH vs BHP predicted

From the graphs a very peculiar observation was made. The BHP of the production well is 1 bar, which is a physical impossibility. In order to understand what is happening one needs to find out what control mode the production well is put under during the history and during the prediction phases. Last reported step from the history data:

WCONHIST

A-3 OPEN RESV 1134.2 99.45 488503.95 3* 100.0 / /

Well control at the beginning of the prediction data:

WCONPROD

A-3 'OPEN' 'ORAT' 2000. 300 1420000 1* 1* 20 15 1 /

The control mode during prediction is the oil rate with a limiting water production of 300 Sm^3 and tubing head pressure of 15 bar and BHP of 20 bar. From the WCONHIST, it can be seen that the control mode is based on observed reservoir volumes, with certain values for oil-,water-, and gas-rates, respectively. The last position in the keyword WCONHIST is the observed bottomhole pressure, which is 100 bar. However, since the control mode is based on reservoir volumes, and it can be seen from the data (the oil rate for instance), that the implemented model cannot obtain the historically observed rates. What ECLIPSE basically does during this period is that it neglects the hydrostatic pressure to get maximum drawdown, in order to reach the observed rates. In reality it is fundamentally wrong to neglect the hydrostatic pressure, due to its omnipresence in the reservoir. Based on this information one can conclude that the model implemented is either pessimistic or that the VFP table employed for predictions does not apply for the hysteresis models. When concluding the results one should take this into consideration.

7 Conclusion

• Hysteresis should be employed to field models due to its impact on the simulation results. Hysteresis affects the fluid flow in the reservoir and cannot be neglected.

• Carlson's hysteresis method proved to be very optimistic, while Killough's method was the least optimistic. This is due to the fact that the oil relative permeabilities calculated were bigger in the case of Carlson's method compared to the other methods.

• Choice of hysteresis end-points have a big impact on the single-, two-phase- and three-phase saturation ranges.

• The ODD3P model extends the range of mobile saturations of the traditional Stone's models. However, the results show that ODD3P estimate a lower oil prediction compared to the other three-phase models. This is due to the fact that compared to the traditional models, the saturation area, in which the oil is mobile, is smaller for ODD3P. Additionally, the input gas-oil data for the traditional models is such that to ensure consistency, closed loops between input bounding curves need to be ensured. A consequence of this is that the relative permeability of oil during decreasing gas saturation is being overestimated for saturations less than S_{gt}. Lastly, based on a recent study[23] done on hysteresis models and WAG, the traditional hysteresis models tend to overestimate oil prediction. It is therefore plausible to assume that the ODD3P model represents a more realistic outcome than the default and Stone's models.

• As the reservoir pressure exceeds MMP, the oil oscillates between oil and gas phases, while the gas oscillates between gas and oil. This causes extreme changes in the saturations, which in turn give improper relative permeabilities. Hysteresis is therefore not modelled correctly in miscible cases where the process path goes from immiscible to miscible conditions. ODD3P, however, treats miscible cases better. The simulator still experienced numerical difficulties.

• Uncertainties play a major role when it comes to reservoir simulation. Different models can give very different results. One method might seem very promising while others might not give good oil predictions at all. Even though there are a lot of uncertainties coupled with the different hysteresis models, they can give us a better understanding of what is happening in the reservoir, especially through complex EOR methods, such as CO_2-injection. It is therefore important to understand the theory and the fundamentals behind the methods employed, in order to fully understand the predicted data.

8 Future Recommendations

• Choose a hysteresis method that corresponds to a good history matching of the model. Alter the relative permeability curves until the model fits the history matched data.

• Find out the effect of capillary pressure hysteresis versus relative permeability hysteresis with regards to different values of $\frac{k_v}{k_h}$.

• CO_2-injection has been the main focus in this thesis. An interesting aspect would be to study the effect of WAG injections with the ODD3P model applied with DSTNUM $\neq$ ISTNUM.

References

[1] Zick A.A. "A Combined Condensing/Vaporizing Mechanism in the Displacement of Oil by Enriched Gases". *SPE 15493*, 1986.

[2] M Adewumi. "Phase Relations in Reservoir Engineering". `https://www.e-education.psu.edu/png520/`, 2014. Cubic EOS and Their Behavior - Part I, II and III,accessed $June 6, 2014$.

[3] W.G. Anderson. "Wettability Literature Survey Part 1: Rock/Oil/Brine interactions and the effect of core handling on wettability.". *Journal of Petroleum Technology*, pages 1125–1144–1262, October 1986.

[4] D.B. Bennion, F.B. Thomas, and R.F. Bietz. "Hysteretic Relative Permeability Effects and Reservoir Conformance - An Overview", 1996.

[5] J.S. Buckley, C. Bousseau, and L. Yu. "Wetting Alteration by Brine and Crude Oil: From Contact Angles to Cores". *SPEJ 30765*, pages 341–350, 1996.

[6] G.L. Chierici. "Novel Relations for Drainage and Imbibition Relative Permeabilities". *SPEJ*, pages 275–276, June 1984.

[7] L.P. Dake. *"Fundamentals of Reservoir Engineering"*. Elsevier, 1977.

[8] Distaso E. "Effect of Relative Permeability and Capillary Pressure Hysteresis in a Wag Process". `http://www.docstoc.com/docs/21952723/Effect-of-Relative-Permeability-and-Capillary-Pressure-Hysteresis-in`, last accessed: $June 6, 2014$, October 2007. Master Igegneria del Petrolio.

[9] R.M. Enick and D.K. Olsen. "Mobility and Conformance Control for Carbon Dioxide Enhanced Oil Recovery via Thickeners, Foams, and Gels - A Detailed Literature Review of 40 years Research". Technical report, National Energy Technology Laboratory, 2012.

[10] D.W. Green and G.P. Willhite. *"Enhanced Oil Recovery"*, volume 6. SPE textbook series, 1998.

[11] O.S. Hustad and Browning D.J. "A Fully Coupled Three-Phase Model for Capillary Pressure and Relative Permeability for Impliecit Compositional Reservoir Simulation". *SPE 125429*, October 2009.

[12] O.S. Hustad and T. Holt. "Gravity Stable Displacement of Oil by Hydrocarbon Gas After Waterflooding". *SPE/DOE 24116*, October 1992.

[13] National Institute if Standards and Technology. "Isothermal Properties for Carbon Dioxide". `webbook.nist.gov/chemistry/fluid/`, url last checked: $June6, 2014$, 2014.

[14] J.E. Killough. "Reservoir Simulation with History-dependent Saturation Functions". *SPEJ*, February 1976.

[15] J. Kleppe. "Handout Note Nr 3: Capillary Pressures and Relative Permeabilities.", August 2012.

[16] L.W. Lake. *"Enhanced Oil Recovery"*. University of Texas, 1989.

[17] P.S. Laplace. "Supplment au dixime livre du Trait de Mcanique Cleste". *Trait de Mcanique Cleste*, 4:1–79, 1808.

[18] O.M. Mathiassen. "CO_2 as Injection Gas for Enhanced Oil Recovery and Estimation of the Potential on the Norwegian Continental Shelf", May 2003.

[19] T.A. Melby. "The Effect of Different Flooding Rates and Ionic Composition with Low Salinity Water in Carbonates". Technical report, University of Stavanger, May 2012.

[20] T.A. Melby. "Compositional Simulation-Model Analysis: An In-depth EOR Study With Focus on CO_2 Injection". Technical report, Norwegian University of Science and Technology, December 2013.

[21] T.F. Moore and R.C. Slobord. " The effect of viscosity and capillarity on the displacement of oil by water". *Producers Monthly*, pages 20–30, August 1956.

[22] Cheng N. *"Special Topics On Developed Miscibility"*. PhD thesis, NTNU, October 2005.

[23] Shahrokhi O., Fatemi M., Ireland S., and Ahmed K. "Assessment of Three Phase Relative Permeability and Hysteresis Models for Simulation of Water-Alternating-Gas (WAG) Injection in Water-wet and Mixed-wet systems". *SPE 169170*, 2014.

[24] M.J. Oak, L.E. Baker, and D.C. Thomas. "Three-Phase Relative Permeability of Berea Sanstone". *SPE 17370*, 1988.

[25] J.D. Rogers and R.B. Grigg. "A literature Analysis of the WAG injectivity Abnormalities in the CO_2 Process". *SPE 59329*, 2000.

[26] Schlumberger. *"ECLIPSE Technical Description"*, 2012.

[27] P. M. Sigmund and F. G. McCaffery. "An improved Unsteady-state Procedure for Determining the Relative Permeability Characteristics of Heterogeneous Porous Media". *SPEJ*, pages 15–28, February 1979.

[28] J.E. Spirteri and R. Juanes. "Impact of Relative Permeability Hysteresis on the Numerical Simulation of WAG injection". *SPE 89921*, 2004.

[29] M.B. Standing. *"Notes on Relative Permeability Relationships"*. PhD thesis, The University of Trondheim, August 1974.

[30] D.C. Standnes and T. Austad. *"Enhanced Oil Recovery from Oil-wet Carbonate Rock by Spontaneous Imbibition of Aquaous Surfactant Solutions"*. PhD thesis, Norwegian University of Science and Technology, 2001.

[31] H.L. Stone. "Probability Model for Estimating Three-phase Relative Permeability". *Esso production Research CO*, pages 214–218, 1970.

[32] S. Strand. *"Wettability Alteration in Chalk: A Study of Surface Chemistry,"*. PhD thesis, University of Stavanger, 2006.

[33] M.A. Torcaso and M.R.J. Wyllie. "A Comparison of Calculated Krg/Kro Ratios with a Correlation of Field Data. *SPE 1180-G*, December 1958.

[34] C.H. Whitson and M.R. Brule. *"Phase Behavior"*, volume 20. SPE Henry l. Doherty series, 2000.

[35] M.R.J. Wyllie and G.H.F Gardner. "The Generalized Kozeny-Carman Equation-Part 2: A Novel Approach to Problems of Fluid Flow". *World Oil*, 5:210–28, April 1958.

[36] T. Young. "An Essay on the Cohesion of Fluids". *Philosophical Transactions of the Royal Society of London*, 95:65–89, 1805.

[37] J.G.J. Ypma. " Analytical and Numerical Modeling of Immiscible Gravity-Stable Gas Injection Into Stratified Reservoirs,". *SPEJ*, pages 554–564, August 1985.

Nomenclature

Symbol	Description
i,j,k	subscripts of fluid phases, oil, water and gas
P_c	Capillary pressure
P_{cog}	Gas-oil capillary pressure
P_{cow}	Oil-water capillary pressure
K_{rij}	Relative permeability of phase i in i-j system
K'_{rij}	End-point relative permeability of phase i in i-j system
S_{irj}	Saturation of phase i in i-j system
T	Temperature
θ	Contact angle between fluid-fluid interface
α	Acentric factor
ω	sphericity of the molecules
β_g	Beta function for gas in Stone's first model
β_w	Beta function for water in Stone's first model
σ_{os}	Interfacial tension between oil-solid
σ_{ow}	Interfacial tension between oil-water
σ_{ws}	Interfacial tension between water-oil

Abbreviation	Description
EOR	Enhanced Oil Recovery
EOS	Equation Of State
MMP	Minimum Miscible Pressure
HCPV	Hydrocarbon Pore Volume
P_i	Phase pressure where i = oil, gas or water
WAG	Water-Alternating-Gas
N_{ca}	Capillary Number
S_i	Saturation of phase i, i = o,w or g
K_{ri}	Relative permeability of phase i, i = o,w or g
S_{in}	Normalized saturation of phase i
OWC	Oil-Water contact
GOC	Gas-Oil contact
FOPR	Field Oil Production Rate
FOPT	Field Oil Production Total
WGOR	Well Gas Oil Ratio
WWPR	Well Water Production Rate
BHP	Bottom Hole Pressure
THP	Tubing Head Pressure
GIR	Gas Injection Rate
SWAG	Simulataneous Water and Gas injection
IOR	Increased Oil Recovery
PR	Peng-Robinsson
SRK	Soave-Redlich-Kwong
BIP	Binary Interaction Parameter
RF	Recovery Factor
WZMF	Component Molar Fraction
$\tilde{J}$	Leverett J-function

A Appendix

A.1 Old Curves

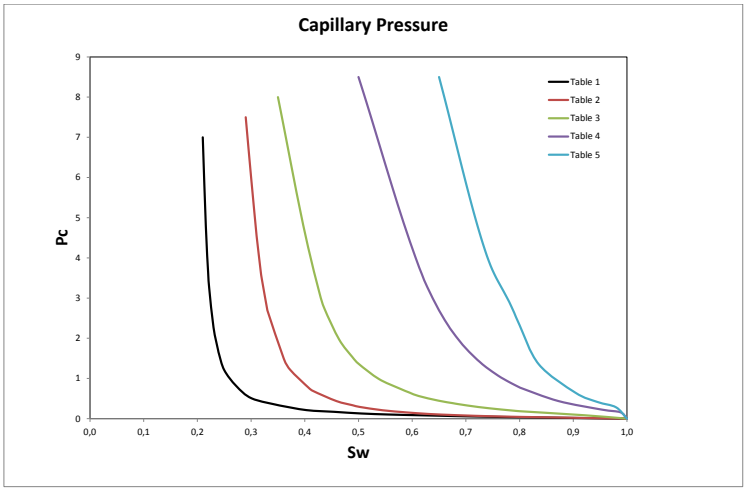

Figure 83: Capillary pressure curves.

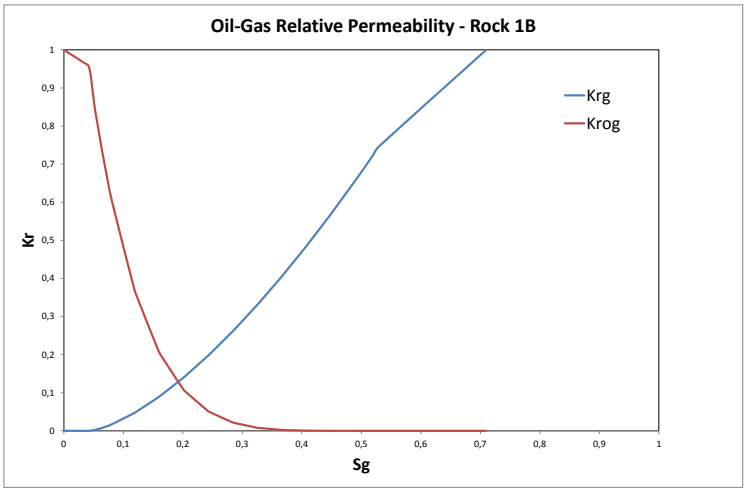

Figure 84: Gas-Oil Drainage Curve, Rock 1B.

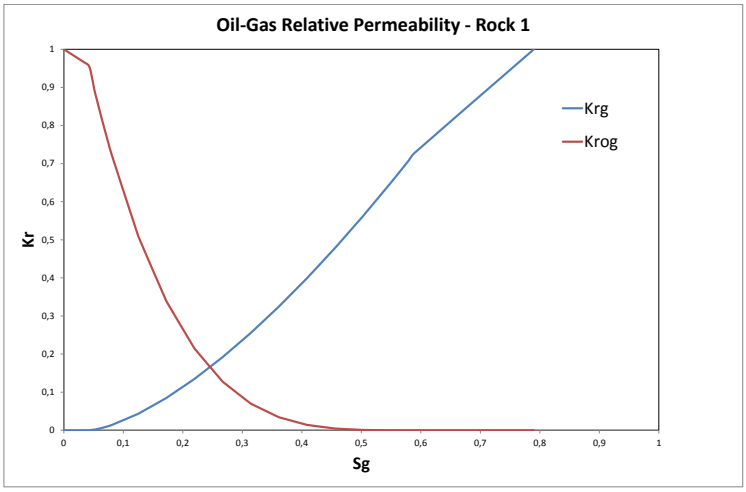

Figure 85: Gas-Oil Drainage Curve,Rock 1.

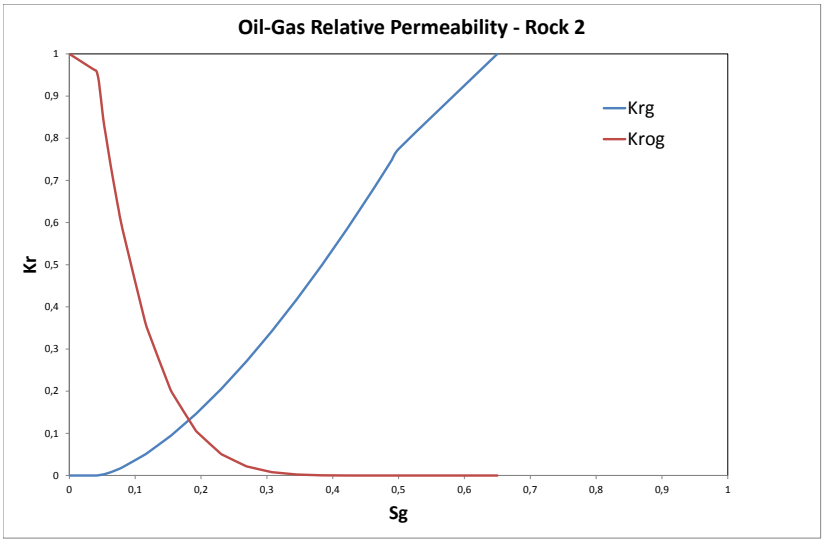

Figure 86: Gas-Oil Drainage Curve,Rock 2.

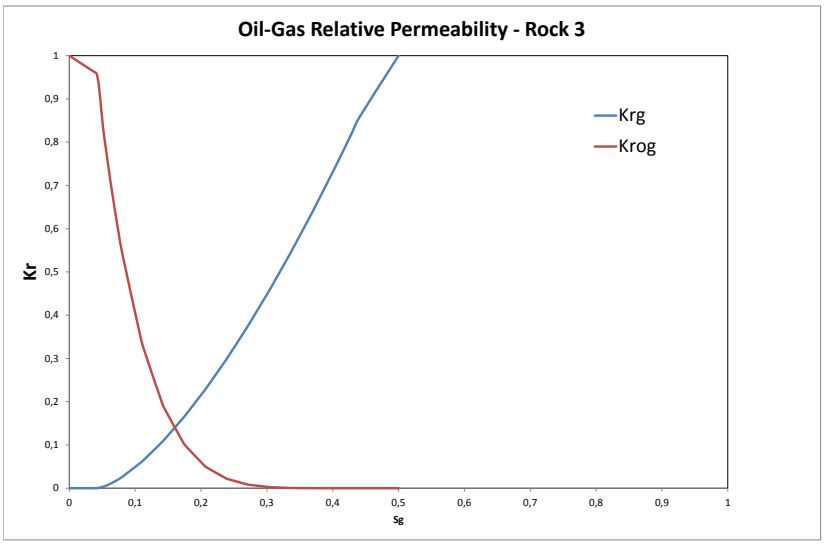

Figure 87: Gas-Oil Drainage Curve, Rock 3.

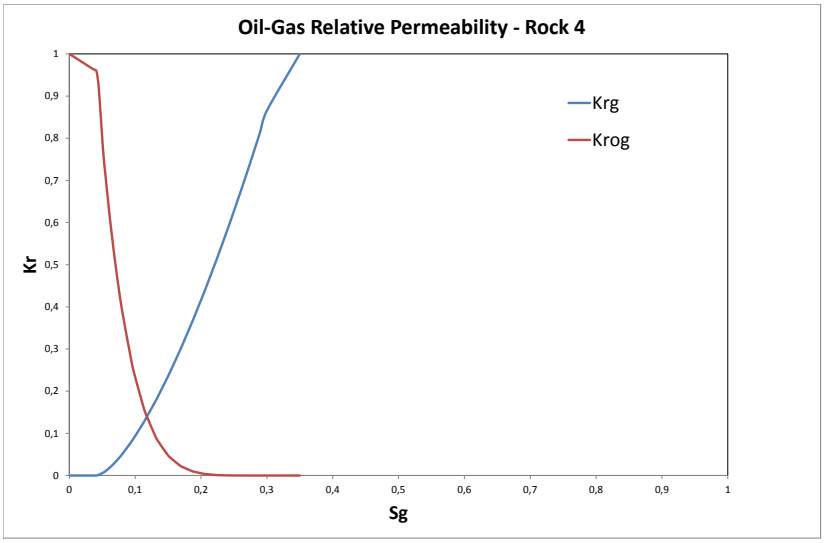

Figure 88: Gas-Oil Drainage Curve, Rock 4.

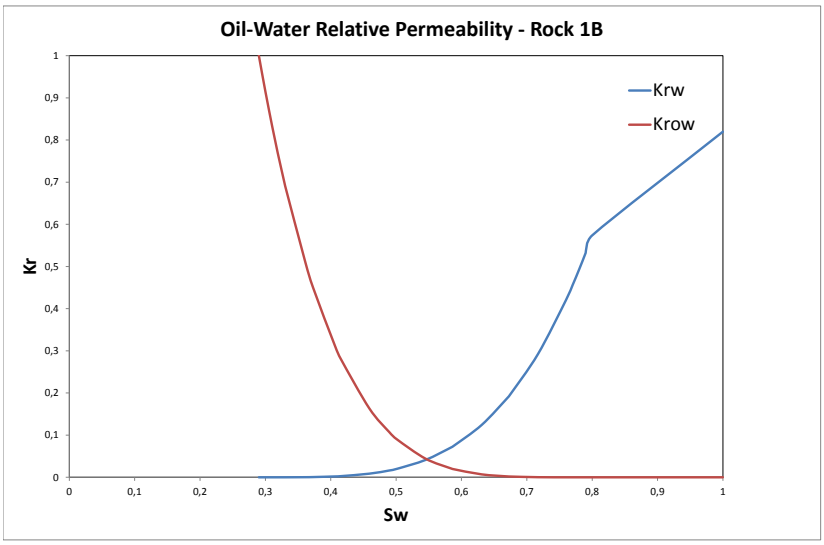

Figure 89: Oil-Water Imbibition Curve, Rock 1B.

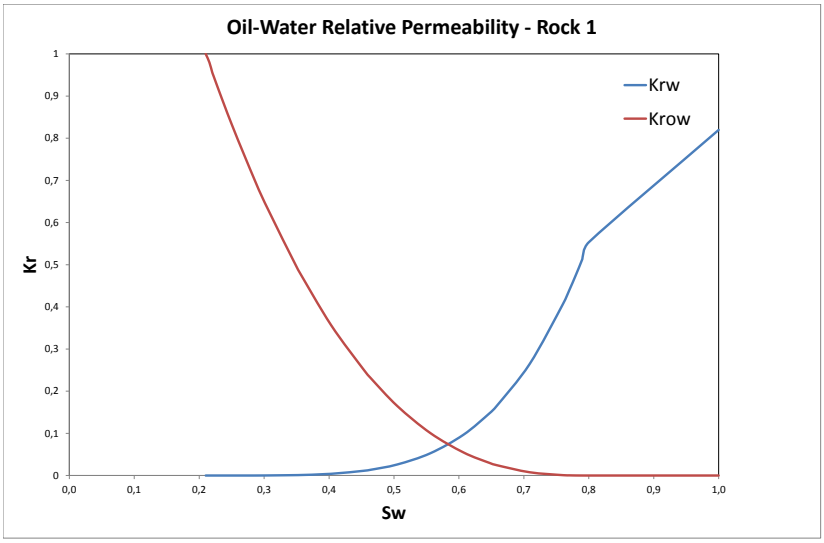

Figure 90: Oil-Water Imbibition Curve, Rock 1.

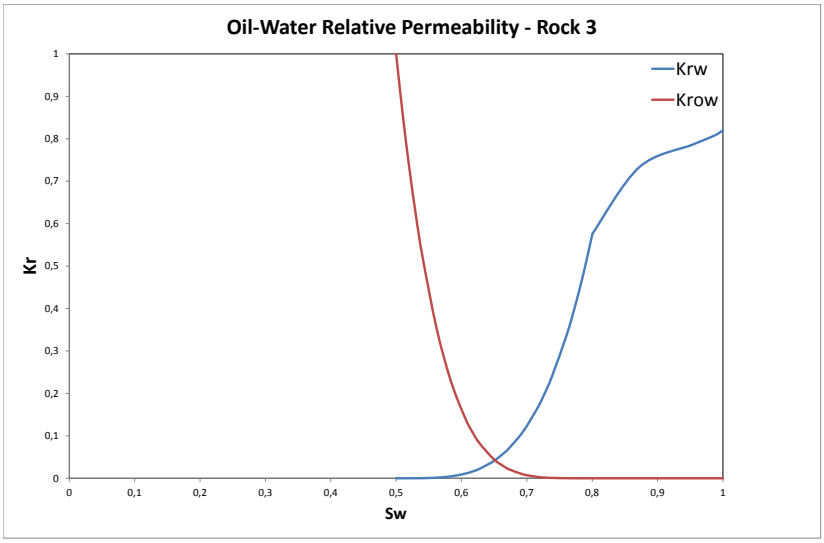

Figure 91: Oil-Water Imbibition Curve, Rock 3.

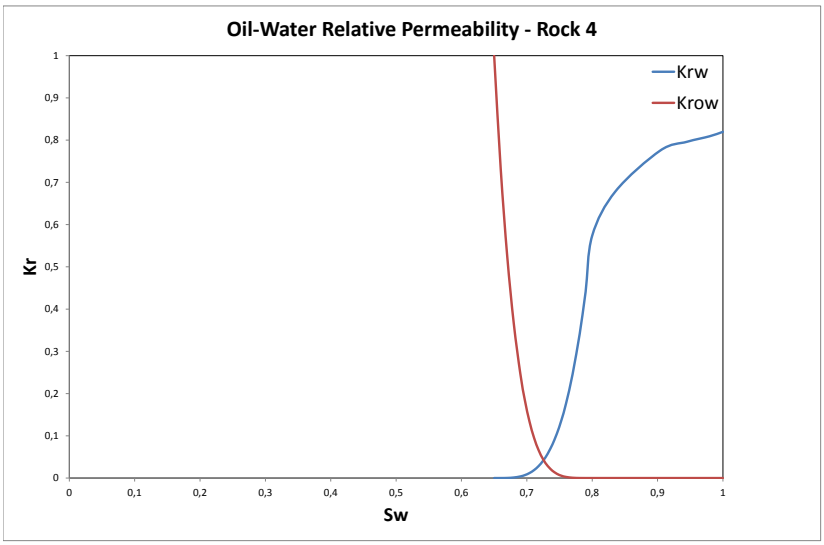

Figure 92: Oil-Water Imbibition Curve, Rock 4.

A.2 New Curves

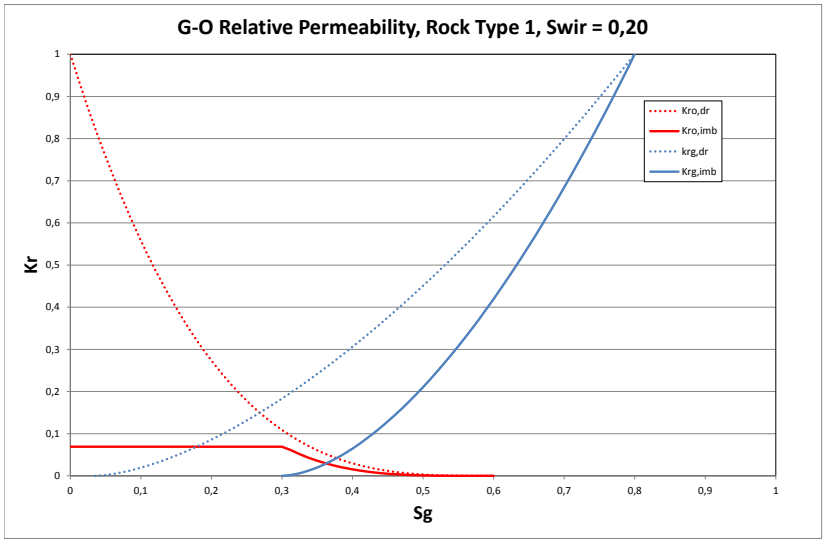

Figure 93: Rocktype 1

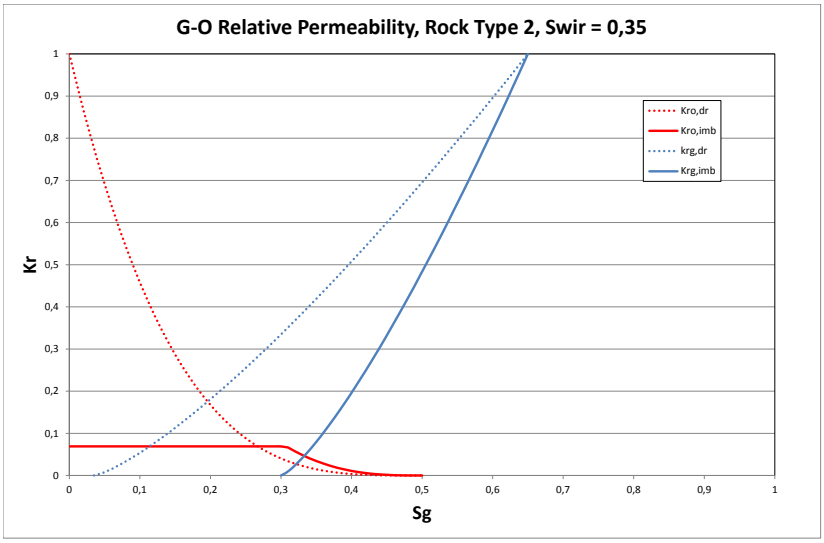

Figure 94: Rocktype 2

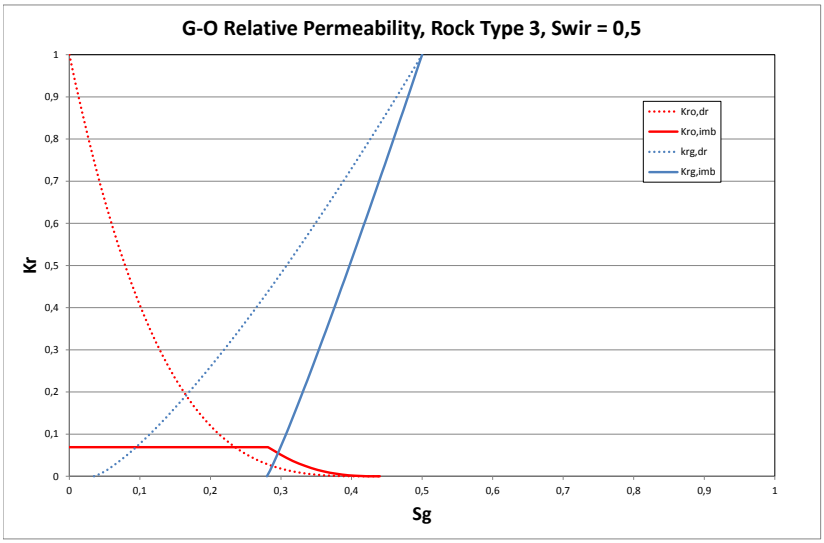

Figure 95: Rocktype 3

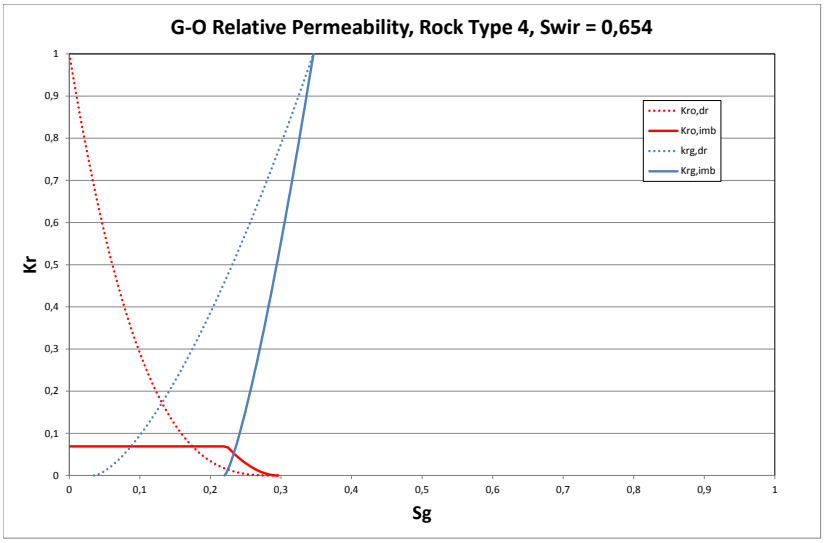

Figure 96: Rocktype 4

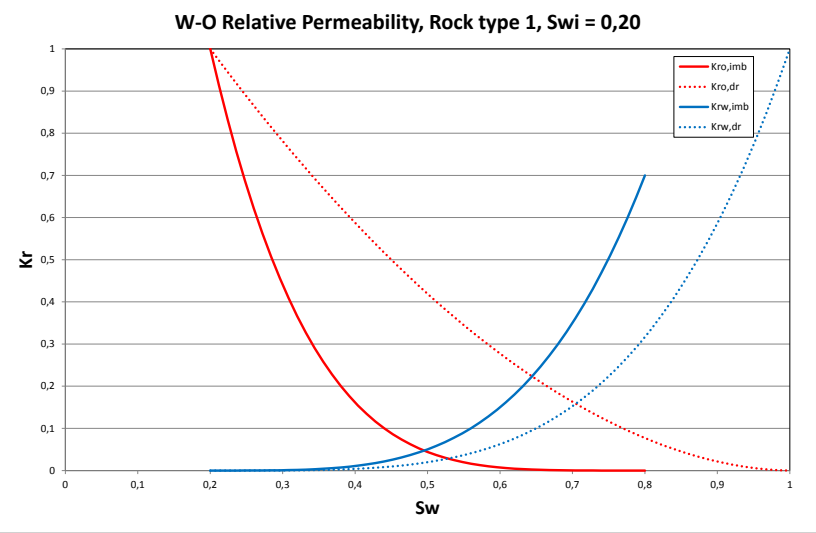

Figure 97: Rocktype 1

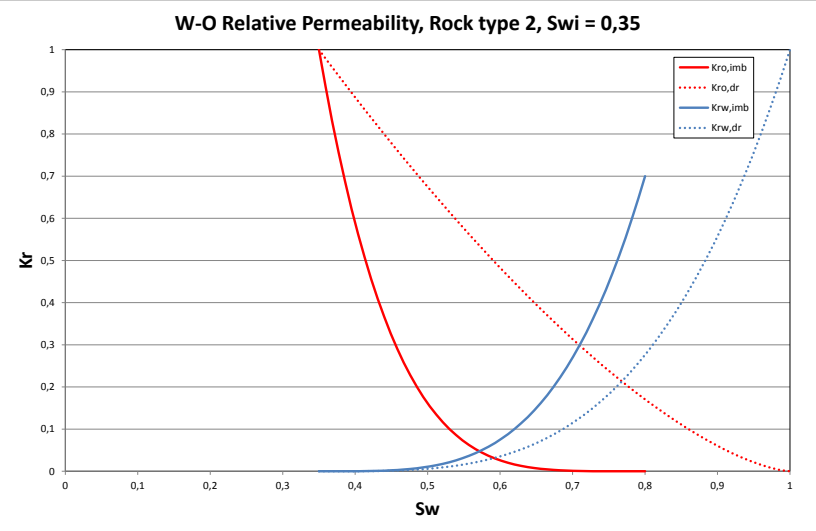

Figure 98: Rocktype 2

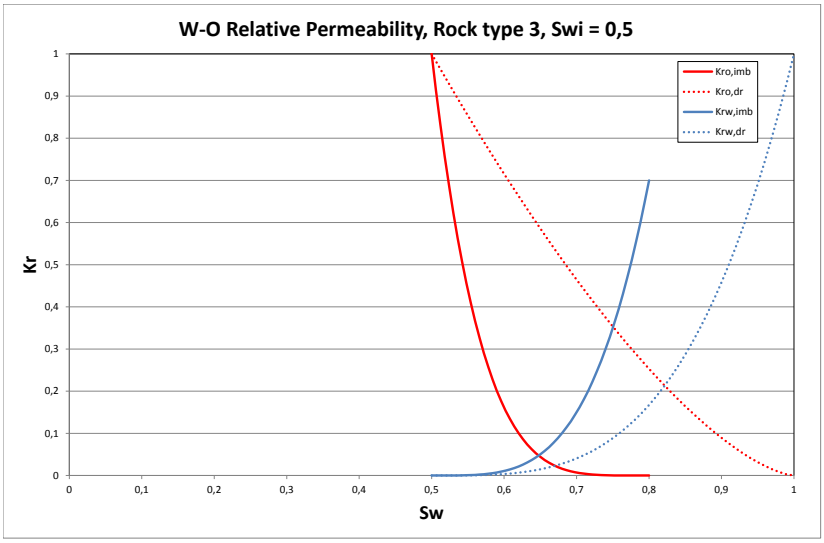

Figure 99: Rocktype 3

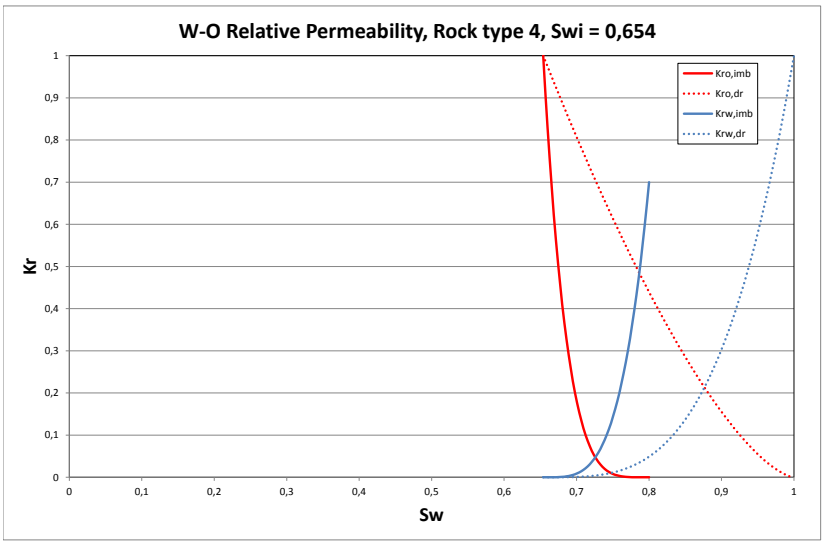

Figure 100: Rocktype 4

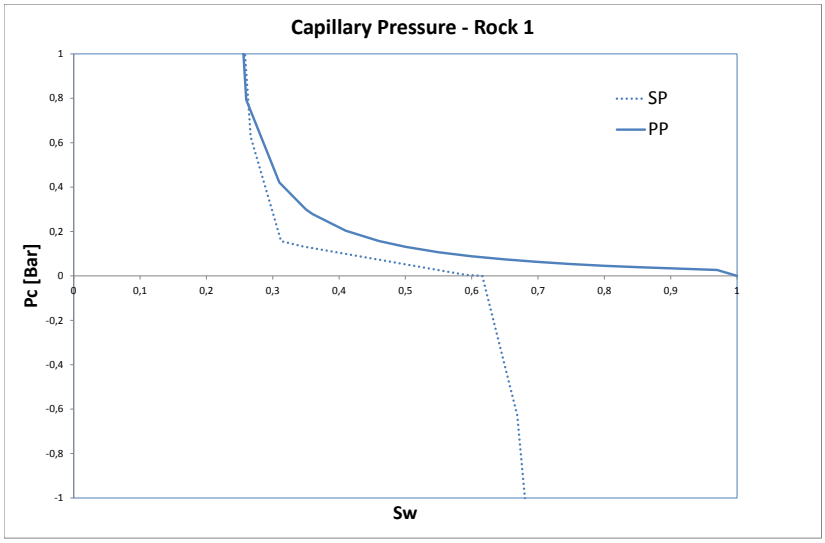

Figure 101: Rocktype 1

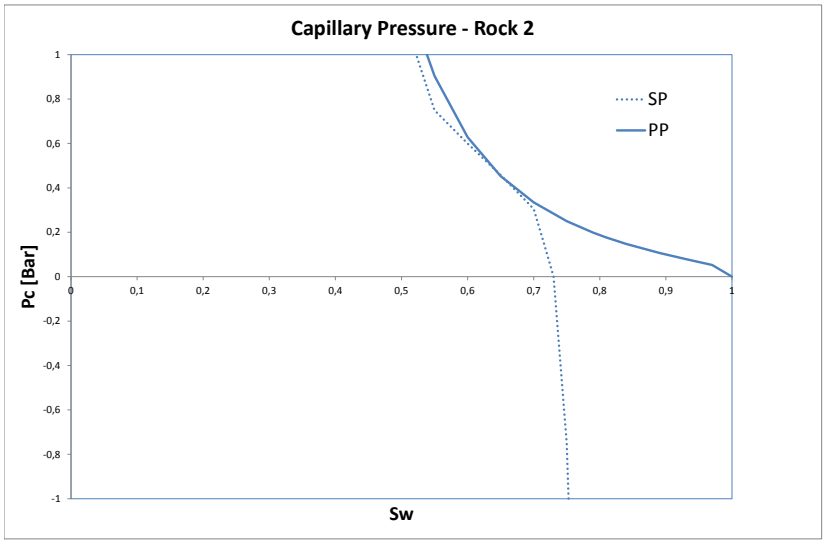

Figure 102: Rocktype 2

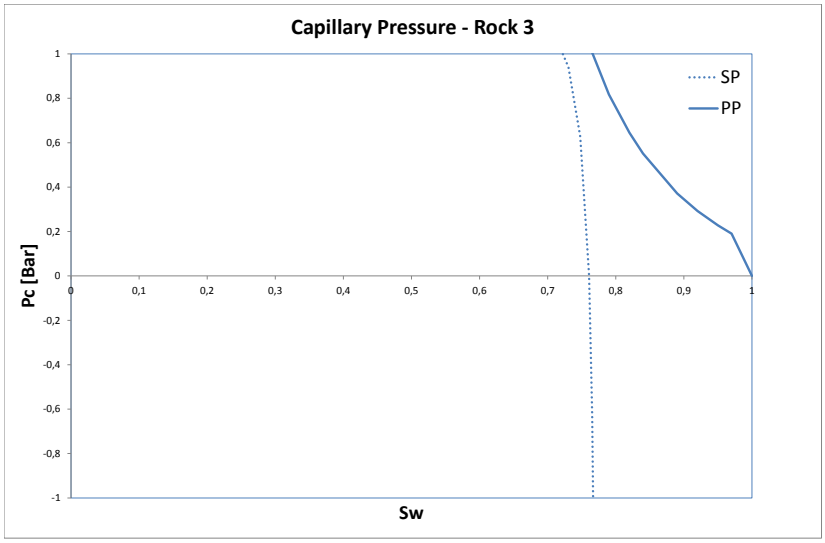

Figure 103: Rocktype 3

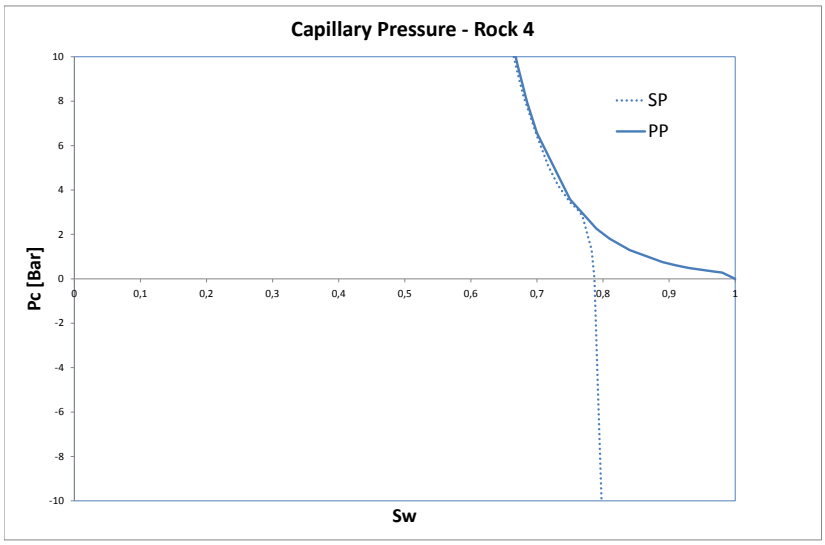

Figure 104: Rocktype 4

A.3 Immiscible CO_2-Injection

Illustration of change in flow pattern with regards to layers at the end of prediction, with an injection pressure of 150 bar. Upper picture showing a reservoir model with no hysteresis. Bottom picture showing reservoir model with hysteresis.

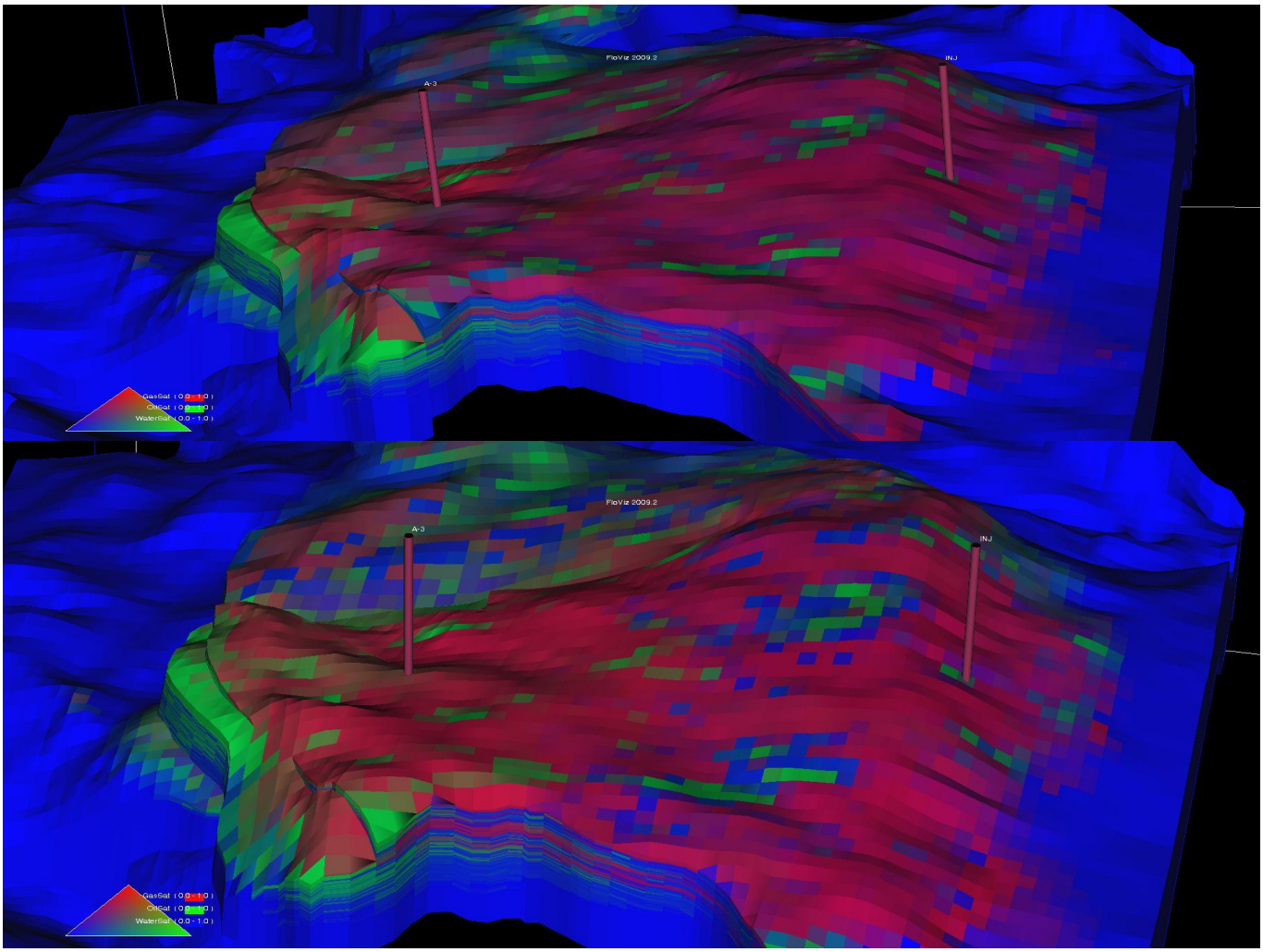

Figure 105: Layer 1.

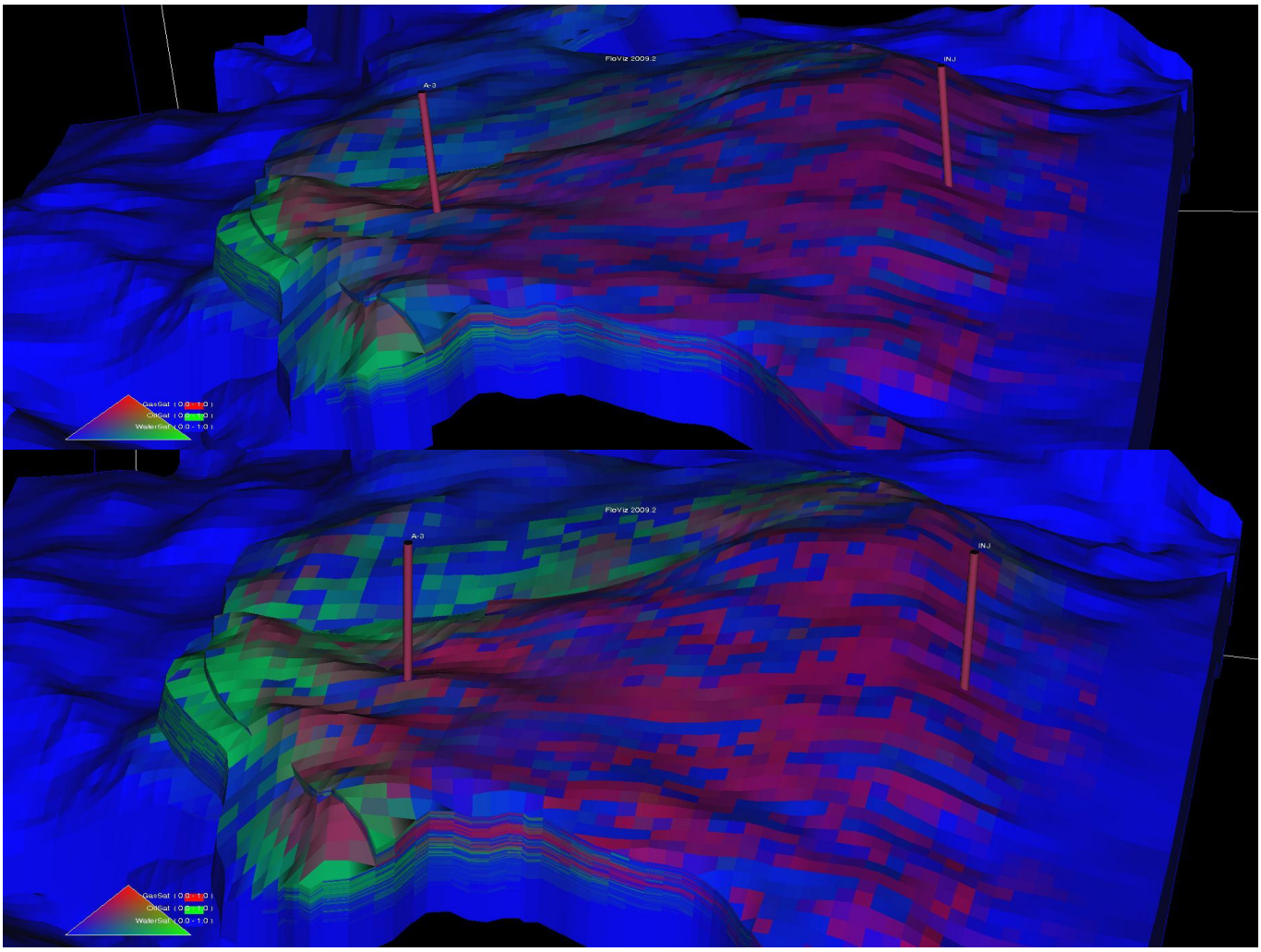

Figure 106: Layer 10.

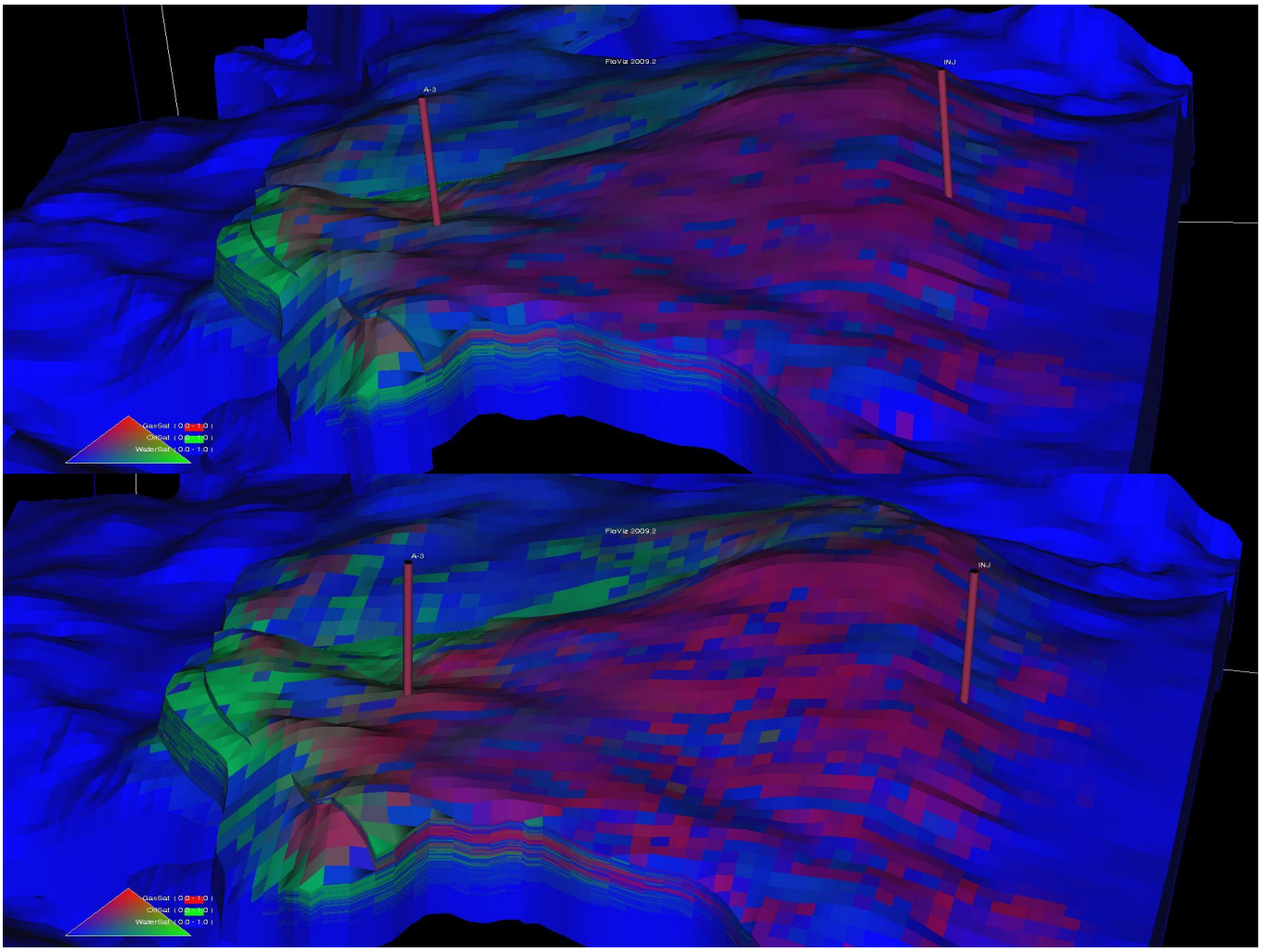

Figure 107: Layer 20.

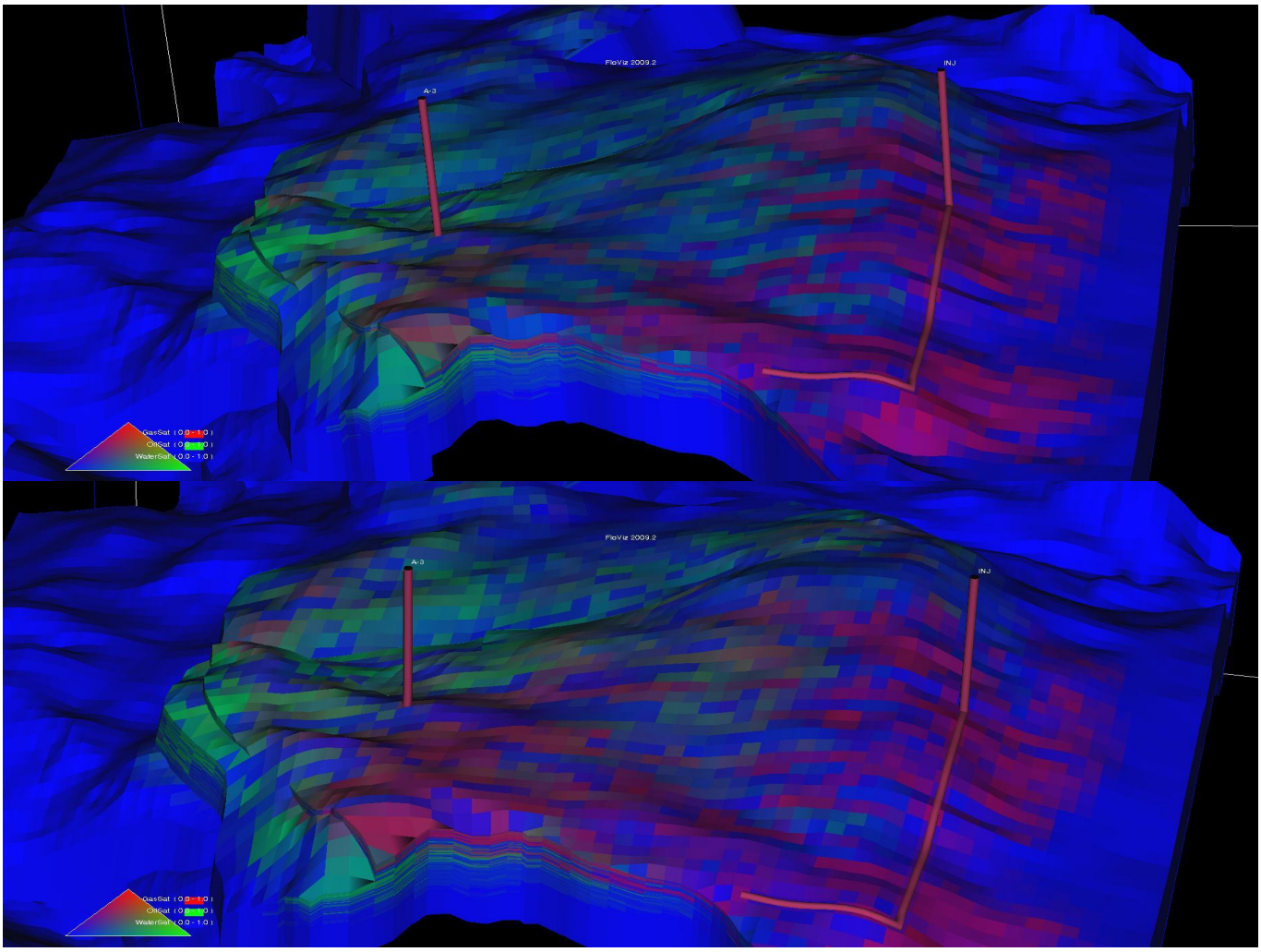

Figure 108: Layer 30.

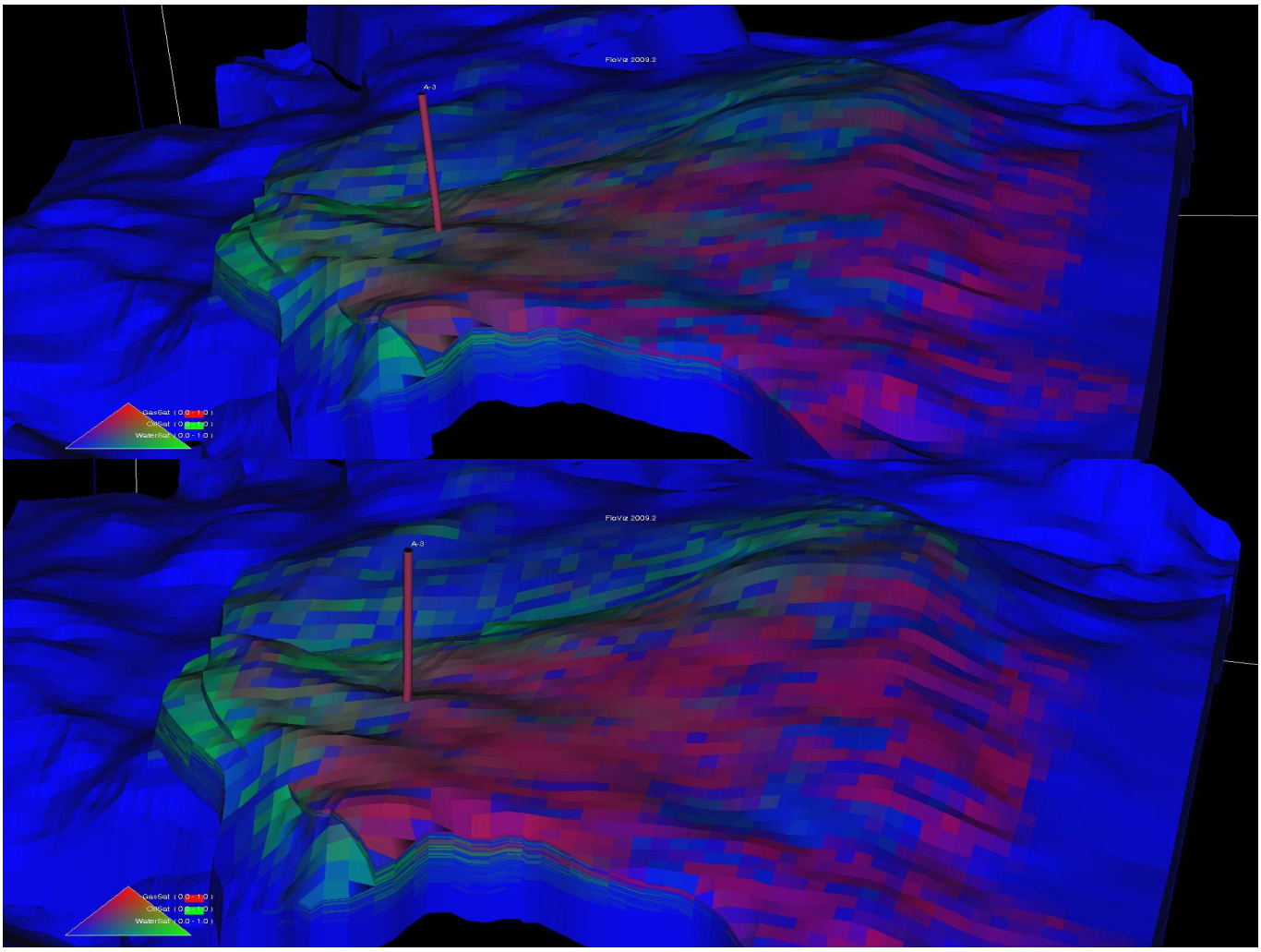

Figure 109: Layer 40.

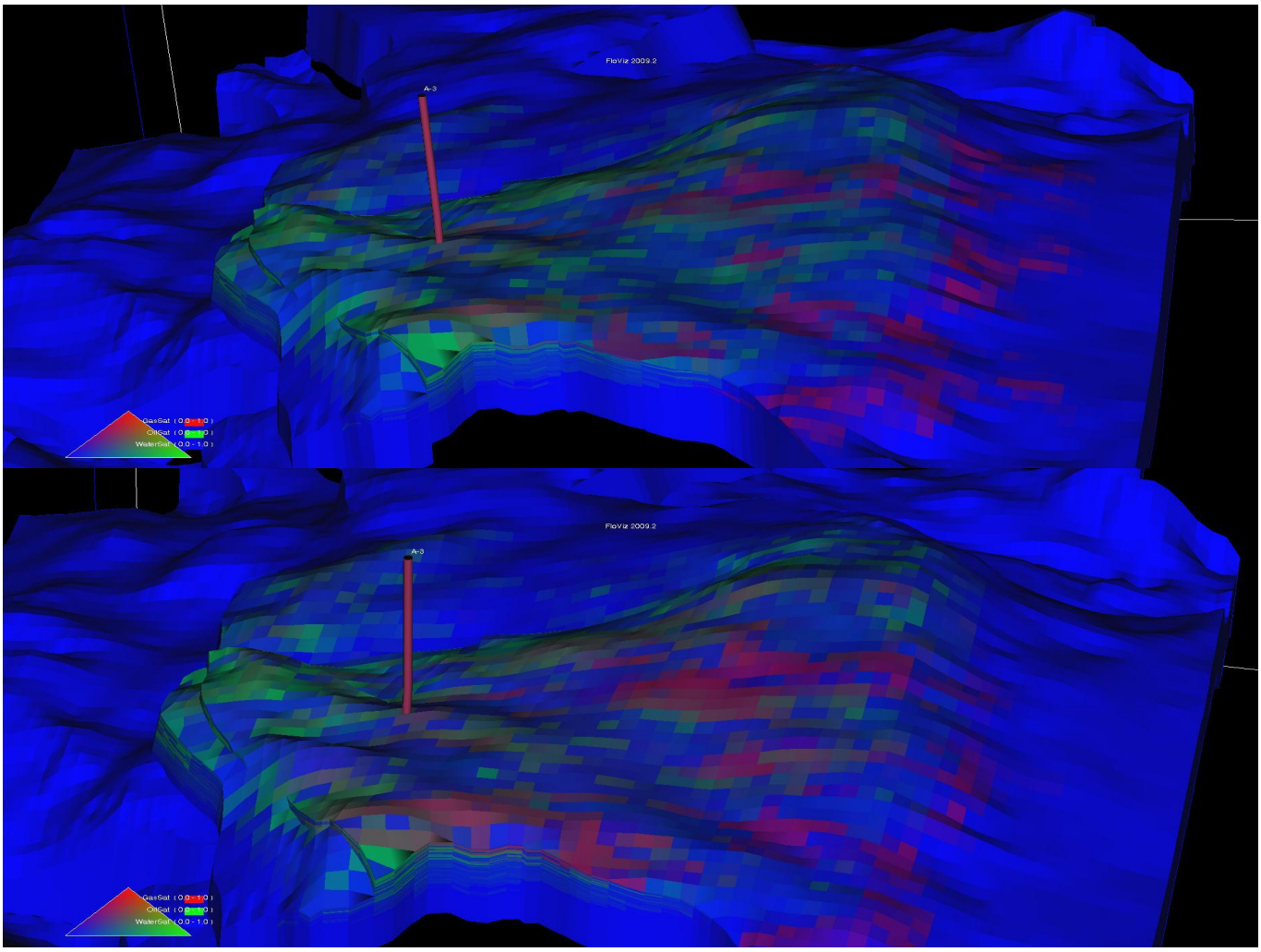

Figure 110: Layer 50.

A.4 Miscible CO_2-Injection

Illustration of change in flow pattern with regards to layers at the end of prediction, with an injection pressure of 310 bar. Upper picture showing a reservoir model with no hysteresis. Bottom picture showing reservoir model with hysteresis.

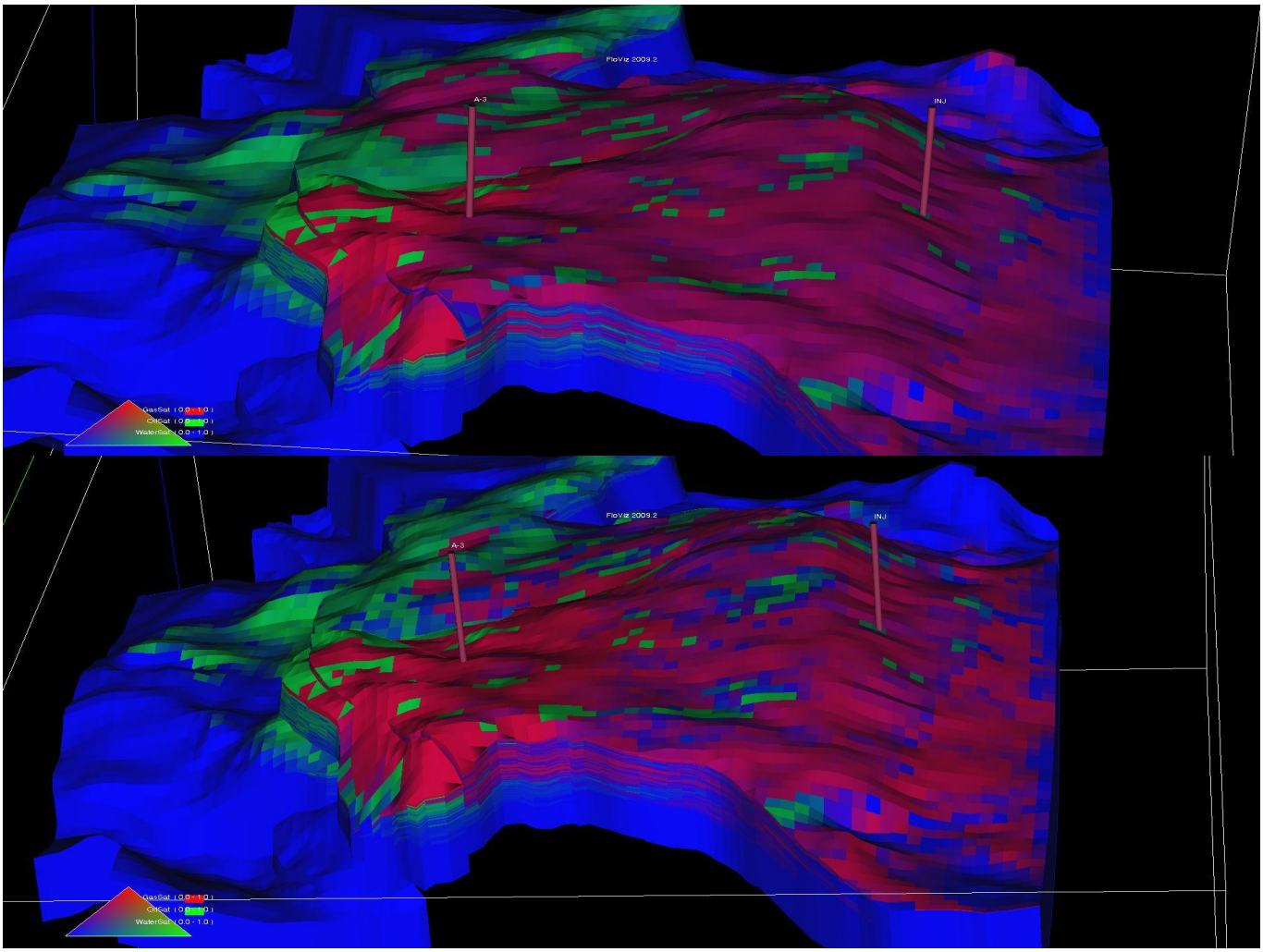

Figure 111: Layer 1.

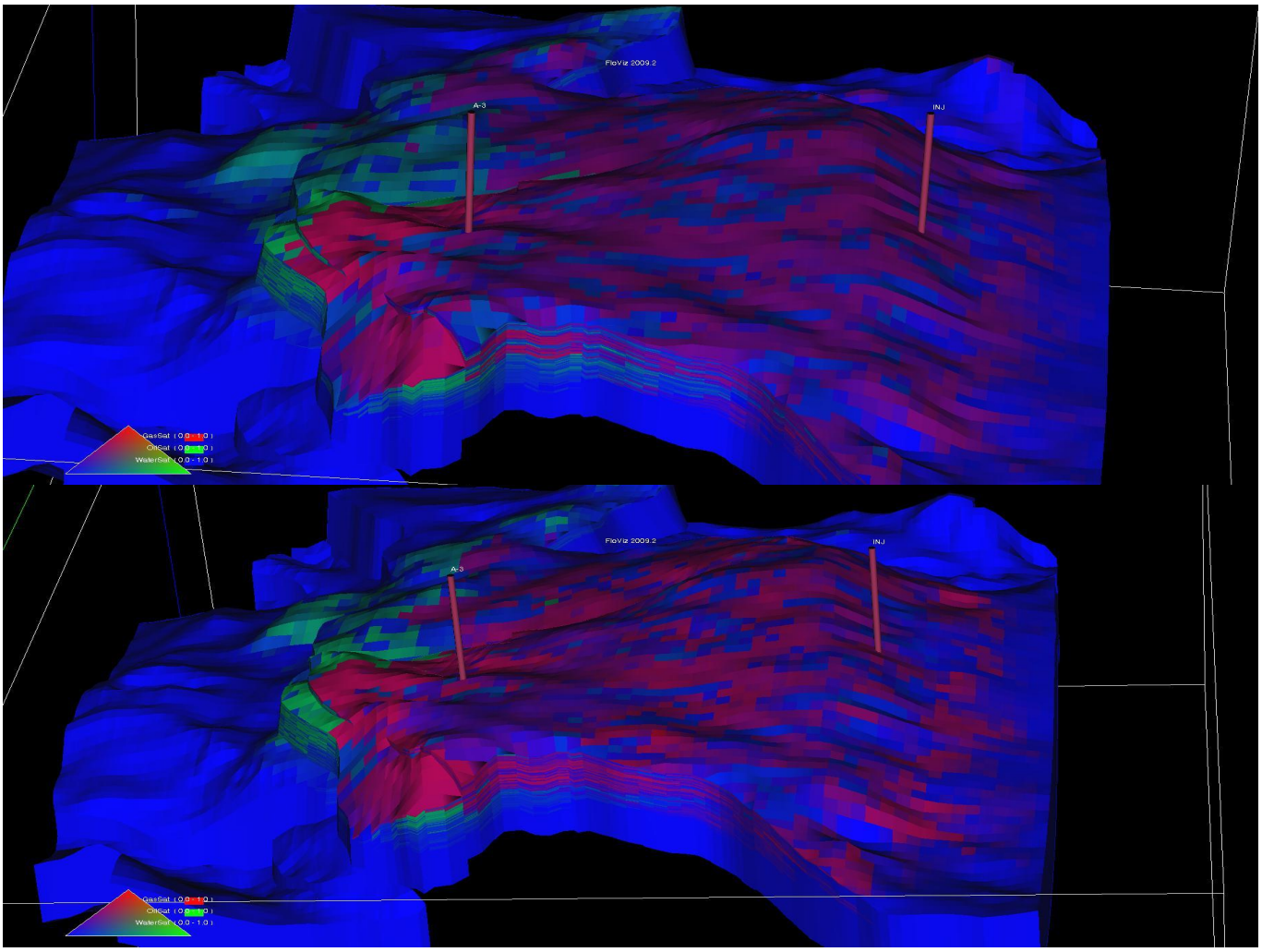

Figure 112: Layer 10.

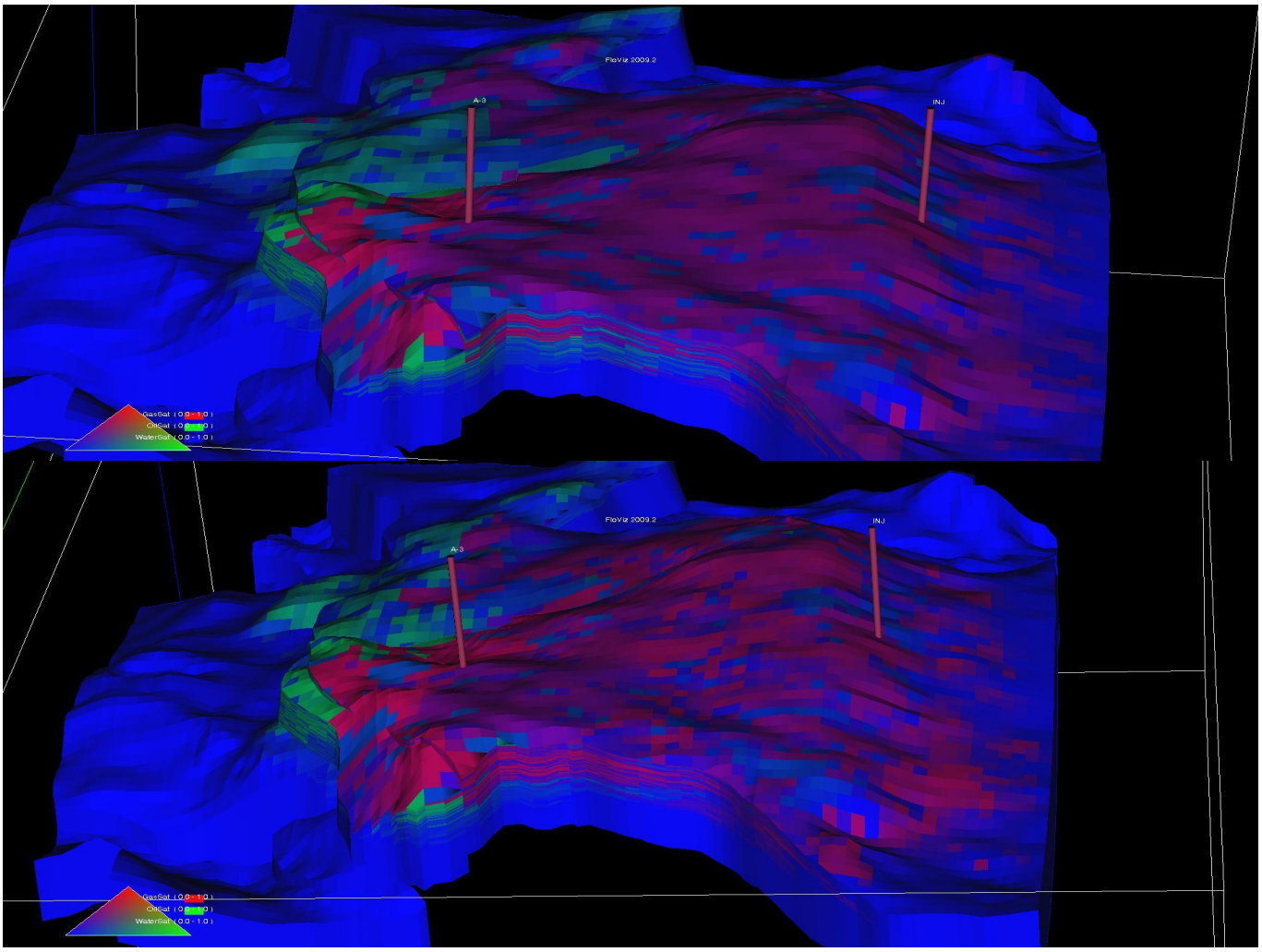

Figure 113: Layer 20.

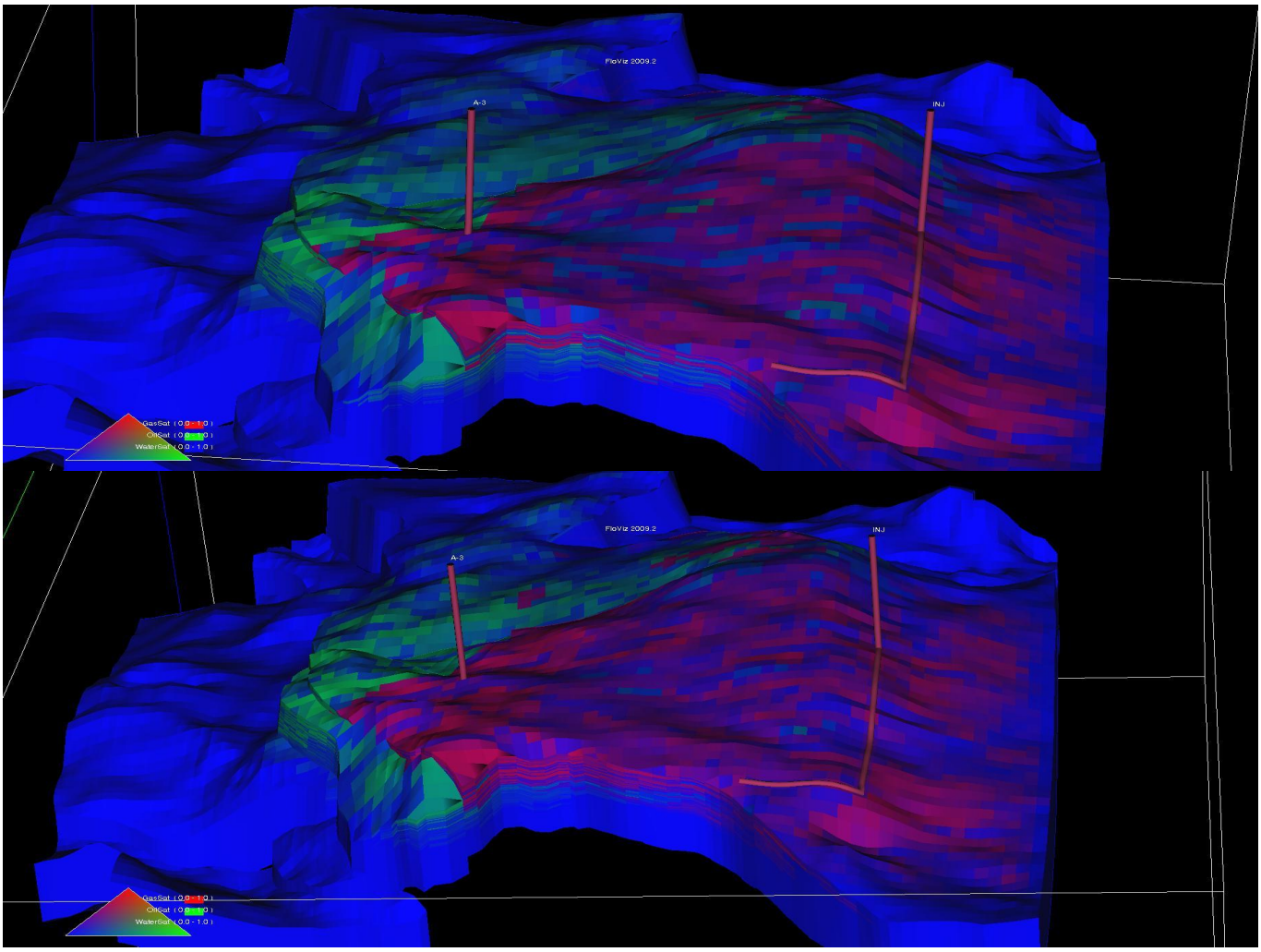

Figure 114: Layer 30.

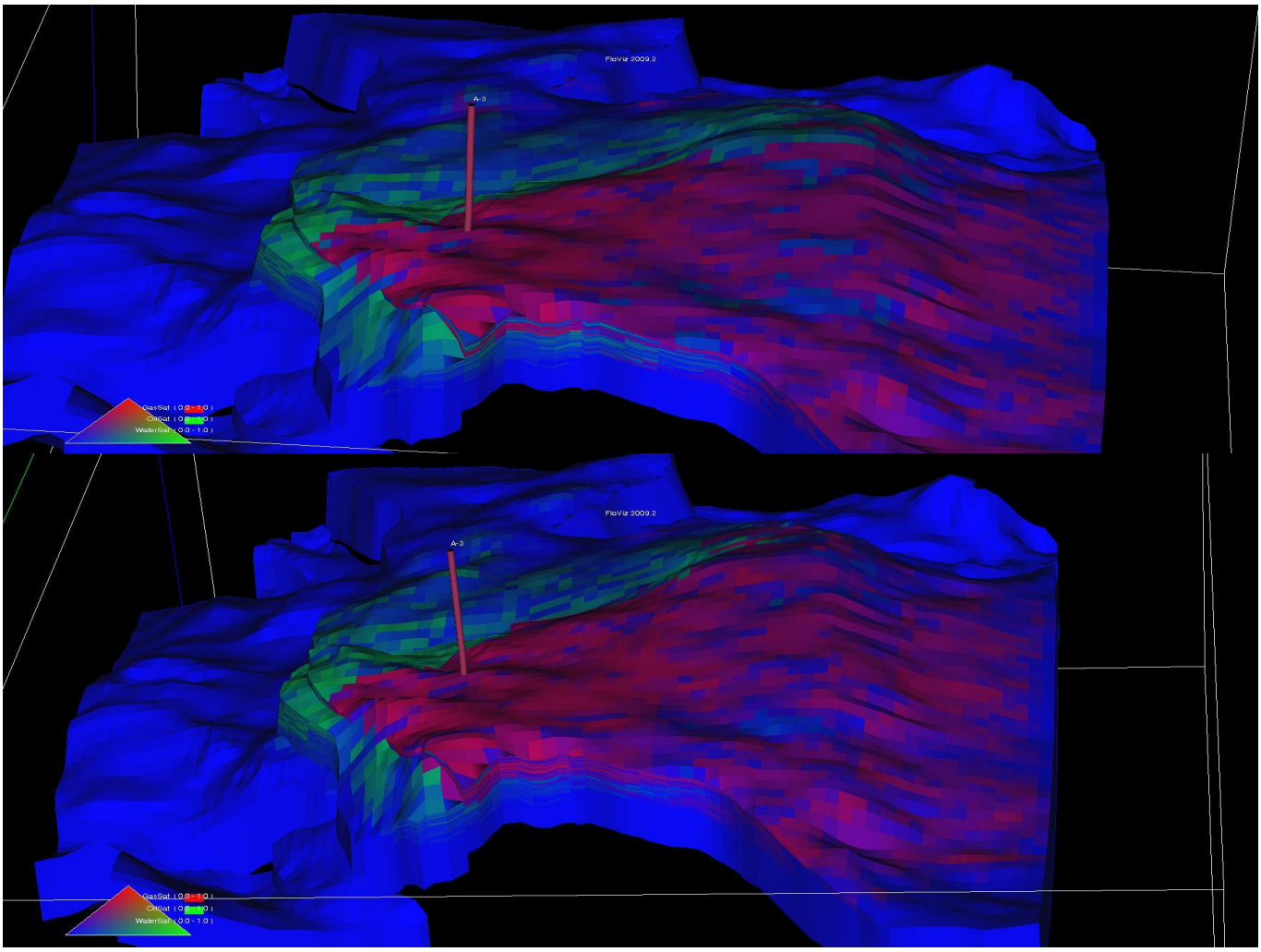

Figure 115: Layer 40.

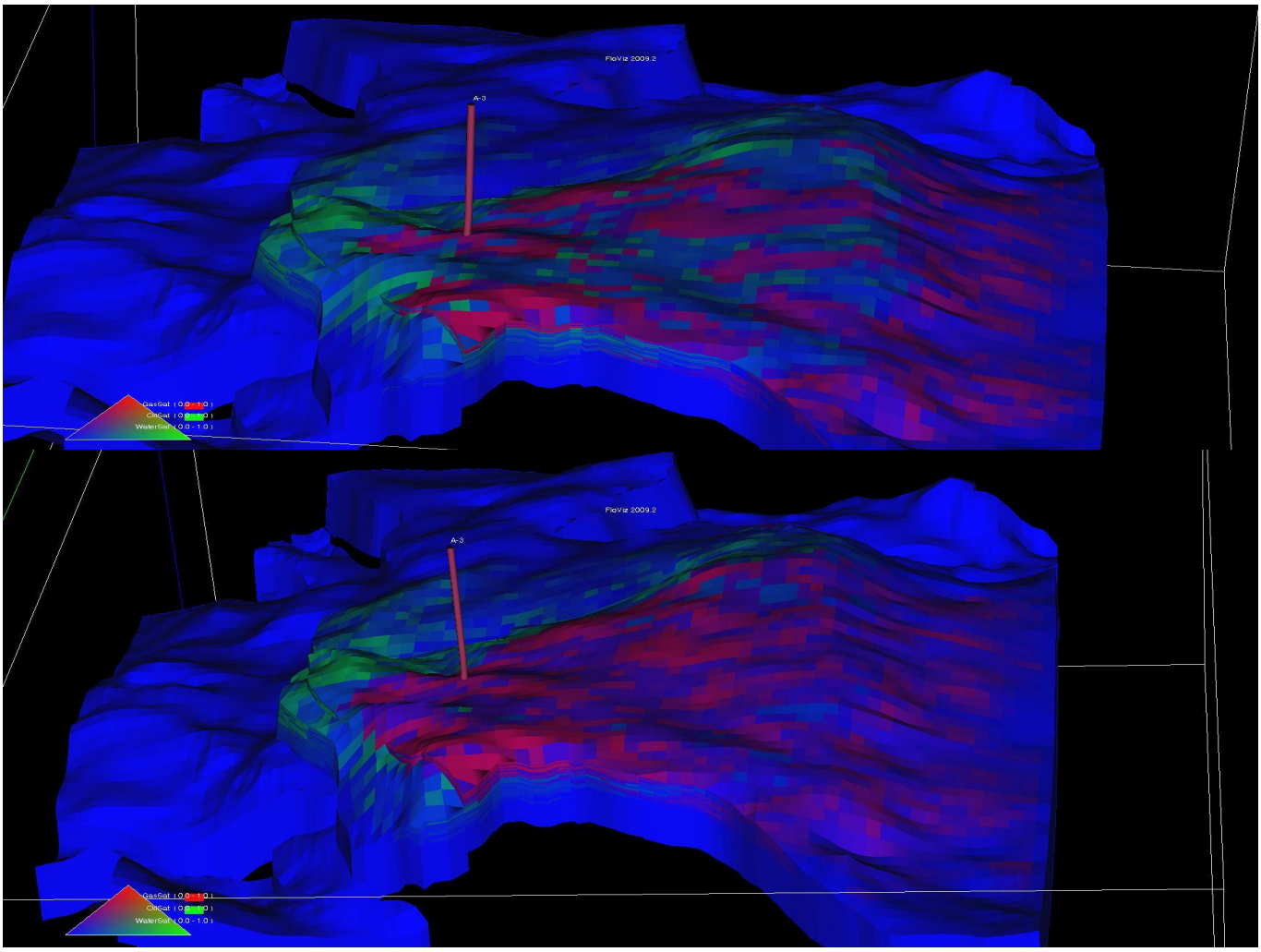

Figure 116: Layer 50.

A.5 ODD3P Immiscible Conditions

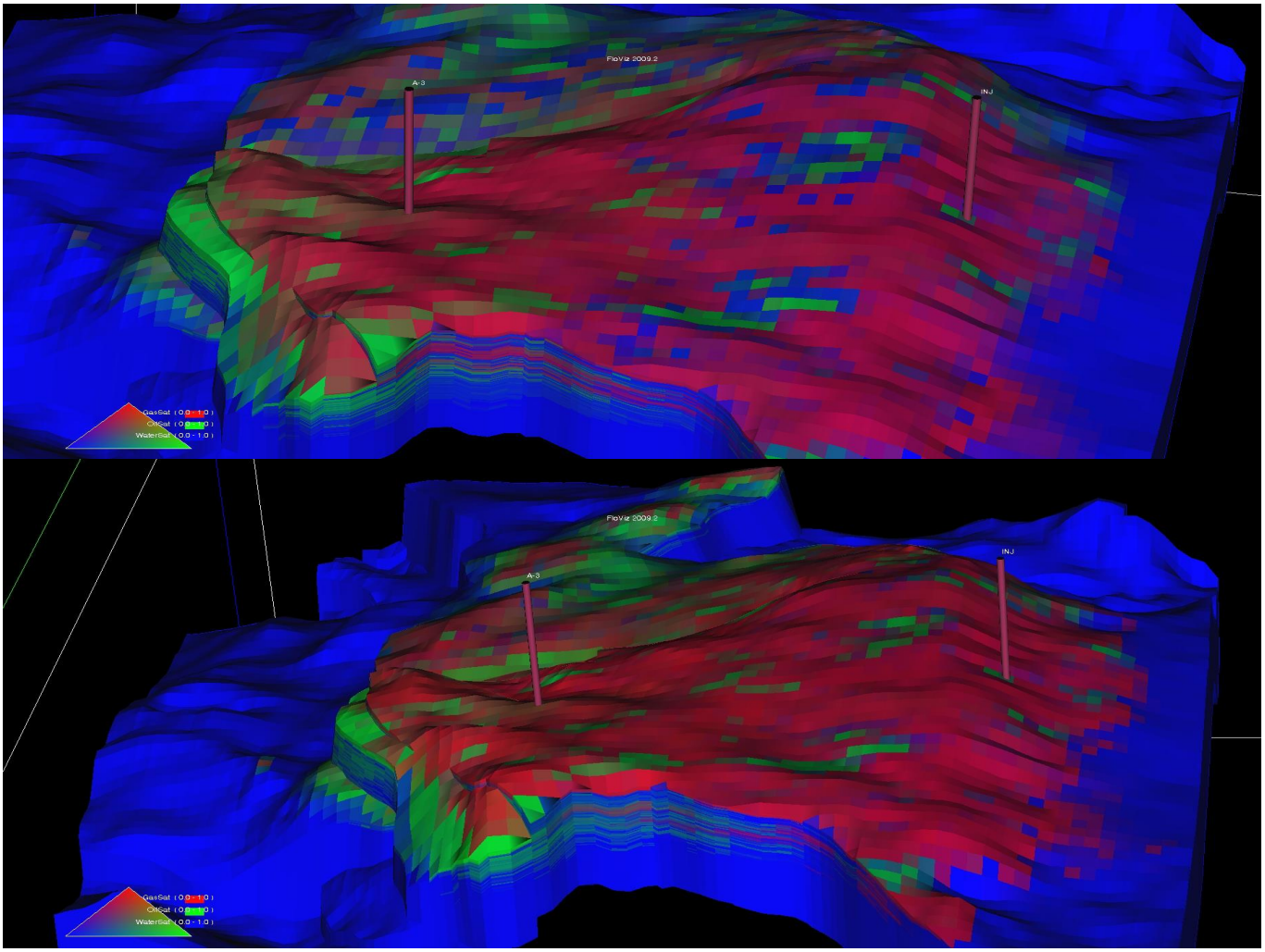

Figure 117: Layer 1.

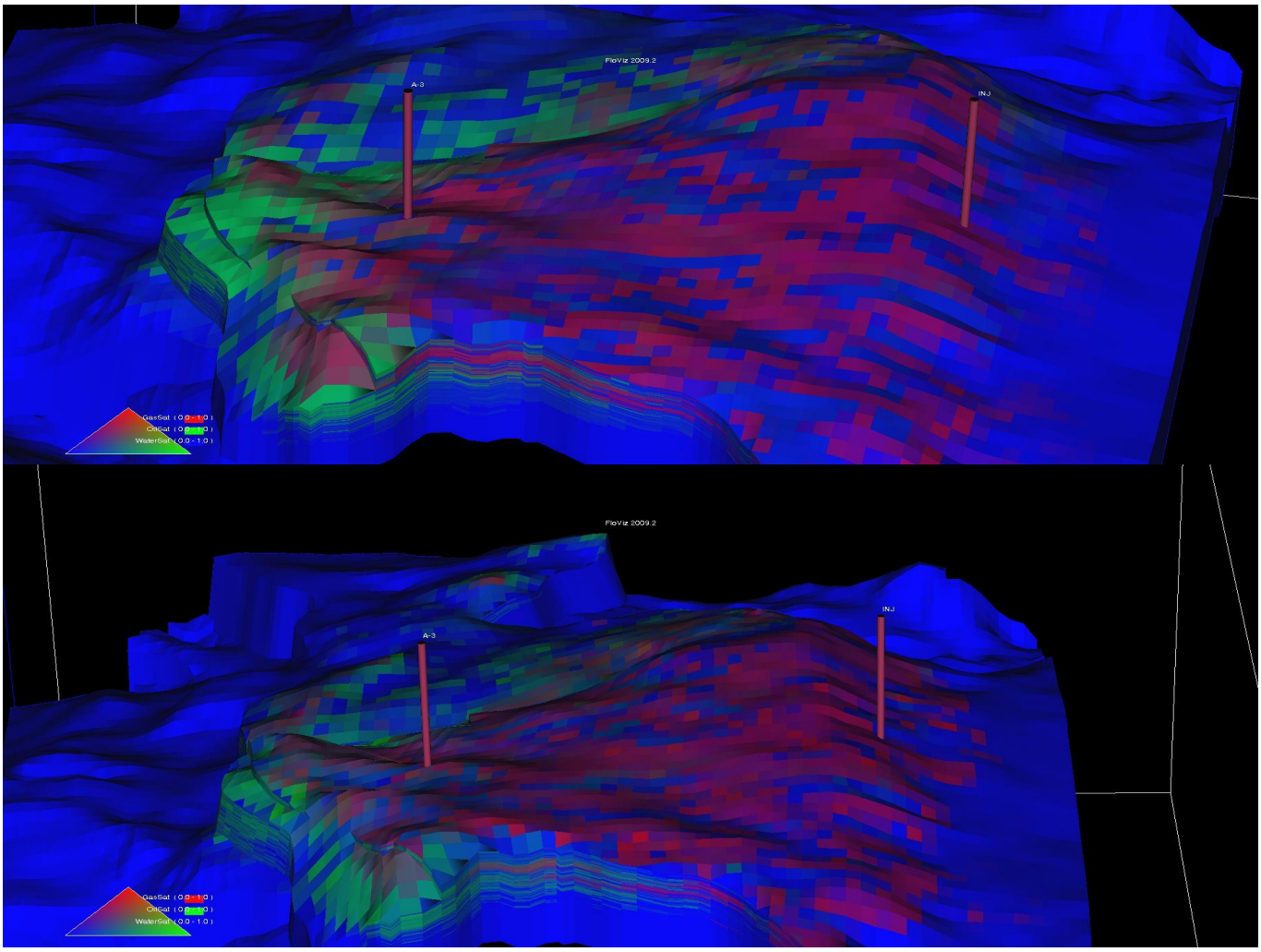

Figure 118: Layer 10.

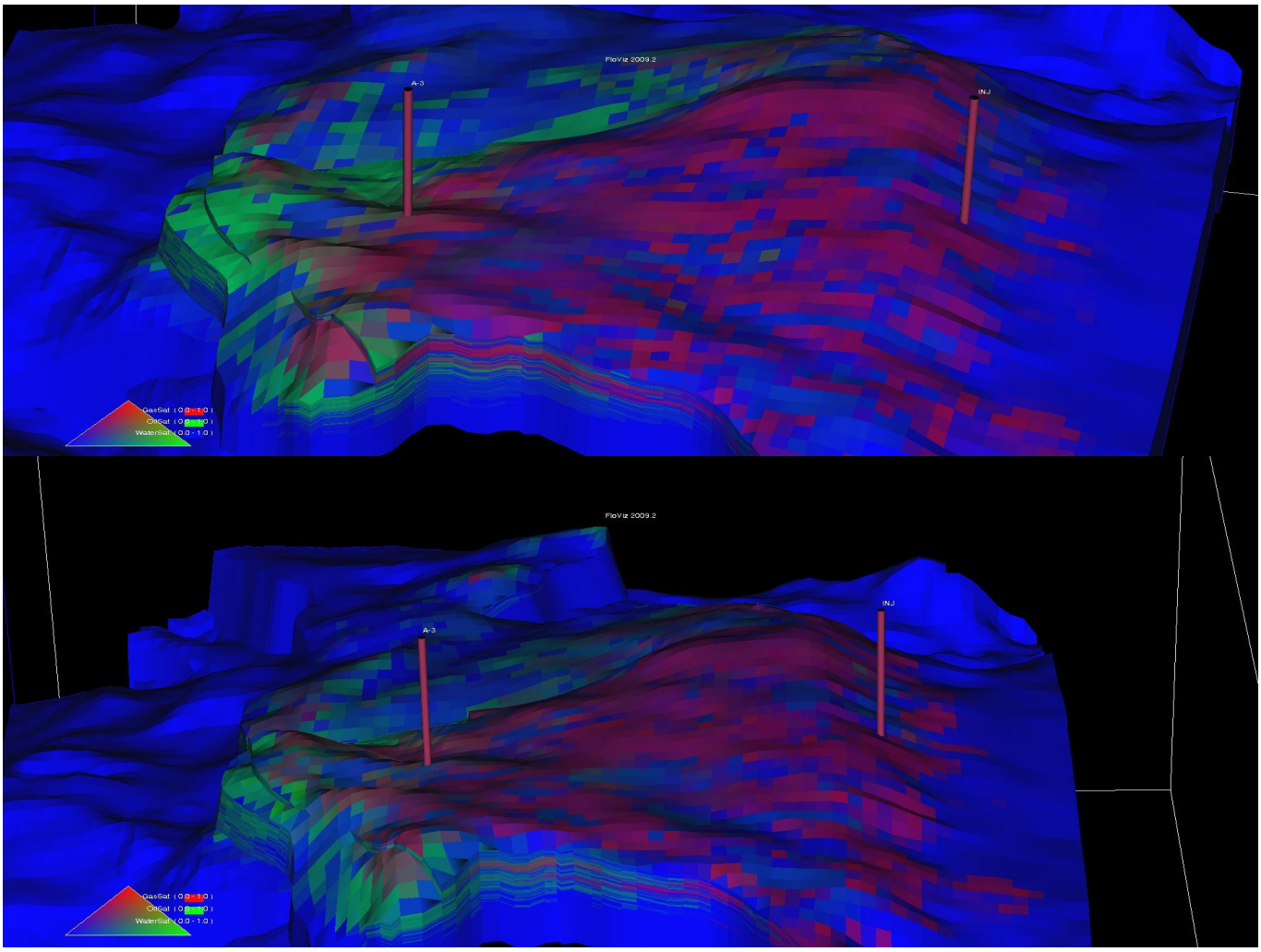

Figure 119: Layer 20.

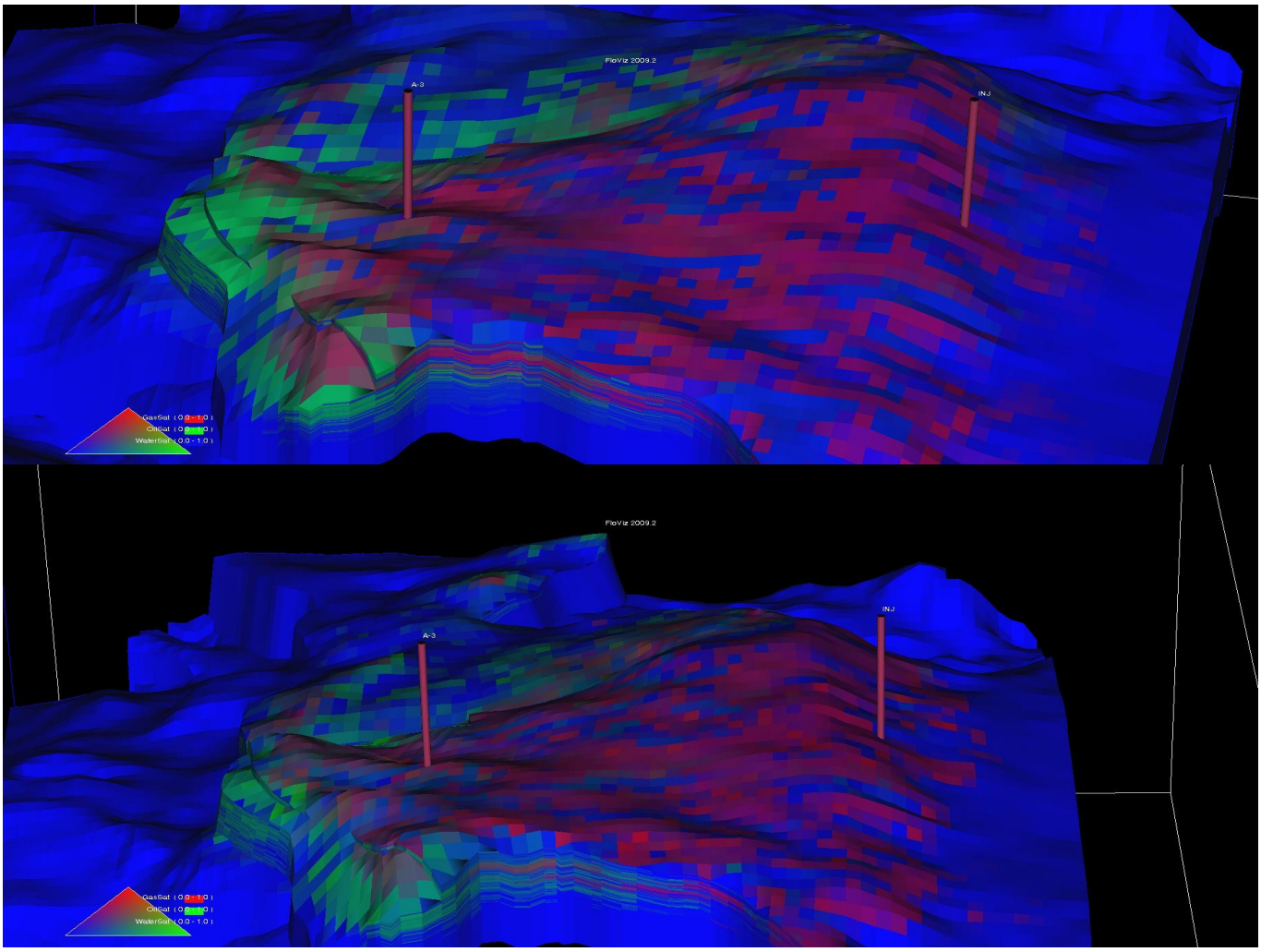

Figure 120: Layer 30.

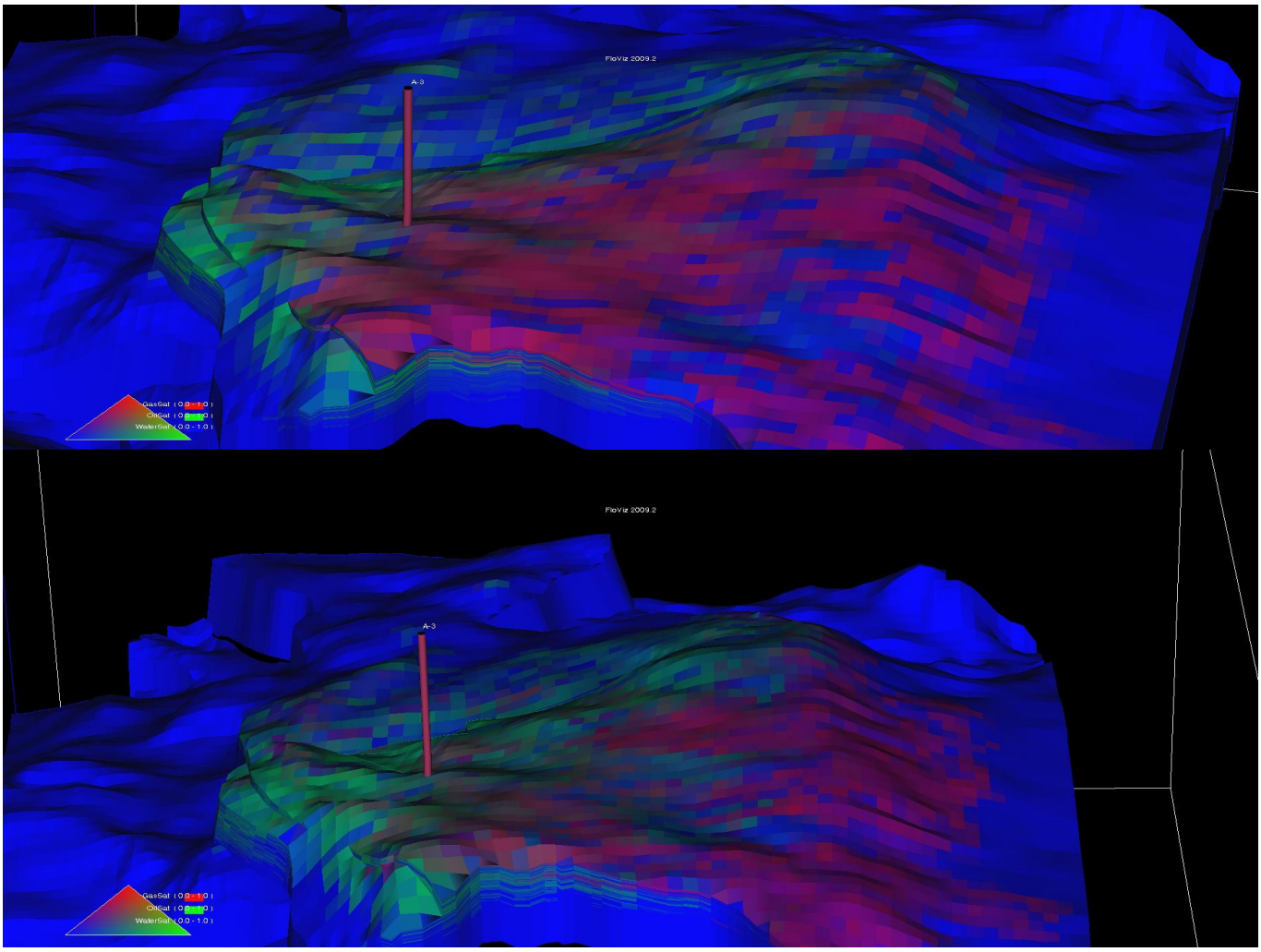

Figure 121: Layer 40.

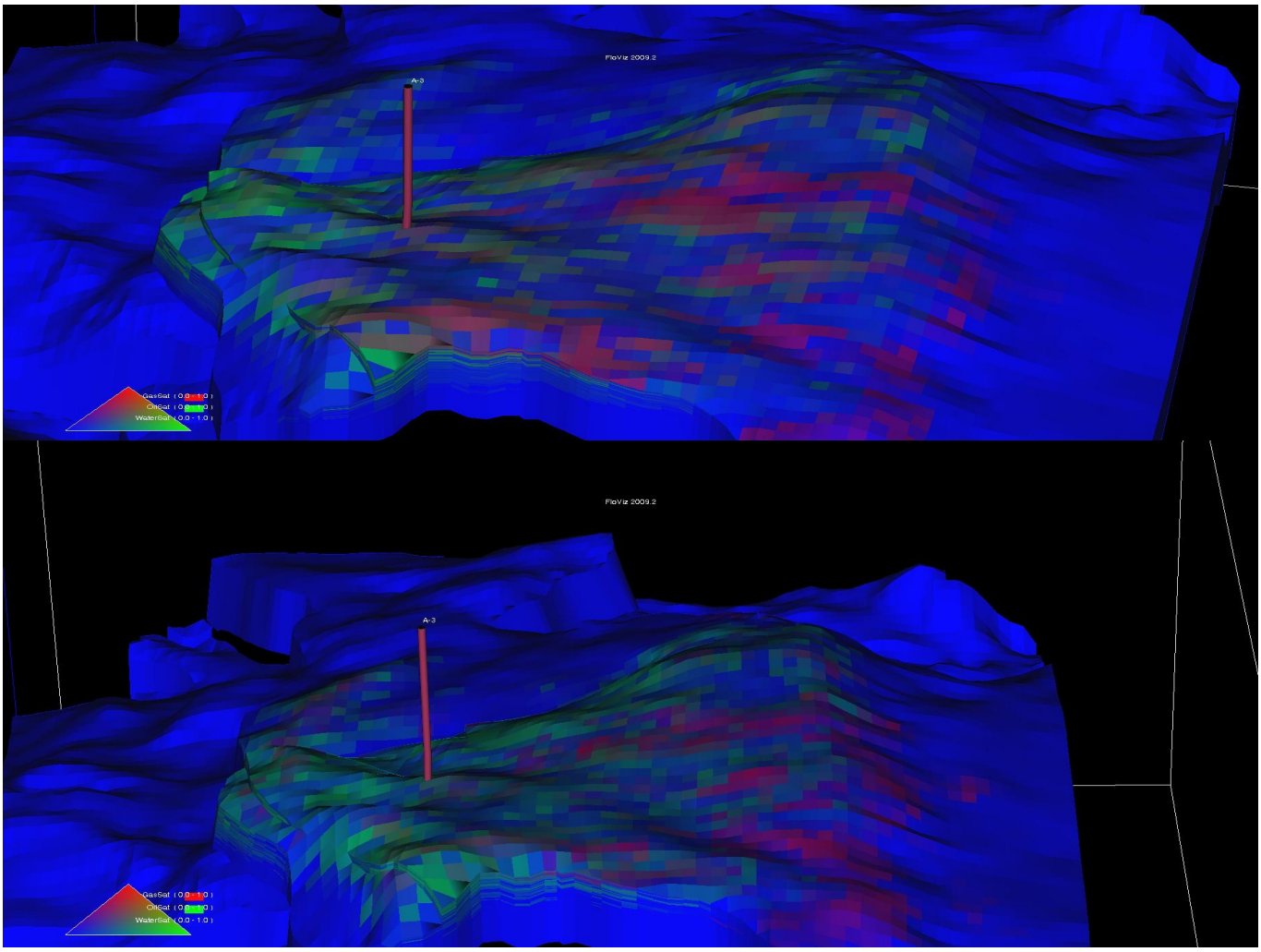

Figure 122: Layer 50.

B Appendix

B.1 Data File

```
-- ******************************************************
RUNSPEC
-- ******************************************************

-- Simulation run title
TITLE
Statoil1

NOECHO

PARALLEL
  4 /

VECTABLE
 8000 /
-- -----------------------------------------------------
-- Simulation grid dimension (Imax, Jmax, Kmax)
DIMENS
    89  104 207 /

-- -----------------------------------------------------
-- Simulation run start
START
 21 DEC 2002 /
-- -----------------------------------------------------
--Activate "Data Check Only" option
--NOSIM

COMPS
 9 /
-- -----------------------------------------------------
-- Fluid phases present
OIL
GAS
WATER
-- -----------------------------------------------------
-- Measurement unit used
METRIC
-- -----------------------------------------------------
--Use saturation table end-point scaling
ENDSCALE
 /
--Table dimensions
TABDIMS
-- NTSFUN NTPVT NSSFUN NPPVT NTFIP NRPVT
     10    /
-- -----------------------------------------------------
-- Dimensions for equilibration tables
EQLDIMS
```

```
  /
-- ------------------------------------------------
--Regions dimension data
REGDIMS
-- NTFIP NMFIPR NRFREG NTFREG
    1    /
-- ------------------------------------------------
--Dimension for well data
WELLDIMS
 3 8* 23 /
-- ------------------------------------------------
--Production well VFP table dimension
VFPPDIMS
--MXMFLO MXMTHP MXMWFR MXMGFR MXMALQ NMMVFT
  15     10      10      10      1      8  /
 /

- ------------------------------------------------
--Summary file dimensions
SMRYDIMS
  /
-- ------------------------------------------------
-- Input and output files format
UNIFIN
UNIFOUT

-- Numerical solution method
AIM
-- Allow horizontal completions
HWELLS
--Allow Hysteresis Option
SATOPTS
 'HYSTER'  /

FORMOPTS
NOHCSCAL /
/
FREEZEPC
/
RUNSUM

-- ************************************************************************
-- In this section simulation grid and static reservoir parameters are given
-- ************************************************************************

GRID

-- ************************************************
------------------------------------------------------

--
--Disable echoing of the input file
NOECHO
```

```
--
--Requests output of an INIT file
--INIT

--
--Control output of the Grid geometry file
GRIDFILE
  0 1  /

--Message print and stop limits
MESSAGES
10000000 /

--
--Generates connections across pinched-out layers
PINCH
 0.01  GAP  1  ALL  TOP  /


MINPV
 10 /


MINNNCT
 0 /
NOECHO
-- ------------------------------------------------
--Include simulation grid
INCLUDE
  '../../../newinclude/east_grid.grdecl' /

NOECHO
-- ------------------------------------------------
--Include ACTNUM data, if any
INCLUDE
  '../../../newinclude/east_actnum.grdecl' /

NOECHO

-- Set lower (water filled) part of model inactive:
EQUALS
     ACTNUM 0  1 89  1 104 132 207 /
/

-- ------------------------------------------------
-- Include faults
-- Make sure that faults' name have 8 characters max.
INCLUDE
  '../../../newinclude/east_all_faults.inc'  /

NOECHO

-- ------------------------------------------------
-- Porosity and permeabiliy:
```

```
INCLUDE
  '../../../newinclude/east_porperm.grdecl' /

NOECHO


COPY
 PERMX PERMY /
/

-- Fault seal
INCLUDE
 'fault_seal_grid.inc' /

-- ***************************************************
-- In this section simulation grid parameters are edited
-- ***************************************************

EDIT

-- ***************************************************
-- Fault seal

MESSAGES
 0 0 1  /

INCLUDE
 'fault_seal_edit.inc' /
-- -------------------------------------------------
-- The pore volume of a row of blocks is increased
-- to model the effect of the aquifer:
INCLUDE
  'aquifer.inc'  /

-- ***************************************************
-- In this section fluid-rock properties and
-- relative permabilities are given
-- ***************************************************

PROPS

MESSAGES
 1000000 1000000 10000 /


-- ***************************************************

-- -------------------------------------------------
-- Relative permeability endpints
NOECHO

-- The following endpoints are set as fields:
--
-- SWL, SGU, SWCR, SWATINIT
```

```
-- Read endpoints (SWL + SWATINIT + Original SWCR = SWATINIT)
INCLUDE
 '../../../newinclude/east_endpoints_swl_swatinit.grdecl' /

-- Reread SWCR (scaled, created by a script)
INCLUDE
 'swcr.inc' /
-- ----------------------------------------------------
-- Next 2 keywords are used to make maximum gas saturation consistent: SGU=1-SWL
--
COPY
 SWL   SGU   /
/
MULTIPLY
 SGU   -1 /
/
ADD
 SGU    1  /
/
------------------------------------------------------------
------------------------------------------------------------
Gas-Oil Rel-perm data:

SGOF
-- Table 1, Rock 1
-- Gas-Oil Imbibition
-- Sg Krg Krog Pc
0 0 1 0
0.02 0 0.897192 0
0.04 0 0.801895 0
0.06 0 0.713799 0
0.08 0 0.632596 0
0.1 0 0.557982 0
0.12 0 0.489652 0
0.14 0  0.427308 0
0.16 0 0.37065 0
0.18 0 0.319384 0
0.2 0 0.273217 0
0.22 0 0.231859 0
0.24 0 0.195022 0
0.26 0 0.162423 0
0.28 0 0.133781 0
0.3 0 0.108819 0
0.32 0.005798 0.087261 0
0.34 0.017577 0.068838 0
0.36 0.033627 0.053283 0
0.38 0.053283 0.040334 0
0.4 0.076146 0.029731 0
0.42 0.101938 0.021222 0
0.44 0.130453 0.014558 0
0.46 0.161525 0.009496 0
0.48 0.195022 0.005798 0
0.5 0.230832 0.003235 0
```

```
0.52 0.268859 0.001584 0
0.54 0.30902 0.000631 0
0.56 0.351241 0.000172 0
0.58 0.395458 0.000019 0
0.6 0.441613 0 0
0.62 0.489652 0 0
0.64 0.539528 0 0
0.66 0.591197 0 0
0.68 0.644617 0 0
0.7 0.699752 0 0
0.72 0.756566 0 0
0.74 0.815028 0 0
0.76 0.875106 0 0
0.78 0.936772 0 0
0.8 1 0 0

-- Table 2. Rock 1B
-- Gas-Oil Imbibition
-- Sg Krg Krog Pc
0 0 1 0
0.02 0 0.88522 0
0.04 0 0.779838 0
0.06 0 0.68342 0
0.08 0 0.595531 0
0.1 0 0.515743 0
0.12 0 0.443631 0
0.14 0 0.378773 0
0.16 0 0.320751 0
0.18 0 0.269153 0
0.2 0 0.223569 0
0.22 0 0.183595 0
0.24 0 0.148833 0
0.26 0 0.118886 0
0.28 0 0.093368 0
0.3 0 0.071893 0
0.32 0.019403 0.054084 0
0.34 0.047777 0.039571 0
0.36 0.080935 0.027989 0
0.38 0.11764 0.018981 0
0.4 0.157231 0.012199 0
0.42 0.199284 0.007303 0
0.44 0.243503 0.003963 0
0.46 0.289663 0.00186 0
0.48 0.337592 0.000689 0
0.5 0.387148 0.000162 0
0.52 0.438215 0 0
0.54 0.490696 0 0
0.56 0.544506 0 0
0.58 0.599574 0 0
0.6 0.655836 0 0
0.62 0.713235 0 0
0.64 0.771721 0 0
0.66 0.831248 0 0
0.68 0.891777 0 0
```

```
0.7 0.953269 0 0
0.715 1 0 0
/
-- Table 3. Rock 2
-- Gas-Oil Imbibition
-- Sg Krg Krog Pc
0 0 1 0
0.02 0 0.891989 0
0.04 0 0.791783 0
0.06 0 0.69912 0
0.08 0 0.613737 0
0.1 0 0.535367 0
0.12 0 0.463744 0
0.14 0 0.398594 0
0.16 0 0.339645 0
0.18 0 0.286618 0
0.2 0 0.239234 0
0.22 0 0.197209 0
0.24 0 0.160254 0
0.26 0 0.128078 0
0.28 0 0.100385 0
0.3 0 0.076872 0
0.32 0.024213 0.057233 0
0.34 0.05962 0.041155 0
0.36 0.100997 0.028317 0
0.38 0.146801 0.01839 0
0.4 0.196206 0.011038 0
0.42 0.248684 0.005909 0
0.44 0.303863 0.002641 0
0.46 0.361466 0.000849 0
0.48 0.421275 0.000122 0
0.5 0.483115 0 0
0.52 0.546841 0 0
0.54 0.612331 0 0
0.56 0.67948 0 0
0.58 0.748199 0 0
0.6 0.818407 0 0
0.62 0.890034 0 0
0.64 0.963017 0 0
0.65 1 0 0

/

-- Table 4. Rock 3
-- Gas-Oil Imbibition
-- Sg Krg Krog Pc
0 0 1 0
0.02 0 0.886076 0
0.04 0 0.780511 0
0.06 0 0.683062 0
0.08 0 0.593485 0
0.1 0 0.511527 0
0.12 0 0.436931 0
0.14 0 0.369435 0
```

```
0.16 0 0.308769 0
0.18 0 0.254656 0
0.2 0 0.20681 0
0.22 0 0.164938 0
0.24 0 0.128736 0
0.26 0 0.097888 0
0.28 0 0.072067 0
0.3 0.071527 0.050928 0
0.32 0.153321 0.034111 0
0.34 0.239498 0.021234 0
0.36 0.32865 0.011887 0
0.38 0.420083 0.005626 0
0.4 0.513375 0.001961 0
0.42 0.608241 0.000323 0
0.44 0.704477 0 0
0.46 0.801927 0 0
0.48 0.900468 0 0
0.5 1 0 0

/
-- Table 5. Rock 4
-- Gas-Oil Imbibition
-- Sg Krg Krog Pc
0 0 1 0
0.02 0 0.875534 0
0.04 0 0.75893 0
0.06 0 0.650247 0
0.08 0 0.549551 0
0.1 0 0.456912 0
0.12 0 0.372409 0
0.14 0 0.29613 0
0.16 0 0.228176 0
0.18 0 0.168661 0
0.2 0 0.117723 0
0.22 0 0.075525 0
0.24 0.091381 0.042277 0
0.26 0.225007 0.018261 0
0.28 0.381167 0.003912 0
0.3 0.554033 0 0
0.32 0.740488 0 0
0.34 0.938542 0 0
0.346 1 0 0
/


-- Table 6. Rock 1. Corey correlated relative permeability curves.
-- Gas-Oil Drainage
-- Sg Krg Krog Pc
0 0 1 0
0.02 0 0.897192383678114 0
0.04 0.000319516809311217 0.801895331681297 0
0.06 0.00419609891815144 0.713799156161152 0
0.08 0.0107468633273278 0.632596374238461 0
0.1 0.0193554411570216 0.557981773149669 0
```

```
0.12 0.0297311689540826 0.489652479892499 0
0.14 0.0416912179168901 0.427308035873609 0
0.16 0.0551058523927666 0.370650477140692 0
0.18 0.0698763976018332 0.319384420877529 0
0.2 0.0859243023231702 0.273217158957549 0
0.22 0.103184976405608 0.231858759495187 0
0.24 0.121604005806986 0.195022177512646 0
0.26 0.141134676696768 0.162423376062915 0
0.28 0.161736275827918 0.133781459432747 0
0.3 0.183372878358846 0.108818820412016 0
0.32 0.206012456063559 0.0872613040874607 0
0.34 0.229626204132833 0.0688383912415472 0
0.36 0.254188021827091 0.0532834052737199 0
0.38 0.279674104307808 0.0403337477076009 0
0.4 0.306062616649357 0.0297311689540826 0
0.42 0.33333342980205 0.0212220833111088 0
0.44 0.361467904068133 0.0145579406084694 0
0.46 0.39044870957662 0.00949567217841166 0
0.48 0.420259675962913 0.00579823730942158 0
0.5 0.450885665382982 0.00323531073505361 0
0.52 0.482312464377283 0.00158417792464182 0
0.54 0.514526691113569 0.000630957344480195 0
0.56 0.547515715290842 0.000172388373082279 0
0.58 0.581267588553579 0.0000187590994115603 0
0.6 0.615770983697209 0 0
0.62 0.651015141278653 0 0
0.64 0.686989822504734 0 0
0.66 0.723685267474857 0 0
0.68 0.761092158015779 0 0
0.7 0.799201584475273 0 0
0.72 0.838005015945429 0 0
0.74 0.877494273470611 0 0
0.76 0.917661505863938 0 0
0.78 0.958499167812714 0 0
0.8 1 0 0
/

-- Table 7. Rock 1B. Corey correlated relative permeability curves.
-- Gas-Oil Drainage
-- Sg Krg Krog Pc
0 0 1 0
0.02 0 0.875159203941741 0
0.04 0.00103049414430682 0.761868397315868 0
0.06 0.00980852118316669 0.65946142486939 0
0.08 0.0223349529272121 0.567285458495794 0
0.1 0.037373710872033 0.484701275152947 0
0.12 0.0544094102060077 0.411083552937324 0
0.14 0.0731395932727521 0.3458211873831 0
0.16 0.0933601499165669 0.288317630400664 0
0.18 0.114921880890535 0.237991254693263 0
0.2 0.137709862326659 0.194275747015726 0
0.22 0.161632221495462 0.156620534296422 0
0.24 0.186613443880572 0.124491247475947 0
0.26 0.212590105554605 0.0973702289841736 0
```

```
0.28 0.239508008883515 0.0747570911684094 0
0.3 0.267320180516383 0.0561693348279201 0
0.32 0.295985425199246 0.0411430394971388 0
0.34 0.325467252163372 0.02923364055124 0
0.36 0.35573305952987 0.020016813063508 0
0.38 0.386753502398585 0.0130894894232723 0
0.4 0.41850199483936 0.00807104841838403 0
0.42 0.450954311524296 0.00460473035940363 0
0.44 0.48408826485505 0.00235936091927493 0
0.46 0.517883440209373 0.00103151651310008 0
0.48 0.552320976569814 0.000348362321589335 0
0.5 0.587383383042483 0.0000716143275246563 0
0.52 0.623054384086515 3.69046566912859E-06 0
0.54 0.659318787950921 0 0
0.56 0.69616237404876 0 0
0.58 0.733571795918505 0 0
0.6 0.771534497117462 0 0
0.62 0.810038637923158 0 0
0.64 0.849073031128811 0 0
0.66 0.888627085538887 0 0
0.68 0.928690756022567 0 0
0.7 0.969254499182757 0 0
0.715 1 0 0
/

-- Table 8. Rock 2. Corey correlated relative permeability curves.
-- Gas-Oil Drainage
-- Sg Krg Krog Pc
0 0 1 0
0.02 0 0.866860702828407 0
0.04 0.00191921378845489 0.746891291445067 0
0.06 0.0155519324336156 0.639277401735678 0
0.08 0.0333917067260381 0.543222188940621 0
0.1 0.0538579368952957 0.457946721791957 0
0.12 0.0763320547137597 0.382690404527942 0
0.14 0.100463531001657 0.31671143023718 0
0.16 0.126021709449296 0.259287269614842 0
0.18 0.152841310364335 0.2097152 0
0.2 0.180797107032644 0.16731288055616 0
0.22 0.209790392947863 0.131418980727139 0
0.24 0.239741031108288 0.101393870748088 0
0.26 0.270582448901919 0.0766203851642629 0
0.28 0.302258316537342 0.0565046732283268 0
0.3 0.334720248757051 0.0404771540501553 0
0.32 0.367926159750264 0.0279936 0
0.34 0.401839052053128 0.0185363800047366 0
0.36 0.436426103568117 0.011615906556098 0
0.38 0.471657965235185 0.00677234924084693 0
0.4 0.507508211200719 0.00357770876399966 0
0.42 0.543952901731149 0.0016384 0
0.44 0.580970231031637 0.000598596759095804 0
0.46 0.618540240054838 0.000144815468787005 0
0.48 0.656644579782829 0.0000128 0
0.5 0.695266314220943 0 0
```

```
0.52 0.734389755005004 0 0
0.54 0.774000321443741 0 0
0.56 0.814084421224417 0 0
0.58 0.854629348054132 0 0
0.6 0.895623193294768 0 0
0.62 0.937054769247481 0 0
0.64 0.97891354220251 0 0
0.65 1 0 0
/
-- Table 9. Rock 3. Corey correlated relative permeability curves.
-- Gas-Oil Drainage
-- Sg Krg Krog Pc
0 0 1 0
0.02 0 0.849744082092905 0
0.04 0.00276040094162393 0.716350555406155 0
0.06 0.0223683099777987 0.598629645735816 0
0.08 0.048027217834441 0.495420969640548 0
0.1 0.0774637513621588 0.40559429898642 0
0.12 0.109788225249041 0.328050388502096 0
0.14 0.144496474152107 0.261721875514284 0
0.16 0.18125674561194 0.205574263019978 0
0.18 0.219831318213073 0.158606999829491 0
0.2 0.260040078649906 0.119854674913009 0
0.22 0.301741057572934 0.0883883476483184 0
0.24 0.34481899411008 0.0633170419293052 0
0.26 0.389178137020936 0.0437894408968557 0
0.28 0.43473746729126 0.0289958317850892 0
0.3 0.481427392512336 0.0181703694273566 0
0.32 0.529187380755719 0.0105937566734872 0
0.34 0.577964218651087 0.00559648871411057 0
0.36 0.627710698248253 0.00256289366017262 0
0.38 0.678384606859151 0.000936364647757882 0
0.4 0.729947936237052 0.000226529935821008 0
0.42 0.78236625391618 0.0000200226067200986 0
0.44 0.835608196670111 0 0
0.46 0.88964505744525 0 0
0.48 0.944450444889754 0 0
0.5 1 0 0
/
-- Table 10. Rock 4. Corey correlated relative permeability curves.
-- Gas-Oil Drainage
-- Sg Krg Krog Pc
0 0 1 0
0.02 0 0.810684954494304 0
0.04 0.00203851740088816 0.646911337926677 0
0.06 0.0227913174085106 0.506828322113202 0
0.08 0.0550399698239803 0.388585078869958 0
0.1 0.0955497271927619 0.29033078001303 0
0.12 0.142885383579865 0.210214597358498 0
0.14 0.196174866196147 0.146385702722445 0
0.16 0.25481467511102 0.0969932679209523 0
0.18 0.318354812813832 0.0601864647701024 0
0.2 0.386442900210177 0.0341144650859771 0
0.22 0.458793238748886 0.0169264406846583 0
```

```
0.24 0.535168087300279 0.00677156338222808 0
0.26 0.615365570029785 0.00179900499476831 0
0.28 0.699211468504639 0.000157937338361002 0
0.3 0.786553426552844 0 0
0.32 0.877256725597071 0 0
0.34 0.971201122046626 0 0
0.346 1 0 0
/


------------------------------------------------------------
------------------------------------------------------------

Water-Oil rel-perm data:
SWOF
-- Table 1. Rock 1. Corey correlated relative permeability curves.
-- Water-Oil Imbibition
-- Sw Krw Krow Pc
0.2 0 1 25
0.21 1.22496389559122E-07 0.927157307625789 11.900001
0.215 5.71834130323352E-07 0.892320294832918 3.000759
0.2166666667 8.53391940631343E-07 0.880937192837913 2.82131661442006
0.26666667 0.000165568038674098 0.588591043182462 0.626959247648903
0.3125 0.00120921318464198 0.392830467142208 0.156739811912226
0.345833 0.00324174715655702 0.285619612955599 0.132634099616858
0.3625 0.00489064429241307 0.241390754058714 0.123936781609195
0.41666667 0.0145926200846313 0.133172333171724 0.0956704980842912
0.46666667 0.0321221400451793 0.0710025141460839 0.0695785440613026
0.5 0.0502555530311202 0.0441941738241593 0.052183908045977
0.5166667 0.061718053520622 0.0341710947578904 0.0434865900383141
0.5625 0.103155818651862 0.0154456303198374 0.0195689655172413
0.59166667 0.138422412386357 0.00856512696456721 0.004348659
0.616 0.174051569930666 0.00489778342120372 0
0.6687 0.273857167493504 0.00107277993176174 -0.627586206896552
0.712 0.383132629505268 0.000177211294462869 -2.03448275862069
0.764 0.553329575234575 3.17453870664701E-06 -6.11034482758621
0.8 0.7 0 -12.0689655172414
1 1 0 -25
/

-- Table 2. Rock 1B. Corey correlated relative permeability curves.
-- Water-Oil Imbibition
-- Sw Krw Krow Pc
0.285 0 1 25
0.28501 0 1 11.7816091954023
0.3 1.02182695316821E-06 0.87545230158109 4.82758620689655
0.31 7.11873133316102E-06 0.79937365196171 4.13793103448276
0.3208333 0.0000279590213599839 0.722864943094814 3.30459770114942
0.3458333 0.000208914557387776 0.567984026750238 1.72413793103448
0.379166 0.00109910686359138 0.40305384045283 0.862068965517241
0.4 0.00234899646387627 0.320728409275427 0.646551724137931
0.45 0.00926124893120257 0.175862672603424 0.413793103448276
0.5 0.0253219249535091 0.0878846678202316 0.275862068965517
0.55 0.056048615680221 0.0386898911908349 0.172413793103448
```

```
0.6 0.108096261470842 0.0141743270698643 0.103448275862069
0.65 0.189209725038526 0.00388399028612581 0.0689655172413793
0.7 0.308186305903191 0.000626422674366072 0
0.720833 0.371234433826461 0.000218931415953589 -0.21551724137931
0.73125 0.406095185138647 0.000116036502628495 -0.431034482758621
0.7479167 0.46681120837347 0.0000332668699298137 -0.827586206896552
0.7604167 0.51655111097463 0.0000096754930522223 -1.72413793103448
0.7708333 0.560895999855938 2.44826295736872E-06 -3.44827586206897
0.78 0.602185543901590 4.48231578409523E-07 -5.45977011494253
0.79 0.649737310666232 1.98092242897075E-08 -8.33333333333333
0.8 0.7 0 -12.0689655172414
1 1 0 -25
/
-- Table 3. Rock 2. Corey correlated relative permeability curves.
-- Water-Oil Imbibition
-- Sw Krw Krow Pc
0.35 0 1 25
0.3501 0 1 11.6941529235382
0.376 0.000013797144410873 8 0.765050393173434 6.89655172413793
0.4 0.000165568038674098 0.588591043182462 4.64767616191904
0.45 0.00230616558930512 0.322737839651785 2.09895052473763
0.5 0.0107655760213687 0.161283275244983 1.19940029985008
0.55 0.0321221400451794 0.0710025141460837 0.749625187406297
0.6 0.0750002171162424 0.0260122948737489 0.599700149925038
0.65 0.149951652313756 0.00712778110110648 0.457974137931035
0.68 0.215398889134774 0.0026113151911219 0.366379310344828
0.7 0.269369894508031 0.00114959188121575 0.305316091954023
0.71667 0.321456286466526 0.000506090378461502 0.137931034482759
0.73 0.368186749485358 0.000230932399479302 0
0.75 0.447423153769726 0.0000508052634252907 -0.749625187406297
0.7604 0.493338995331713 0.0000177561712159449 -1.69415292353823
0.7708 0.542636483340806 4.49297787906632E-06 -3.22338830584708
0.78125 0.595471661696715 6.15246869068078E-07 -5.09745127436282
0.793 0.659514954037216 7.3027236788245E-09 -8.39580209895052
0.8 0.70 0 -12.2938530734633
1 1 0 -25
/

-- Table 4. Rock 3. Corey correlated relative permeability curves.
-- Water-Oil Imbibition
-- Sw Krw Krow Pc
0.5 0 1 25
0.501 0 1 11.833855799373
0.512174 3.60306431440648E-06 0.829927287505331 10.2664576802508
0.54783 0.000652775278631737 0.45772545253219 6.81818181818182
0.6 0.0107655760213687 0.161283275244983 3.91849529780564
0.62174 0.0227337989180926 0.0960962514511705 2.97805642633229
0.652174 0.0530798960572313 0.0413841670413069 2.06896551724138
0.678261 0.0968389675923585 0.0172738933027146 1.56739811912226
0.7 0.149951652313756 0.0071277811011065 1.25391849529781
0.708696 0.176273974685113 0.00473332056334154 1.09717868338558
0.730435 0.25687379367195 0.0013922557289616 0.940438871473354
0.747826 0.338684987631803 0.000381500137568198 0.627586206896552
0.76087 0.411572403169028 0.000104537084629636 0
```

```
0.76522 0.438252970306876 0.0000615295916934113 -0.626959247648903
0.7826087 0.557881873189426 2.71924947062819E-06 -5.40752351097179
0.8 0.70000 0 -12.0689655172414
1 1 0 -25
/

-- Table 5. Rock 4. Corey correlated relative permeability curves.
-- Water-Oil Imbibition
-- Sw Krw Krow Pc
0.654 0 1 25
0.65401 0 1 12.0689655172414
0.664583 0.000032668003442752 0.712749113263367 10.0383141762452
0.66875 0.000115336525773087 0.619240073222137 9.50191570881226
0.679167 0.000878405075066145 0.426827656335349 8.27586206896552
0.7 0.00869034360881069 0.182142858910339 6.4367816091954
0.7174 0.0293947656618609 0.0770953334508995 5.05747126436782
0.73182 0.0640715588167939 0.0325027981674188 4.21455938697318
0.75 0.142294421242653 0.00804965316751283 3.44827586206897
0.76087 0.213895944154634 0.00267133392377022 3.14176245210728
0.768696 0.279792209425297 0.000978662890561774 2.83524904214559
0.78261 0.432299223925448 0.0000694875257313604 1.30268199233716
0.786956 0.490516746776864 0.0000190406834565938 0
0.79130 0.554316094829945 3.07094379078244E-06 -4.06130268199234
0.8 0.7000 0 -12.1072796934866
1 1 0 -25
/

-- Table 6. Rock 1. Corey correlated relative permeability curves.
-- Water-Oil Drainage
-- Sw Krw        Krow Pc
0.2 0 1 25
0.21 2.44140624999998E-08 0.950929711914063 12.0031
0.215 1.2359619140625E-07 0.927083131408692 3.000759
0.26 0.000031640625 0.732094140625 0.793241
0.31 0.0003574462890625 0.553396508789063 0.421172
0.35 0.0012359619140625 0.435806274414062 0.299793
0.36 0.0016 0.4096 0.278828
0.41 0.0047480712890625 0.295834008789063 0.203655
0.46 0.011156640625 0.207594140625 0.157103
0.5 0.019775390625 0.152587890625 0.131034
0.55 0.0366363525390625 0.100112915039062 0.10669
0.6 0.0625 0.0625 0.088483
0.65 0.100112915039062 0.0366363525390625 0.074276
0.7 0.152587890625 0.019775390625 0.062897
0.75 0.223403930664062 0.0095367431640625 0.053586
0.8 0.31640625 0.00390624999999999 0.045793
0.81 0.338033227539063 0.0031816650390625 0.044414
0.85 0.435806274414062 0.0012359619140625 0.039172
0.97 0.858228540039063 0.0000019775390625 0.026897
1 1 0 0
/
-- Table 7. Rock 1B. Corey correlated relative permeability curves.
-- Water-Oil Drainage
-- Sw Krw Krow Pc
```

```
0.285 0 1 25
0.28501 0 1 12.0031
0.3 1.33735978733403E-06 0.968697094944636 6.364345
0.32 0.0000259517715148018 0.927479472532604 3.478483
0.35 0.00022652993582101 0.866784172041448 1.812828
0.37 0.000579288749030844 0.827088079359627 1.291034
0.42 0.00292480585489951 0.730605483824283 0.663586
0.47 0.0088110953923026 0.638196975523907 0.397241
0.5 0.0149095131848666 0.584784622382581 0.305172
0.52 0.0203547780727358 0.550050790757171 0.259448
0.55 0.0309948409759424 0.499297863790018 0.206552
0.6 0.0567565243028713 0.418437813710079 0.146
0.65 0.095050384778139 0.342486142375531 0.106138
0.7 0.148969442401723 0.271783332432712 0.078621
0.75 0.221826889155692 0.206752586010169 0.058897
0.79 0.296107001932638 0.15917317508727 0.046828
0.81 0.339223878724749 0.136984471567572 0.041724
0.84 0.412054152024712 0.105857324037207 0.034966
0.89 0.557278983546373 0.0603434261963644 0.025655
0.93 0.697248927512291 0.0306328918281344 0.01931
0.97 0.860688210053326 0.0085945436055808 0.013517
1 1 0 0
/
-- Table 8. Rock 2. Corey correlated relative permeability curves.
-- Water-Oil Drainage
-- Sw Krw Krow Pc
0.35 0 1 25
0.3501 0 1 12.0031
0.37 5.10985100005918E-06 0.954203025433276 8.826345
0.42 0.000409870245419509 0.842892045552196 3.454345
0.47 0.00270356996414778 0.736281298285394 1.858966
0.5 0.00590367795093858 0.674660014851561 1.380345
0.52 0.00914901788491054 0.63458794991802 1.154897
0.55 0.0161587676642761 0.576034819156969 0.904069
0.6 0.0352852567675263 0.482747409570915 0.628276
0.65 0.0667924914088028 0.395122746149031 0.453172
0.7 0.114562216339068 0.313553640224657 0.334483
0.75 0.182815587056441 0.238528335748478 0.249931
0.79 0.255204083638615 0.183636457865152 0.198345
0.81 0.298164313478598 0.15803757842618 0.176414
0.84 0.371954255540466 0.122126507903221 0.147448
0.89 0.522614447077346 0.0696175912560143 0.106966
0.93 0.671121619227832 0.035340852793825 0.079241
0.97 0.847567245648844 0.00991543671746909 0.052759
1 1 0 0
/
-- Table 9. Rock 3. Corey correlated relative permeability curves.
-- Water-Oil Drainage
-- Sw Krw Krow Pc
0.5 0 1 25
0.501 0 1 12.0031
0.51 1.13137084989848E-06 0.970150503787943 10.54855
0.55 0.000316227766016838 0.853814968245462 6.781724
0.58 0.0016384 0.769872716752581 4.996
```

```
0.6 0.00357770876399966 0.715541752799933 4.114966
0.65 0.0147885090526395 0.585662018573853 2.602345
0.7 0.0404771540501552 0.46475800154489 1.693655
0.75 0.0883883476483184 0.353553390593274 1.123862
0.79 0.148592872223132 0.27219110933313 0.816828
0.82 0.2097152 0.216 0.644828
0.84 0.259287269614842 0.181019335983756 0.551172
0.89 0.419112978263761 0.103189146716115 0.371793
0.92 0.543222188940621 0.0639999999999999 0.292276
0.95 0.691590124278824 0.0316227766016838 0.227724
0.97 0.805281065338457 0.0146969384566991 0.190552
1 1 0 0
/
-- Table 10. Rock 4. Corey correlated relative permeability curves.
-- Water-Oil Drainage
-- Sw Krw Krow Pc
0.654 0 1 25
0.65401 0 1 12.0031
0.67 0.000021264422543919 0.931444026025444 9.705931
0.685 0.00021527796659132 0.868663718084582 7.961862
0.7 0.000856813035317722 0.807360938901418 6.568966
0.75 0.0112507887400279 0.614180275395634 3.575862
0.79 0.0380732397411112 0.472840637194685 2.256897
0.81 0.0615417367915925 0.406926762541963 1.803793
0.84 0.113901372938734 0.314460301002565 1.295586
0.89 0.262075042333267 0.179256486386953 0.753172
0.91 0.348396298959568 0.132662939485457 0.60731
0.93 0.453331024162638 0.0909982230560485 0.489862
0.97 0.728011841480483 0.0255309946078053 0.31731
0.98 0.811886377402651 0.0138973132033048 0.283379
1 1 0 0
/
------------------------------------------------------------
------------------------------------------------------------
/

--Hysteresis Option
EHYSTR
1* 8 /
/
------------------------------------------------------------
-- ------------------------------------------------------
-- Include PVT data


NCOMPS
 9 /
-- Equation of state
EOS
SRK /
-- Reservoir temperature (C)
RTEMP
    100.00 /
-- Standard Conditions (C and bara)
```

```
STCOND
   14.99999    1.01325  /
-- Component names
CNAMES
 CO2
 N2
 C1
 C2
 C3
 C4C5
 C6
 C7C12
 C13P /
-- Tc (K)
TCRIT
   304.200
   126.200
   190.600
   305.400
   369.800
   435.439
   552.063
   574.782
   722.281 /
-- Pc (Bar)
PCRIT
   73.7646
   33.9439
   46.0015
   48.8387
   42.4552
   36.1095
   34.5976
   26.4128
   16.5345 /
-- Omega
ACF
   0.22500
   0.04000
   0.00800
   0.09800
   0.15200
   0.20545
   0.27079
   0.65111
   0.84844 /
-- OmegaA
OMEGAA
     0.42748
     0.42748
     0.42748
     0.42748
     0.42748
     0.42748
```

```
     0.42748
     0.42748
     0.42748 /
-- OmegaB
OMEGAB
     0.08664
     0.08664
     0.08664
     0.08664
     0.08664
     0.08664
     0.08664
     0.08664
     0.08664 /
-- Molecular weights
MW
   44.0098
   28.0135
   16.0429
   30.0698
   44.0968
   62.5206
   91.0980
  119.9064
  231.6094 /
-- Boiling points (K)
TBOIL
   194.650
    77.400
   111.600
   184.600
   231.100
   281.665
   364.522
   423.789
   573.044 /
-- Critical volumes (m3/kg-mole)
VCRIT
   0.09400
   0.08980
   0.09900
   0.14800
   0.20300
   0.27502
   0.35476
   0.58169
   1.03573 /
-- Critical Z-factors
ZCRIT
   0.27414
   0.29049
   0.28737
   0.28465
   0.28029
```

```
   0.27429
   0.26739
   0.32148
   0.28516 /
-- Volume translation/co-volume
SSHIFT
  0.101924
  0.034350
  0.021107
  0.058382
  0.080639
  0.102064
  0.126500
  0.067049
  0.099923 /
-- Parachors (dyn/cm)
PARACHOR
    78.000
    41.000
    77.300
   108.900
   151.900
   202.863
   273.747
   340.660
   623.609 /
-- Overall composition
ZI
  0.002398
  0.015589
  0.352157
  0.151296
  0.181475
  0.142502
  0.061383
  0.065330
  0.027870 /
-- Binary interaction coefficients for SRK
BIC
 -0.0315
  0.1200  0.0278
  0.1200  0.0407  0.0000
  0.1200  0.0763  0.0000  0.0000
  0.1200  0.0817  0.0000  0.0000  0.0000
  0.0472  0.0340  0.0005  0.0007  0.0005  0.0001
  0.1000  0.0800  0.0000  0.0000  0.0000  0.0000  0.0000
  0.1000  0.0800  0.0000  0.0000  0.0000  0.0000  0.0000  0.0000
/
BICS
 -0.0315
  0.1200  0.0278
  0.1200  0.0407  0.0000
  0.1200  0.0763  0.0000  0.0000
  0.1200  0.0817  0.0000  0.0000  0.0000
```

```
  0.0472  0.0340  0.0005  0.0007  0.0005  0.0001
  0.1000  0.0800  0.0000  0.0000  0.0000  0.0000  0.0000
  0.1000  0.0800  0.0000  0.0000  0.0000  0.0000  0.0000  0.0000
/
-- LBC coefficients
LBCCOEF
   0.1023000    0.0233640    0.0585330   -0.0407580    0.0093324 /


------------------------------------------------------------
------------------------------------------------------------
INCLUDE
 '../../../newinclude/kvalues9.inc' /

-- Rock compressibility:
INCLUDE
 'compress.inc' /

-- Water properties

DENSITY
 1* 1000.0 1* /

PVTW
 300.0 1.0 4.0E-5  0.4 /

-- ************************************************************
-- In this section simulation grid region parameters are given
-- ************************************************************

REGIONS
-- Region parameters, SATNUM, PVTNUM, etc.
-- In this example:
-- only 1 PVTNUM, 1 SATNUM, 2 FIPNUM for entire grid
-- PVTNUM & SATNUM are defined in this file
-- FIPNUM & FLUXNUM are imported from files
-- Normally these parameters are established using RMS
--Include SATNUM regions
--Include IMBNUM regions
INCLUDE
'../../../newinclude/east_imbnum.grdecl' /

--Include SATNUM regions
INCLUDE
  'NEWsatnum.grdecl' /

NOECHO

EQUALS
 PVTNUM     1      /
/
-- ************************************************
-- In this section the initialization parameters aand
-- dynamic parameters are defined
```

```
-- ************************************************

SOLUTION

RESTART
--START 22 OCT 2012
'../../../sim/NEWBASE2RE3/NEWBASE2RE3' 119 /
-- ************************************************
--
--Simulation model initialisation data
--
--   DATUM  DATUM   OWC     OWC    GOC    GOC    RSVD   RVVD   SOLN
--   Depth  Pres.   Depth   Pcow   Depth  Pcog   Table  Table  Method
EQUIL
     2597   290      2597  0.0       500    0.0  /

-- Controls on output from SOLUTION section
--RPTSOL
-- /
--Controls on output to the RESTART file
RPTRST
 BASIC=4 CONV=1000 SGAS SOIL SWAT XMF YMF ZMF RPORV DENG DENO
 DENW VGAS VOIL XMF YMF ZMF PART /

-- Separator (use k-values):
FIELDSEP
 1 15.0 1.013250 0 0 1 /
/
-- ************************************************************************
-- In this section simulation output data to be written to summary file are defined
-- ************************************************************************
SUMMARY

-- Summary data to be written to summary file
INCLUDE
 'summary2.inc'   /

-- ************************************************************************
-- In this section data required to describe history and prediction is given
-- - well completions, well production/injection, well constraints
-- - platform/production unit constraints, etc.
-- ************************************************************************

SCHEDULE

CVCRIT
-- DPM         CompDV
  2     5*      0.2   /
/
MESSOPTS
 ACCPTIME 1 /
/
SKIPREST
```

```
-- **************************************************
NOECHO
--TSCRIT
-- 0.1 0.01 14.0 1.5 0.5 2* 0.5 1* 0.1 1* 0.5 /
-- --------------------------------------------------
-- Well definitions:
INCLUDE
 '../../../newinclude/wells.sch' /
-- Well productivity:
INCLUDE
 'wpi.inc' /
-- Schedule with allocated rates:

INCLUDE
 '../../../include/hist.sch' /
-- --------------------------------------------------
-- Production well VFP table (used for predictions)
INCLUDE
 'A-3H.ecl'  /

INCLUDE
  'prediction.inc' /

END
```

B.2 ODD3P tables

```
PCODD3P
0 1.0 1.0 1.0  1.0 1.0 1.0 / -- PSTNUM = 1
0 1.0 1.0 1.0  1.0 1.0 1.0 / -- PSTNUM = 2
0 1.0 1.0 1.0  1.0 1.0 1.0 / -- PSTNUM = 3
0 1.0 1.0 1.0  1.0 1.0 1.0 / -- PSTNUM = 4
0 1.0 1.0 1.0  1.0 1.0 1.0 / -- PSTNUM = 5
/ --ISTNUM = 6
/ --ISTNUM = 7
/ --ISTNUM = 8
/ --ISTNUM = 9
/ --ISTNUM = 10
/ --DSTNUM = 11
/ --DSTNUM = 12
/ --DSTNUM = 13
/ --DSTNUM = 14
/ --DSTNUM = 15


--PCODD3PG
--0.0  0.0
--0.57 0.0
--0.6  1.0
--/
--PCPDD3PW
--0.0 0.0
--0.8 0.0
--1.0 1.0
--/

EPSODD3P
1 1 1  1    0   1.7   27.0  27.0 0.25 0.25 0.25 20.0 1.0 15.0   1.0    1.0    1.0
1 1 1  1    0   1.7   27.0  27.0 0.25 0.25 0.25 20.0 1.0 15.0   1.0    1.0    1.0
1 1 1  1    0   1.7   27.0  27.0 0.25 0.25 0.25 20.0 1.0 15.0   1.0    1.0    1.0
1 1 1  1    0   1.7   27.0  27.0 0.25 0.25 0.25 20.0 1.0 15.0   1.0    1.0    1.0
1 1 1  1    0   1.7   27.0  27.0 0.25 0.25 0.25 20.0 1.0 15.0   1.0    1.0    1.0
/ --ISTNUM = 6
/ --ISTNUM = 7
/ --ISTNUM = 8
/ --ISTNUM = 9
/ --ISTNUM = 10
/ --DSTNUM = 11
/ --DSTNUM = 12
/ --DSTNUM = 13
/ --DSTNUM = 14
/ --DSTNUM = 15

OPTODD3P
4
/
SOF3
--primary table
--So Krow Krog
```

```
0 0 0
0.03 0.002301 0
0.15 0.045191 0
0.19 0.069981 0
0.2 0.076947 0
0.24 1* 0.000069
0.25 0.116271 1*
0.28 1* 0.000631
0.3 0.162914 1*
0.32 1* 0.002309
0.35 0.216675 1*
0.36 1* 0.005798
0.4 0.277392 0.011842
0.44 1* 0.021222
0.45 0.344927 1*
0.48 1* 0.034755
0.5 0.419158 1*
0.52 1* 0.053283
0.54 0.483295 1*
0.56 1* 0.077675
0.59 0.569324 1*
0.6 1* 0.108819
0.64 0.661784 0.147625
0.65 0.681041 1*
0.68 1* 0.195022
0.69 0.760597 1*
0.72 1* 0.251955
0.74 0.86569 1*
0.76 1* 0.319384
0.785 0.965589 1*
0.79 0.976998 1*
0.8 1 0.398287
0.84 1 0.489652
0.88 1 0.594485
0.92 1 0.713799
0.96 1 0.848624
1 1 1
/
--So Krow Krog
0 0 0
0.03 0.008595 0
0.07 0.030633 0
0.11 0.060343 0
0.16 0.105857 0
0.18 1* 0
0.19 0.136984 1*
0.21 0.159173 1*
0.221 1* 0.000028
0.25 0.206753 1*
0.262 1* 0.000316
0.3 0.271783 1*
0.303 1* 0.001307
0.344 1* 0.003578
0.35 0.342486 1*
```

```
0.385 1* 0.007813
0.4 0.418438 1*
0.426 1* 0.014789
0.45 0.499298 1*
0.467 1* 0.025365
0.48 0.550051 1*
0.5 0.584785 1*
0.508 1* 0.040477
0.53 0.638197 1*
0.549 1* 0.061129
0.58 0.730605 1*
0.59 1* 0.088388
0.63 0.827088 1*
0.631 1* 0.123387
0.65 0.866784 1*
0.672 1* 0.167313
0.68 0.927479 1*
0.7 0.968697 1*
0.713 1* 0.22141
0.715 1 1*
0.754 1 0.286974
0.795 1 0.365354
0.836 1 0.457947
0.877 1 0.566195
0.918 1 0.69159
0.959 1 0.835666
1 1 1
/--primary table
--So.w Krow Krog
0 0 0
0.03 0.00992 0
0.07 0.03534 0
0.11 0.06962 0
0.15 1* 0
0.16 0.12213 1*
0.1925 1* 0.00003
0.2 0.17068 1*
0.21 0.18364 1*
0.235 1* 0.00032
0.25 0.23853 1*
0.2775 1* 0.00131
0.3 0.31355 1*
0.32 1* 0.00358
0.35 0.39512 1*
0.3625 1* 0.00781
0.4 0.48275 1*
0.405 1* 0.01479
0.4475 1* 0.02537
0.45 0.57603 1*
0.48 0.63459 1*
0.49 1* 0.04048
0.5 0.67466 1*
0.53 0.73628 1*
0.5325 1* 0.06113
```

```
0.575 1* 0.08839
0.58 0.84289 1*
0.6175 1* 0.12339
0.63 0.9542 1*
0.65 1 1*
0.66 1 0.16731
0.7 1 0.21
0.7025 1 0.22141
0.745 1 0.28697
0.7875 1 0.36535
0.83 1 0.45795
0.8725 1 0.5662
0.915 1 0.69159
0.9575 1 0.83567
1 1 1
/
--So Krow Krog
0 0 0
0.03 0.0147 0
0.05 0.03162 0
0.06 1* 0
0.08 0.064 1*
0.107 1* 0.00003
0.11 0.10319 1*
0.154 1* 0.00032
0.16 0.18102 1*
0.18 0.216 1*
0.201 1* 0.00131
0.21 0.27219 1*
0.248 1* 0.00358
0.25 0.35355 1*
0.295 1* 0.00781
0.3 0.46476 1*
0.342 1* 0.01479
0.35 0.58566 1*
0.389 1* 0.02537
0.4 0.71554 1*
0.42 0.76987 1*
0.436 1* 0.04048
0.45 0.85381 1*
0.483 1* 0.06113
0.49 0.97015 1*
0.5 1 1*
0.53 1 0.08839
0.577 1 0.12339
0.624 1 0.16731
0.671 1 0.21
0.718 1 0.22141
0.72 1 0.28697
0.765 1 0.36535
0.812 1 0.45795
0.859 1 0.5662
0.906 1 0.69159
0.953 1 0.83567
```

```
1 1 1
/
--So Krow Krog
0 0 0
0.02 0.0139 0
0.03 0.02553 0
0.05 1* 0
0.07 0.091 1*
0.09 0.13266 1*
0.0975 1* 0.00013
0.11 0.17926 1*
0.145 1* 0.001
0.16 0.31446 1*
0.19 0.40693 1*
0.1925 1* 0.00338
0.21 0.47284 1*
0.24 1* 0.008
0.25 0.61418 1*
0.2875 1* 0.01563
0.3 0.80736 1*
0.315 0.86866 1*
0.33 0.93144 1*
0.335 1* 0.027
0.3459 0.99957 1*
0.346 1 1*
0.3825 1 0.04288
0.43 1 0.064
0.4775 1 0.09113
0.525 1 0.125
0.5725 1 0.16638
0.62 1 0.216
0.6675 1 0.27463
0.715 1 0.343
0.7625 1 0.42188
0.81 1 0.512
0.8575 1 0.61413
0.905 1 0.729
0.9525 1 0.85738
1 1 1
/
---------------Secondary tables-----------------
--So Krow Krog
0 0 0
0.2 0 0
0.2225 0 1*
0.24 1* 0.000011
0.28 1* 0.000158
0.3125 0.000535 1*
0.32 1* 0.00074
0.3425 0.001551 1*
0.35 0.001953 1*
0.36 1* 0.002208
0.3875 0.005331 1*
0.4 1* 0.005154
```

```
0.425 0.01211 1*
0.44 1* 0.010305
0.4625 0.024233 1*
0.48 1* 0.018512
0.5 0.044194 1*
0.52 1* 0.030749
0.5375 0.075085 1*
0.56 1* 0.048107
0.575 0.120631 1*
0.6 1* 0.071794
0.605 0.170556 1*
0.64 1* 0.103128
0.6425 0.254056 1*
0.68 0.366357 0.143541
0.6875 0.39283 1*
0.7 1* 0.16
0.7175 0.513944 0.16
0.72 1* 0.16
0.755 0.704106 0.16
0.78875 0.918351 0.16
0.7925 0.944968 0.16
0.8 1 0.16
1 1 0.16
/
--So Krow Krog
0 0 0
0.18 0 0
0.2 0 1*
0.221 1* 0.000069
0.22161 0.000001 1*
0.25042 0.000029 1*
0.262 1* 0.000631
0.27923 0.00022 1*
0.303 1* 0.002309
0.31524 0.001186 1*
0.33685 0.00257 1*
0.344 1* 0.005798
0.35126 0.004033 1*
0.38007 0.008838 1*
0.385 1* 0.011842
0.41608 0.020074 1*
0.426 1* 0.021222
0.4521 0.040174 1*
0.467 1* 0.034755
0.48811 0.073262 1*
0.508 1* 0.053283
0.52413 0.124481 1*
0.54573 0.166412 1*
0.549 1* 0.077675
0.56014 0.199981 1*
0.58175 0.25994 1*
0.59 1* 0.108819
0.61776 0.389976 1*
0.631 1* 0.147625
```

```
0.65378 0.565811 1*
0.66818 0.651216 1*
0.672 1* 0.195022
0.68979 0.797833 1*
0.7 1* 0.22
0.7042 0.909034 0.22
0.71428 0.993724 0.22
0.715 1 0.22
1 1 0.22
/
--So.w Krow Krog
0 0 0
0.15 0 0
0.1925 0 0.00023
0.2 0 1*
0.22077 0.00000001 1*
0.235 1* 0.00158
0.24846 0.00004 1*
0.27615 0.00034 1*
0.2775 1* 0.00493
0.31077 0.00182 1*
0.32 1* 0.01104
0.33846 0.00497 1*
0.34538 0.00619 1*
0.3625 1* 0.02062
0.37308 0.01357 1*
0.405 1* 0.03435
0.40769 0.03083 1*
0.44231 0.06169 1*
0.4475 1* 0.05289
0.47692 0.1125 1*
0.49 1* 0.07687
0.51154 0.19114 1*
0.53231 0.25555 1*
0.5325 1* 0.1069
0.54615 0.30708 1*
0.56692 0.39915 1*
0.575 1* 0.14359
0.60154 0.59885 1*
0.6175 1* 0.18751
0.63615 0.86881 1*
0.65 1 1*
0.66 1 0.23923
0.7 1 0.3
1 1 0.3
/
--So Krow Krog
0 0 0
0.06 0 0
0.107 0 0
0.154 0 0.0004
0.2 0 1*
0.201 1* 0.0025
0.218 0 1*
```

```
0.23 0 1*
0.248 0.0003 0.0072
0.266 0.0011 1*
0.295 1* 0.0152
0.296 0.0059 1*
0.308 0.0101 1*
0.326 0.0202 1*
0.342 1* 0.0272
0.35 0.0442 1*
0.38 0.1004 1*
0.389 1* 0.0437
0.41 0.2009 1*
0.436 1* 0.0652
0.44 0.3664 1*
0.452 0.4563 1*
0.47 0.6224 1*
0.483 1* 0.0923
0.494 0.9131 1*
0.5 1 1*
0.53 1 0.1254
0.577 1 0.1649
0.624 1 0.2113
0.671 1 0.265
0.718 1 0.3263
0.72 1 0.33
1 1 0.33
/
--So Krow Krog
0 0 0
0.0975 0 0.00337
0.145 0 0.01259
0.1925 0 0.0272
0.2 0 1*
0.20844 0 1*
0.21266 0.00002 1*
0.22954 0.00075 1*
0.23798 0.00233 1*
0.24 1* 0.04698
0.24642 0.00576 1*
0.26751 0.0311 1*
0.28017 0.06738 1*
0.2875 1* 0.07179
0.28861 0.10572 1*
0.30549 0.23168 1*
0.32659 0.52626 1*
0.33292 0.65547 1*
0.335 1* 0.10152
0.33925 0.80811 1*
0.34596 0.9987 1*
0.346 1 1*
0.3825 1 0.13606
0.43 1 0.17535
0.4775 1 0.21933
0.525 1 0.26794
```

```
0.5725 1 0.32114
0.62 1 0.37887
0.6675 1 0.4411
0.715 1 0.50779
0.7625 1 0.57892
0.78 1 0.65
1 1 0.65
/
---------------tertiary = Secondary tables-----------------
--So Krow Krog
0 0 0
0.2 0 0
0.2225 0 1*
0.24 1* 0.000011
0.28 1* 0.000158
0.3125 0.000535 1*
0.32 1* 0.00074
0.3425 0.001551 1*
0.35 0.001953 1*
0.36 1* 0.002208
0.3875 0.005331 1*
0.4 1* 0.005154
0.425 0.01211 1*
0.44 1* 0.010305
0.4625 0.024233 1*
0.48 1* 0.018512
0.5 0.044194 1*
0.52 1* 0.030749
0.5375 0.075085 1*
0.56 1* 0.048107
0.575 0.120631 1*
0.6 1* 0.071794
0.605 0.170556 1*
0.64 1* 0.103128
0.6425 0.254056 1*
0.68 0.366357 0.143541
0.6875 0.39283 1*
0.7 1* 0.16
0.7175 0.513944 0.16
0.72 1* 0.16
0.755 0.704106 0.16
0.78875 0.918351 0.16
0.7925 0.944968 0.16
0.8 1 0.16
1 1 0.16
/
--So Krow Krog
0 0 0
0.18 0 0
0.2 0 1*
0.221 1* 0.000069
0.22161 0.000001 1*
0.25042 0.000029 1*
0.262 1* 0.000631
```

```
0.27923 0.00022 1*
0.303 1* 0.002309
0.31524 0.001186 1*
0.33685 0.00257 1*
0.344 1* 0.005798
0.35126 0.004033 1*
0.38007 0.008838 1*
0.385 1* 0.011842
0.41608 0.020074 1*
0.426 1* 0.021222
0.4521 0.040174 1*
0.467 1* 0.034755
0.48811 0.073262 1*
0.508 1* 0.053283
0.52413 0.124481 1*
0.54573 0.166412 1*
0.549 1* 0.077675
0.56014 0.199981 1*
0.58175 0.25994 1*
0.59 1* 0.108819
0.61776 0.389976 1*
0.631 1* 0.147625
0.65378 0.565811 1*
0.66818 0.651216 1*
0.672 1* 0.195022
0.68979 0.797833 1*
0.7 1* 0.22
0.7042 0.909034 0.22
0.71428 0.993724 0.22
0.715 1 0.22
1 1 0.22
/
--So.w Krow Krog
0 0 0
0.15 0 0
0.1925 0 0.00023
0.2 0 1*
0.22077 0.00000001 1*
0.235 1* 0.00158
0.24846 0.00004 1*
0.27615 0.00034 1*
0.2775 1* 0.00493
0.31077 0.00182 1*
0.32 1* 0.01104
0.33846 0.00497 1*
0.34538 0.00619 1*
0.3625 1* 0.02062
0.37308 0.01357 1*
0.405 1* 0.03435
0.40769 0.03083 1*
0.44231 0.06169 1*
0.4475 1* 0.05289
0.47692 0.1125 1*
0.49 1* 0.07687
```

```
0.51154 0.19114 1*
0.53231 0.25555 1*
0.5325 1* 0.1069
0.54615 0.30708 1*
0.56692 0.39915 1*
0.575 1* 0.14359
0.60154 0.59885 1*
0.6175 1* 0.18751
0.63615 0.86881 1*
0.65 1 1*
0.66 1 0.23923
0.7 1 0.3
1 1 0.3
/
--So Krow Krog
0 0 0
0.06 0 0
0.107 0 0
0.154 0 0.0004
0.2 0 1*
0.201 1* 0.0025
0.218 0 1*
0.23 0 1*
0.248 0.0003 0.0072
0.266 0.0011 1*
0.295 1* 0.0152
0.296 0.0059 1*
0.308 0.0101 1*
0.326 0.0202 1*
0.342 1* 0.0272
0.35 0.0442 1*
0.38 0.1004 1*
0.389 1* 0.0437
0.41 0.2009 1*
0.436 1* 0.0652
0.44 0.3664 1*
0.452 0.4563 1*
0.47 0.6224 1*
0.483 1* 0.0923
0.494 0.9131 1*
0.5 1 1*
0.53 1 0.1254
0.577 1 0.1649
0.624 1 0.2113
0.671 1 0.265
0.718 1 0.3263
0.72 1 0.33
1 1 0.33
/
--So Krow Krog
0 0 0
0.0975 0 0.00337
0.145 0 0.01259
0.1925 0 0.0272
```

```
0.2 0 1*
0.20844 0 1*
0.21266 0.00002 1*
0.22954 0.00075 1*
0.23798 0.00233 1*
0.24 1* 0.04698
0.24642 0.00576 1*
0.26751 0.0311 1*
0.28017 0.06738 1*
0.2875 1* 0.07179
0.28861 0.10572 1*
0.30549 0.23168 1*
0.32659 0.52626 1*
0.33292 0.65547 1*
0.335 1* 0.10152
0.33925 0.80811 1*
0.34596 0.9987 1*
0.346 1 1*
0.3825 1 0.13606
0.43 1 0.17535
0.4775 1 0.21933
0.525 1 0.26794
0.5725 1 0.32114
0.62 1 0.37887
0.6675 1 0.4411
0.715 1 0.50779
0.7625 1 0.57892
0.78 1 0.65
1 1 0.65
/
SGF3
--Sg Krgo(Sg) Krgw(Sg) Pcog
0 0 0 0
0.035 0 0 0
0.0351 0.0005 0.0005 1.00E-06
0.07325 0.008286135 0.008286135 1.00E-04
0.1115 0.025118864 0.025118864 0.001345
0.14975 0.048055822 0.048055822 0.0019585
0.188 0.076146158 0.076146158 0.0022205
0.22625 0.10881882 0.10881882 0.0022895
0.2645 0.145678012 0.145678012 0.0026795
0.30275 0.186427026 0.186427026 0.003145
0.341 0.230831985 0.230831985 0.003714
0.37925 0.278701959 0.278701959 0.004424
0.4175 0.329876978 0.329876978 0.0053345
0.45575 0.384220297 0.384220297 0.0065515
0.494 0.441613154 0.441613154 0.007855
0.53225 0.501951054 0.501951054 0.010183
0.5705 0.565141063 0.565141063 0.0139415
0.60875 0.631099769 0.631099769 0.0149895
0.647 0.699751727 0.699751727 0.0210585
0.68525 0.771028233 0.771028233 0.039662
0.7235 0.844866354 0.844866354 0.150038
0.76175 0.921208143 0.921208143 0.600155
```

```
0.8 1 1 1.25
/
--Sg Krgo Krgw Pcog
0 0 0 0
0.035 0 0 0.000676
0.07425 0.015085441 0.015085441 0.0009655
0.1135 0.039810717 0.039810717 0.001283
0.15275 0.070230824 0.070230824 0.0017485
0.192 0.105061112 0.105061112 0.002086
0.23125 0.143587294 0.143587294 0.0023415
0.2705 0.185340255 0.185340255 0.002945
0.30975 0.22998275 0.22998275 0.003931
0.349 0.277257937 0.277257937 0.005307
0.38825 0.326962179 0.326962179 0.0073
0.4275 0.378929142 0.378929142 0.0103275
0.46675 0.43301981 0.43301981 0.0129725
0.506 0.489115866 0.489115866 0.0152585
0.54525 0.547115098 0.547115098 0.019862
0.5845 0.606928115 0.606928115 0.0331795
0.62375 0.668475922 0.668475922 0.0645515
0.663 0.731688083 0.731688083 0.0906415
0.70225 0.796501313 0.796501313 0.173924
0.7415 0.862858364 0.862858364 0.3182175
0.78075 0.930707144 0.930707144 0.6
0.82 1 1 1.25
/
--Sg Krgo Krgw Pcog
0 0 0 0
0.0001 0 0 1.00E-10
0.035 0 0 1*
0.0758 0.0204 0.0204 1*
0.1165 0.0501 0.0501 1*
0.1573 0.0849 0.0849 0.0026
0.198 0.1234 0.1234 0.004
0.2388 0.1649 0.1649 0.0054
0.2795 0.2091 0.2091 0.0074
0.3203 0.2554 0.2554 0.0088
0.361 0.3039 0.3039 0.0099
0.4018 0.3541 0.3541 0.0125
0.4425 0.4061 0.4061 0.0167
0.4833 0.4597 0.4597 0.0227
0.524 0.5148 0.5148 0.0314
0.5648 0.5712 0.5712 0.0452
0.6055 0.629 0.629 0.0577
0.6463 0.688 0.688 0.069
0.687 0.7482 0.7482 0.093
0.7278 0.8096 0.8096 0.1727
0.7685 0.872 0.872 0.4413
0.8093 0.9355 0.9355 0.6002
0.85 1 1 1.25
/
--Sg Krgo Krgw Pcog
0 0 0 0
0.035 0 0 0
```

```
0.08025 0.02035 0.02035 1.00E-10
0.1255 0.05012 0.05012 1*
0.17075 0.0849 0.0849 1*
0.216 0.12341 0.12341 1*
0.26125 0.16494 0.16494 0.00953
0.3065 0.20905 0.20905 0.01139
0.35175 0.25544 0.25544 0.01462
0.397 0.30386 0.30386 0.01859
0.44225 0.35414 0.35414 0.02756
0.4875 0.40613 0.40613 0.03224
0.53275 0.4597 0.4597 0.04084
0.578 0.51475 0.51475 0.0562
0.62325 0.5712 0.5712 0.08469
0.6685 0.62897 0.62897 0.13012
0.71375 0.68799 0.68799 0.20575
0.759 0.7482 0.7482 0.2498
0.80425 0.80955 0.80955 0.33909
0.8495 0.872 0.872 0.52743
0.907 0.94514 0.94514 0.60016
0.94 1 1 1.25
/
--Sg Krgo Krgw Pcog
0 0 0 0
0.035 0 0 0
0.08075 0.01118 0.01118 0
0.1265 0.03162 0.03162 0
0.17225 0.05809 0.05809 0
0.218 0.08944 0.08944 0
0.26375 0.125 0.125 0
0.3095 0.16432 0.16432 0
0.35525 0.20706 0.20706 0.01417
0.401 0.25298 0.25298 0.01587
0.44675 0.30187 0.30187 0.02449
0.4925 0.35355 0.35355 0.03037
0.53825 0.40789 0.40789 0.03766
0.584 0.46476 0.46476 0.06478
0.62975 0.52405 0.52405 0.09019
0.6755 0.58566 0.58566 0.11285
0.72125 0.64952 0.64952 0.17879
0.767 0.71554 0.71554 0.32845
0.81275 0.78366 0.78366 0.39809
0.8585 0.85381 0.85381 0.4853
0.90425 0.92595 0.92595 0.60016
0.95 1 1 1.25
/
-------------------------secondary tables-----------------
--Sg Krgo(Sg) Krgw(Sg) Pcog
0 0 0 0
0.3 0 0 0
0.3001 0.0005 0.0005 1.00E-06
0.325 0.00614114 0.00614114 0.0001
0.35 0.019952623 0.019952623 0.001345
0.375 0.039751648 0.039751648 0.0019585
0.4 0.064826264 0.064826264 0.0022205
```

```
0.425 0.094732285 0.094732285 0.0022895
0.45 0.129153486 0.129153486 0.0026795
0.475 0.167847809 0.167847809 0.003145
0.5 0.210621153 0.210621153 0.003714
0.525 0.257312731 0.257312731 0.004424
0.55 0.307786103 0.307786103 0.0053345
0.575 0.361923324 0.361923324 0.0065515
0.6 0.419620914 0.419620914 0.007855
0.625 0.480786989 0.480786989 0.010183
0.65 0.545339139 0.545339139 0.0139415
0.675 0.613202826 0.613202826 0.0149895
0.7 0.684310144 0.684310144 0.0210585
0.725 0.758598839 0.758598839 0.039662
0.75 0.836011528 0.836011528 0.150038
0.775 0.916495061 0.916495061 0.600155
0.8 1 1 1.25
/--Sg Krgo Krgw Pcog
0 0 0 0
0.3 0 0 0
0.3001 1* 1* 1.00E-10
0.326 0.020354527 0.020354527 0.0009655
0.352 0.050118723 0.050118723 0.001283
0.378 0.08490214 0.08490214 0.0017485
0.404 0.123406773 0.123406773 0.002086
0.43 0.164938489 0.164938489 0.0023415
0.456 0.209053591 0.209053591 0.002945
0.482 0.255439737 0.255439737 0.003931
0.508 0.303863117 0.303863117 0.005307
0.534 0.354141048 0.354141048 0.0073
0.56 0.406126198 0.406126198 0.0103275
0.586 0.459696817 0.459696817 0.0129725
0.612 0.51475032 0.51475032 0.0152585
0.638 0.571198902 0.571198902 0.019862
0.664 0.628966409 0.628966409 0.0331795
0.69 0.687986066 0.687986066 0.0645515
0.716 0.748198758 0.748198758 0.0906415
0.742 0.809551727 0.809551727 0.173924
0.768 0.871997545 0.871997545 0.3182175
0.794 0.935493312 0.935493312 0.6
0.82 1 1 1.25
/
--Sg Krgo Krgw Pcog
0 0 0 0
0.3 0 0 0
0.3001 0 0 1.00E-10
0.3275 0.0204 0.0204 1*
0.355 0.0501 0.0501 1*
0.3825 0.0849 0.0849 1*
0.41 0.1234 0.1234 1*
0.4375 0.1649 0.1649 1*
0.465 0.2091 0.2091 1*
0.4925 0.2554 0.2554 1*
0.52 0.3039 0.3039 0.0075
0.5475 0.3541 0.3541 0.0125
```

```
0.575 0.4061 0.4061 0.0167
0.6025 0.4597 0.4597 0.0227
0.63 0.5148 0.5148 0.0314
0.6575 0.5712 0.5712 0.0452
0.685 0.629 0.629 0.0577
0.7125 0.688 0.688 0.069
0.74 0.7482 0.7482 0.093
0.7675 0.8096 0.8096 0.1727
0.795 0.872 0.872 0.4413
0.8225 0.9355 0.9355 0.6002
0.85 1 1 1.25
/
--Sg Krgo Krgw Pcog
0 0 0 0
0.28 0 0 0
0.313 0.03706 0.03706 1.00E-10
0.346 0.07943 0.07943 1*
0.379 0.12408 0.12408 1*
0.412 0.17027 0.17027 1*
0.445 0.21764 0.21764 1*
0.478 0.26597 0.26597 1*
0.511 0.31512 0.31512 1*
0.544 0.36498 0.36498 0.03138
0.577 0.41546 0.41546 0.04702
0.61 0.46652 0.46652 0.05486
0.643 0.51808 0.51808 0.0627
0.676 0.57012 0.57012 0.07837
0.709 0.62259 0.62259 0.10345
0.742 0.67547 0.67547 0.14891
0.775 0.72873 0.72873 0.19593
0.808 0.78235 0.78235 0.34091
0.841 0.8363 0.8363 0.45
0.874 0.89057 0.89057 0.52
0.893 1 1 1.25
/
--Sg Krgo Krgw Pcog
0 0 0 0
0.22 0 0 0
0.2565 0.02035 0.02035 0
0.293 0.05012 0.05012 0
0.3295 0.0849 0.0849 0
0.366 0.12341 0.12341 0
0.4025 0.16494 0.16494 0
0.439 0.20905 0.20905 0
0.4755 0.25544 0.25544 0
0.512 0.30386 0.30386 0
0.5485 0.35414 0.35414 0
0.585 0.40613 0.40613 0
0.6215 0.4597 0.4597 0
0.658 0.51475 0.51475 0.05
0.6945 0.5712 0.5712 0.09019
0.731 0.62897 0.62897 0.11285
0.7675 0.68799 0.68799 0.17879
0.804 0.7482 0.7482 0.32845
```

```
0.8405 0.80955 0.80955 0.39809
0.877 0.872 0.872 0.4853
0.9135 0.93549 0.93549 0.60016
0.95 1 1 1.25
/
-----------------------tertiary tables-------------------
--Sg Krgo(Sg) Krgw(Sg) Pcog
0 0 0 0
0.3 0 0 0
0.3001 0.0005 0.0005 1.00E-06
0.325 0.006 0.006 0.0001
0.35 0.02 0.02 0.00195
0.375 0.04 0.04 0.003
0.4 0.065 0.065 0.0033
0.425 0.095 0.095 0.00345
0.45 0.129 0.129 0.00405
0.475 0.168 0.168 0.00465
0.5 0.211 0.211 0.00555
0.525 0.257 0.257 0.0066
0.55 0.308 0.308 0.00795
0.575 0.362 0.362 0.0099
0.6 0.42 0.42 0.01185
0.625 0.481 0.481 0.0153
0.65 0.545 0.545 0.02
0.675 0.613 0.613 0.024
0.7 0.684 0.684 0.03165
0.725 0.759 0.759 0.05955
0.75 0.836 0.836 0.225
0.775 0.916 0.916 0.9003
0.8 1 1 1.25
/
--Sg Krgo Krgw Pcog
0 0 0 0
0.3 0 0 0
0.3001 1* 1* 1.00E-10
0.326 0.020354527 0.020354527 0.0009655
0.352 0.050118723 0.050118723 0.001283
0.378 0.08490214 0.08490214 0.0017485
0.404 0.123406773 0.123406773 0.002086
0.43 0.164938489 0.164938489 0.0023415
0.456 0.209053591 0.209053591 0.002945
0.482 0.255439737 0.255439737 0.003931
0.508 0.303863117 0.303863117 0.005307
0.534 0.354141048 0.354141048 0.0073
0.56 0.406126198 0.406126198 0.0103275
0.586 0.459696817 0.459696817 0.0129725
0.612 0.51475032 0.51475032 0.0152585
0.638 0.571198902 0.571198902 0.019862
0.664 0.628966409 0.628966409 0.0331795
0.69 0.687986066 0.687986066 0.0645515
0.716 0.748198758 0.748198758 0.0906415
0.742 0.809551727 0.809551727 0.173924
0.768 0.871997545 0.871997545 0.3182175
0.794 0.935493312 0.935493312 0.6
```

```
0.82 1 1 1.25
/
--Sg Krgo Krgw Pcog
0 0 0 0
0.3 0 0 0
0.3001 0 0 1.00E-10
0.3275 0.0204 0.0204 1*
0.355 0.0501 0.0501 1*
0.3825 0.0849 0.0849 1*
0.41 0.1234 0.1234 1*
0.4375 0.1649 0.1649 1*
0.465 0.2091 0.2091 1*
0.4925 0.2554 0.2554 1*
0.52 0.3039 0.3039 0.0075
0.5475 0.3541 0.3541 0.0125
0.575 0.4061 0.4061 0.0167
0.6025 0.4597 0.4597 0.0227
0.63 0.5148 0.5148 0.0314
0.6575 0.5712 0.5712 0.0452
0.685 0.629 0.629 0.0577
0.7125 0.688 0.688 0.069
0.74 0.7482 0.7482 0.093
0.7675 0.8096 0.8096 0.1727
0.795 0.872 0.872 0.4413
0.8225 0.9355 0.9355 0.6002
0.85 1 1 1.25
/
--Sg Krgo Krgw Pcog
0 0 0 0
0.28 0 0 0
0.313 0.03706 0.03706 1.00E-10
0.346 0.07943 0.07943 1*
0.379 0.12408 0.12408 1*
0.412 0.17027 0.17027 1*
0.445 0.21764 0.21764 1*
0.478 0.26597 0.26597 1*
0.511 0.31512 0.31512 1*
0.544 0.36498 0.36498 0.03138
0.577 0.41546 0.41546 0.04702
0.61 0.46652 0.46652 0.05486
0.643 0.51808 0.51808 0.0627
0.676 0.57012 0.57012 0.07837
0.709 0.62259 0.62259 0.10345
0.742 0.67547 0.67547 0.14891
0.775 0.72873 0.72873 0.19593
0.808 0.78235 0.78235 0.34091
0.841 0.8363 0.8363 0.45
0.874 0.89057 0.89057 0.52
0.893 1 1 1.25
/
--Sg Krgo Krgw Pcog
0 0 0 0
0.22 0 0 0
0.2565 0.02035 0.02035 0
```

```
0.293 0.05012 0.05012 0
0.3295 0.0849 0.0849 0
0.366 0.12341 0.12341 0
0.4025 0.16494 0.16494 0
0.439 0.20905 0.20905 0
0.4755 0.25544 0.25544 0
0.512 0.30386 0.30386 0
0.5485 0.35414 0.35414 0
0.585 0.40613 0.40613 0
0.6215 0.4597 0.4597 0
0.658 0.51475 0.51475 0.05
0.6945 0.5712 0.5712 0.09019
0.731 0.62897 0.62897 0.11285
0.7675 0.68799 0.68799 0.17879
0.804 0.7482 0.7482 0.32845
0.8405 0.80955 0.80955 0.39809
0.877 0.872 0.872 0.4853
0.9135 0.93549 0.93549 0.60016
0.95 1 1 1.25
/

SWF3
--Rock1
--primary
--Sw Krwo(Sw)Krwg(Sw)Pcwo
0.0 0.0 0.0 2000
0.2 0.0 0.0 200
0.2001 1E-20 1E-20 25
0.21 1* 1* 12.0031
0.215 1* 1* 3.00076
0.26 0.00003 0.00003 0.79324
0.31 0.00036 0.00036 0.42117
0.35 0.00124 0.00124 0.29979
0.36 0.0016 0.0016 0.27883
0.41 0.00475 0.00475 0.20366
0.46 0.01116 0.01116 0.1571
0.5 0.01978 0.01978 0.13103
0.55 0.03664 0.03664 0.10669
0.6 0.0625 0.0625 0.08848
0.65 0.10011 0.10011 0.07428
0.7 0.15259 0.15259 0.0629
0.75 0.2234 0.2234 0.05359
0.8 0.31641 0.31641 0.04579
0.81 0.33803 0.33803 0.04441
0.85 0.43581 0.43581 0.03917
0.97 0.85823 0.85823 0.0269
1 1 1 0
/

---------------------------------
--rock1B
--primary table
--Sw Krwo Krwg Pcwo
0 0 0 2000
```

```
0.285 1E-12 1E-12 200
0.28501 1* 1* 25
0.28502 1* 1* 12
0.3 1* 1* 6.36435
0.32 0.00003 0.00003 3.47848
0.35 0.00023 0.00023 1.81283
0.37 0.00058 0.00058 1.29103
0.42 0.00292 0.00292 0.66359
0.47 0.00881 0.00881 0.39724
0.5 0.01491 0.01491 0.30517
0.52 0.02035 0.02035 0.25945
0.55 0.03099 0.03099 0.20655
0.6 0.05676 0.05676 0.146
0.65 0.09505 0.09505 0.10614
0.7 0.14897 0.14897 0.07862
0.75 0.22183 0.22183 0.0589
0.79 0.29611 0.29611 0.04683
0.81 0.33922 0.33922 0.04172
0.84 0.41205 0.41205 0.03497
0.89 0.55728 0.55728 0.02566
0.93 0.69725 0.69725 0.01931
0.97 0.86069 0.86069 0.01352
1 1 1 0
/

-----------------------------------
--rock2
--primary table
--Sw Krwo Krwg Pcow
0 0 0 2000
0.35 0 0 25
0.3501 1.00E-10 1.00E-10 12.0031
0.37 1* 1* 8.8263
0.42 0.0004 0.0004 3.4543
0.47 0.0027 0.0027 1.859
0.5 0.0059 0.0059 1.3803
0.52 0.0091 0.0091 1.1549
0.55 0.0162 0.0162 0.9041
0.6 0.0353 0.0353 0.6283
0.65 0.0668 0.0668 0.4532
0.7 0.1146 0.1146 0.3345
0.75 0.1828 0.1828 0.2499
0.79 0.2552 0.2552 0.1983
0.8 0.2761 0.2761 0.1764
0.84 0.372 0.372 0.1474
0.89 0.5226 0.5226 0.107
0.93 0.6711 0.6711 0.0792
0.97 0.8476 0.8476 0.0528
1 1 1 0
/
-------------------------------
--rock3
--primary table
--Sw Krwo Krwg Pcow
```

```
0 0 0 2000
0.5 0 0 25
0.5001 1E-10 1E-10 12.0031
0.51 1* 1* 10.5486
0.55 0.0003 0.0003 6.7817
0.58 0.0016 0.0016 4.996
0.6 0.0036 0.0036 4.115
0.65 0.0148 0.0148 2.6023
0.7 0.0405 0.0405 1.6937
0.75 0.0884 0.0884 1.1239
0.79 0.1486 0.1486 0.8168
0.82 0.2097 0.2097 0.6448
0.84 0.2593 0.2593 0.5512
0.89 0.4191 0.4191 0.3718
0.92 0.5432 0.5432 0.2923
0.95 0.6916 0.6916 0.2277
0.97 0.8053 0.8053 0.1906
1 1 1 0
/

--------------------
--rock4
--primary table
--Sw Krwo Krwg Pcwo
0 0 0 2000
0.654 0 0 25
0.6541 1E-10 1E-10 12.0031
0.67 0.00002 0.00002 9.70593
0.685 0.00022 0.00022 7.96186
0.7 0.00086 0.00086 6.56897
0.75 0.01125 0.01125 3.57586
0.79 0.03807 0.03807 2.2569
0.81 0.06154 0.06154 1.80379
0.84 0.1139 0.1139 1.29559
0.89 0.26208 0.26208 0.75317
0.91 0.3484 0.3484 0.60731
0.93 0.45333 0.45333 0.48986
0.97 0.72801 0.72801 0.31731
0.98 0.81189 0.81189 0.28338
1 1 1 0
/
----------------------------------------------------ISTNUM6-10-------------------
--increasing table
--Sw Krwo(Sw)Krwg(Sw)Pcwo
0.0 0.0 0.0 2000
0.2 0.0 0.0 200
0.2001 1E-20 1E-20 25
0.2075 1* 1* 12.0031
0.21125 1* 1* 3.00076
0.245 0.00004 0.00004 0.79324
0.2825 0.00037 0.00037 0.42117
0.3125 0.00121 0.00121 0.29979
0.32 0.00155 0.00155 0.25
0.3575 0.00434 0.00434 0.15
```

```
0.395 0.00978 0.00978 0.09567
0.425 0.01684 0.01684 0.06958
0.4625 0.03026 0.03026 0.05218
0.5 0.05026 0.05026 0.04349
0.5375 0.07863 0.07863 0.02
0.575 0.11734 0.11734 0.004
0.6125 0.16855 0.16855 0
0.65 0.2346 0.2346 -1
0.6575 0.24981 0.24981 -1.5
0.6875 0.318 0.318 -3
0.7775 0.60537 0.60537 -10
0.8 0.7 0.7 -12
/

--secondary table. increasing sat.
--Sw Krwo Krwg Pcwo
0 0 0 2000
0.285 1E-12 1E-12 200
0.28501 1* 1* 25
0.28502 1* 1* 12
0.2958 1* 1* 6.36435
0.31021 0.00001 0.00001 3.47848
0.33182 0.00008 0.00008 1.81283
0.34622 0.00021 0.00021 0.64552
0.38224 0.00124 0.00124 0.33179
0.41825 0.00411 0.00411 0.19862
0.43986 0.00728 0.00728 0.15259
0.45427 0.0102 0.0102 0.12972
0.47587 0.01611 0.01611 0.10328
0.51189 0.03107 0.03107 0.073
0.5479 0.05438 0.05438 0.05307
0.58392 0.08858 0.08858 0
0.61993 0.13648 0.13648 -0.21552
0.64874 0.18674 0.18674 -0.43103
0.66315 0.21644 0.21644 -0.82759
0.68476 0.26733 0.26733 -1.72414
0.72077 0.37103 0.37103 -3.44828
0.74958 0.47322 0.47322 -5.45977
0.77839 0.59478 0.59478 -8.33333
0.8 0.7 0.7 -12
/

--secondary table. increasing sat
--Sw Krwo Krwg Pcow
0 0 0 2000
0.35 0 0 25
0.3501 1.00E-10 1.00E-10 12.0031
0.37 1* 1* 8.8263
0.3985 0.0001 0.0001 3.4543
0.4331 0.0011 0.0011 1.859
0.4538 0.0027 0.0027 1.3803
0.4677 0.0043 0.0043 1.1549
0.4885 0.0079 0.0079 0.9041
0.5231 0.0185 0.0185 0.6283
```

```
0.5577 0.0371 0.0371 0.4532
0.5923 0.0666 0.0666 0.3345
0.6269 0.1106 0.1106 0.2499
0.6546 0.1589 0.1589 0.15
0.6615 0.1731 0.1731 0
0.6892 0.2392 0.2392 -1.6942
0.7238 0.346 0.346 -3.2234
0.7515 0.454 0.454 -5.0975
0.7792 0.5849 0.5849 -8.3958
0.8 0.7 0.7 -12
/
--secondary table
--Sw Krwo Krwg Pcow
0 0 0 2000
0.5 0 0 25
0.5001 1E-10 1E-10 11.8339
0.506 1* 1* 10.2665
0.53 0.0001 0.0001 6.8182
0.548 0.0007 0.0007 3.9185
0.56 0.0015 0.0015 2.9781
0.59 0.0072 0.0072 2.069
0.62 0.0215 0.0215 1.5674
0.65 0.0503 0.0503 1.2539
0.674 0.0883 0.0883 1.0972
0.692 0.1284 0.1284 0.9404
0.704 0.1617 0.1617 0.6276
0.734 0.2723 0.2723 0
0.752 0.3609 0.3609 -0.627
0.77 0.4691 0.4691 -5.4075
0.782 0.5533 0.5533 -8
0.8 0.7 0.7 -12
/
--secondary table
--Sw Krwo Krwg Pcwo
0 0 0 2000
0.654 0 0 25
0.6541 1E-10 1E-10 12.0031
0.66075 0.00001 0.00001 9.70593
0.66708 0.00007 0.00007 7.96186
0.67341 0.00033 0.00033 6.56897
0.69451 0.00536 0.00536 3.57586
0.71139 0.02014 0.02014 2.2569
0.71983 0.03392 0.03392 1.80379
0.73249 0.06618 0.06618 1
0.75358 0.16356 0.16356 0
0.76202 0.2228 0.2228 -0.01
0.77046 0.29653 0.29653 -0.1
0.78734 0.49593 0.49593 -1
0.79156 0.55826 0.55826 -5
0.8 0.7 0.7 -12
/
------------------------------------------------------------DSTNUM11-15----------------
--decreasing table
--Sw Krwo(Sw)Krwg(Sw)Pcwo
```

```
0.0 0.0 0.0 2000
0.2 0.0 0.0 200
0.2001 1E-20 1E-20 25
0.2075 1* 1* 12.0031
0.21125 1* 1* 3.00076
0.245 0.00004 0.00004 0.79324
0.2825 0.00037 0.00037 0.42117
0.3125 0.00121 0.00121 0.29979
0.32 0.00155 0.00155 0.25
0.3575 0.00434 0.00434 0.15
0.395 0.00978 0.00978 0.09567
0.425 0.01684 0.01684 0.06958
0.4625 0.03026 0.03026 0.05218
0.5 0.05026 0.05026 0.04349
0.5375 0.07863 0.07863 0.02
0.575 0.11734 0.11734 0.004
0.6125 0.16855 0.16855 0
0.65 0.2346 0.2346 -1
0.6575 0.24981 0.24981 -1.5
0.6875 0.318 0.318 -3
0.7775 0.60537 0.60537 -10
0.8 0.7 0.7 -12
/
--tertiary table. decreasing sat.
--Sw Krwo Krwg Pcwo
0 0 0 2000
0.285 1E-12 1E-12 200
0.28501 1* 1* 25
0.28502 1* 1* 12
0.2958 1* 1* 11.45583
0.31021 0.00001 0.00001 6.261264
0.33182 0.00008 0.00008 3.263094
0.34622 0.00021 0.00021 1.161936
0.38224 0.00124 0.00124 0.597222
0.41825 0.00411 0.00411 0.357516
0.43986 0.00728 0.00728 0.274662
0.45427 0.0102 0.0102 0.233496
0.47587 0.01611 0.01611 0.185904
0.51189 0.03107 0.03107 0.1314
0.5479 0.05438 0.05438 0.095526
0.58392 0.08858 0.08858 0
0.61993 0.13648 0.13648 -0.10776
0.64874 0.18674 0.18674 -0.215515
0.66315 0.21644 0.21644 -0.413795
0.68476 0.26733 0.26733 -0.86207
0.72077 0.37103 0.37103 -1.72414
0.74958 0.47322 0.47322 -5.45977
0.77839 0.59478 0.59478 -8.33333
0.8 0.7 0.7 -12
/
--tertiary table. decreasing sat
--Sw Krwo Krwg Pcow
0 0 0 2000
0.35 0 0 25
```

```
0.3501 1.00E-10 1.00E-10 12.0031
0.37 1* 1* 8.8263
0.3985 0.0001 0.0001 5.1815
0.4331 0.0011 0.0011 2.7884
0.4538 0.0027 0.0027 2.0705
0.4677 0.0043 0.0043 1.7323
0.4885 0.0079 0.0079 1.3561
0.5231 0.0185 0.0185 0.9424
0.5577 0.0371 0.0371 0.6798
0.5923 0.0666 0.0666 0.5017
0.6269 0.1106 0.1106 0.3749
0.6546 0.1589 0.1589 0.15
0.6615 0.1731 0.1731 0
0.6892 0.2392 0.2392 -1.1859
0.7238 0.346 0.346 -2.2564
0.7515 0.454 0.454 -3.5682
0.7792 0.5849 0.5849 -5.8771
0.8 0.7 0.7 -12
/

--tertiary table
--Sw Krwo Krwg Pcow
0 0 0 2000
0.5 0 0 25
0.5001 1E-10 1E-10 11.8339
0.506 1* 1* 10.2665
0.53 0.0001 0.0001 6.8182
0.548 0.0007 0.0007 3.9185
0.56 0.0015 0.0015 2.9781
0.59 0.0072 0.0072 2.069
0.62 0.0215 0.0215 1.5674
0.65 0.0503 0.0503 1.2539
0.674 0.0883 0.0883 1.0972
0.692 0.1284 0.1284 0.9404
0.704 0.1617 0.1617 0.6276
0.734 0.2723 0.2723 0
0.752 0.3609 0.3609 -0.627
0.77 0.4691 0.4691 -5.4075
0.782 0.5533 0.5533 -8
0.8 0.7 0.7 -12
/

--tertiary table
--Sw Krwo Krwg Pcwo
0 0 0 2000
0.654 0 0 25
0.6541 1E-10 1E-10 12.0031
0.66075 0.00001 0.00001 9.70593
0.66708 0.00007 0.00007 7.96186
0.67341 0.00033 0.00033 6.56897
0.69451 0.00536 0.00536 3.57586
0.71139 0.02014 0.02014 2.2569
0.71983 0.03392 0.03392 1.80379
0.73249 0.06618 0.06618 1
```

```
0.75358 0.16356 0.16356 0
0.76202 0.2228 0.2228 -0.01
0.77046 0.29653 0.29653 -0.1
0.78734 0.49593 0.49593 -1
0.79156 0.55826 0.55826 -5
0.8 0.7 0.7 -12
/
```

B.3 Prediction File

```
-------------Well producer control--------------
WCONPROD
--NAME  STATUS  C-RATE  O-TARG  W-TARG  G-TARG  L-TARG  RES-TARG  BHP  THP VFP
 A-3    'OPEN'  'ORAT'   2000.    300  1420000     1*      1*        20  15   1 /
/
-------------------------------------------------

--------------------Dates-----------------------
NEXTSTEP
0.1 /

DATES
1 'NOV' 2012 /
1 'JAN' 2013 /
1 'MAR' 2013 /
1 'AUG' 2013 /
1 'NOV' 2013 /
1 'JAN' 2014 /
1 'AUG' 2014 /
1 'JAN' 2015 /
/
-----------------------------------------------------
-------Injection well completion data for 2015--------
WELSPECS
INJ 'EAST' 64 66 1* 'GAS' /
/

COMPDAT
 INJ 64 66 30 30 OPEN 2*  .25  1*  .0  1* 'Y' /
 INJ 64 67 30 30 OPEN 2*  .25  1*  .0  1* 'Y' /
 INJ 64 68 30 30 OPEN 2*  .25  1*  .0  1* 'Y' /
 INJ 64 69 30 30 OPEN 2*  .25  1*  .0  1* 'Y' /
 INJ 64 70 30 30 OPEN 2*  .25  1*  .0  1* 'Y' /
 INJ 64 71 30 30 OPEN 2*  .25  1*  .0  1* 'Y' /
 INJ 64 72 30 30 OPEN 2*  .25  1*  .0  1* 'Y' /
 INJ 64 73 30 30 OPEN 2*  .25  1*  .0  1* 'Y' /
 INJ 64 74 30 30 OPEN 2*  .25  1*  .0  1* 'Y' /
 INJ 64 75 30 30 OPEN 2*  .25  1*  .0  1* 'Y' /
 INJ 64 76 30 30 OPEN 2*  .25  1*  .0  1* 'Y' /
 INJ 64 77 30 30 OPEN 2*  .25  1*  .0  1* 'Y' /
 INJ 64 78 30 30 OPEN 2*  .25  1*  .0  1* 'Y' /
 INJ 64 79 30 30 OPEN 2*  .25  1*  .0  1* 'Y' /
 INJ 64 80 30 30 OPEN 2*  .25  1*  .0  1* 'Y' /
 INJ 64 81 30 30 OPEN 2*  .25  1*  .0  1* 'Y' /
 INJ 64 82 30 30 OPEN 2*  .25  1*  .0  1* 'Y' /
 INJ 64 83 30 30 OPEN 2*  .25  1*  .0  1* 'Y' /
 INJ 64 84 30 30 OPEN 2*  .25  1*  .0  1* 'Y' /
 INJ 64 85 30 30 OPEN 2*  .25  1*  .0  1* 'Y' /
 INJ 64 86 30 30 OPEN 2*  .25  1*  .0  1* 'Y' /
 INJ 63 86 30 30 OPEN 2*  .25  1*  .0  1* 'X' /
 INJ 62 86 30 30 OPEN 2*  .25  1*  .0  1* 'X' /
 INJ 61 86 30 30 OPEN 2*  .25  1*  .0  1* 'X' /
```

```
 INJ 60 86 30 30 OPEN 2*  .25  1*  .0  1* 'X' /
 INJ 59 86 30 30 OPEN 2*  .25  1*  .0  1* 'X' /
 INJ 58 86 30 30 OPEN 2*  .25  1*  .0  1* 'X' /
 INJ 57 86 30 30 OPEN 2*  .25  1*  .0  1* 'X' /
 INJ 56 86 30 30 OPEN 2*  .25  1*  .0  1* 'X' /
 INJ 55 86 30 30 OPEN 2*  .25  1*  .0  1* 'X' /
 /

------------------------------------------------------
---------------Well conditions and production terms----
WEFAC
 A-3 0.95 /
 INJ 0.95 /
/
WCONPROD
 A-3 OPEN ORAT 10000 300 500000000 2* 40 15 1 /
/
------------------------------------------------------
-----------------Gas-Injection data----------------------

WELLSTRE
 DILCO2 0.998 0.001 0.001 0 0 0 0 0 0 /
/

WINJGAS
 INJ STREAM DILCO2 2* /
/
WCONINJE
 INJ GAS OPEN BHP 2* 150 /
/
------------------------------------------------------
-----------------WAG-Injection data----------------------
WELLWAG
 INJ T G 30.0 W 30.0 2* BHP BHP 150 150 /
/
------------------------------------------------------
-----------------Water-Injection data----------------------
Additionally the injection well was set to 'water' in WELSPECS
WCONINJE
 INJ WATER OPEN BHP 2* 150 /
/


-------------------------------------------------
-----------------SWAG-Injection data----------------------
For SWAG, 2 identical wells were made, one with water control and the other
with gas control. INJ2 had same WELSPECS and COMPDAT as INJ, the only difference be
control instead of gas.

WCONINJE
 INJ GAS OPEN BHP 2* 150 /
 INJ2 WATER OPEN BHP 2* 150 /
/
------------------------------------------------------------
```

```
DATES
1 'JAN' 2016 /
1 'JAN' 2017 /
1 'JAN' 2018 /
1 'JAN' 2019 /
1 'JAN' 2020 /
1 'JAN' 2021 /
1 'JAN' 2022 /
1 'JAN' 2023 /
1 'JAN' 2024 /
1 'JAN' 2025 /
/
```